

---

# Techno-Economic Assessment of Processes that Produce Jet Fuel from Plant-Derived Sources

---

by

**Gabriel Wilhelm Diederichs**

Thesis presented in partial fulfilment  
of the requirements for the Degree

of  
The crest of Stellenbosch University, featuring a shield with a blue and red design, topped with a crown and surrounded by red and white decorative elements. Below the shield is a banner with the Latin motto 'Pacta sunt quibus recti'.  
MASTER OF ENGINEERING  
(CHEMICAL ENGINEERING)

in the Faculty of Engineering  
at Stellenbosch University

Supervisor  
Professor JF Görgens

December 2015

## Declaration

By submitting this thesis electronically, I declare that the entirety of the work contained therein is my own, original work, that I am the sole author thereof (save to the extent explicitly otherwise stated), that reproduction and publication thereof by Stellenbosch University will not infringe any third party rights and that I have not previously in its entirety or in part submitted it for obtaining any qualification.

Date: 16/09/2015.....

Copyright © 2015 Stellenbosch University

All rights reserved

## Abstract

The use of alternative jet fuels are being considered to reduce the dependency of the air transport sector on fossil derived fuel. Jet fuel produced from plant-derived sources has the potential to decrease the net greenhouse gas (GHG) emissions of the aviation industry. Lignocellulosic biomass is a particularly promising plant-derived feedstock for jet fuel production. The market jet fuel price has experienced significant variability in the past 10 years ranging between \$0.42 and \$1.28 per kg jet fuel. There is, however, an uncertainty concerning the most promising process option to produce jet fuel from plant-derived sources.

Based on screening assessments from studies in literature, six processes were chosen to be investigated. Four processes that converted lignocellulose to mainly jet fuel were the GFT-J (gasification and Fischer-Tropsch) process, the FP-J (fast pyrolysis with upgrading) process, the L-ETH-J (biochemical conversion to ethanol with upgrading) process and the SYN-FER-J (gasification, syngas fermentation to ethanol with upgrading) process. Two processes which converted first generation feedstock to mainly jet fuel were the HEFA (hydroprocessing of vegetable oil) process and the S-ETH-J (sugarcane to ethanol by sugar fermentation with upgrading) process.

Mass and energy balances were constructed for the investigated processes based on detailed process models on Aspen Plus<sup>®</sup>. With exception to the FP-J process that fed additional natural gas and did not aim for mainly jet fuel, all the processes were hydrogen and electricity self-sufficient, and thus independent of fossil sources, whilst also producing mainly jet fuel.

Furthermore, the process economics of the processes were investigated on an international estimate basis. Based on cash flow analyses, minimum jet selling prices (MJSP) were determined for the processes. An economic sensitivity analysis was also performed for the processes.

The following energy efficiencies and economic results emerged for the investigated processes.

## Energy efficiencies and economic results of processes in this study

Processes	FP-J	GFT-J	L-ETH-J	SYN-FER-J	HEFA	S-ETH-J
<b>Energy Efficiencies</b>						
<b>Liquid fuel</b>	48.2%	36.7%	32.0%	27.6% - 29.6%	75.3%	34.4%
<b>Overall</b>	33.7%	37.2%	33.3%	27.6% - 29.6%	75.3%	37.1%
<b>Economic Results</b>						
<b>Fixed capital investment (US\$ million)</b>	719.2	515.7	440.1	368.0 - 378.0	147.2	295.5
<b>Minimum jet selling price (\$ per kg jet fuel)</b>	2.59	1.86	2.55	1.90 - 2.05	1.67	1.79

The energy efficiencies (higher heating value basis) are defined as follows: 1) Liquid fuel = (energy in fuels) / (energy in biomass - thermal energy required for electricity); 2) Overall = (energy in fuels + electrical energy) / (energy in biomass and fossil feed)

For the lignocellulose fed processes, the GFT-J process achieved the highest overall energy efficiency, whilst the HEFA process had the highest overall energy efficiency for all processes.

The thermochemical processes (GFT-J and FP-J processes) required the highest fixed capital investment (FCI), whereas the first generation fed processes (HEFA and S-ETH-J processes) had the lowest FCI.

At the base economic parameters the HEFA process attained the lowest MJSP of all the investigated processes, whilst the GFT-J and SYN-FER-J processes obtained the lowest MJSP of all the lignocellulose fed processes.

Based on the economic sensitivity analysis, it was found that the main feedstock cost and FCI generally had the largest effect on the processes' resulting MJSP. The economic sensitivity analysis also showed that there was substantial overlap between the MJSP of the first generation fed processes and certain lignocellulose fed processes (especially the GFT-J and SYN-FER-J processes). As lignocellulose is plentiful (whilst not contending with food crops) further investigation on especially lignocellulose fed jet fuel production processes, was recommended.

## SAMEVATTING

Die gebruik van alternatiewe vliegtuigbrandstowwe word oorweeg om die lugvaartvervoersektor se afhanklikheid op fossielbrandstowwe te verminder.

Vliegtuigbrandstowwe wat van plantverworwe bronne geproduseer is, het die potensiaal om die kweekhuisgas (KHG) emissies van die lugvaartbedryf te verminder. Lignosellulose is veral 'n belowende plantverworwe bron vir vliegtuigbrandstofproduksie. Die markprys van vliegtuigbrandstof het beduidende veranderlikheid in die afgelope 10 jaar ondergaan (wissel tussen \$0.42 en \$1.28 per kg vliegtuigbrandstof). Daar is egter onsekerheid oor die mees belowende proses vir die produksie van vliegtuigbrandstof van plantverworwe bronne.

Met behulp van 'n siftings assessering van studies in die literatuur, is ses prosesse gekies om te ondersoek. Vier prosesse wat lignosellulose na hoofsaaklik vliegtuigbrandstof omgeskakel het, sluit in die GFT-J (vergassing en Fischer-Tropsch) proses, die FP-J (vinnige pirolise en opgradering) proses, die L-ETH-J (biochemiese omskakeling na etanol met opgradering) proses en die SYN-FER-J (vergassing, sintese-gas fermentasie na etanol met opgradering) proses. Twee prosesse wat eerste generasie roumateriaal omgeskakel het na hoofsaaklik vliegtuigbrandstof was die HEFA (hidrogenasie van plant-olie) proses en die S-ETH-J (suikerriet na etanol m.b.v. suikerfermentasie met opgradering) proses.

Massa- en energiebalanse was vir die ondersoekte prosesse saamgestel, gebaseer op gedetailleerde proses simulasie op Aspen Plus<sup>®</sup>. Met uitsondering van die FP-J proses (wat aardgas gevoer het en nie hoofsaaklik vir vliegtuigbrandstof gemik het nie), was al die prosesse waterstof- en elektrisiteitsselfonderhoudend, en as gevolg onafhanklik van fossiel brandstowwe, terwyl hulle hoofsaaklik vliegtuigbrandstof geproduseer het.

Die ekonomiese vatbaarheid van die prosesse was bepaal op 'n internasionale basis. Minimum vliegtuigbrandstofverkooppryse (MVVP) was bepaal vir die prosesse, gebaseer op kontantvloei ontledings. 'n Ekonomiese sensitiwiteit analise was uitgevoer vir die prosesse.

Die volgende energiedoeltreffendhede en ekonomiese resultate was bepaal vir die ondersoekte prosesse.

## Energiedoeltreffendheid en ekonomiese resultate van prosesse in hierdie studie

Prosesse	FP-J	GFT-J	L-ETH-J	SYN-FER-J	HEFA	S-ETH-J
<b>Energiedoeltreffendheid</b>						
<b>Vloeibare brandstof</b>	48.2%	36.7%	32.0%	27.6% - 29.6%	75.3%	34.4%
<b>Algehele</b>	33.7%	37.2%	33.3%	27.6% - 29.6%	75.3%	37.1%
<b>Ekonomiese Resultate</b>						
<b>Vaste kapitaal belegging (US\$ miljoen)</b>	719.2	515.7	440.1	368.0 - 378.0	147.2	295.5
<b>Minimum vliegtuigbrandstof verkoopprijs (\$ per kg vliegtuigbrandstof)</b>	2.59	1.86	2.55	1.90 - 2.05	1.67	1.79

Die energie doeltreffendheid (hoër verbrandingswaarde basis) is as volg gedefinieer: 1) Vloeibare brandstof = (energie in brandstof) / (energie in biomassa - termiese energie benodig vir elektrisiteit); 2) Algehele = (energie in brandstof + elektriese energie) / (energie in biomassa en fossielbrandstof voer)

Vir die prosesse met lignosellulose as voer, het die GFT-J proses die hoogste algehele energiedoeltreffendheid bereik, terwyl die HEFA proses het die hoogste algehele energiedoeltreffendheid gehad van alle prosesse.

Die termochemiese prosesse (GFT-J en FP-J prosesse) het die hoogste vaste kapitaal belegging (VKB) benodig, terwyl die prosesse met eerste generasie voer (HEFA en S-ETH-J proses) het die laagste VKB vereis.

By die basis ekonomiese parameters het die HEFA proses die laagste MVVP behaal van alle prosesse, terwyl die GFT-J en SYN-FER-J proses die laagste MVVP behaal het van alle prosesse met lignosellulose in die voer.

Volgens die ekonomiese sensitiwiteit analise het die hoof roumateriaal koste en die VKB oor die algemeen die grootste effek op die prosesse se MVVP gehad. Die ekonomiese sensitiwiteit analise het ook getoon dat daar heelwat oorvleueling tussen die MVVP van die prosesse met eerste generasie voer en sekere prosesse met lignosellulose voer (veral die GFT-J en SYN-FER-J prosesse) was. Omdat lignosellulose volop is (sonder om met voedsel gewasse te kompeteer) was verdere ondersoek op vliegtuigbrandstof produksie prosesse, spesifiek prosesse met lignosellulose in die voer, aanbeveel.

## A Word of Thanks

I would like to thank the following for the roles they have played in my work and my life in the last two years:

- Firstly, I would like to thank my **God**.
- **Professor Johann Görgens** for his insight, enthusiasm and for providing guidance in this project.
- **Abdul Petersen, Suandrie McLaren** and other **postgraduate students** who provided models as a basis for this study.
- The **Centre for Renewable and Sustainable Energy Studies**, for providing financial support.
- **Dr Asfaw Daful** for proofreading my thesis.
- To my **parents** for supporting and believing in me.
- To my **friends** and **loved ones** for their support.
- To my girlfriend, **Liezl**, for her love, support and for keeping life *light*.

# Table of Contents

Declaration.....	ii
Abstract.....	iii
A Word of Thanks .....	vii
Table of Contents.....	viii
Nomenclature .....	xiv
1 Introduction .....	1
1.1 Background.....	1
1.1.1 Jet Fuel.....	1
1.1.2 Sustainability.....	4
1.1.3 Feedstock .....	5
1.1.4 Alternative Production Pathways.....	7
1.1.5 Commercial Developments .....	10
1.2 Research Proposal .....	11
1.2.1 Problem Statement .....	11
1.2.2 Aims .....	12
1.2.3 Investigated Processes.....	12
1.2.4 Project Objectives.....	14
1.2.5 Project Deliverables .....	14
1.2.6 Thesis Layout .....	15
2 Screening Assessment.....	16
2.1 Screening Assessment Results.....	17
2.2 Process Selection .....	19
3 Literature Study.....	20
3.1 HEFA Process .....	20
3.1.1 Studies in literature .....	20
3.1.2 State of technology, proposed yields and process conditions .....	21
3.2 Ethanol to Jet Process Section .....	23

3.2.1	Studies in literature .....	23
3.2.2	State of technology, proposed yields and process conditions .....	23
3.3	S-ETH-J Process .....	25
3.3.1	Studies in literature .....	26
3.3.2	State of technology, proposed yields and process conditions .....	26
3.4	L-ETH-J Process .....	27
3.4.1	Studies in literature .....	27
3.4.2	State of technology, proposed yields and process conditions .....	28
3.5	FP-J Process .....	28
3.5.1	Studies in literature .....	29
3.5.2	State of technology, proposed yields and process conditions .....	30
3.6	GFT-J Process.....	30
3.6.1	Studies in literature .....	31
3.6.2	State of technology, proposed yields and process conditions .....	32
3.7	SYN-FER-J Process .....	34
3.7.1	Studies in literature .....	35
3.7.2	State of technology, proposed yields and process conditions .....	36
4	Approach and Design Basis .....	39
4.1	Approach .....	39
4.2	Feedstock, Jet Fuel Product and Plant Size.....	40
4.2.1	Lignocellulose .....	40
4.2.2	Sugarcane .....	41
4.2.3	Vegetable oil.....	42
4.2.4	Jet fuel product .....	43
4.3	Process Descriptions .....	44
4.3.1	HEFA process.....	44
4.3.2	SYN-FER-J process.....	45
4.3.3	S-ETH-J process .....	46
4.3.4	L-ETH-J process.....	48

4.3.5	FP-J process.....	49
4.3.6	GFT-J process.....	50
4.4	Mass and Energy Balances .....	51
4.4.1	General.....	52
4.4.2	Pressure changers.....	56
4.4.3	Heat exchangers.....	56
4.4.4	Separation equipment.....	56
4.4.5	Biochemical reactors.....	59
4.4.6	Ethanol upgrading to jet fuel section .....	62
4.4.7	Thermochemical reactors.....	65
4.4.8	Utilities and waste water plant.....	69
4.4.9	Biomass drying and grinding.....	71
4.4.10	Hydrogen production.....	71
4.4.11	Power generation.....	73
4.5	Equipment Sizing and Cost Estimation .....	76
4.5.1	General.....	76
4.5.2	Aspen Icarus.....	76
4.5.3	Capital costs from literature .....	77
4.6	Economic Analysis.....	77
4.6.1	Capital Investment .....	77
4.6.2	Variable operating cost .....	78
4.6.3	Fixed operating cost.....	79
4.6.4	Discounted cash flow analysis .....	80
4.6.5	Economic sensitivity analysis.....	82
5	Process Mass and Energy Overview .....	83
5.1	HEFA Process .....	83
5.2	SYN-FER-J Process .....	84
5.3	S-ETH-J Process .....	86
5.4	L-ETH-J Process .....	88

5.5	FP-J Process .....	89
5.6	GFT-J Process.....	91
6	Process Economics.....	94
6.1	HEFA Process .....	94
6.1.1	Project Capital and Operating Cost.....	94
6.1.2	Discounted Cash Flow and Sensitivity Analyses .....	95
6.2	SYN-FER-J Process .....	96
6.2.1	Project Capital and Operating Cost.....	96
6.2.2	Discounted Cash Flow and Sensitivity Analyses .....	98
6.3	S-ETH-J Process .....	100
6.3.1	Project Capital and Operating Cost.....	100
6.3.2	Discounted Cash Flow and Sensitivity Analyses .....	101
6.4	L-ETH-J Process .....	103
6.4.1	Project Capital and Operating Cost.....	103
6.4.2	Discounted Cash Flow and Sensitivity Analyses .....	104
6.5	FP-J Process .....	105
6.5.1	Project Capital and Operating Cost.....	105
6.5.2	Discounted Cash Flow and Sensitivity Analyses .....	107
6.6	GFT-J Process.....	108
6.6.1	Project Capital and Operating Cost.....	108
6.6.2	Discounted Cash Flow and Sensitivity Analyses .....	110
7	Comparisons of Processes.....	112
7.1	Process Properties.....	112
7.1.1	Process properties of processes in this study .....	112
7.1.2	Comparison of process properties of this study with literature.....	115
7.2	Process Economics .....	119
7.2.1	Capital and operating costs of processes in this study .....	119
7.2.2	Capital cost comparison with previous studies .....	120
7.2.3	Minimum jet selling prices .....	122

7.3	Concluding remarks .....	126
8	Conclusions.....	128
9	Recommendations for Future Work.....	130
10	References.....	132
Appendix A.	Screening Assessment.....	148
	Scope of the Screening Assessment.....	148
	Methods used to Perform Screening of Investigated Processes.....	149
Appendix B.	Proposed Yields .....	150
	HEFA Process .....	150
	Ethanol to Jet Process Section.....	151
	FP-J Process .....	152
	GFT-J Process.....	153
	SYN-FER-J Process .....	154
	Cooling Tower Calculations.....	154
Appendix C.	Capital Cost Estimation .....	157
	Aspen Icarus.....	157
	Capital Costs from Literature.....	158
Appendix D.	Power and Water Calculations .....	162
	HEFA Process .....	162
	SYN-FER-J Process .....	163
	S-ETH-J Process .....	164
	L-ETH-J Process.....	165
	FP-J Process .....	166
	GFT-J Process.....	167
Appendix E.	Additional Capital Costs .....	168
	SYN-FER-J Process .....	168
Appendix F.	Capital Cost Comparison to Literature.....	169
	HEFA Process .....	169
	Ethanol to Jet Process Section.....	169

Gasification and Syngas Fermentation Process Section .....	170
Sugarcane to Ethanol Process Section .....	170
Lignocellulose to Ethanol Process Section .....	171
FP-J Process .....	171
GFT-J Process .....	172
Appendix G. Operating Costs .....	173
Variable Operating Cost Assumptions .....	173
HEFA Process .....	174
SYN-FER-J Process .....	175
S-ETH-J Process .....	177
L-ETH-J Process .....	178
FP-J Process .....	179
GFT-J Process .....	180
Appendix H. Discounted Cash Flow Sheets .....	181
HEFA Process .....	181
SYN-FER-J Process .....	181
S-ETH-J Process .....	182
L-ETH-J Process .....	183
FP-J Process .....	184
GFT-J Process .....	184
Appendix I. Indices .....	186
Appendix J. Aspen Plus Simulation Flow Sheets .....	187
HEFA Process .....	188
SYN-FER-J Process .....	193
S-ETH-J Process .....	201
L-ETH-J Process .....	202
GFT-J Process .....	203

## Nomenclature

1G	First Generation	L-FFA-J	Lignocellulos to FFA to Jet
2G	Second Generation	LHSV	Liquid Hourly Space Velocity
3G	Third Generation	LHV	Lower Heating Value
AEA	Aspen Energy Analyzer	L-LIP-J	Lignocellulose to Lipid to Jet
AJF	Alternative Jet Fuels	LRT	Liquid Retention Time
ALC-J	Alcohol to Jet	LT	Low-Temperature
ASTM	American Society for Testing and Materials	LTFT	Low-Temperature Fischer-Tropsch
ASU	Air Separation Unit	MC	Moisture Content
ATR	Auto-thermal Reformer	MFSP	Minimum Fuel Selling Price
Biojet fuel	Biomass derived Jet fuel	MJSP	Minimum Jet fuel Selling Price
<i>C. ljungdahlii</i>	<i>Clostridium ljungdahlii</i>	MM	Million (e.g. MM\$)
CFP-J	Catalytic Fast Pyrolysis with upgrading to Jet	MOC	Material of Construction
COP	Coefficient of Performance	MSW	Municipal Solid Waste
CSTR	Continuous Stirred-Tank Reactor	MT	Metric Ton
DCFROR	Discounted Cash Flow Rate of Return	MW	Mega-watt
DFB gasifier	Dual Fluidized Bed gasifier	NPV	Net Present Value
DFSTJ	Direct Fermentation of Sugar to Jet	NREL	National Renewable Energy Laboratory
ETH-J	Ethanol to Jet	Petrojet fuel	Petroleum Jet fuel
FCI	Fixed Capital Investment	PFD	Process Flow Diagram
FFA	Free Fatty Acids	PSA	Pressure Swing Adsorption
FP-F	Fast Pyrolysis with upgrading to Fuel	<i>S. cerevisiae</i>	<i>Saccharomyces cerevisiae</i>
FT	Fischer-Tropsch	SEP-CAT	Separation of Lignocellulose and Catalytic conversion to Jet
FP-J	Fast Pyrolysis with upgrading to Jet	S-ETH-J	Sugarcane to Ethanol to Jet
GFT	Gasification and Fischer-Tropsch synthesis	SHCF	Separate Hydrolysis and Co-Fermentation
GFT-J	Gasification and Fischer-Tropsch synthesis to Jet	SHSF	Separate Hydrolysis and Separate Fermentation
GHG	Greenhouse Gas	SKA	Synthetic Kerosene with Aromatics
GHSV	Gas Hourly Space Velocity	SOT	State of Technology
GRT	Gas Retention Time	SPK	Synthetic Paraffinic Kerosene
HEFA	Hydro-processed Esters and Fatty Acids	SSCF	Simultaneous Saccharification and Co-Fermentation
HHV	Higher Heating Value	SYN-CAT-J	Catalytic synthesis of Alcohols to Jet fuel process
HRSG	Heat Recovery Steam Generators	SYN-FER	Gasification and Syngas Fermentation
HT	High-Temperature	SYN-FER-J	Gasification, Syngas Fermentation with upgrading to Jet fuel
IATA	International Air Transport Association	TCI	Total Capital Investment
IRR	Internal Rate of Return	TIC	Total Installed Cost
JTF ratio	Jet-to-fuel ratio	WHSV	Weight Hourly Space Velocity
L-ACID-J	Lignocellulose to Jet via Organic Acids	Wt	Weight
L-ALC-J	Lignocellulose to Alcohol to Jet	WWT	Wastewater Treatment
L-BUT-J	Lignocellulose to Butanol to Jet	XRT	Cell Retention Time
L-ETH-J	Lignocellulose to Ethanol to Jet (specifically via hydrolysis and fermentation)	<i>Z. mobilis</i>	<i>Zymomonas mobilis</i>

# 1 Introduction

In 2010, air transport consumed 10% of global transportation energy [1], with the world consumption of jet fuel being over 800 million litres per day [2]. Conventional fossil-derived jet fuel produces a large amount of greenhouse gas (GHG) emissions [3]. According to Bond et al. [4], there seems to be uncertainties surrounding the future availability of crude oil, whilst alternatives to liquid fuel for aviation (e.g. battery powered transportation) are also unlikely in the near future [5].

Jet fuel produced from plant-derived sources, a promising energy source, has the potential to decrease the net GHG emissions associated with jet fuel [3], [5] as well as possibly increasing energy security [4]. Lignocellulose, a second generation (2G) plant-derived source, has particularly large potential as a carbon source [6].

Although a variety of processes exist which convert plant-derived sources to jet fuel (discussed in section 1.1.4), only three processes have been approved for use in conventional aircraft [7]. These include the gasification with Fischer-Tropsch synthesis (GFT) process, the HEFA process (process that hydroprocesses vegetable oil to fuel) and the direct fermentation of sugar to jet (DFSTJ) process [7], [8]. Further investigation and development is therefore needed for alternative routes.

Due to the lack of comprehensive techno-economic assessments on processes which produce jet fuel from plant-derived sources, there is an uncertainty concerning the most promising process option [5]. This study will aim to compare process pathways which convert plant-derived sources to mainly jet fuel with particular emphasis on lignocellulose to jet fuel processes. Comparison will be made in terms of technical and economic basis, with future follow-up work to quantify environmental impacts.

## 1.1 Background

### 1.1.1 Jet Fuel

Jet fuel is a type of aviation fuel that is designed for aircraft which are powered by gas-turbine engines [9]. The fuel used by commercial aviation fleets consist almost solely of conventional petroleum derived jet fuel including Jet A, Jet B and Jet A-1 [10], [11]. These three fuels are correspondingly in use in commercial aviation in the US, by the US Air Force and commercial aviation in Europe (as well as most of the rest of the world) [12].

Jet fuel derived from crude oil (petrojet fuel) consists of a mixture of different hydrocarbons including alkanes, saturated cycloalkanes, saturated aromatics and olefins [13]. The properties of jet fuel are significantly influenced by the distribution of the hydrocarbons. The kerosene jet fuels (Jet A and Jet A-1) have a carbon number distribution between 8 and 16, whereas wide-cut jet fuel (Jet B) has a carbon distribution ranging between 5 and 15 [14], [11]. The carbon distribution of Jet A-1 is compared to motor gasoline and diesel fuel in Figure 1.

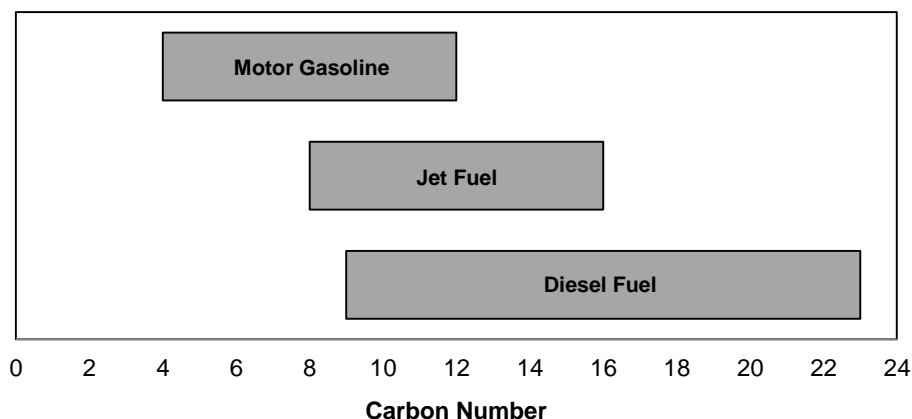


Figure 1: Carbon distribution of Jet A-1 alongside motor gasoline and diesel fuel, [15].

The basic specification for petrojet fuels are given in Table 1.

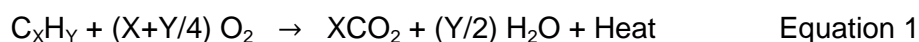
Table 1: Basic specifications of Jet A, B and A-1, [16].

Property	Units	Jet A	Jet B	Jet A-1
Net heat of combustion	MJ/kg	42.8	42.8	42.8
Density (@ 15°C)	kg/m <sup>3</sup>	775 - 840	751 - 802	775 - 840
Maximum freezing point	°C	-40	-50	-47
Maximum vapour pressure	kPa	- <sup>1</sup>	21	- <sup>1</sup>
Minimum flash point	°C	38	- <sup>1</sup>	38
Maximum viscosity @ -20°C	cSt	8	- <sup>1</sup>	8
Maximum aromatic content	Volume%	25	25	25

<sup>1</sup> Not limited by the specification

The main function of jet fuel is to provide a source of energy to propel the aircraft [9], [17].

The combustion of the jet fuel can be described by the following reaction.



The minimization of mass and volume of fuel on an aircraft is desired, thus the importance of gravimetric and volumetric energy content of the fuel [9]. Higher gravimetric energy content will permit an aircraft to carry more people or cargo or carry the same amount of people or

cargo for longer distances [9]. Higher volumetric content is especially desirable in smaller aircraft [9].

The search for alternative jet fuels (AJF) has increased in recent times due to economic and sustainability concerns. AJF consist of jet fuels which are derived from other sources than conventional petroleum including oil shale, coal, natural gas and biomass [14]

It would be desirable if the AJF are drop-in fuels [3], which would require that the AJF can be mixed with petrojet fuel, that the same supply infrastructure can be used and that no adaptations of aircraft or engines are necessary for AJF use [18]. This will ease the transition from petrojet fuel to AJF [18]. Other roles of jet fuel include absorption of heat and functioning as hydraulic operating fluids and lubricants in engine control systems and pumps [17], [9]. The AJF need to be thermally stable during operation to prevent deposits in the fuel system [9]. The compatibility of the AJF with the materials in the aircraft fuel system is also a necessity [9].

As shown in Table 2, certain AJF pathways produce synthetically paraffinic kerosene (SPK), which does not contain aromatic hydrocarbons. Some type of elastomers in aircraft systems swell due to the aromatics in petrojet fuel [9], [11]. There is thus a concern that if SPK is used in current aircrafts, the shrinking of the elastomers could cause leaks [11], [9]. This can be prevented by blending SPK with petrojet fuel or adding additives to SPK [9].

Table 2: The approval status of AJF processes, [19], [8].

<b>Class</b>	<b>Process</b>	<b>Feedstock</b>
<b>Completed</b>		
SPK <sup>1</sup>	GFT	Coal, natural gas, biomass
SPK <sup>1</sup>	HEFA	Triglyceride oils
SPK <sup>1</sup>	DFSTJ	Sugars
<b>In the approval process</b>		
SKA <sup>2</sup>	GFT	Coal, natural gas, biomass
SPK <sup>1</sup>	ALC-J <sup>3</sup>	Sugar, alcohol
SKA <sup>2</sup>	ALC-J <sup>3</sup>	Sugar, alcohol
SKA <sup>2</sup>	Catalytic Hydrothermolysis	Triglyceride oils
SKA <sup>2</sup>	Sugar Catalysis	Sugars
SKA <sup>2</sup>	CFP-J <sup>4</sup>	Biomass

<sup>1</sup> SPK – Synthetically Paraffinic Kerosene; <sup>2</sup> SKA – Synthetic Kerosene with Aromatics; <sup>3</sup> Alcohol to Jet process; <sup>4</sup> Catalytic fast pyrolysis with upgrading to jet fuel.

The ASTM D7566 is a specification standard for AJF which aims to integrate new fuels as drop-in fuels [19]. The approval and certification of AJF is a vital step for incorporation in

aviation as the process guarantees the safety and performance of the AJF and enables the commercial use of AJF [19]. As petrojet fuel consists of a number of different types of hydrocarbons [13], it is not possible (neither necessary) to control the detailed composition in a specification of a jet fuel. The specification approval process therefore seeks to make sure that the AJF will either have similar properties to petrojet fuel or have properties which are suitable for aviation use [14].

The ASTM D7566 approval status of AJF processes are shown in Table 2. The HEFA SPK and GFT SPK products are approved to be blended up to fifty percent with petrojet fuel [3], whilst the SPK product from the DFSTJ process is approved to be blended up to ten percent with petrojet fuel [8].

As kerosene jet fuel (Jet A and Jet A-1), which are used for commercial aviation, is the most widely used type of jet fuel [11], targeting production of alternative kerosene jet fuel is the most sensible. Further use of the term “jet fuel” will therefore refer to kerosene jet fuel.

### **1.1.2 Sustainability**

According to IATA (International Air Transport Association), the sustainability of the production and use of jet fuel can be measured by the environmental, economic and societal impacts [20]. In recent years, conventional fossil-sourced fuel, including jet fuel, has been found to be environmental unsustainable [3]. The net GHG emissions associated with petrojet fuel are currently contributing significantly to climate change [12]. According to Stratton et al. [12], alternatively produced jet fuels, especially based on renewable pathways (discussed in section 1.1.4), have the potential to significantly reduce the GHG emissions associated with the aviation industry. This is because these biojet<sup>A</sup> fuels use feedstock which grows on a GHG emission (CO<sub>2</sub>), creating a closed carbon-cycle.

Various biojet fuels have been developed which meet the technical specifications for use [21]; however, to be able to serve as a promising replacements for petrojet fuel, they need to meet the different sustainability requirements [20], [12]. Trade-offs between the various sustainability criterions will most likely need to be made to determine the most promising biojet fuel production process.

When assessing the impact of a biojet fuel (or any other fuel) on the environment, the GHG emissions and effect on ecosystems and biodiversity associated with the production and use of the fuel need to be determined [20]. When assessing the GHG emissions associated with

---

<sup>A</sup> Jet fuel produced out of biomass

a biojet fuel, a life-cycle assessment of the biojet fuel needs to be performed. This provides a sound basis for evaluating the environmental impacts of the biojet fuel [3]. This includes determining the GHG emissions associated with the jet fuel production (including biomass acquiring) and use. For a biojet fuel to be considered, the biojet fuel's life-cycle GHG emissions must be considerably less than petrojet fuel [20]. It has been found that biojet fuel on a unit energy basis can reduce GHG emissions by as much as 85% in comparison to petrojet fuel [22].

The economic viability of a biojet fuel is a very important sustainability criterion [3]. According to IATA [20], biojet fuels are not currently financially viable in comparison to petrojet fuel. Although financial viability will most likely not be met in the near future, blending mandates or government financing can be used to overshadow the economic stumbling block associated with the processes [20]. Research and innovations are also necessary to make biojet fuel more economically attractive.

The societal sustainability of a biojet fuel is also another important criterion of the fuel. The production and use of a biojet fuel should not significantly affect the food security or drastically increase food prices [20]. The production and use of biojet fuel should also not decrease the standard of water resources and should not pollute the air significantly. The waste production associated with the production and use of biojet fuel should also be reduced, whilst the technology used to produce biojet fuel should also promote decent work for people [20].

### **1.1.3 Feedstock**

Various phases in which biofuels have been produced exist, and are determined by their feedstock [23]. These were followed in order to strive to sustainable energy production.

Initially, first generation (1G) biofuels were produced. This phase produces biofuel using 1G feedstock such as food crops by either extracting oils or using sugars or starch [23]. These biofuels have some drawbacks. The major disadvantage associated with 1G biofuels are the possible negative effects on food prices [23].

Second generation (2G) biofuels were then considered, which produce energy from feedstock that does not have direct impacts on the food chain. 2G feedstock includes wood waste, crop waste and municipal solid waste (MSW). According to Lucian [24], lignocellulosic biomass is an especially promising feedstock as it is abundant and has a relatively low cost [18]. If not managed correctly, 2G feedstock could also have impacts on land use and food production if they compete with crops for land and water.

Biofuels were further developed by producing third generation (3G) biofuels from feedstock which can be produced, whilst not competing with crops for land and water. The feedstock includes the use of algae [23]. These processes are, however, still immature.

Figure 2 displays the relative cost and relative technical effort to process feedstock to sustainable aviation fuel. As indicated, lignocellulosic feedstock is relatively low cost but generally requires higher technical efforts. The high technical effort is due to the complex and rigid structure of lignocellulose, shown in Figure 3. It thus requires substantial pretreatment for biochemical processes or other complex technical processes for thermochemical processes.

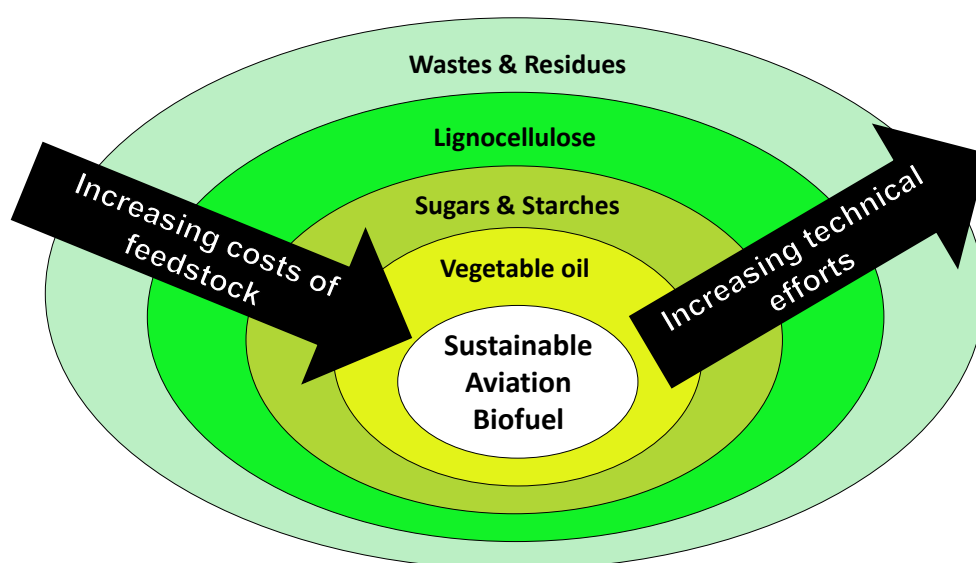


Figure 2: Relative cost of feedstock and technical efforts to process feedstock to sustainable aviation biofuels, redrawn from [18].

As lignocellulosic biomass is a promising feedstock and significant assessments on the conversion of lignocellulose to jet fuel have not been performed (shown in section 2), comparisons on processes converting lignocellulose to jet fuel will be the core of this study. A detailed discussion on lignocellulose as feedstock will therefore be performed in this section.

Lignocellulosic biomass (or lignocellulose) is the non-food fraction of biomass and can be derived from various sources. Lignocellulose from wastes include agricultural wastes, crop residues, mill wood wastes and urban wood wastes, whilst forest products include wood and logging residues [25]. Energy crops are also a possible source of lignocellulose and include short rotation woody crops, herbaceous woody crops and grasses [25].

As depicted in Figure 3, lignocellulose consists of a complex structure of three main chemical components: cellulose, hemicellulose and lignin [20]. Minor components include ash and extractives [20].

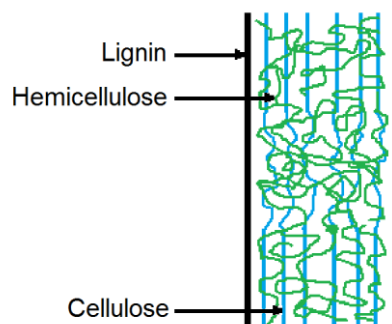


Figure 3: Simplified lignocellulose structure, redrawn from [26]

The composition of various lignocellulosic plant materials differ greatly. This is illustrated in Figure 4.

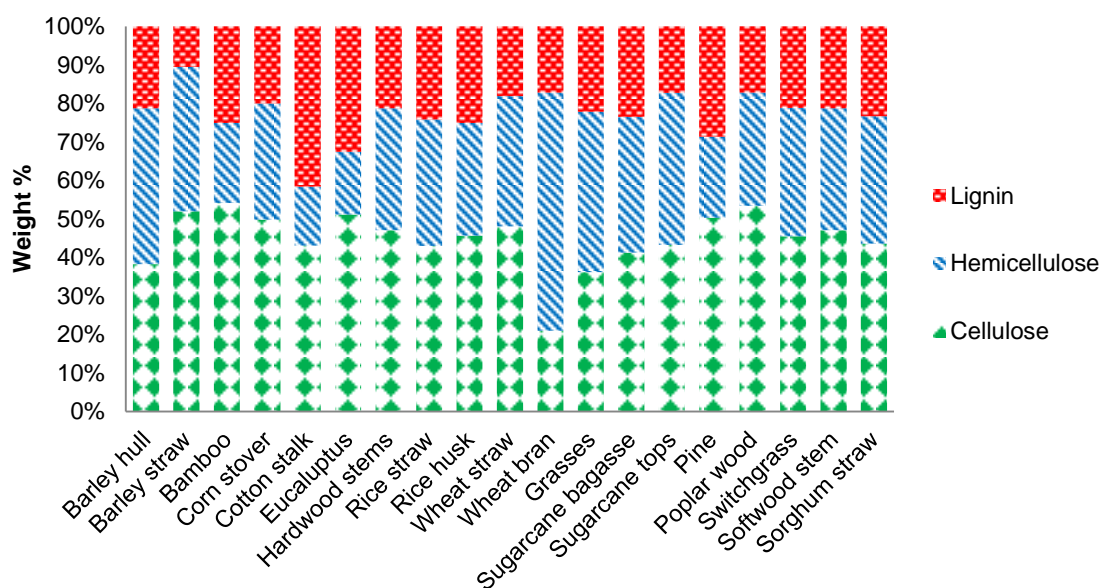


Figure 4: Typical lignocellulose contents of some plant materials (normalized for cellulose, hemicellulose and lignin), [27].

#### 1.1.4 Alternative Production Pathways

According to Hemighaus et al. [9], most of the world’s jet fuel is produced by refining of crude oil. However, the search for sustainable fuel, especially decreased GHG emissions, has led to an increase in research on alternative jet fuel production pathways [9]. These possible alternative production pathways consist of renewable and non-renewable pathways. Non-renewable pathways are generally only being investigated due to economic

considerations, whereas the renewable pathways are mainly being investigated due to the large potential to decrease the net GHG emissions associated with jet fuel [3], [5].

#### Non-renewable alternative production pathways:

Other than crude oil, non-renewable feedstock which can be used to produce jet fuel include shale oil, oil sands, natural gas and coal [9].

Upgraded shale oil and oil sands can be used in conventional refining processes to produce various hydrocarbons including jet fuel. The upgrading of the liquids mainly includes purification [28].

Because the Fischer-Tropsch (FT) synthesis process starts with carbon monoxide, any source of carbon can be used. The two fossil sources, coal and natural gas, are generally used to produce FT synthetic fuel [29]. The carbon monoxide and hydrogen (syngas) required for the FT synthesis process is produced differently for the coal and natural gas [9]. The coal is first gasified and then purified from the contaminants and ash. The syngas can be produced from natural gas by various processes including steam reforming, auto-thermal reforming and direct oxidation [30]. As shown for FT synthesis in Equation 2, the carbon monoxide is catalytically polymerized to hydrocarbons, accompanied by the reaction with hydrogen [9].



The FT process primarily produces straight chain hydrocarbons. Further processing such as cracking of the raw product is done to produce more useful fuel. Coal can also be converted to jet fuel by direct liquefaction, which consists of selectively depolymerizing coal by cleaving the coal structure into smaller parts, with continuous addition of hydrogen at specific process conditions, producing a synthetic crude oil [31].

#### Renewable alternative production pathways:

Various pathways can be followed to convert renewable feedstock (non-fossil sources) to jet fuel. Presented in Figure 5 is a simplified diagram of the potential routes that exist. The conversion pathways can broadly be divided into lipid, biochemical, thermochemical and catalytic conversion pathways, whilst some process pathways consist of a combination between the conversion pathways (referred to as hybrids). The renewable feedstock in Figure 5 consists of 1G, 2G and 3G feedstock with a variety of intermediates.

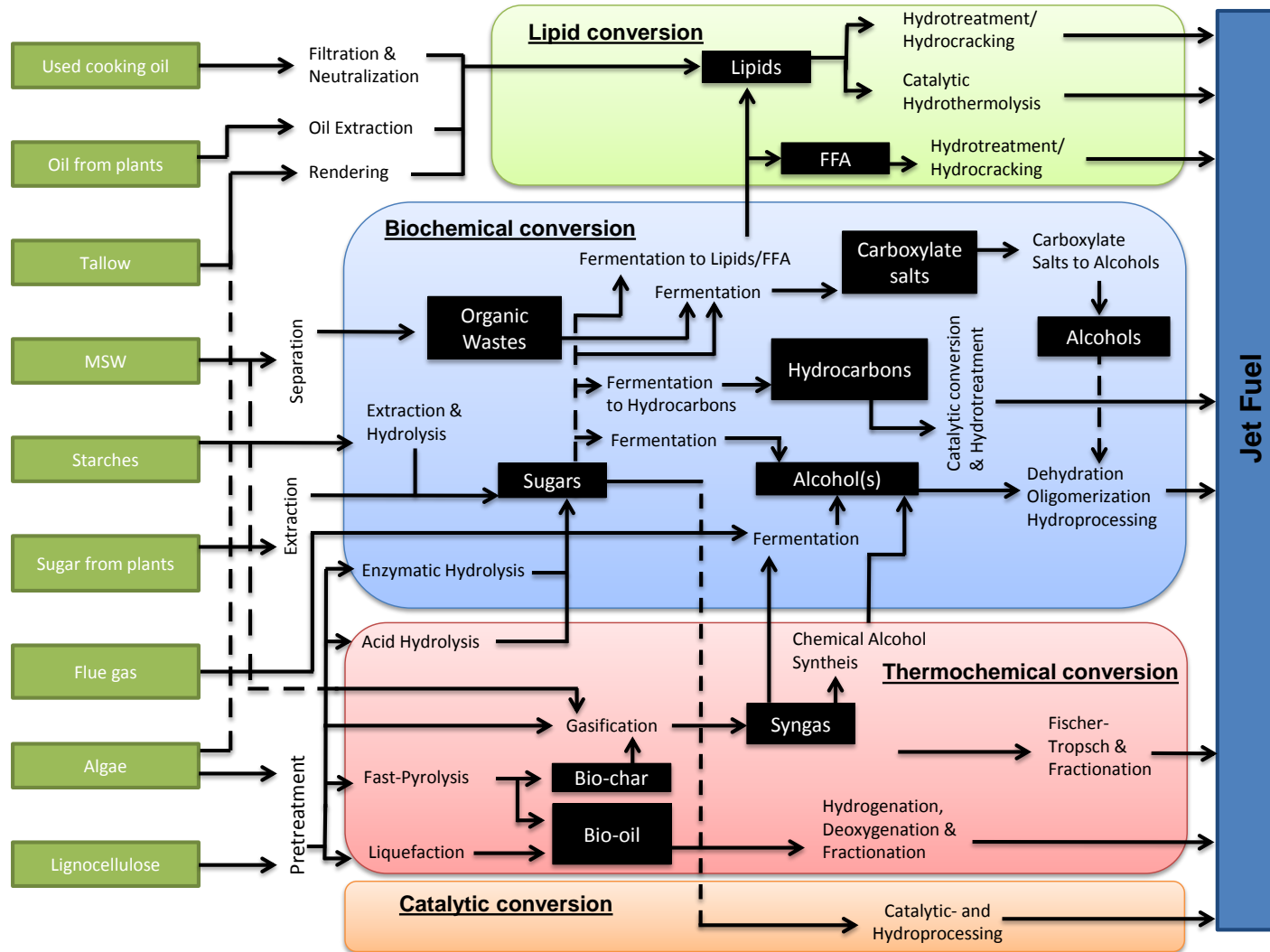


Figure 5: Mind-map of various pathways to produce jet fuel from the various non-fossil sources, redrawn based on [18].

The feed to the lipid conversion pathway consist of lipids or free-fatty acids (FFA). The feed to the conversion pathway can be derived from plants, wastes, algae as well as sugar fermentation. The lipids and FFA are upgraded by hydroprocessing units such as hydrotreatment or hydrocracking.

A biochemical process refers to a process that converts raw material with organisms or enzymes [7]. It can be seen in Figure 5 that sugars derived from 1G and 2G feed are precursors for most of the biochemical process pathways. In contrast to the 1G feed which only requires simple hydrolysis for releasing of its sugars, 2G feedstock such as lignocellulose requires significant pretreatment and hydrolysis to release its sugars [32]. Sugars derived from 1G or 2G fed processes can be fermented to lipids, FFA, carboxylate salts, higher hydrocarbons or alcohols [18]. The production of lipids, FFA and hydrocarbons with long carbon chain lengths are favourable as it requires less significant upgrading to jet fuel, but the carbon yields are generally lower compared to lower alcohols such as ethanol or even butanol [33]. The hydrocarbons can be upgraded catalytically to jet fuel (largely dependent on chain length), whilst the alcohols can be upgraded by dehydration, oligomerization and hydroprocessing.

A thermochemical process treats its feed with high temperatures. The main intermediates of the thermochemical process pathway in Figure 5 are bio-oil and syngas. Bio-oil can be produced by fast pyrolysis or liquefaction of lignocellulose [34]. Bio-oil production by hydrothermal liquefaction of algae has also been investigated [35]. Bio-oil can be upgraded to jet fuel by hydroprocessing units such as hydrotreatment or hydrocracking. Syngas can be produced by gasification of biomass or municipal solid waste. The syngas can either be upgraded by chemical alcohol synthesis to different alcohols [36], by syngas fermentation to mainly ethanol [37] or by FT synthesis to hydrocarbons.

The catalytic processes which convert sugars derived from 1G or 2G feed to jet fuel, consists of multiple pathways with different intermediates using a variety of catalytic reactions [4], [38].

### **1.1.5 Commercial Developments**

Although biofuels have been used in more than 1600 commercial flights [39], these have all been produced from batches of fuel from demo plants [7]. In 2014, IATA reported that the first regular commercial production of jet fuel should start in 2015, even though still at a limited scale [7]. According to IATA, cost still remains a major hurdle for the large-scale commercial production of biojet fuels. Four companies that are close to commercial

production of biojet fuel (including AltAir, Fulcrum BioEnergy, Solena and Amyris) are briefly discussed below [7].

AltAir intend to utilize the UOP renewable jet fuel process to produce HEFA-SPK from vegetable oil [40]. AltAir had ambitions to be the first full-scale plant devoted to renewable jet fuel for commercial use [40] by starting production of 90 000 metric ton (MT) of diesel and jet fuel per year at the beginning of 2015 [7].<sup>B</sup>

Fulcrum BioEnergy, in partnership with Cathay Pacific, intend to produce 30 000 MT per year of drop-in fuel by 2016 [7]. The plant will be based on Fulcrum BioEnergy's demonstration facility which converted municipal solid waste to FT-SPK fuel by gasification with steam reforming, FT synthesis and hydroprocessing [41], [7].

By 2017, Solena, in partnership with British Airways, are aiming to produce 50 000 MT of jet fuel per year [7]. The plant will consist of Solena's plasma gasification technology and microchannel FT synthesis reactors [42].

Amyris is currently producing farnesene at an initial commercial scale in a plant that can produce 40 000 MT of fuel per year [7]. Amyris produces farnesene from sugarcane by the process of direct fermentation of sugar to hydrocarbons [43]. Farnesene can be converted into a jet fuel substitute by hydroprocessing, whilst there are also prospects of utilizing cellulosic sugars from woody biomass as feed [7].

## 1.2 Research Proposal

### 1.2.1 Problem Statement

Jet fuel produced from plant-derived sources is an essential step in mitigating the GHG emissions associated with the aviation industry [5]. There are a wide variety of processes which convert plant-derived sources, including lignocellulose, to jet fuel [44].

The literature does consist of a few biojet fuel production process assessments. However, comprehensive assessments of lignocellulose to jet fuel processes (a promising route) are limited. Assessments on the same basis are also scarce [5]. For assessments to be comparable, various factors including feedstock and product price, economic assumptions, type of yields (current state of technology or possible future yields) and estimation methods need to be the same.

---

<sup>B</sup> At the time of publication of this study, no evidence of AltAir producing jet fuel on a commercial scale was available.

There is therefore still uncertainty concerning the best process option(s) to convert plant-derived sources, especially lignocellulose, to jet fuel [5].

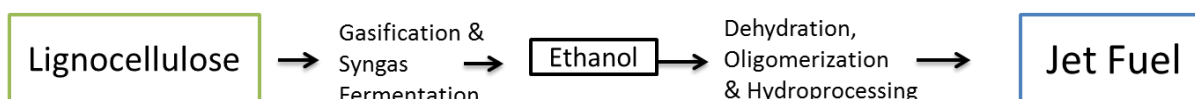
### 1.2.2 Aims

The main aim of this study is to compare process options that convert plant-derived sources to jet fuel. Specific emphasis will be placed on lignocellulose to jet fuel processes. It is aimed that a comparison be made in terms of technical and economic basis. If these processes are studied and compared on the same basis, better understanding of the best process option(s) will result.

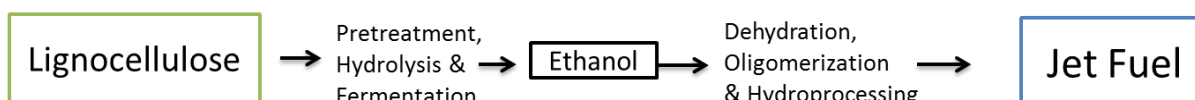
### 1.2.3 Investigated Processes

Selection of lignocellulose to jet fuel processes to be investigated only commences after the screening assessment in section 2. Selection of the processes were based on the promise associated with the processes, the abundance of detailed experimental data to allow computer simulation of the processes, the maturity of the process technologies, the novelty of the study on the processes in comparison to literature and the time required to investigate the processes. For the lignocellulose to jet fuel processes in this study, the feed-rate of dry, ash-free lignocellulose was fixed to 75 MT/h. Illustrations of the chosen lignocellulose to jet fuel processes are given below.

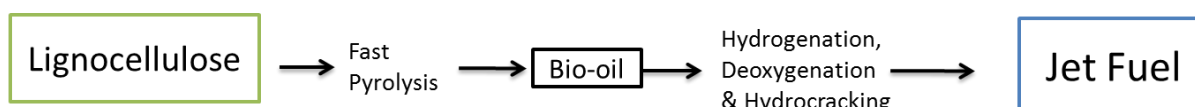
#### SYN-FER-J process

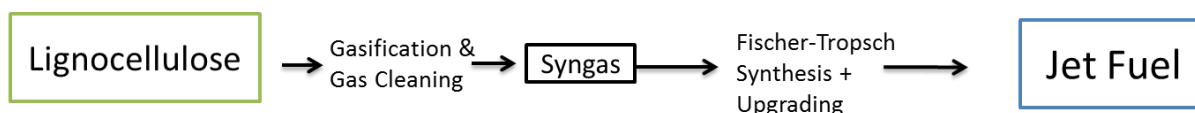


#### L-ETH-J process



#### FP-J process



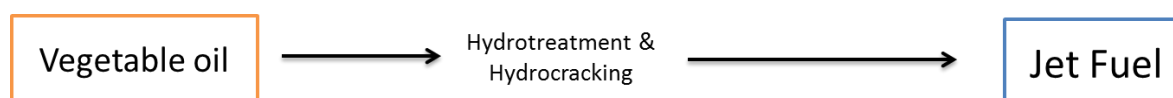
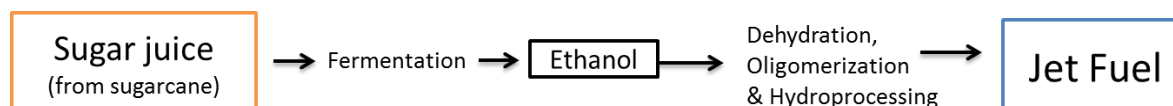
GFT-J process

Along with the chosen lignocellulose to jet fuel processes, it was decided that two processes which convert 1G feedstock to jet fuel would also be investigated as benchmark processes as these processes generally utilize more mature technology [45].

The first selected 1G fed process was the HEFA process, which is a relatively mature process that converts vegetable oil to jet fuel. The HEFA process, which was the first process to be approved for commercial aircraft use [3], was the source of jet fuel for the majority of the commercial test flights thus far [7].

Considerable amounts of ethanol, which is feed to the almost approved alcohol to jet process [7], are produced commercially from 1G feedstock such as sugarcane and starch [46]. It has been found that the sugarcane to ethanol process (with sucrose fermentation) generally has a greater GHG reduction potential than the starch to ethanol process [47]. Therefore, the sugarcane to ethanol with upgrading to jet process was also chosen to be investigated.

A feed-rate of 14.9 MT/h of vegetable oil to the HEFA process and 222.5 MT/h of wet sugarcane to the S-ETH-J process were chosen so that these processes produced similar amounts of jet fuel to the lignocellulose to jet fuel processes. The investigated 1G fed processes are illustrated below.

HEFA processS-ETH-J process

#### 1.2.4 Project Objectives

Process simulations will be constructed for the processes illustrated in section 1.2.3, based on literature and previous simulations in the writer's research group.<sup>C</sup> Capital and operating costs of the various processes will then be determined based on the simulations, which will be incorporated into a cash flow analysis. An economic sensitivity analysis will also be performed.

From the process simulation and economic study the following objectives can be met:

- I. Determine the process properties (e.g. mass ratios, energy ratios and energy efficiencies) of the processes
- II. Determine the absolute economic feasibility of the investigated processes
- III. Determine the comparative economic feasibility of the investigated processes
- IV. Determine which factors (e.g. capital cost, feedstock cost, by-product costs, interest rate, stream factor, etc.) have the greatest influence on the ultimate process economics

#### 1.2.5 Project Deliverables

The project deliverables of this study include:

- Process configurations of investigated processes
- Published experimental data for process sections of processes
- Integrated process simulations of investigated processes (Aspen Plus<sup>®</sup>)
- Mass and energy balances of investigated processes
- Process properties of the investigated processes
- Capital and operating costs of investigated processes
- Economic feasibility and sensitivity assessments of investigated processes

---

<sup>C</sup> The process simulation which was performed in this study or based on previous simulations is specified in section 4.3.

### 1.2.6 Thesis Layout

The approach which was followed in this thesis is presented in Figure 6.

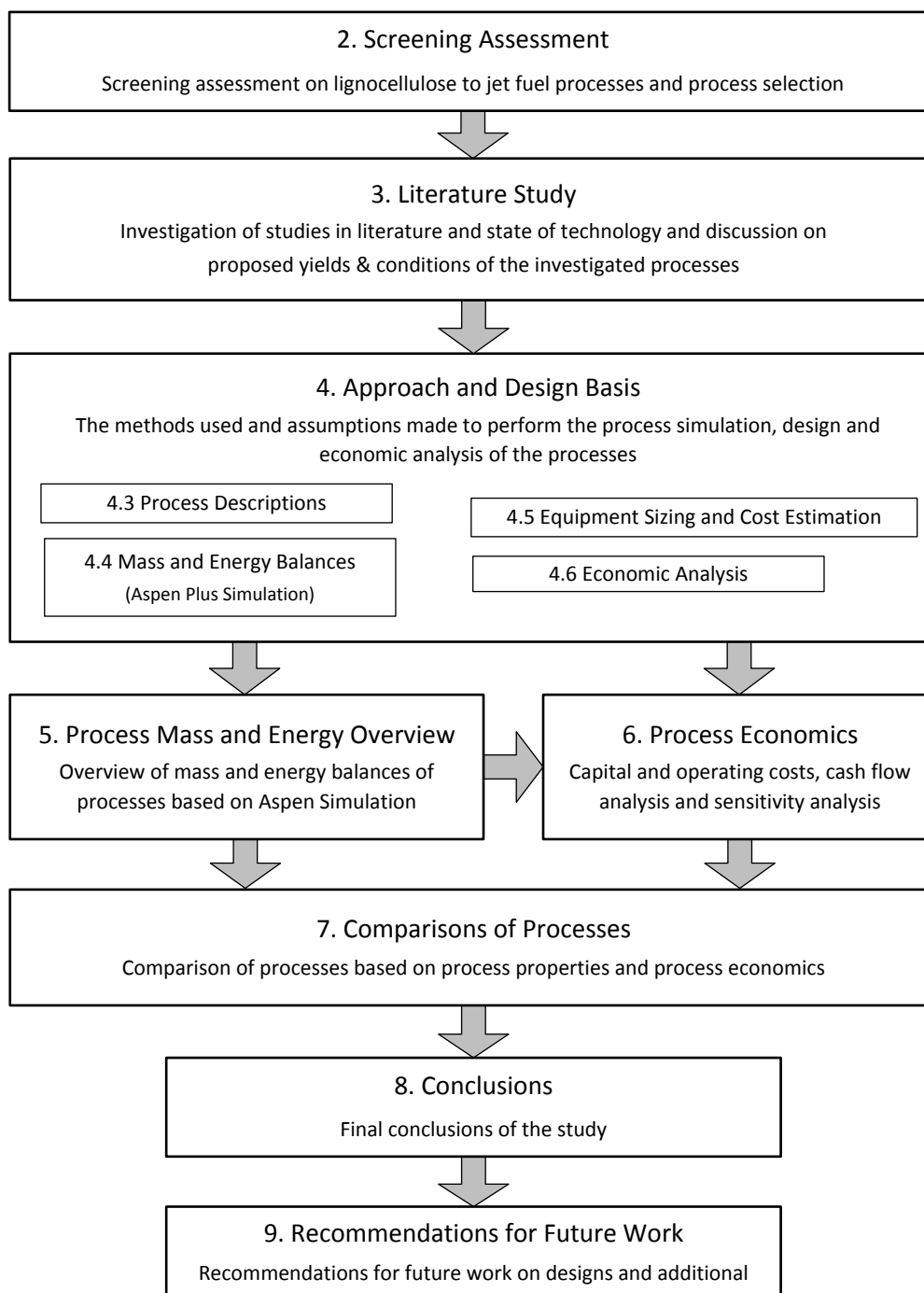


Figure 6: Thesis layout

## 2 Screening Assessment

From section 1.1.4 it is evident that there are a wide variety of process pathways for the conversion of lignocellulose to jet fuel. As this project has a time constraint, only a certain number of processes can be assessed in detail. Many techno-economic studies have been performed for a wide variety of processes that produce fuel from lignocellulose, produce intermediates from lignocellulosic biomass or produce fuel from intermediates (discussed in section 3). However, limited comprehensive techno-economic assessments were found which convert lignocellulose to mainly jet fuel.

The literature consists of three techno-economic assessments which aimed for mainly jet fuel from lignocellulose comprising of a study by Ekbom et al. [48], Bond et al. [4] and Crawford [49]. Ekbom et al. performed a study on the gasification with FT synthesis pathway to mainly jet fuel; the study by Bond et al. examined a process which catalytically converted cellulose and hemicellulose fractions from lignocellulose to mainly jet fuel, whilst the study by Crawford performed lignocellulose fermentation to acetic acid, with conversion to ethanol, followed by upgrading to mainly jet fuel. Pham et al. [50] also performed a techno-economic assessment of lignocellulose to jet fuel via the MixAlco process, but it did not aim at mainly jet fuel. The outcome of these and other studies in literature can, however, not be compared with each other due to differing assumptions, different levels of detail or different type of results.

A **screening assessment** – a high-level assessment comparing processes on a similar basis, based on information from studies in literature – was therefore deemed to be more valuable than purely comparing literature. The screening assessment was only for lignocellulose to jet fuel processes. The **screening assessment aided at the selection of processes for detailed assessment later in the present project**. The screening assessment aimed at determining the promise associated with the various process pathways from literature based on the current state of technology. In contrast, the detailed assessment of processes in this study (which is mainly conducted in section 4, 5, and 6) will be based on process simulation.

The processes, the type of pathway and the literature sources used in the screening assessment are shown in Table 3. A brief description of each process is given in Appendix A. The method that was used to perform the screening assessment is described in Appendix A. The outputs of the screening assessment were jet fuel energy ratios, overall energy efficiencies and minimum jet selling prices (MJSP).

Table 3: Processes in the screening assessment

Processes <sup>1</sup>	Pathways	Sources
FP-J	Thermochemical	[51], [52], [53], [54], [55]
CFP-J	Thermochemical	[56], [51], [57], [52]
L-ETH-J	Biochemical	[58], [59], [60], [61], [62]
SYN-FER-J	Biochemical and thermochemical	[6], [59], [60], [61], [62]
SYN-CAT-J	Thermochemical	[36], [59], [60], [61], [62]
L-BUT-J	Biochemical	[63], [59], [60], [64]
L-LIP-J	Biochemical and lipid	[65], [66]
L-FFA-J	Biochemical and lipid	[65], [67], [68]
L-ACID-J	Biochemical	[50]
SEP-CAT	Catalytic	[4]
GFT-J (HT) <sup>2</sup>	Thermochemical	[48], [69]
GFT-J (LT) <sup>3</sup>	Thermochemical	[48], [69]
Small GFT-J (HT) <sup>2</sup>	Thermochemical	[48], [69], [70]

<sup>1</sup> Refer to nomenclature on page xiv for abbreviations of the processes; <sup>2</sup> High-temperature gasification scenario; <sup>3</sup> Low-temperature gasification scenario.

## 2.1 Screening Assessment Results

The overall energy efficiencies and jet fuel energy ratios for the screening processes are depicted in Figure 7. The varying degree of heat integration in the investigated literature studies may to some extent reduce the comparability of the processes.

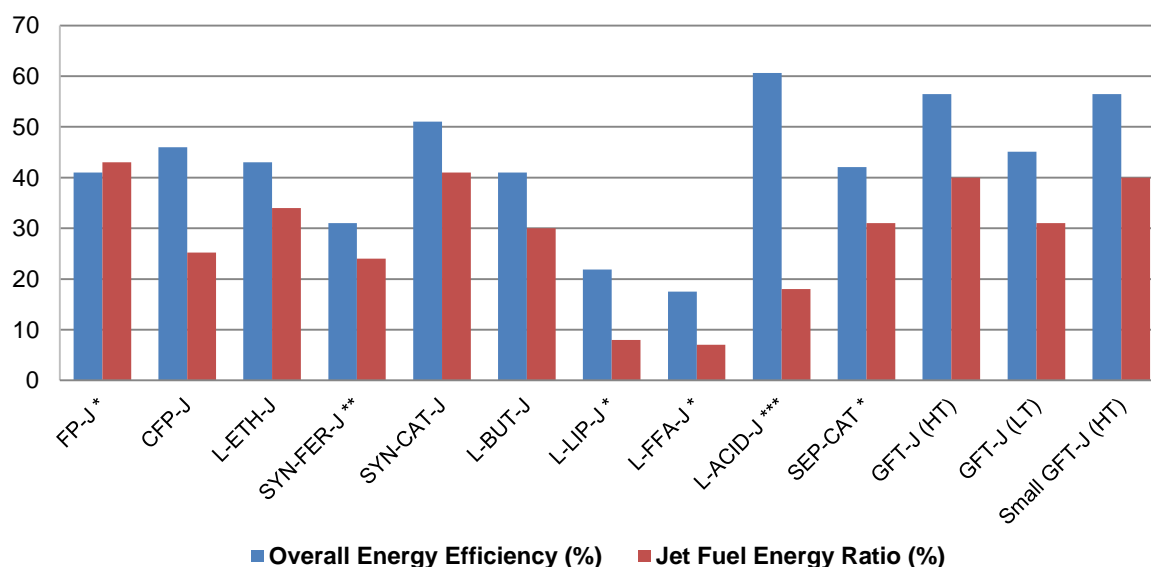


Figure 7: Energy efficiencies and energy ratios of screening processes

\* Purchase of hydrogen; \*\* Yield used by main reference is somewhat outdated; \*\*\* Not for maximum jet production.

Small jet fuel energy ratios and overall energy efficiencies associated with the L-LIP-J and L-FFA-J process make them unpromising. The low jet fuel energy ratio associated with the SYN-FER-J process is somewhat due to outdated yields by Piccolo et al. [6], whilst the low jet fuel energy ratio of the L-ACID-J is because the process was not aimed at maximum jet fuel production. From Figure 7 it can be seen that the thermochemical processes generally have higher energy efficiencies. The source of the hydrogen also plays a crucial role. The process properties of the FP-J and SEP-CAT processes are somewhat optimistic due to hydrogen purchase.<sup>D</sup>

Based on the high-level economic assessment performed in the screening assessment (discussed in Appendix A) the following MJSP were determined for the screening processes (shown in Figure 8). It needs to be stressed that the MJSP values have considerable uncertainty as the technical and economic assumptions have not been scrutinised.

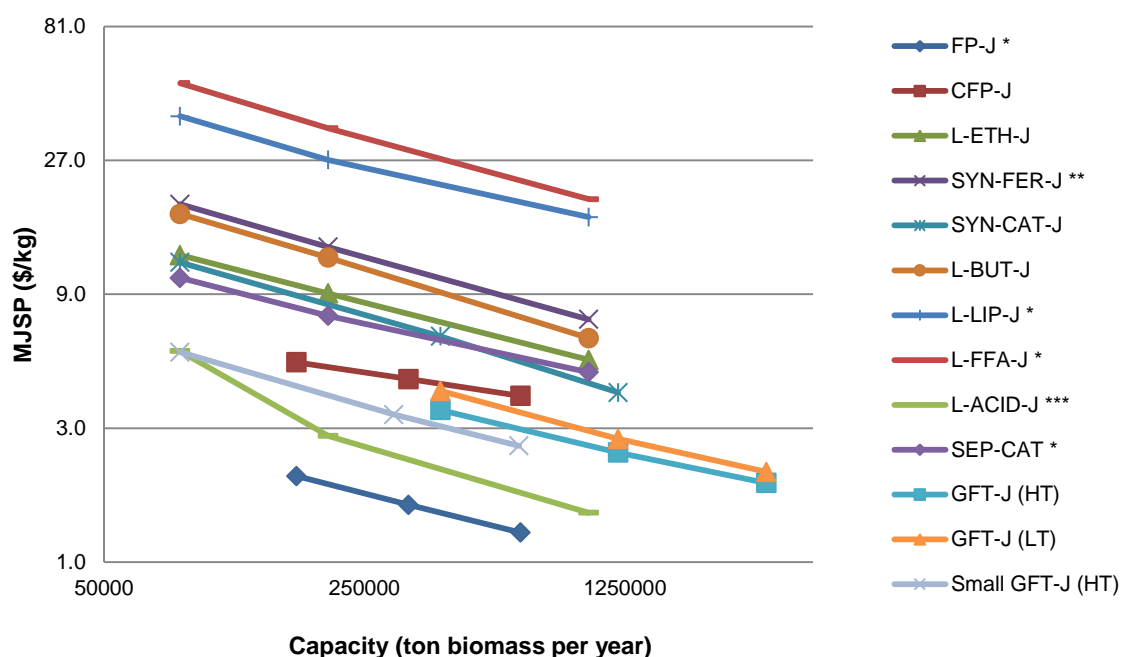


Figure 8: MJSP versus capacity for screening processes

\* Purchase of hydrogen; \*\* Yield used by main reference is somewhat outdated; \*\*\* Not for maximum jet production.

The low MJSP for the L-ACID-J process is somewhat due to its low capital cost, based on Pham et al. [50]. The thermochemical processes generally obtained the lowest MJSP.

<sup>D</sup> This inequality can be removed if hydrogen was produced from part of the feedstock or an intermediate.

## 2.2 Process Selection

The decision on which processes to evaluate in a greater level of detail were based on various factors including: promise associated with the processes (process properties and economics), the abundance of sufficiently detailed experimental data to allow process simulations to be constructed, the maturity of the process technology, the novelty of the study on the process (in comparison to what is in literature) and the time needed for the study. The processes were also chosen to constitute of a variety of pathways. The decision on which processes to further investigate does therefore not necessarily indicate that processes that are not chosen are not promising. The main reason for the exclusion of promising routes include the seeming lack of detailed experimental data (L-ACID-J), the investigation to produce jet fuel from lignocellulose will not be novel (L-ACID-J and SEP-CAT) and the time limitation associated with this project (L-BUT-J and SYN-CAT-J).

The chosen lignocellulose to jet fuel processes are listed below:

- **GFT-J process**  
Gasification and Fischer-Tropsch pathway
- **FP-J process**  
Fast pyrolysis with upgrading pathway
- **L-ETH-J process**  
Biochemical conversion of lignocellulose to ethanol; upgrading to jet fuel
- **SYN-FER-J process**  
Gasification, syngas fermentation to ethanol; upgrading to jet fuel

The main reasons why these processes were selected are given in Table 4.

Table 4: Reasons for lignocellulose to jet fuel process selection

Reasons	GFT-J	FP-J	L-ETH-J	SYN-FER-J
Relative mature technology	✓	-	✓ <sup>1</sup>	-
Obtained very high energy efficiencies	✓	-	-	-
Obtained very low MJSP	✓	✓	-	-
In-house Aspen Plus <sup>®</sup> model available	✓	✓	✓ <sup>2</sup>	-
Product flexibility - pathway can produce high proportions of jet fuel	✓	✓	✓	✓
Pathway has been approved for commercial use	✓	-	-	-
Pathway is in approval process for commercial use	-	✓	✓	✓
Pathway investigation will be novel	-	✓ <sup>3</sup>	✓	✓

<sup>1</sup> Especially the ethanol production section; <sup>2</sup> In-house model available for the ethanol production section; <sup>3</sup> Only the economic assessment will be novel.

### 3 Literature Study

In section 1.2.3 and section 2.2, certain processes were concluded to be assessed in detail, through process simulation and economic evaluation. These included four lignocellulose to jet fuel processes (GFT-J, FP-J, L-ETH-J and SYN-FER-J process) and two processes that convert 1G feedstock to jet fuel (HEFA and S-ETH-J process).

For these processes, techno-economic studies performed in literature will be discussed and compared. The state of technology (SOT) of the main conversion sections will be investigated and yields and conditions will be proposed. As a few of these processes have been previously investigated and simulated on Aspen Plus® in our research group (with the models available for updating), the proposed yields and conditions of these processes are closely linked to these previous studies.

Although a variety of scenarios are available for each process pathway, this study will only aim at producing a single scenario for each process pathway which is **feasible, promising** and **representative** of the pathway. This study aims to use current SOT for the assessment.

#### 3.1 HEFA Process

The conventional HEFA process comprises of two reactor sections (the single-step reactor configuration is still immature [71]). As shown in Figure 9, the two-steps include a hydrodeoxygenation (or hydrotreating) reactor section and a hydrocracking and isomerization reactor section [15]. In the first reactor section, the vegetable oil is upgraded by saturating the oil, generating FFA's and removing oxygen from the FFA's [72]. The second reactor section generates desired hydrocarbons by cracking and isomerization. The jet fuel fraction can be maximized by correct choice of reactor conditions [73].

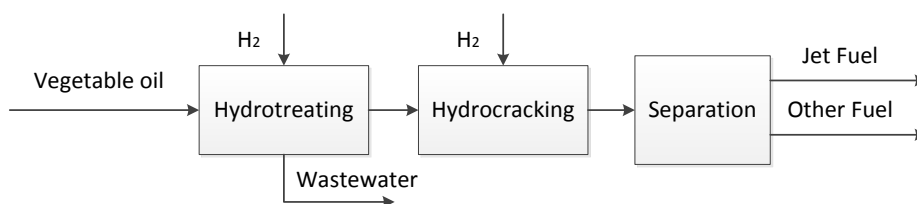


Figure 9: Overall process flow diagram of the HEFA process

##### 3.1.1 Studies in literature

Thorough techno-economic studies of the HEFA process in literature include the study by Klein-Marcuschamer et al. [5] and Pearlson [15]. Klein-Marcuschamer et al. and Pearlson both investigated the two-step conversion of vegetable oil with the addition of hydrogen to

light fuel gas, naphtha, diesel fuel and jet fuel. Klein-Marcuschamer et al. fed pongomia oil, whereas Pearlson fed soybean oil. Both studies had scenarios which aimed for maximum jet fuel production. Klein-Marcuschamer et al. used SuperPro Designer for mass and energy balance modelling purposes, in contrast to Aspen Plus<sup>®</sup> which was used by Pearlson. Process economics were investigated by both studies by calculation of minimum selling prices of distillate products and of economic indicators such as net present value (NPV) [5], [15]. Base minimum selling prices were \$1.05 per litre distillate product by Pearlson (2010 US\$) and \$2.35 per litre distillate product by Klein-Marcuschamer et al. (2011 US\$) [15], [5].

### 3.1.2 State of technology, proposed yields and process conditions

The possible yields and conditions for the HEFA process are discussed below for the two reactor sections.

#### Hydrodeoxygenation section:

A variety of investigations have been performed on the hydrodeoxygenation section for a variety of feedstock, conditions and catalysts. Although a thorough review is not deemed necessary for this relatively well researched process section, a comparison of independent promising experimental literature will be performed. As the hydrodeoxygenation reaction of oil (triglyceride) follows certain stoichiometric reactions as shown in Figure 10, a certain maximum liquid hydrocarbon production exists. The maximum liquid hydrocarbon production occurs if the conversion of the triglyceride is highest and no significant cracking to gas hydrocarbons occur.

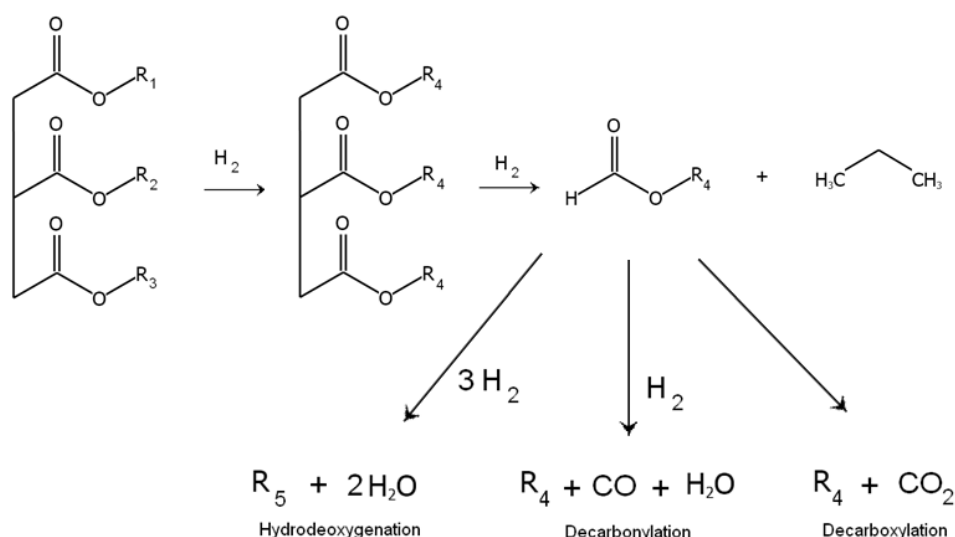


Figure 10: Deoxygenation reaction pathways of triglyceride, redrawn from [72]

With R<sub>1</sub>, R<sub>2</sub> and R<sub>3</sub> being hydrocarbons with 0, 1 or 2 double bonds and R<sub>4</sub> being hydrocarbons with only single bonds; R<sub>5</sub> being a hydrocarbon with one more carbon atom than R<sub>4</sub>.

A promising investigation of the hydrodeoxygenation reactor (or hydrotreater) for jatropha oil was performed by Gong et al. [74]. Desirable results (low degree of cracking and complete conversion) were obtained by Gong et al. [74], whilst using a NiMoP/Al<sub>2</sub>O<sub>3</sub> structure catalyst with reactor conditions of 350°C, 3 MPa in a fixed bed reactor with a liquid hourly space velocity (LHSV) of 2h<sup>-1</sup> and a H<sub>2</sub>/feed volume ratio (v/v) of 600. The study by Gong et al. [74] obtained 83.9 wt% yield of liquid hydrocarbons. The study by Gong et al. [74] is particularly useful as sufficient information is available for calculation of the hydrogen use by stoichiometric calculations. The results by Gong et al. [74] agree well with Kumar et al. [75], who also found complete conversions of jatropha oil and similar yields using similar reactor conditions.<sup>E</sup> According to Huo et al. [76], similar overall yields are achieved by UOP<sup>F</sup> (close to complete conversion of oil and 84.2 wt% yield of liquid hydrocarbons on the oil fed) in comparison to Gong et al. [74]. However, according to Klein-Marcuschamer et al. [5], UOP convert the vegetable oil in three stages with 90% conversion achieved in the first two stages, 98% achieved in the last stage with recycle of products. This reduces the likelihood of catalyst deactivation [77]. The main reactor conditions of UOP are 350°C and 32.5 bar [76].

The yields of Gong et al. [74], which are proposed for modelling in the present work, are given in Table 89 and Table 90 in Appendix B.

#### Hydrocracking and isomerization section:

A range of investigations have also been performed on the hydrocracking and isomerization reactor section. A very useful investigation was performed by Robota et al. [73], who used a similar feed to the products of Gong et al. [74], for the hydrodeoxygenation reactor section. The catalyst used by Robota et al. was a bi-functional PT/US-Y zeolite catalyst with reactor conditions of 55.16 bar, a variable temperature for the various degrees of cracking ranging between 268°C and 278°C (three alternatives), a LHSV of 1h<sup>-1</sup> and a H<sub>2</sub>/feed volume ratio (v/v) of 850. In a study by Gong et al. [78], hydrocarbons, derived from hydrodeoxygenated jatropha oil, were cracked and isomerized to smaller hydrocarbons.<sup>G</sup> However, the study by Gong et al. [78] had a lower degree of cracking (in comparison to Robota et al.) producing less amounts of hydrocarbons in the jet fuel range. In-depth characterization of the product by Gong et al. [78] was also lacking (which is required for process modelling).

---

<sup>E</sup> Reactor conditions of Kumar et al. were 360°C, 50 bar in a fixed bed reactor using a Ni-Mo structure catalyst with a H<sub>2</sub>/feed volume ratio (v/v) of 1500 and a LHSV of 1h<sup>-1</sup>.

<sup>F</sup> UOP is a company currently producing jet fuel and diesel by hydroprocessing of vegetable oil.

<sup>G</sup> Reactor conditions were a pressure of 3 MPa, temperature between 350°C and 375°C using a Pd/SAPO-11 catalyst, a LHSV of 2h<sup>-1</sup> and a H<sub>2</sub>/feed volume ratio (v/v) of 1200.

The cracking data used by Klein-Marcuschamer et al. [5] was derived from McCall et al. [79]. A comparison between the maximum jet fuel scenarios by McCall et al., Pearlson [15] and Robota et al. is performed in Table 5. Significant amounts of jet fuel were produced by all studies. Unfortunately, the studies by McCall et al. and Pearlson also lack the in-depth characterization of the products that is needed for process simulations in Aspen Plus®.

Table 5: Hydrocracking, jet fuel yield based on C<sub>5+</sub>

	McCall et al. [79]	Pearlson [15]	Robota et al. [73]
Jet Fuel Fraction of C <sub>5+</sub>	0.70	0.62	0.58

The product yields of Robota et al. [73], for the maximum jet fuel scenario at 278°C, are proposed for modelling in this study (yields are shown in Table 91 in Appendix B).

### 3.2 Ethanol to Jet Process Section

An ethanol to jet (ETH-J) conversion process section is required by the S-ETH-J, L-ETH-J and SYN-FER-J process. The overall process flow diagram of the ETH-J section is shown in Figure 11.

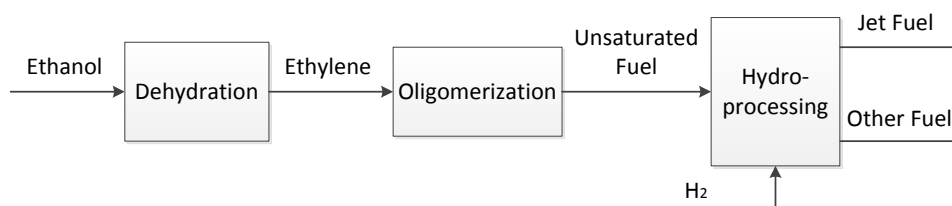


Figure 11: Overall process flow diagram of the ETH-J process section

#### 3.2.1 Studies in literature

To the best of the writer's knowledge, the only techno-economic evaluation available in literature of the conversion of ethanol to heavy hydrocarbons or jet fuel is the study by Crawford [49]. The jet fuel production process investigated by Crawford consisted of ethanol dehydration to ethylene, a two-step oligomerization with recycle of hydrocarbons by distillation, and hydrotreating of jet fuel.

#### 3.2.2 State of technology, proposed yields and process conditions

The process configuration of the ETH-J section for this study was largely based on [59] and the study by Keuchler et al. [60]. Similarly to the study by Crawford [49], this project's ETH-J section consisted of ethanol dehydration, a two-step oligomerization section with recycle of hydrocarbons, and hydrotreating of the final fuel.

Ethanol dehydration section:

An investigation of the dehydration of ethanol to ethylene was performed by Fan et al. [80]. A comparative table of promising catalysts, produced by Fan et al., is given in Table 6. The SynDol catalyst is the only commercially used catalyst [80]. The catalyst, conditions and yields by Haishi et al. [62] are proposed for this study.

Table 6: Comparison of ethanol dehydration catalysts, from [80]

Catalyst	Maximum ethylene selectivity	Ethanol conversion	Reaction temperature (°C)	LHSV <sup>a</sup> / WHSV <sup>b</sup> / GHSV <sup>c</sup>	Stability	Reference
TiO <sub>2</sub> /γ-Al <sub>2</sub> O <sub>3</sub>	99.40%	100%	360–500	26–234 h <sup>-1 a</sup>	400h, stable	[81]
0.5% La-2% P-HZSM-5	99.90%	100%	240–280	2 h <sup>-1 b</sup>	Very stable	[82]
<b>Meso-porous silica</b>	<b>99.90%</b>	<b>100%</b>	<b>350</b>	<b>400 h<sup>-1 c</sup></b>	<b>Stable</b>	[62]
Nano-CAT	99.70%	100%	240	1 h <sup>-1 b</sup>	630 h, very stable	[83]
SynDol (Halcon SD, USA)	96.80%	99%	450	26–234 h <sup>-1 a</sup>	Very stable	[81]

<sup>a</sup> LHSV - Liquid hourly space velocity; <sup>b</sup> WHSV - Weight hourly space velocity; <sup>c</sup> GHSV - Gas hourly space velocity.

Oligomerization section:

The oligomerization section converts ethylene to heavy hydrocarbons. According to Keuchler et al. [60], the conversion of ethylene to heavy hydrocarbons in one step requires significant processing, in comparison to the conversion of slightly higher olefins. A two-step conversion of ethylene is thus proposed [59]. As Keuchler et al. patented a promising process that produces higher hydrocarbons, mainly the jet fuel range, by oligomerization and recycling of a fed olefinic fraction (mainly C<sub>4</sub> and also C<sub>6</sub> and C<sub>8</sub> hydrocarbons); a sub-section first converting ethylene to the fed olefinic fraction is therefore required.

This type of sub-section was investigated by Mahdavian et al. [61]. The product obtained by Mahdavian et al. (with ethylene as feed) is very similar to the olefinic feed of Keuchler et al. The reactor conditions for Mahdavian et al. were 55°C, 22 bar in the presence of a Ti(IV)/Al/THF/EDC catalyst with molar ratios of 1:4:4:5 and in a n-heptane solvent. Comparable yields were obtained by Al-Sa'doun [84] for the conversion of ethylene (slightly higher fraction of butene produced). The reactor conditions of Al-Sa'doun were precisely the

same, except for the different catalyst,  $\text{Ti}(\text{OBU})_4\text{-AlEt}_3$ . The yields obtained by Mahdaviani et al. are proposed for this study and are shown in Table 92 in Appendix B.

It is proposed that the hydrocarbons produced by Mahdaviani et al. are oligomerized to larger hydrocarbons by the process described by Keuchler et al. The light hydrocarbons ( $\text{C}_8$ ) are recycled for further oligomerization. The range of hydrocarbons produced by this process is shown in Table 93 in Appendix B. The reactor conditions used by Keuchler et al. are a temperature of  $235^\circ\text{C}$ , a pressure of 7 MPa and a WHSV of about 3.5, whilst employing a zeolite catalyst (ZSM-5).

#### Hydrogenation section:

Hydrogenation (or hydroprocessing) of the product is required to improve the quality of the jet fuel (by saturating of the double bonds). Keuchler et al. hydrogenated the product obtained from the oligomerization reactor using a platinum/palladium containing catalyst at a pressure of 34.5 bar and a temperature of  $185^\circ\text{C}$ . This is similar to the hydrogenation which was employed by Garwood et al. [85] for hydrogenation of gasoline, using a Ni-catalyst at a pressure of 3550 kPa with temperatures ranging between  $177\text{-}191^\circ\text{C}$ . According to Keuchler et al., hydroprocessing does not significantly affect the composition of the hydrocarbons. The conditions of Keuchler et al. are proposed for this study.

### 3.3 S-ETH-J Process

The S-ETH-J process consists of two main sections: ethanol production from sugarcane and ethanol conversion to jet fuel. Only the sugarcane to ethanol section will be discussed as the ETH-J section has already been discussed in section 3.2. The term ‘**sugarcane to ethanol**’ only refers to the **1G feedstock fermentation** process. The overall process flow diagram of the S-ETH-J process is given in Figure 12.

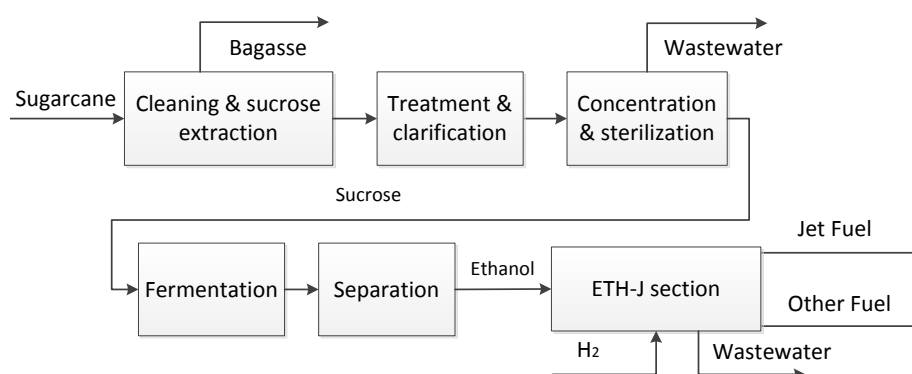


Figure 12: Overall process flow diagram of the S-ETH-J process

### 3.3.1 Studies in literature

According to Leal [86], the sugarcane to ethanol pathway is a well-established technology. Useful techno-economic assessments available in literature include studies by Dias et al. [87], [88], [89], Macrelli et al. [90] and van der Westhuizen [91]. According to van der Westhuizen, the main sub-sections of this pathway include sugarcane conversion to juice, juice treatment and clarification, juice concentration and sterilisation, sugar syrup fermentation, ethanol recovery and cogeneration of heat and power [91].

Various scenarios were investigated by the above mentioned literature and they can be broadly divided into processes with only 1G fed fermentation with heat integration using the by-product bagasse and additional 2G feed [88], [91] and processes with thermal integration of facilities with separate 1G and 2G fed fermentation [87], [89], [90], [91]. All the assessments were based on process simulation. Cane cleaning and sucrose extraction was performed by mills for all the studies except by van der Westhuizen, who used a diffuser. The sucrose concentration was achieved by all the studies using a multi-effect evaporator. For all the above literature, the 1G fermentation was performed using the Melle-Boinot process – fed-batch fermentation with recycling of yeast. The above studies used a variety of ethanol recovery processes including conventional distillation, double effect distillation, azeotropic distillation, extractive distillation and molecular sieves. Four of the mentioned studies above performed an economic analysis with Dias et al. [88], Macrelli et al. and van der Westhuizen performing minimum fuel selling price (MFSP) calculations, while Dias et al. [89] performed an economic analysis using discounted cash flow rate of return (DCFROR) as a criterion.

### 3.3.2 State of technology, proposed yields and process conditions

As van der Westhuizen [91] was in the writer's research group and the mass and energy balance simulation performed by van der Westhuizen is available for updating, the yields and conditions of van der Westhuizen are proposed for this study. As van der Westhuizen derived yields from the other five studies, the simulation performed by van der Westhuizen should provide a good indication of the SOT of the sugarcane to ethanol process. Only the main conversion section (the sugar syrup fermentation section) will be discussed.

#### Sugar syrup fermentation section:

The concentrated and sterilized sugar syrup consisting of mainly sucrose is hydrolysed by the yeast to produce hexose sugar [91]. The maximum yield of ethanol per gram of hexose sugar is 0.511 [91]. Van der Westhuizen used yields by Leal [86], who determined that the current fermentation time for the Melle-Boinot process (using yeast such as *S. cerevisiae*) is

approximately 8 hours with a fermentation yield of about 91% and a final ethanol concentration of 13% (w/v). This compares well with the other four studies, with their assumed fermentation yield of the 1G fed processes ranging from 90% to 94%.

### 3.4 L-ETH-J Process

The L-ETH-J process consists of two main sections: ethanol production from lignocellulose and ethanol conversion to jet fuel. Only the lignocellulose to ethanol section will be discussed as the ETH-J section has already been discussed in section 3.2. The overall process flow diagram of the L-ETH-J process is given in Figure 13.

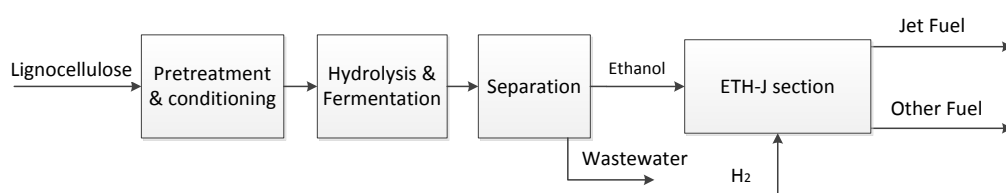


Figure 13: Overall process flow diagram of the L-ETH-J process

#### 3.4.1 Studies in literature

A variety of studies have been performed on the biochemical conversion of lignocellulose to ethanol. Thorough techno-economic studies include NREL (National Renewable Energy Laboratory) reports by Kazi et al. [58] and Humbird et al. [32] and investigations which were performed in the writer's research group, Leibbrandt [92] and Petersen [93]. According to Petersen, the typical lignocellulose to ethanol process consists of pretreatment, hydrolysis, fermentation, ethanol recovery and cogeneration of steam and electricity [93].

The lignocellulose feeds of the NREL reports were corn stover, whereas the feeds of the other two studies were sugarcane bagasse. Along with the ethanol product, all of the above studies included cogeneration of the residual solids to produce steam and electricity. Many types of pretreatment are available with steam explosion established by Kazi et al. (who investigated a variety of scenarios) to be the most promising. Subsequently, all of the studies consisted of steam explosion with Humbird et al. and Leibbrandt investigating  $\text{H}_2\text{SO}_4$  catalysed steam explosion, and Petersen investigating  $\text{SO}_2$  impregnated steam explosion. All of the studies investigated fermentation processes with separate hydrolysis and co-fermentation (SHCF). Alternative fermentation scenarios, separate hydrolysis and separate fermentation (SHSF) and simultaneous saccharification and co-fermentation (SSCF), were also investigated by Kazi et al. and Petersen respectively. The NREL reports utilized the microorganism *Z. mobilis*, whereas the other two studies employed *S. cerevisiae*. Ethanol recovery was performed by conventional distillation for all the studies. All the studies

investigated the economics of the process based on process simulation of the processes on Aspen Plus<sup>®</sup>. The process economics were investigated by the NREL reports and Leibbrandt by the calculation of MFSP, whilst Leibbrandt and Petersen both determined economic criterion, such as NPV and DCFROR.

### 3.4.2 State of technology, proposed yields and process conditions

As Petersen [93] is the last investigation which was performed in the writer's research group (adapted from Leibbrandt [92]) and the simulation performed by Petersen is available for updating, the yields and conditions of Petersen are proposed for this study. Although Petersen determined that the SHCF and SSCF processes have similar economic prospective, as the latest NREL report (Humbird et al. [32]) also investigated SHCF, the SHCF scenario is proposed for this study. The overall energy efficiency of 39% of the SHCF process by Petersen compares fairly well to the energy efficiency of 45% and 42% of the SHCF process by Humbird et al. and Leibbrandt respectively. Only the main conversion sections (the pretreatment section and hydrolysis and fermentation section) will be discussed.

#### Pretreatment section and hydrolysis and fermentation section:

Petersen [93] established from literature that SO<sub>2</sub> impregnated steam explosion is a promising pretreatment method [94], [95]. Sendelius [94] determined that the xylose yields from xylan were higher in the case of SO<sub>2</sub> impregnation in comparison to H<sub>2</sub>SO<sub>4</sub> catalysed steam explosion. It was also determined that the enzymatic hydrolysis of glucan to glucose on pulps treated with SO<sub>2</sub> could reach up to 87% [95] in comparison to the 83% determined by Leibbrandt [92] for H<sub>2</sub>SO<sub>4</sub> catalysed steam explosion. Petersen performed the SO<sub>2</sub> impregnated steam explosion at similar conditions to Sendelius [94], with a maximum temperature of 205°C. Petersen based the SHCF on work by Martin et al. [96] who found that a promising co-fermenting strain of *S. cerevisiae* had conversions of xylose to ethanol of 44% and glucose to ethanol of 88%.

## 3.5 FP-J Process

The process consisting of fast pyrolysis of lignocellulosic biomass followed with upgrading to fuel can be broadly divided into two process scenarios; consisting of catalytic or thermal fast pyrolysis sections. The process consisting of thermal fast pyrolysis will be investigated as a previous investigation in the writer's research group has been performed on this process scenario [97]. The term "**FP-J process**" will therefore refer to the **thermal fast pyrolysis** process with catalytic upgrading of the bio-oil to jet fuel (overall process flow diagram shown in Figure 14).

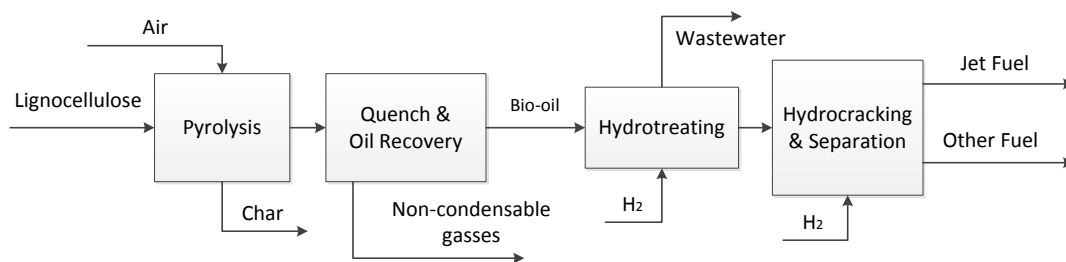


Figure 14: Overall process flow diagram of the FP-J process

### 3.5.1 Studies in literature

The thermal fast pyrolysis process followed by upgrading to fuels has been investigated in a variety of techno-economic studies including Gebreslassie et al. [52], Wright et al. [54], Brown et al. [51], Jones et al. [55] and Jones et al. [98]. The study by Brown et al. is an update of the work by Wright, whilst the study by Jones et al. [98] is also an update of the study by Jones et al. [55]. A FP-J process simulation has been performed in our research group by McLaren [97]. This simulation used the fast pyrolysis simulation performed by Leibbrandt [92], modifying it with a catalytic upgrading section. The study by McLaren aimed for jet fuel aromatics, but it did not achieve close to the potential maximum jet fuel yield. To the best of the writer's knowledge, there is no techno-economic study on the FP-J process available in literature.

The biomass feeds of the studies include poplar wood [55], [52], woody feedstocks [98], corn stover [54], [51] and pine wood [97]. The hydrogen source for upgrading of bio-oil, is an important consideration as the entire hydrogen feed generally cannot be obtained by reforming of off-gasses [55], [52]. Wright et al. investigated two process scenarios: hydrogen purchase and hydrogen production from bio-oil. According to Wright et al., the economics of the hydrogen purchase scenario far outweigh the latter scenario which has significantly lower fuel yields due to use of the bio-oil.<sup>H</sup> The study by Brown et al. subsequently only investigated hydrogen purchase. Co-reforming of natural gas and off-gas from the process were investigated by the other literature [55], [52], [98], [97]. The study by McLaren produced light gasses, petrol, jet fuel, diesel and gas oil, whilst all the other studies only produced petrol and diesel [55], [52], [98], [54], [51], [97].

The simulation of mass and energy balances were performed by various software including CHEMCAD by Jones et al. [55], Jones et al. [98] and Brown et al., Aspen Plus<sup>®</sup> by Wright et al., Jones et al. [98] and McLaren and an algebraic modelling system (GAMS) by Gebreslassie et al. Economic assessments were performed by all the studies except by

<sup>H</sup> However, the use of fossil-derived hydrogen negatively impacts the GHG emission associated with the feed.

McLaren. MFSP were investigated by Jones et al. [55], Jones et al. [98], Brown et al. and by Wright et al., whilst Gebreslassie et al. determined the economic criterion NPV.

### 3.5.2 State of technology, proposed yields and process conditions

The FP-J process consists of two main sections: fast pyrolysis of biomass to bio-oil and upgrading of the bio-oil to fuel, including jet fuel. As the study by McLaren [97] has not been published, the main references of McLaren will be used for proposing of yields and conditions. As the Aspen Plus<sup>®</sup> simulation by McLaren is not available for updating<sup>1</sup>, an assessment using McLaren's results from Aspen Plus<sup>®</sup> will be performed.

#### Fast pyrolysis of biomass:

The conditions of the fast pyrolysis process of the study by McLaren were based on Piskorz et al. [99] and Leibbrandt [92], and are 500°C at atmospheric pressure. An in-depth characterization of bio-oil was performed by McLaren. Yields from literature, which was used for calculation of the pyrolysis reactor yields by McLaren, are shown in Table 94 in Appendix B. The overall reactor yields of McLaren are compared to Jones et al. [55] in Table 94 in Appendix B. The main hydrocarbons in the pyrolysis oil obtained by both McLaren and Jones et al. [55] range from C<sub>2</sub> to C<sub>18</sub>, although the study by McLaren obtained a small fraction (2%) of larger hydrocarbons (C<sub>18+</sub>).

#### Bio-oil upgrading:

The upgrading of the bio-oil consists of two reactors; a hydrotreater and a hydrocracker. These reactors were investigated by Elliot et al. [100] and Christensen et al. [101] (the main upgrading references of the study by McLaren). The reactor conditions, reactor hydrogen consumption and total phase yields derived from these references are given in Table 95 and Table 96, both in Appendix B. The reactor conditions of the study by McLaren are compared to Jones et al. [55] in Table 95 and Table 96; showing good agreement between the studies. The overall phase yields and hydrocarbon distillate yields obtained from Elliot et al. and Christensen et al., which were employed by McLaren to converge the complex mass and molar balance for the upgrading section, is given in Table 97 and Table 98 in Appendix B.

## 3.6 GFT-J Process

According to Petersen et al. [102], the main sections of a typical GFT process include gasification of biomass, clean-up of syngas, FT synthesis, upgrading and separation as well as cogeneration of steam and electricity (overall process flow diagram shown in Figure 15).

---

<sup>1</sup> The Aspen Plus<sup>®</sup> simulation of McLaren was initially believed to be available for updating; this was not the case.

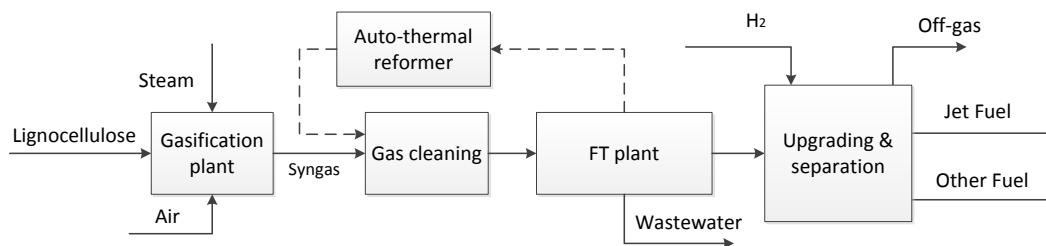


Figure 15: Overall process flow diagram of the GFT-J process

### 3.6.1 Studies in literature

Significant investigation and simulation have been performed on the GFT and GFT-J processes with thorough techno-economic studies including Trippe et al. [103], Kreutz et al. [104], Ekbom et al. [48], Swanson et al. [69], Leibbrandt [92] and Petersen et al. [102]. Petersen et al. is the last investigation and simulation which was performed in the writer's research group.

Of these techno-economic studies, all the processes produce petrol, diesel and electricity, except for Petersen et al. and Ekbom et al. Petersen et al. produced gasses, naphtha, diesel, hydrowax and electricity, whilst Ekbom et al. produced naphtha, diesel, hydrowax, district heat and jet fuel (aimed at specifically jet fuel). The feed investigated by Trippe et al. (whom only investigated the FT synthesis, product recovery and upgrading sections) was clean syngas. Lignocellulose was used as the feed for the remaining studies and included mixed prairie grass [104], corn stover [69], wood chips [48], and sugarcane bagasse [92], [102].

All the studies accompanied their assessment with simulations on Aspen Plus<sup>®</sup> except for the assessment of Ekbom et al.<sup>J</sup> All the assessments investigated the low-temperature FT (LTFT) synthesis, ranging between 493K and 523K [103]. According to de Klerk [105] and Ekbom et al., the LTFT is the most appropriate FT synthesis scenario for jet fuel production as the products from a LTFT scenario contain higher amount of kerosene and less refining is required for upgrading of the FT product. Economics were investigated by all the studies with the outputs being either MFSP [92], [103], [104], [69], [48] or economic criterion such as NPV or IRR (internal rate of return) [102], [92].

According to Petersen and Kreutz et al., the heat integration of the GFT process is particularly important for the economic viability of the process. Varying degrees of heat integration were performed by all the studies.

<sup>J</sup> It is unclear from the assessment of Ekbom et al. whether process simulation was the basis for the mass and energy balance.

### 3.6.2 State of technology, proposed yields and process conditions

The last investigation of the GFT process in the writers' research group by Petersen et al. [102] used the refining section by Ekbom et al. [48] to determine the mass and energy balance surrounding the refining section. Consequently, the proposed yields and conditions for this study will be derived from the studies by Petersen et al. and Ekbom et al.

#### Gasification section:

The gasification section of Petersen et al. consisted of a dual-fluidized bed (DFB) configuration. Petersen et al. predicted the composition of the syngas through thermodynamic calculations, by minimization of the Gibbs Free Energy [106]. Thermodynamic equilibrium calculations have been found to be accurate at gasification temperatures between 800-1000°C in the presence of a gasification catalyst (such as dolomite or nickel-based) [92], [102]. For tar-free syngas, the gasifier temperature is required to be above 900°C [107], [102]. The optimized variables for the DFB gasifier given in Table 7 were determined by Petersen et al. (based on efficiencies and economics) and are proposed for this study.

Table 7: GFT-J process DFB gasifier optimized variables, [102]

Steam to biomass <sup>1</sup>	Moisture content (%) <sup>2</sup>	Biomass split (%) <sup>3</sup>
1	5	42

<sup>1</sup> Ratio of steam to biomass going to the gasification section of the DFB gasifier; <sup>2</sup> Moisture content of biomass to the gasification section of the DFB gasifier; <sup>3</sup> Fraction of biomass split to the combustor section of the DFB gasifier.

#### Syngas cleaning section:

The syngas cleaning performed by Petersen et al. first removed ash and particulates by a cyclone. As the syngas produced by Petersen et al. was assumed to be tar-free due to the use of a gasification catalyst and high temperatures, no additional tar-crackers were deemed necessary [107]. As CO<sub>2</sub> build-up occurs due to recycling of unconverted syngas from the FT reactor and CO<sub>2</sub> is undesired in the syngas (due to reduction of conversion efficiency in the FT reactor), CO<sub>2</sub> removal is necessary [92]. Kreutz et al. [104] proposed a Rectisol unit for acid gas removal. The Rectisol unit employed by Petersen et al. is based on a study by Sun et al. [108]. The Rectisol unit performance (which is proposed for this study) is given in Table 8.

Table 8: Rectisol unit performance, [108]

Acid gas removal	(%)
CO <sub>2</sub>	95
H <sub>2</sub> S	100

FT synthesis section:

As FT refining aimed at jet fuel production was only investigated by Ekbom et al., the study by Ekbom et al. will be followed for proposing of yields and conditions. Ekbom et al. assumed that the FT reactor change growth reactions can be described by the Anderson-Schultz-Flory model. The equation of the Anderson-Schultz-Flory model is shown below.

$$M_n = \alpha^{n-1} \times (1 - \alpha) \quad \text{Equation 3}$$

With     $n$         - Carbon number of hydrocarbon  
            $M_n$       - Mole fraction of produced hydrocarbon  
            $\alpha$         - Chain growth probability

The chain growth probability,  $\alpha$ , is a function of catalyst and the FT process conditions [103]. The specific value for the chain growth probability was assumed to be 0.9 by Ekbom et al. Chain growth probability was determined in the study by Swanson et al. [69] using an equation developed by Song et al. [109] based on a specific cobalt catalyst. The catalyst, along with Equation 4, is proposed for the calculation of the value for  $\alpha$ . For significant jet fuel production, the value for  $\alpha$  needs to be at least 0.85 [69], [48].

$$\alpha = \left[ 0.2332 \times \frac{P_{CO}}{P_{CO} + P_{H_2}} + 0.6330 \right] \times [1 - 0.0039 \times (T(K) - 533)] \quad \text{Equation 4}$$

With     $P_{CO}$       - Partial pressure of carbon monoxide in the fed syngas  
            $P_{H_2}$       - Partial pressure of hydrogen in the fed syngas  
            $T(K)$      - Temperature of FT synthesis reactor in Kelvin

The reactor design of Swanson et al. of a fixed-bed reactor is proposed for this study (this enabled the use of Swanson et al.'s method for simulation of a fixed-bed FT reactor). A one-pass conversion of 40% was set by Swanson et al. and Petersen et al. for a fixed-bed reactor.

FT-liquid upgrading section:

Varying degrees of FT product refining for maximization of the jet fuel fraction is possible. A promising configuration based on Ekbom et al. is proposed for this study (shown in Figure 16). The hydrocracking data used by Ekbom et al. are given in Figure 54 in Appendix B. As the configuration by Ekbom et al. recycles the waxes from the distillation section, the feed to the hydrocracker constitutes of FT reactor products without the light components ( $C_1 - C_4$ ) with significant amount of waxes. A thorough investigation of the hydrocracking of FT wax was performed by Regalli [110]. It is proposed that by investigation of the study by Regalli

and yields of Ekbohm et al., empirical yields which are a function of the feed to the hydrocracker can be determined.

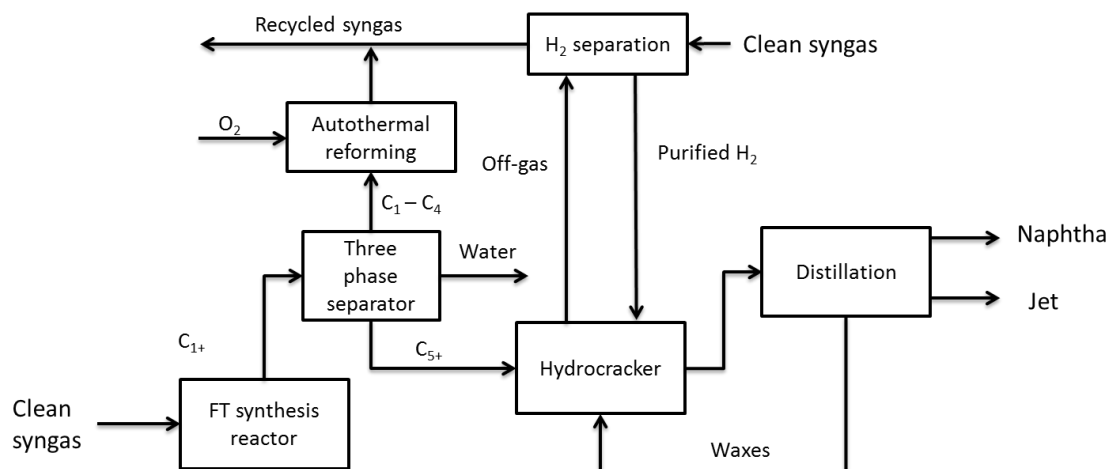


Figure 16: FT-synthesis and refinery configuration for maximum jet fuel production, based on [48].

#### Auto-thermal reforming section:

According to Petersen et al., an auto-thermal reformer (ATR) is essential due to the low per pass conversion in the FT reactor (40% per pass conversion). Equilibrium modelling of the ATR was performed by Petersen et al. based on the study by Leibbrandt. The conditions employed by Petersen et al. for the ATR (which are proposed for this study) is 33 bar [104], a 1:1 molar ratio between the steam and the hydrocarbons [111], whilst oxygen is fed to maintain a temperature of 1000°C [92].

### 3.7 SYN-FER-J Process

The SYN-FER-J process consists of two main sections: ethanol production by biomass gasification and syngas fermentation, and ethanol conversion to jet fuel. The overall process flow diagram of the SYN-FER-J process is given in Figure 17. Only the gasification and fermentation section will be discussed as the ETH-J section has already been discussed in section 3.2.

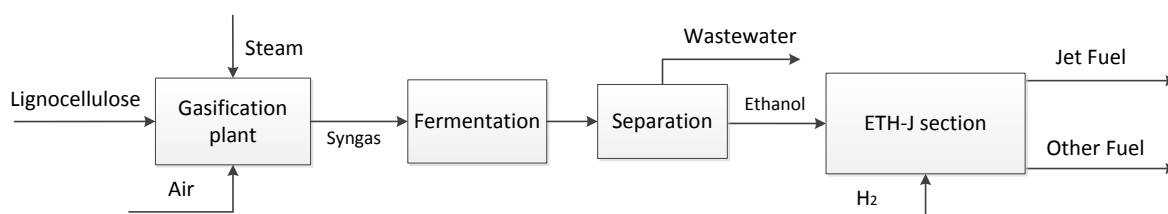


Figure 17: Overall process flow diagram of the SYN-FER-J process

### 3.7.1 Studies in literature

A variety of studies have been performed on the SYN-FER process (conversion of lignocellulose to ethanol via gasification and syngas fermentation) with noteworthy techno-economic studies including Putsche [112], Piccolo et al. [6], Martin et al. [113] and van Kasteren et al. [114].

Various feedstocks were used by the studies, including wood chips [114], [6], [112] and switchgrass [113]. Although all of the studies aimed for ethanol, only one study recovered acetic acid [114]. Electricity was only produced by Piccolo et al. and Putsche, whilst the other processes are in need of external electricity supply. The net electricity production is closely linked to the achieved conversion, with Piccolo et al. and Putsche, who achieved the lowest net conversion of about 204-282 and 270 litres ethanol per ton dry biomass, producing electricity, whilst Martin et al. and van Kasteren et al., who achieved the highest conversion of about 330-415 and 350 litre ethanol per ton dry biomass, not producing electricity. These yields are similar to the conversions achieved by gas fermentation companies Ineos Bio and Coskata of about 380 litre ethanol per ton dry biomass [37].

Mass and energy balance simulations were performed by all the studies using Aspen Plus<sup>®</sup>, except for Martin et al. who used GAMS. An economic analysis was performed by all the studies using MFSP calculations. Economic criterion, such as NPV and DCFROR, were also determined by Piccolo et al. A description of the types of equipment used by the studies is given in Table 9.

Table 9: Equipment used by the studies investigating the SYN-FER process

	van Kasteren et al. [114]	Piccolo et al. [6]	Martin et al. [113]	Putsche [112]
<b>Gasification</b>	Circulating fluidized-bed	Circulating fluidized-bed	Indirect & direct gasifiers	BCL/FERCO gasifier (indirect)
<b>Fermentation</b>	Bubble loop/ trickle bed reactor	One-stage continuous stirred tank reactor (CSTR)	One-stage CSTR	- <sup>3</sup>
<b>Cleaning</b>	Olga process (advanced scrubbing)	Crude purification <sup>1</sup>	Steam reforming/partial oxidation; ceramic filter/scrubber; PSA <sup>2</sup>	- <sup>3</sup>

<sup>1</sup> No specification of cleaning process by literature; <sup>2</sup> Pressure-swing adsorption; <sup>3</sup> Equipment used for the fermentation and cleaning sections are not known.

### 3.7.2 State of technology, proposed yields and process conditions

As no SYN-FER process investigation has been performed in our research group, a new Aspen Plus® model will be developed for the SYN-FER process; the literature will therefore be used to guide the proposing of yields and conditions for the sections. The gasification, gas-cleaning and fermentation sections will be discussed for the SYN-FER process.

#### Gasification section:

According to reviews on the SYN-FER process by Daniell et al. [37] and Mohammadi et al. [115], a fluidized bed gasifier is the preferred technology for biomass gasification intended for gas fermentation (especially for large scale gas production). The investigation by Petersen et al. [102], whose gasification section model is available for updating, consisted of a DFB gasifier. The investigation by Petersen et al. is subsequently proposed for this study (refer to the *Gasification section* in section 3.6.2). The conditions of the DFB gasifier will be chosen to match the feed syngas composition of the proposed fermentation step literature.

#### Gas cleaning section:

The required cleaning step of the syngas associated with the SYN-FER process is less extreme in comparison to processes which catalytically convert the syngas [37]. The syngas cleaning performed by Petersen et al. first removed ash and particulates by a cyclone. As the study by Petersen et al. employed a gasifier with a gasification catalyst at high temperatures, it was assumed to be tar-free [107]. No additional cleaning equipment or tar-crackers were therefore deemed necessary.

#### Fermentation section:

The most important consideration for a bioreactor is the mass transfer coefficient [37]. According to Daniell et al., there is significant uncertainty of the best bioreactor design with designs which are being investigated by gas fermentation companies including gas lift, bubble column, immobilised cell, trickle-bed and microbubble reactors.

The three most important parameters of the fermentation step data is final ethanol concentration, overall yields and ethanol productivity. In general there is a play-off between these three parameters [116]. Firstly, higher final ethanol concentration can significantly reduce the energy input necessary for the recovery of the ethanol. This is illustrated in Figure 18 for a conventional distillation column where separation energy required doubles from 40 g/l to 20 g/l and immense increase of separation energy occurs below a concentration of 20 g/l.

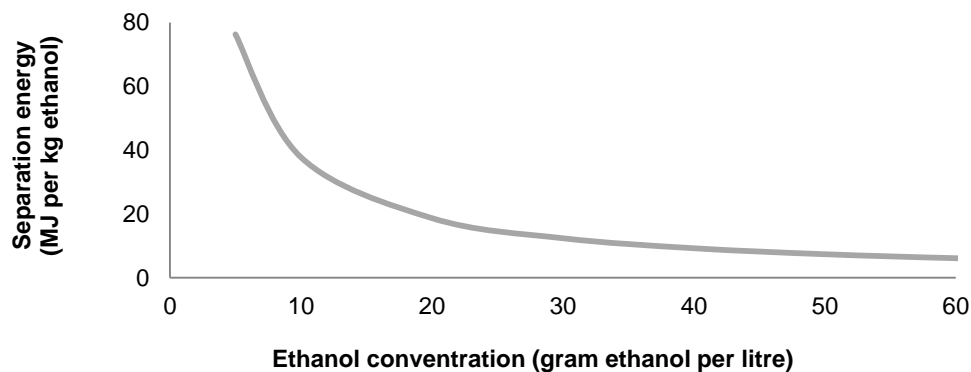


Figure 18: Separation energy versus ethanol concentration, redrawn from [117].

High ethanol yields are essential as Piccolo et al. determined that the feedstock cost is the main production cost of the SYN-FER process [6]. Lower ethanol productivities usually translate into increased number of fermenters, resulting in higher capital costs to ensure the same output. Although high overall yields can be achieved by the syngas fermentation, challenges are associated with the final ethanol concentration and ethanol productivity for this process [37].

As all three these parameters are important and inter-dependent, literature that does not provide the information for all three these parameters is of little use. Although reviews of the syngas fermentation process have been performed in literature [37], [118], [115], the comparisons of fermentative literature were not focused specifically on ethanol production or the comparisons were not thorough. In Table 99 in Appendix B, a comparison of promising syngas fermentation experimental literature is performed.

The studies in Table 99 consisted of a variety of syngas compositions. All the experiments in Table 99 performed the fermentation using the promising *C. ljungdahlii* strain. Generally, the experiments were performed using a CSTR, with cell recycling being employed by some of the studies. The patent by Gaddy et al. [116] from Ineos Bio, described a range of fermentation experiments performed with various syngas feeds. These set of experiments are very comprehensive with experiment 1 to 3 in Table 99 consisting of 16, 18 and 14 experimental runs using different conditions. In general, productivities around 15-40 g ethanol/l.day were achieved by the studies. Significantly higher productivities were achieved by experiment 4 and 5 in Table 99 by performing the reactions under high pressure with high concentrations of hydrogen in the syngas feed. For all the studies the conversion efficiencies of the carbon monoxide were always more than the hydrogen with the carbon monoxide conversions ranging between 80-96%, whilst the hydrogen conversions ranged between 14-81%. Although the maximum ethanol concentration achieved was 48 g/l, this was achieved

under transient conditions. The highest steady-state ethanol concentration of 33 g/l was achieved by experiment 1, but at these conditions the conversions and productivities were significantly compromised. As the maximum concentration of acetate achieved by the studies is 5 g/l, recovery of the acetate is not economically feasible [119].

The promising experimental runs by Gaddy et al. (specifically experiment number 3 and 5 in Table 99) are proposed for the fermentation section.

## 4 Approach and Design Basis

This section will describe the approach and methods that were taken to perform the techno-economic analysis. This includes comprehensive discussions on the simulation methodology in Aspen Plus<sup>®</sup> (section 4.4), the methods used for sizing and cost estimation (section 4.5) and the economic analysis approach and methodology (section 4.6).

### 4.1 Approach

The approach which will be followed to perform the techno-economic analysis is shown in Figure 19. Firstly, a literature search will be done on possible process configurations and published experimental data on process yields and conditions. Process flow diagrams will be constructed followed by mass and energy balances using Aspen Plus<sup>®</sup> (including updating of Aspen models previously simulated in research group). Pinch-analysis and heat integration, aided by Aspen Energy Analyzer, will be performed for the processes. Process properties can then be determined from the mass and energy balances. Capital and operating cost estimation will be performed based on capital and operating costs obtained from the literature. Lastly, a sensitivity analysis on the economic inputs will be performed.

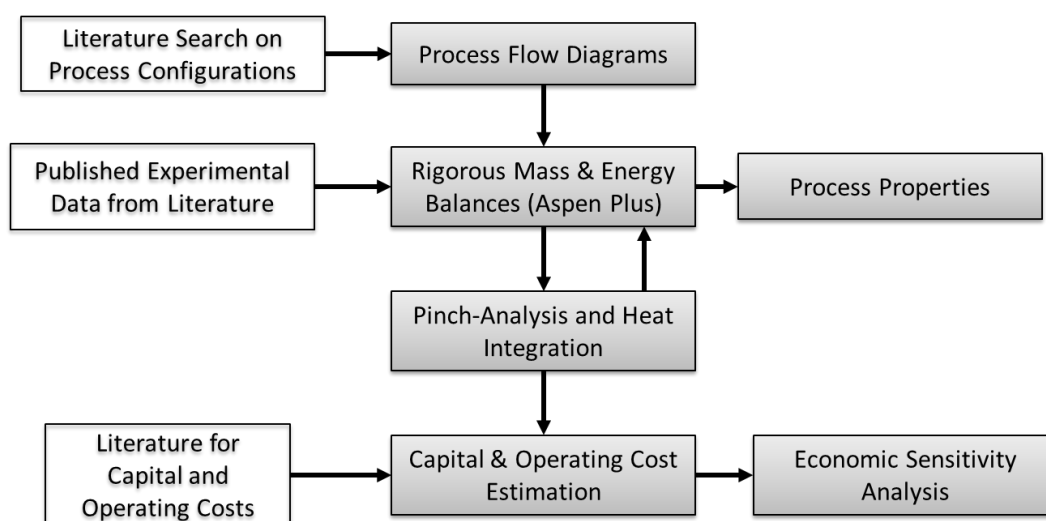


Figure 19: Approach to the techno-economic analysis

As discussed in section 3, a variety of possible scenarios are available for each process. This study will aim at producing a single scenario for each process pathway which is **feasible**, **promising** and **representative** of the process pathway.<sup>K</sup>

<sup>K</sup> The only exception is the SYN-FER-J process for which three scenarios were constructed based on different fermentation data as the interplay between fermentation output parameters on the process promise was unclear.

The scenarios will be constructed such that the processes are **electrical power** and **hydrogen self-sufficient**; independent of fossil sources. Thus all the steam, electricity and hydrogen required by the processes will be obtained from the biomass feedstock itself. Dutta et al. [120], made a similar assumption. The reasoning by Dutta et al. was:

“Though economics may improve by purchasing electricity and natural gas for plant operations, the long-term sustainability of the processes will suffer. The consistent assumption allows for easy comparison (a level playing field) among the various technology platforms without adjustments.”

The only exception for this assumption is the FP-J process, which uses natural gas for the hydrogen production section.<sup>L</sup>

## 4.2 Feedstock, Jet Fuel Product and Plant Size

### 4.2.1 Lignocellulose

The feed-rate of dry, ash-free lignocellulose was fixed to 75 MT/h. This is a similar size to the 83.3 MT dry lignocellulose per hour generally investigated by NREL reports [32], [69], [98]. As discussed in section 1.1.3, the composition of lignocellulose can vary significantly between various types of lignocellulose. A generic lignocellulose composition was chosen based on previous simulations performed in the writer's research group [93], [97]. These compositions were chosen to represent a wide variety of lignocellulose in terms of composition (cellulose, hemicellulose and lignin) and heating value (with a higher heating value of ~18.6 MJ/kg). The fed lignocellulose has a moisture content (MC) of 50% and an ash fraction of 3.70% (based on dry weight).

The biomass compositions for the processes were either specified using proximate analysis and ultimate analysis (SYN-FER-J and GFT-J processes) or using the chemical composition (FP-J and L-ETH-J processes). The composition of the ultimate analysis of the feed was chosen to compare well with the chemical composition in terms of energy content and chemical atoms (hydrogen, carbon, oxygen and ash content). The assumed proximate analysis, ultimate analysis and chemical composition of the lignocellulose are given in Table 10, Table 11 and Table 12. As the study by McLaren [97] was not available for updating, the composition of the biomass fed to the FP-J process was not altered (see Table 12).

---

<sup>L</sup> The FP-J process simulation by McLaren was not available for updating.

Table 10: Proximate analysis of the dry lignocellulose. Based on [102].

Proximate analysis	Content (Mass%)
MOISTURE	0.00
FIXED CARBON	23.03
VOLATILE MATTER	73.27
ASH	3.70

Table 11: Ultimate analysis of the dry lignocellulose. Based on [102].

Ultimate analysis	Content (Mass%)
ASH	3.70
CARBON	47.44
HYDROGEN	5.72
NITROGEN	0.00
CHLORINE	0.00
SULFUR	0.00
OXYGEN	43.13

Table 12: Chemical composition of the dry lignocellulose.

Information from [93] and [97].

Component	This project Content (Mass%)	FP-J process Content (Mass%)
EXTRACT	7.50	9.86
ASH	3.70	0.99
CELLULOSE	40.60	41.24
LIGNIN	25.50	27.22
XYLAN	20.00	9.00
ARABINAN	1.70	0.86
MANNAN	0.20	10.83
GALACTAN	0.80	0

#### 4.2.2 Sugarcane

The S-ETH-J process assessment has sugarcane and trash as its feed. Sugarcane constitutes of mainly sucrose and bagasse (lignocellulose) with a few other minor components [91]. Sugarcane trash refers to the parts of the sugarcane that do not form part of the sucrose containing stalks, such as tops and the leaves of the sugarcane [91]. Although the constituents of sugarcane have high variability, the composition in Table 13 was assumed. The feed-rate of wet sugarcane was fixed to 222.5 MT/h so that the amount of jet fuel produced in the S-ETH-J process is similar to the lignocellulose to jet fuel processes. 140 dry kg of trash was assumed to be fed along with each metric ton of wet cane [87], [91]. The composition of wet trash is given in Table 14.

Table 13: Constituents of wet sugarcane. Information from [87].

Component	Content (Mass%)
SUCROSE	13.30
CELLULOSE	4.77
XYLAN	4.53
LIGNIN	2.62
REDUCING SUGARS	0.62
MINERALS	0.20
IMPURITIES	1.79
WATER	71.57
DIRT	0.60

Table 14: Constituents of wet trash. Information from [91].

Component	Content (Mass%)
WATER	15.00
XYLAN	32.30
LIGNIN	18.68
CELLULOSE	34.01

### 4.2.3 Vegetable oil

Vegetable oil is used in the HEFA process assessment. Vegetable oil consists of three long carbon chains connected with an acid group to a glycerine backbone [15]. The compositions of a few vegetable oils are shown in Table 15.

Table 15: The chain length composition of various vegetable oil, (wt%), [15], [74].

Carbon chain length	Soybean	Palm	Pongamia	Canola	Jatropha
<b>16</b>	11	44	5.4	4	15.6
<b>18</b>	87.6	56	74.8	62	84.2
<b>20</b>	1.4	-	13.3	34	0.2
<b>20+</b>	-	-	6.5	-	-

The vegetable oil composition in the project assessment is taken to be similar to jatropha oil. The assumed composition of the vegetable oil is shown in Table 16.

Table 16: Composition of vegetable oil to HEFA process. Information from [74].

Fatty acid	Structure	Molar%
PALMITIC ACID	C16:0	17.17
LINOLEIC ACID	C18:2	33.42
OLEIC ACID	C18:1	42.05
STEARIC ACID	C18:0	7.15
GADOLEIC ACID	C20:1	0.23

The feed-rate of vegetable oil was fixed to 14.9 MT/h so that the amount of jet fuel produced is similar to the lignocellulose to jet fuel processes. As the composition for jatropha oil is similar to soybean oil and pongamia oil, the assessment of jatropha oil should still be comparable to assessments performed by Pearlson [15] and Klein-Marcuschamer et al. [5]. Since all of the triglycerides were not available in Aspen Plus<sup>®</sup> databanks, the oil was modelled using TRIOLEIN with slightly adjusted molecular formulae (shown in Table 17). This was done to ensure an atom balance in the oil conversion reactor (further discussed in section 4.4.7.2).

Table 17: Adjusted molecular formulae for oil feed

TRIOLEIN	Carbon	Hydrogen	Oxygen
Actual	57	104	6
Adjusted	60.2	102.6	6.6

#### 4.2.4 Jet fuel product

##### 4.2.4.1 Jet fuel properties

It is essential that the jet fuel product meets the strict jet fuel property specifications (illustrated in Table 1 in section 1.1.1) to be suitable for current aviation aircrafts. The properties of the jet fuel are influenced by its carbon distribution and types of hydrocarbons.

According to Robota et al. [73], the jet fuel product should consist of mainly C<sub>9</sub> - C<sub>15</sub> hydrocarbons with only minor contributions from C<sub>8</sub> and C<sub>16+</sub> hydrocarbons. This was therefore used as a specification for the simulation of the hydrocarbon distillation columns (further discussed in section 4.4.4.3).

When producing jet fuel from alcohols (S-ETH-J, L-ETH-J and SYN-FER-J processes), hydrogenation of the product was required to ensure the quality of the jet fuel by saturating of the double bonds [60], [4]. Hydroprocessing of products from the HEFA, FP-J and GFT-J processes by hydrotreating or hydrocracking reactors was also required to improve the properties of the jet fuel [5], [98], [48]. The methods used to simulate the hydroprocessing units are discussed in sections 4.4.6.3, 4.4.7.2 and 4.4.7.4.

The FP-J process is the only investigated process that produces jet fuel containing significant amounts of aromatics [8]. Based on the current ASTM specifications, blending with petroleum derived jet fuel will therefore be required for the jet fuel without aromatics derived from the other investigated processes [9]. As shown in Table 2 in section 1.1.1, a variety of other processes, which have the ability to produce jet fuel containing significant amounts of aromatics, are currently in the approval process.

Further investigation of the jet fuel products is required to ensure the jet fuel products meet the different property specifications.

#### 4.2.4.2 Jet fuel product flowrate

For the chosen feed-rates for feedstock (given in section 4.2.1, 4.2.2 and 4.2.3), the investigated processes achieved jet fuel product flowrates of up to 8 000 kg/h (~0.22 million litre jet fuel per day), see section 5.

In an international context, the world consumption of jet fuel is over 800 million litres per day [2]. A variety of targets have been set for the replacing of fossil jet fuels. Boeing targeted replacing of 1% of the global jet fuel demand with biojet fuels by 2015 [121], whilst IATA aimed at replacing up to 6% of the global jet fuel demand by 2020 [122].

For the processes investigated, ~37 process plants would be required to replace 1% of the global jet fuel demand, whilst ~222 process plants would be required to replace 6% of the global jet fuel demand (for processes with jet fuel product rate of 8 000 kg/h, based on current global jet fuel demand). Further, to achieve the 6% replacement of the global jet fuel demand either requires ~17 500 MT/h of dry lignocellulose, ~14 500 MT/h of dry sugarcane or ~3 700 MT/h of vegetable oil.

### 4.3 Process Descriptions

Process descriptions of the six investigated processes, accompanied by simplified block flow diagrams, are given in this section. As the simulation of the processes was not solely done by the writer, but also based on past work done in the writer's research group, a modelling work allocation factor is included on the block flow diagrams. Further in-depth discussion on the processes as well as specific modelling done in this study is performed in section 4.4.

The work allocation factors indicate the following:

- 1 Writer performed 10% or less of simulation
- 2 Writer performed 10 - 30 % of simulation
- 3 Writer performed 30 - 50 % of simulation
- 4 Writer performed 50 - 75 % of simulation
- 5 Writer performed 75 - 100% of simulation

#### 4.3.1 HEFA process

A simplified block flow diagram of the HEFA process is given in Figure 20. The HEFA process includes the following sections:

- *Hydrotreating*: The vegetable oil is deoxygenated by catalytic hydrotreating at raised pressures with excess hydrogen fed.
- *Hydrocracking*: The hydrotreated vegetable oil is cracked and isomerized to form diesel, jet fuel and naphtha fractions. The reactor conditions are set to aim for maximum jet fuel production.
- *Separation*: The hydrocarbons from the hydrocracker are fractionated into a light fraction and naphtha, jet fuel and diesel boiling range blend stocks. A fraction of the naphtha is sent to the reforming section to satisfy the plants' hydrogen and electrical power demand.
- *Hydrogen plant*: Make-up hydrogen is produced by steam reforming of a fraction of the naphtha product along with the light fraction from the separation section. Hydrogen purification, from the reformed gas and the off-gas from the hydrotreater and hydrocracker, is performed using two PSA units.
- *Steam & power plant*: Electrical power is produced in a steam turbine generator (no surplus). The steam is generated from a variety of heat sources in the process plant.
- *WWT & utilities*: This section includes a wastewater treatment (WWT) plant and a cooling water system.

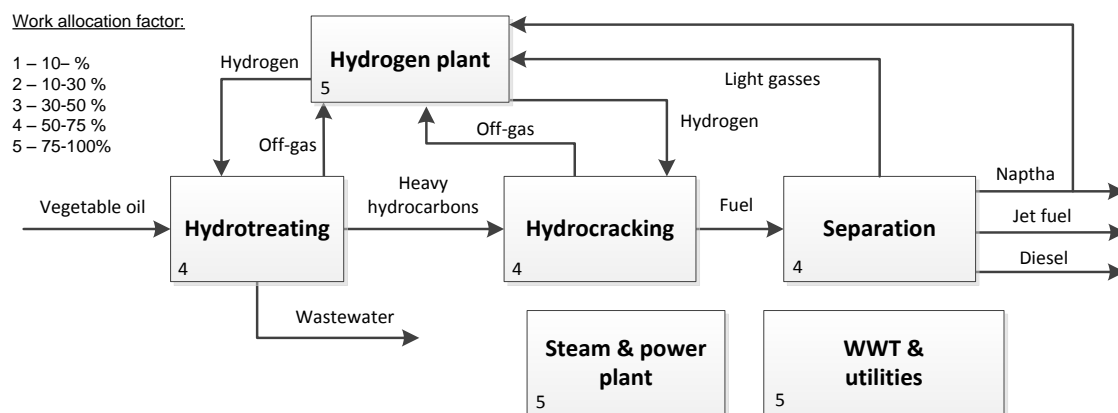


Figure 20: HEFA process overall block flow diagram

#### 4.3.2 SYN-FER-J process

A simplified block flow diagram of the SYN-FER-J process is given in Figure 21. Although three scenarios will be investigated, the block flow diagram fully represents the three scenarios. The SYN-FER-J process includes the following sections:

- *Gasification plant*: The lignocellulosic biomass, along with steam, is converted to syngas in a DFB gasifier. A fraction of the syngas product is sent to the power plant to satisfy the process plants' electrical power demand.

- *Fermentation*: Syngas fermentation using *C. ljungdahlii* occurs in bubble-loop reactors with syngas and cell recycle. Syngas is converted into mainly ethanol with acetone as a by-product.
- *Separation*: The ethanol in the fermentation broth is recovered to 93 wt% by two distillation columns and a water scrubber.
- *Hydrogen recovery plant*: Hydrogen is recovered from the fermentation off-gas using a membrane and a PSA unit.
- *Dehydration*: The ethanol (93 wt%) is dehydrated to mainly ethylene in isothermal fixed bed reactors. Purification of ethylene is accomplished by water condensation and adsorption towers.
- *Oligomerization*: The ethylene stream is oligomerized in a two reactor setup that produces mainly jet fuel by recycling the light hydrocarbons (C<sub>8</sub>-) for further oligomerization.
- *Hydroprocessing*: The jet fuel and diesel fractions are hydrogenated to ensure the quality of the fuels.
- *Steam & power plant*: Electrical power is produced in a steam turbine generator. The steam is generated mainly from the cooling of the gasification product streams and the combustion of the split fraction of the syngas product and the biogas produced in the anaerobic WWT plant. No surplus electricity is produced.
- *WWT & utilities*: This section includes a WWT plant and a cooling water system.

Work allocation factor:

- 1 – 10- %
- 2 – 10-30 %
- 3 – 30-50 %
- 4 – 50-75 %
- 5 – 75-100%

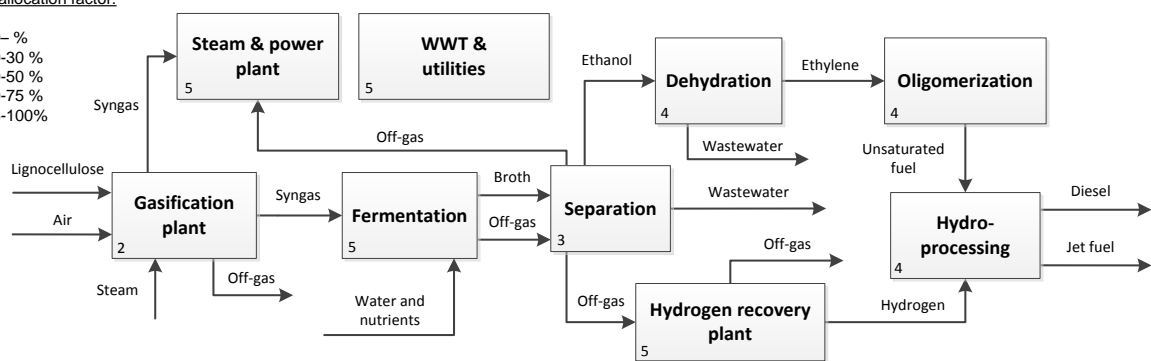


Figure 21: SYN-FER-J process overall block flow diagram

### 4.3.3 S-ETH-J process

A simplified block flow diagram of the S-ETH-J process is given in Figure 22. The S-ETH-J process includes the following sections:

- *Cleaning & sucrose extraction:* The fed sugarcane is first cleaned and the sucrose is then extracted in a diffuser. The resulting bagasse is dewatered to 50% MC and sent to the steam & power plant.
- *Treatment & clarification:* Physical treating of the sucrose liquid is first performed by screens and hydrocyclones. The liquid is clarified to remove remaining dirt.
- *Concentrating & sterilization:* The sucrose is concentrated in a multiple effect evaporator to a concentration of 22 wt% and is subsequently sterilised.
- *Fermentation:* The sucrose liquid is fermented to ethanol by *S. cerevisiae* in a fed-batch manner to an ethanol concentration of 13% (w/v).
- *Separation:* The ethanol in the fermentation product is recovered to 93 wt% by two distillation columns and a water scrubber.
- *Hydrogen plant:* Steam reforming of a small fraction of the ethanol is performed to satisfy the process plants' hydrogen consumption. Hydrogen purification from the reformed gas is performed using a PSA unit.
- *Dehydration:* The ethanol (93 wt%) is dehydrated to mainly ethylene in isothermal fixed bed reactors. Purification of ethylene is accomplished by water condensation and adsorption towers.
- *Oligomerization:* The ethylene stream is oligomerized in a two reactor setup that produces mainly jet fuel by recycling the light hydrocarbons (C<sub>8</sub>-) for further oligomerization.
- *Hydroprocessing:* The jet fuel and diesel fractions are hydrogenated to ensure the quality of the fuels.
- *Steam & power plant:* Excess electrical power is produced in a steam turbine generator. The steam is generated from the combustion of the dewatered bagasse and additional trash fed.
- *WWT & utilities:* This section includes a WWT plant and a cooling water system.

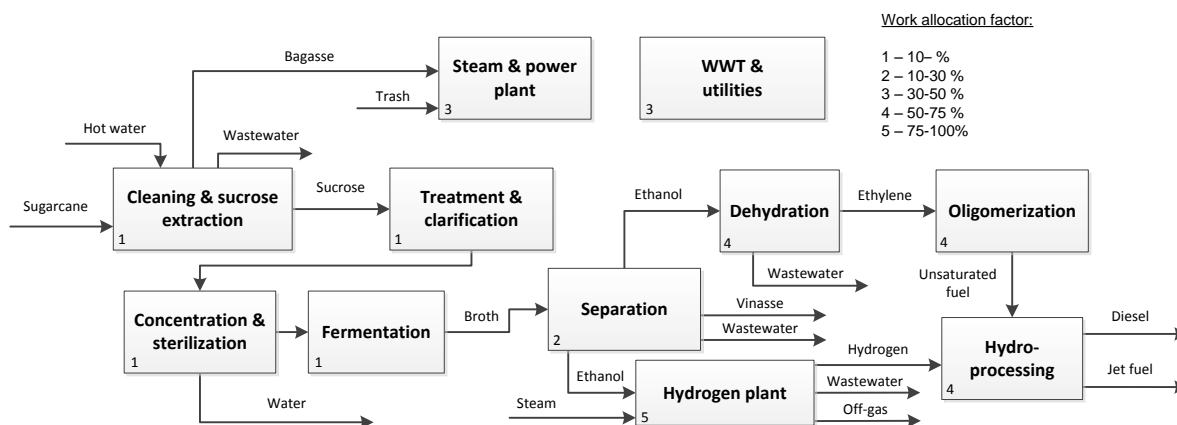


Figure 22: S-ETH-J process overall block flow diagram

#### 4.3.4 L-ETH-J process

A simplified block flow diagram of the L-ETH-J process is given in Figure 23. The L-ETH-J process includes the following sections:

- *Pretreatment & conditioning:* The pretreatment of lignocellulosic biomass consists of SO<sub>2</sub> impregnated steam explosion.
- *Hydrolysis & fermentation:* Separate hydrolysis and fermentation were performed comprising of enzymatic hydrolysis of pretreated biomass and continuous fermentation performed by modified yeast. Seed generation is performed on-site.
- *Separation:* The ethanol in the fermentation product is recovered to 93 wt% by two distillation columns and a water scrubber.
- *Evaporator:* The solid residue from the separation section is concentrated by evaporation, a pneumatic press and a multiple effect evaporator.
- *Hydrogen plant:* Steam reforming of a small fraction of the ethanol is performed to satisfy the process plants' hydrogen consumption. Hydrogen purification from the reformed gas is performed using a PSA unit.
- *Dehydration:* The ethanol (93 wt%) is dehydrated to mainly ethylene in isothermal fixed bed reactors. Purification of ethylene is accomplished by water condensation and adsorption towers.
- *Oligomerization:* The ethylene stream is oligomerized in a two reactor setup that produces mainly jet fuel by recycling the light hydrocarbons (C<sub>8</sub>-) for further oligomerization.
- *Hydroprocessing:* The jet fuel and diesel fractions are hydrogenated to ensure the quality of the fuels.

- *Steam & power plant*: Surplus electrical power is produced in a steam turbine generator. The steam is generated from the combustion of solids from the evaporator section and biogas produced in the anaerobic WWT plant.
- *WWT & utilities*: This section includes a WWT plant and a cooling water system.

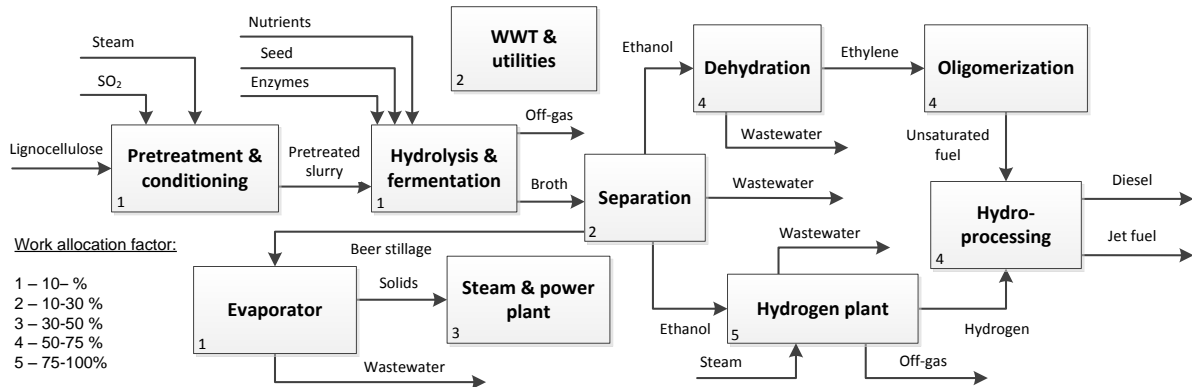


Figure 23: L-ETH-J process overall block flow diagram

#### 4.3.5 FP-J process

A simplified block flow diagram of the FP-J process is given in Figure 24. The FP-J process includes the following sections:

- *Pyrolysis*: The lignocellulosic biomass is pyrolyzed producing mainly bio-oil (water and organic compounds), solid char and non-condensable gasses.
- *Quench*: The bio-oil is cooled by air which is used for drying of biomass. The cooled bio oil is recovered from the fluidising gas by scrubbing and electrostatic precipitation.
- *Oil recovery*: A portion of the bio-oil from the quench section is recycled to the scrubber. A fraction of the resulting bio-oil is sent to the steam & power plant (23%), whilst the remainder is sent to the hydrotreating section.
- *Hydrotreating*: The product bio-oil is deoxygenated by catalytic hydrotreating in the presence of excess hydrogen.
- *Hydrocracking & separation*: The deoxygenated bio-oil is cracked and isomerized to hydrocarbons fractions which are separated by conventional distillation into gas oil, diesel, jet fuel, naphtha and lighter fractions.
- *Hydrogen plant*: Steam reforming of mainly natural gas (and some plant off-gas) is performed to satisfy the process plants' hydrogen requirement. Hydrogen purification

from the reformed gas and hydrotreating and hydrocracking recycle gas is performed using two separate PSA units.

- *Steam & power plant:* Excess electrical power is produced in a steam turbine generator. The steam is mainly generated from process plant cooling and from the combustion of char, off-gas, and a fraction of the bio-oil.
- *WWT & utilities:* This section includes a WWT plant and a cooling water system.

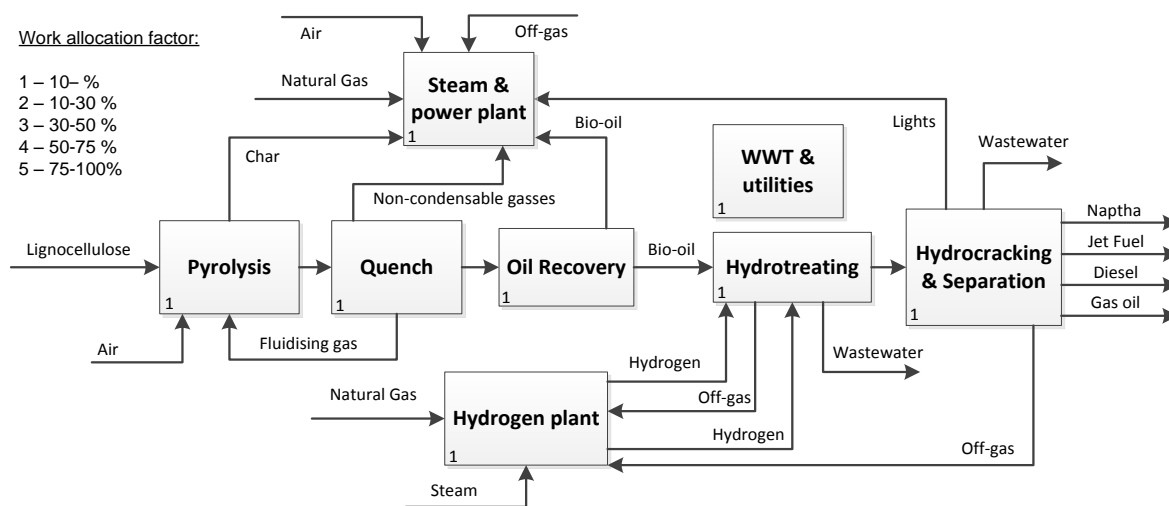


Figure 24: FP-J process overall block flow diagram

#### 4.3.6 GFT-J process

A simplified block flow diagram of the GFT-J process is given in Figure 25. The GFT-J process includes the following sections:

- *Gasification plant:* The lignocellulosic biomass, along with steam, is converted to syngas in a DFB gasifier. The product syngas is compressed.
- *Gas cleaning:* Syngas from the gasification plant and auto-thermal reformer are sent to the gas cleaning section. The syngas is cleaned in a Rectisol unit, by removing most of the CO<sub>2</sub>.
- *FT-plant:* A fraction of the syngas is directed to the hydrogen recovery plant, before the final compression of the syngas is performed. In a LTFT reactor, the syngas is converted into fuel fractions. The gas and liquid fractions are first separated, followed by the aqueous phase removal from the liquid hydrocarbons.
- *Air separation unit:* An air separation unit (ASU) provides purified oxygen to the ATR.
- *Auto-thermal reformer:* The gas fraction from the FT-plant (consisting of light hydrocarbons and unconverted syngas) are reformed in an ATR with oxygen and steam and is then recycled to the gas-cleaning section.

- *Upgrading & separation:* The liquid hydrocarbon fraction from the FT-plant is upgraded in a hydrocracker unit which cracks and isomerizes the FT-liquids. Hydrogen is co-fed to the hydrocracker to enable upgrading. Fractionation of the upgraded liquids to heavy hydrocarbons, light hydrocarbons, naphtha product and jet fuel product is performed. The heavy fraction is recycled to the hydrocracker, whilst the light fraction is sent to the steam & power plant.
- *Hydrogen recovery plant:* Hydrogen is recovered from the hydrocracker off-gas and a fraction of the syngas from the FT-plant in two successive PSA units.
- *Steam & power plant:* Surplus electrical power is produced in a steam turbine generator. The steam is generated mainly from the cooling of the gasification and FT reactor product streams and the combustion of the upgrading section off-gas, PSA off-gas and a purge stream from the recycle gas to the ATR section.
- *WWT & utilities:* This section includes a WWT plant and a cooling water system.

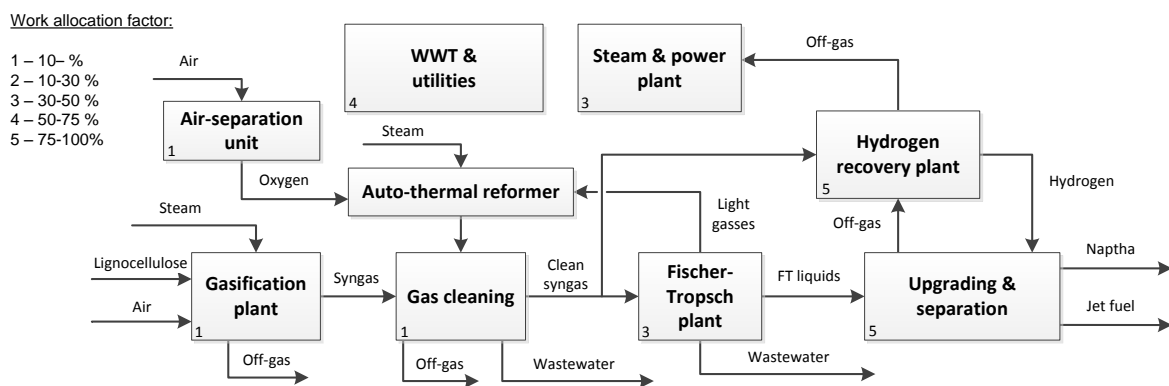


Figure 25: GFT-J process overall block flow diagram

#### 4.4 Mass and Energy Balances

Mass and energy balances were constructed using mainly Aspen Plus<sup>®</sup>. Aspen Plus<sup>®</sup> is a steady-state process simulator which is comprised of physical property and unit operation models [123]. The Aspen Plus<sup>®</sup> simulations for the sections which consisted of significant new work (where the writer performed 50%+ of the simulation) are shown in Appendix J.

The methods and assumptions which were used to perform the mass and energy balances are discussed in the following sub-sections. In-depth discussion will only be performed for process sections which were performed in this study or which were significantly updated in this study.

#### 4.4.1 General

##### 4.4.1.1 Physical properties

Physical properties for compounds are required, whilst performing mass and energy balances in simulators, such as Aspen Plus®. Without suitable physical properties, either a compromised mass and energy balance will result or the simulation will not run [124]. A few steps that can be followed when deciding on physical properties are available in studies by Carlson [124] and van der Merwe [125]. These methods along with literature prescription of physical properties were used to guide decision-making surrounding physical properties for simulations.

##### 4.4.1.2 Process properties

There are various process properties which can be used to compare processes. For converting biomass into fuel, three valuable process properties are mass ratio, energy ratio and energy efficiency [20].

For the calculation of the following process properties, a complete mass and energy balance is required.

##### Mass ratio:

Mass ratios can be calculated for each process using the equation below [20].

$$\eta_m = \frac{m_{fuel}}{m_{biomass}} \quad \text{Equation 5}$$

Where  $\eta_m$  is the mass ratio of the process,  $m_{fuel}$  is the mass of fuel produced and  $m_{biomass}$  is the mass of the dry feedstock input. A jet mass ratio can also be determined as a mass ratio between the jet fuel and the biomass.

##### Energy ratio:

Energy ratios can be calculated for each process using one of the equations below [20]. Equation 6 determines the energy ratio based on biomass in the feed, whilst Equation 7 determines the energy ratio based on the total feed.

$$\eta_e = \frac{|m_{fuel} \cdot HHV_{fuel}|}{|m_{biomass} \cdot HHV_{biomass}|} \quad \text{Equation 6}$$

or

$$\eta_e = \frac{|m_{fuel} \cdot HHV_{fuel}|}{|m_{biomass} \cdot HHV_{biomass}| + |m_{fossil} \cdot HHV_{fossil}|} \quad \text{Equation 7}$$

Where  $\eta_e$  is the energy ratio of the process,  $HHV_{fuel}$  is the higher heating value (HHV) of the fuel,  $HHV_{biomass}$  is the HHV of the biomass feedstock,  $m_{fossil}$  is the mass of fossil input and  $HHV_{fossil}$  is the HHV of the fossil input. The energy ratio represents a ratio between the energy content of the fuel and the feedstock. A jet fuel energy ratio can also be determined as a ratio between the energy in the jet fuel and the energy in the feed.

#### Energy efficiency:

Energy efficiency can be calculated for each process using various equations. The following equations will be used [92].

$$n_{liquid\ fuel} = \frac{|m_{fuel} \cdot HHV_{fuel}|}{|m_{biomass} \cdot HHV_{biomass}| - \frac{E_{elec.power}}{n_{elec}}} \quad \text{Equation 8}$$

$$n_{overall} = \frac{|m_{fuel} \cdot HHV_{fuel}| + E_{elec.power}}{|m_{biomass} \cdot HHV_{biomass}| + |m_{fossil} \cdot HHV_{fossil}|} \quad \text{Equation 9}$$

The liquid fuel energy efficiency ( $\eta_{liquid\ fuel}$ ) determines the amount of biomass energy which is converted into fuel energy, deducting the energy for electricity generation from the biomass energy. The overall energy efficiency ( $\eta_{overall}$ ) determines the efficiency of the process taking the energy in the fuels and electricity power produced ( $E_{elec.power}$ ) as a product, whilst taking into account the energy in the biomass and the fossil fuel inputs. The electrical energy is converted to thermal energy in Equation 8 by assuming a 45% conversion efficiency for direct conversion of biomass to electricity ( $n_{elec} = 45\%$ ) [92].

#### 4.4.1.3 Hydrogen considerations

All the processes require a certain amount of make-up hydrogen. As stated in section 4.1, the scenarios are aimed to be **hydrogen self-sufficient**; independent of fossil sources. The various possible sources for the hydrogen include part of the feed, intermediates or product. The simplest source of producing hydrogen will be investigated. A discussion on the simulation of hydrogen production and separation is performed in section 4.4.10.

The SYN-FER-J process requires some hydrogen for the hydrogenation of the fuels. A fraction of the unconverted syngas from the fermentation sections will be used as a hydrogen source. The GFT-J process requires substantial hydrogen for the hydrocracker. With syngas as an intermediate in the process, the source of the hydrogen will be taken from a fraction of the cleaned syngas. The L-ETH-J and S-ETH-J both requires some hydrogen for the hydrogenation of the fuels. As both processes have ethanol as an intermediate, it will

be used as a precursor for hydrogen production by steam reforming. Significant hydrogen is needed by the HEFA process for the hydroprocessing of vegetable oil. Steam reforming of the light hydrocarbon product was found to be insufficient in meeting the process' hydrogen demand. Additional naphtha product was reformed to meet the process' hydrogen demand. A large amount of hydrogen is needed by the FP-J process for the hydroprocessing of the bio-oil. As no updating of the study by McLaren [97] was performed, natural gas was kept as the hydrogen source. Alternative sources of hydrogen are steam reforming of a fraction of the bio-oil or hydrogen production from a fraction of the biomass. According to literature, sufficient hydrogen generally cannot be obtained by reforming of process off-gas [55], [52].

#### 4.4.1.4 Electrical power considerations

Significant amounts of electrical power are required for all the investigated processes. As stated in section 4.1, the scenarios are aimed to be **electrical power self-sufficient**; independent of fossil sources. Power production therefore needs to be performed by all the processes. A discussion on the simulation of power generation is done in section 4.4.11.

For the investigated processes, there are two cases:

- Case 1:** Excess energy is generated by the process; sufficient energy is therefore available to meet process' energy requirements and meet process' electrical power demand.
- Case 2:** Insufficient energy is generated by the process; an alternative source of energy is needed to meet process' energy requirements and/or meet process' electrical power demand.

The processes in case 1 are the FP-J, GFT-J, S-ETH-J and L-ETH-J process. The FP-J process, however, has natural gas co-fed as an energy source to the steam reforming section.

The processes in case 2 are the SYN-FER-J and HEFA process. For the SYN-FER-J process, a fraction of the syngas from the gasification section is sent to a combustor in order to meet the process' energy and electrical power demand (a similar scenario was employed by [36]). For the HEFA process, a fraction of the naphtha product along with process off-gas was combusted in the reformer to meet the process' energy and electrical power demand.

#### 4.4.1.5 Heat integration

This study intended to perform reasonable heat integration on the investigated processes. The method that was followed to perform the heat integration is shown below. The method is much more iterative than what is illustrated.

- I. First construct simulation without any heat integration
- II. Determine the duties of the streams that need heating and streams that need cooling
- III. Perform heat integration that is clear from inspection (a clear example is preheating of the feed to a distillation column by using the bottoms)
- IV. Input remaining duties into Aspen Energy Analyzer (AEA)

AEA first constructs a base case – a simulation with no heat integration but only heating and cooling utilities. A pinch analysis was then performed on the base case using AEA; determining the maximum heat-recovery possible. Heat exchangers were added into the base case one at a time guided by the suggested configurations of the AEA optimization. For each possible heat exchange configuration, AEA determines the amount of energy and the economics (in comparison to base-case) related to the configuration.

Advantage was given to heat-integration configurations which:

- Are physically close to each other
- Constitutes of large amounts of energy recovery
- Are economically attractive

Heat exchangers were added until all reasonable heat integration was performed.

As processes in case 1 have excess energy, it was aimed that the lower temperature streams be used for heating, such that excess energy can be used for steam and excess power generation. As the processes in case 2 have just sufficient energy with an additional source of energy, a very iterative approach was followed. As the additional source of energy was introduced to ensure sufficient energy and power requirements, revision on heat-integration configurations needed to be made. For processes in case 2, it was also aimed that the lower temperature streams be used for heating, such that sufficient energy was available for power generation.

#### 4.4.1.6 Steam considerations

Steam was utilized across the process plants for heat recovery and heat supply. Steam generation across the process plants (e.g. FT synthesis reactor cooling, hot syngas cooling, C<sub>4+</sub> oligomerization reactor cooling) were performed by feeding pressurized water to the heat

sources with subsequent use of the steam across the process plants (e.g. heat supply in reboilers). A variety of types of steam were employed including low pressure, medium pressure and high pressure steam. Steam was also generated by the processes specifically for power generation (further discussed in section 4.4.11). Saturated steam was generally utilized for process plant steam, whilst superheated steam was required for power generation in steam turbines.

#### 4.4.2 Pressure changers

Pressure drop is neglected across most equipment in the process plants. Pressure increase is only simulated in pumps and compressors.

##### 4.4.2.1 Pumps

Pumps were generally specified by the discharge pressure. No efficiencies were defined such that Aspen Plus<sup>®</sup> can calculate the pump efficiencies.

##### 4.4.2.2 Compressors

The specifications for compressors are shown in Table 18. For compressors run in series, discharge pressures were specified such that compressors have equal power inputs.

Table 18: Compressor specifications

Specification	
Type	Polytropic using ASME method
Discharge pressure	Process Specific
Polytropic Efficiency	0.75

#### 4.4.3 Heat exchangers

Reasonable heat-integration was performed on the processes as discussed in section 4.4.1.5. A minimum approach temperature of at least 10°C was adhered to when simulating heat exchangers.

#### 4.4.4 Separation equipment

The main separation equipment includes vapour-liquid separators, liquid-liquid separators, distillation columns, adsorption columns and a Rectisol unit. Correct choice of physical properties is especially important for the separation sections. The steps that were followed to decide on physical properties for separation are available in studies by Carlson [124] and van der Merwe [125].

#### 4.4.4.1 Vapour-liquid and liquid-liquid separation

The vapour-liquid separators and liquid-liquid separators were specified by a specific pressure and a duty of zero. Large quantities of vapour-liquid separators were modelled in the processes, but in-depth discussion is not warranted. Liquid-liquid separation is performed on the FT reactor product to separate the aqueous phase from the hydrocarbon phase using the *UNIF-LL* property method. Three-phase separation was performed on the HEFA processes' hydrotreater product to separate the aqueous phase from the hydrocarbon phases. The *RKSMHV2* property method was employed.

#### 4.4.4.2 Ethanol recovery section

An ethanol recovery section, employed by the L-ETH-J, S-ETH-J and SYN-FER-J processes, recovers ethanol from the fermentation broths. The bottoms of the beer column for the L-ETH-J, S-ETH-J and SYN-FER-J processes consist of evaporator feed, vinasse or waste water respectively. The section is simulated using the *ELEC-NRTL* property method [32]. Although the fermentation broths have varying ethanol concentrations (L-ETH-J – 3.9 wt% ethanol; S-ETH-J – 12.3 wt% ethanol; SYN-FER-J – 2-2.5 wt%), the recovery sections are alike. A simplified flow diagram of the ethanol recovery section is shown in Figure 26.

The feed to the beer column is concentrated to an ethanol mass purity of 0.55 by removing the dissolved CO<sub>2</sub> in the top product and significant water and other in the bottoms. A scrubber, with H<sub>2</sub>O as liquid, is used to recover ethanol from the fermentation vents and the beer columns' top product. The scrubber liquid product is sent to the beer column. The ethanol stream from the beer column is further concentrated in the rectification column to an ethanol mass purity of 0.93 by removal of water. The recovery of the ethanol is specified in both columns such that no significant ethanol is lost. The combined ethanol recovery of the scrubber and beer column system were ~99.8% whilst the ethanol recovery of the rectification column was ~99.9%. Complete water removal from ethanol by molecular sieves is not required as the ethanol conversion process (described in section 4.4.6.1) can handle a small fraction of water (7 wt% H<sub>2</sub>O) without being negatively affected [126], [127].

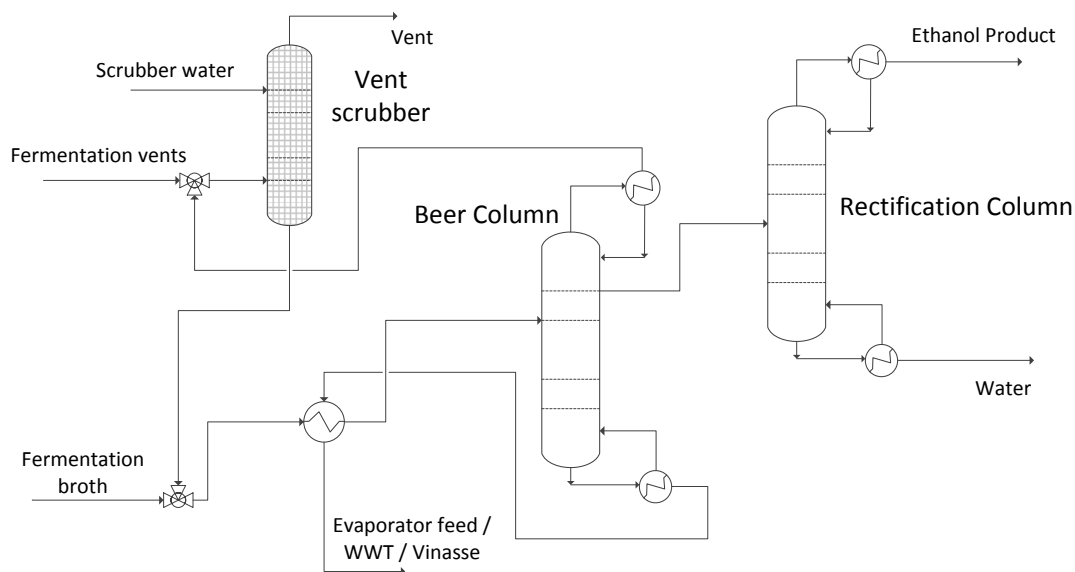


Figure 26: Flow diagram of ethanol recovery section

#### 4.4.4.3 Hydrocarbon distillation columns

The GFT-J and HEFA processes both employ two hydrocarbon distillation columns to separate the fuel products based on the *RK-SOAVE* property method. See Figure 27 for a simplified flow diagram. For the GFT-J and HEFA processes the hydrocarbon feed is split by product splitter 1 to a heavy fraction or diesel respectively, a jet fuel fraction and a C<sub>8</sub>-fraction. Product splitter 1 is specified so that all the jet fuel (C<sub>9</sub> - C<sub>15</sub>) is recovered. Product splitter 2 separates the C<sub>8</sub>-fraction into naphtha (mainly C<sub>6</sub> - C<sub>8</sub>) and a light fraction.

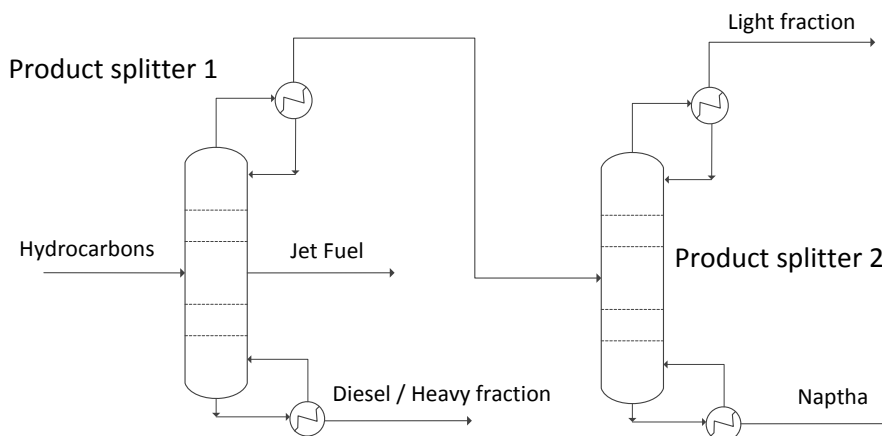


Figure 27: GFT-J and HEFA process separation section

The L-ETH-J, S-ETH-J and SYN-FER-J processes utilize a hydrocarbon distillation column to recycle the light fraction from the oligomerization reactor (C<sub>8</sub>) to the oligomerization

reactor. The *RK-SOAVE* property method is also employed. The column is specified so that the feed is separated into a jet fuel fraction ( $C_9 - C_{15}$ ), a diesel fraction and the  $C_8$  fraction. Figure 30 in section 4.4.6.2 shows a simplified flow diagram of the oligomerization product splitter section. Very good comparison was achieved between the separation in Aspen Plus<sup>®</sup> and [60].

The hydrocarbon separation of the FP-J process was not simulated in Aspen Plus<sup>®</sup> by the study by McLaren [97], but rather based on literature [101]. The product fractions are gas oil, diesel, jet fuel, naphtha and lighter fractions.

#### 4.4.4.4 Adsorption column

An adsorption column (along with knock-out drums) is employed by the L-ETH-J, S-ETH-J and SYN-FER-J processes after the dehydration reactor to purify the ethylene. Contaminant removal (mainly diethyl ether) can be achieved by correct choice of adsorbent [128]. A process configuration similar to Cameron et al. [129] (who also investigated ethylene purification after ethanol dehydration) was assumed. Since the column was simulated in Aspen Plus<sup>®</sup> in this study using a separator block, the utility demands of Cameron et al. were used.

#### 4.4.4.5 Rectisol unit

The Rectisol unit, employed in the GFT-J process, was originally simulated in Aspen Plus<sup>®</sup> by Petersen et al. [102] using a black-box approach. The method by Petersen et al., which is based on a study by Sun et al. [108], was also used in this study. The proposed performance of the Rectisol unit is discussed in the *syngas cleaning section* in section 3.6.2.

### 4.4.5 **Biochemical reactors**

The L-ETH-J, S-ETH-J and SYN-FER-J are the only processes with biochemical reactors.

#### 4.4.5.1 L-ETH-J process

The L-ETH-J process consists of the pretreatment reactor section, the hydrolysis reactor and fermentation reactor section and the seed generation section. As these were originally simulated by Petersen [93] in Aspen Plus<sup>®</sup>, the method by Petersen is referenced. The main assumptions are discussed in section 3.4.2.

#### 4.4.5.2 S-ETH-J process

The S-ETH-J process consists of a fermentation reactor section. As this was originally simulated by van der Westhuizen [91] in Aspen Plus<sup>®</sup>, the method by van der Westhuizen is referenced. The main assumptions are discussed in section 3.3.2.

#### 4.4.5.3 SYN-FER-J process

The SYN-FER-J process consists of a fermentation reactor section. The simulation for the fermentation reactor in Aspen Plus® was constructed in this project and will be discussed comprehensively. Three scenarios were developed for the fermentation reactor sections (A.1, A.2 and B) based on different fermentation data. The selected conditions and experimental results, performed by Gaddy et al. [116] on a *C. ljungdahlii* strain using a CSTR with cell recycling, are shown in Table 19 and Table 20.

Table 19: Conditions of the selected syngas fermentation experiments, [116]

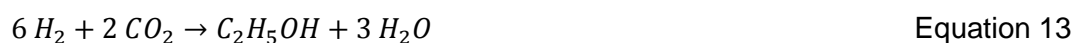
	Feed (mol%)				GRT <sup>1</sup> (min)	XRT <sup>2</sup> (hr)	LRT <sup>3</sup> (hr)
	H <sub>2</sub>	CO	CO <sub>2</sub>	CH <sub>4</sub>			
A.1	50	45	0	5	12.5	46.4	23.2
A.2					6.8	54.3	16.3
B	55	30	10	5	6	24	1.62

<sup>1</sup> Gas retention time, ratio of reactor liquid volume to inlet gas flow rate; <sup>2</sup> Cell retention time, average amount of time cells spend in reactor; <sup>3</sup> Liquid retention time, ratio of reactor liquid volume to liquid flow rate.

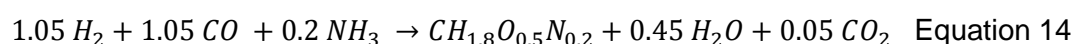
Table 20: Results of the selected syngas fermentation experiments, [116]

	Gas conversion (%)		Products (g/l)		Ethanol Productivity (g/l.day)	Cell concentration (g dry Cell/l)
	CO	H <sub>2</sub>	Ethanol	Acetate		
A.1	96.3	81.2	20.4	4.4	21.1	3.8
A.2	84.7	57.7	23.4	5.7	34.5	4.7
B	95	60	25	3	369	2

Piccolo et al. [6] described the syngas fermentation process by the following equations.



Equation 14 is assumed to represent the production of *C. ljungdahlii* from syngas and nutrients (based on [125]).



Based on the conditions and experimental results by Gaddy et al., whilst assuming Equation 10 to Equation 14 accurately describes the syngas fermentation by *C. ljungdahlii*, fractional conversions for each reaction can be determined with the use of mass and molar balances. As the calculated fractional conversion for Equation 10 to Equation 13 is a function of the fractional conversion of Equation 14 (which is solved for in the simulation), the determination of conversions are iterative. The converged fractional conversions for the three scenarios are shown in Table 21.

Table 21: Calculated fractional conversion for syngas fermentation

Fractional conversion	A.1	A.2	B
<b>Equation 10</b> - (conversion based on CO)	0.118	0.183	0.042
<b>Equation 11</b> - (conversion based on H <sub>2</sub> )	0.052	-0.021	0.042
<b>Equation 12</b> - (conversion based on CO)	0.797	0.639	0.906
<b>Equation 13</b> - (conversion based on H <sub>2</sub> )	0.717	0.575	0.557
<b>Equation 14</b> - (conversion based on H <sub>2</sub> )	0.043	0.023	0.001

According to van Kasteren et al. [114], the approach to achieve sufficient gas-to-liquid mass transfer in very large CSTR's for commercial syngas fermentation by increasing power input, is not economically feasible due to excessive power costs. This was validated by rule-of-thumb calculations based on data by [130]. A bubble loop reactor, a promising reactor proposed by van Kasteren et al., was employed in the simulation. Consequently, it is assumed that the data by Gaddy et al. for a CSTR can be applied for a bubble column with syngas recycle.

Figure 28 compares the actual process flow diagram (PFD) for the syngas fermentation process (proposed by van Kasteren et al.) to the Aspen simulated PFD. The actual PFD consists of syngas, water and nutrients fed to a bubble column. For the actual PFD, a fraction of the product gas is compressed and recycled, whilst the the rest is removed as off-gas. Liquid, containing cells, is removed from the bubble column. A fraction of the cells are recycled. The Aspen simulation models the syngas fermentation in a stoichiometric reactor based on Equation 10 to Equation 14 and the fractional conversions in Table 21. The water feed is adjusted such that the product concentrations obtained by Gaddy et al. are achieved. Sufficient nitrogen (by means of ammonia) is added to the reactor to enable cell production. As the data by Gaddy et al. was assumed for the bubble column with syngas recycle, no syngas recycle modelling is necessary. A syngas recycle compressor was modelled separately solely to determine the economics associated with the recycle stream compressor. The removal of off-gas is modelled in a separate vapour-liquid separator. The modelling of cell recycle is similar to the actual PFD.

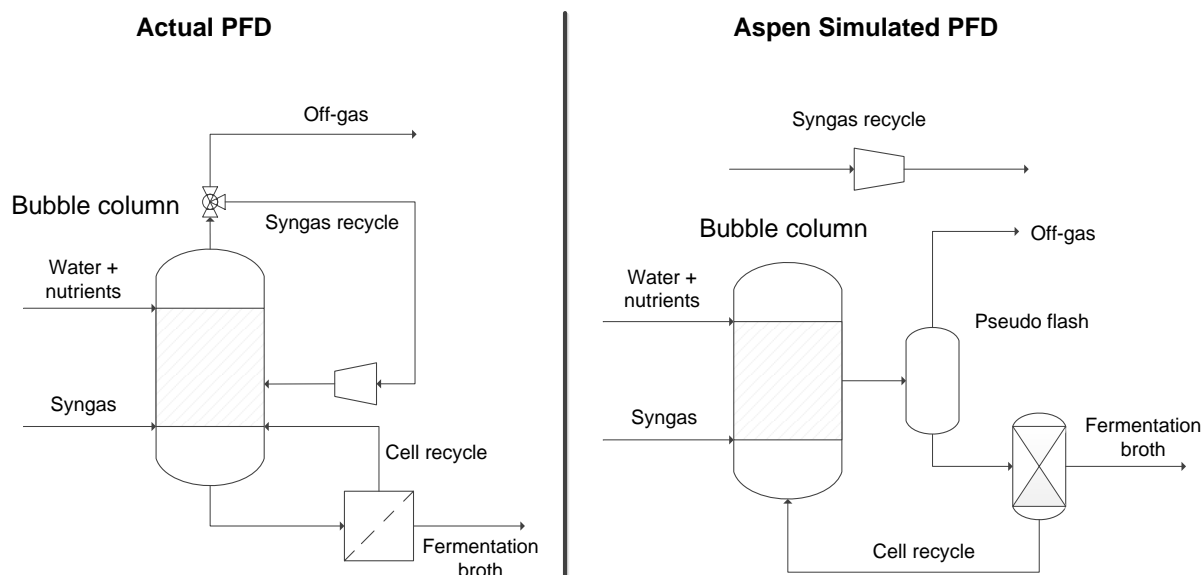


Figure 28: PFD of "actual" and "Aspen simulated" syngas fermentation process

#### 4.4.6 Ethanol upgrading to jet fuel section

An identical ethanol upgrading to jet fuel (ETH-J) section was employed by the L-ETH-J, S-ETH-J and SYN-FER-J processes. The ETH-J section consists of a dehydration reactor, an oligomerization section, and hydroprocessing.

By combining the yields proposed for modelling of the ETH-J section, an overall yield of 541 kg jet fuel per MT of ethanol fed was determined. This compares well to the study of Crawford [49], who obtained an overall yield of 556 kg jet fuel per MT of ethanol fed. According to Crawford, the theoretical maximum yield is 616 kg jet fuel per MT of ethanol fed.

##### 4.4.6.1 Dehydration reactor

The feed to the dehydration reactor consists of 93 wt% ethanol (the balance is water). The simulated dehydration reactor, which is based on experiments by Haishi et al. [62] for a fixed bed reactor, has the following conditions.

Table 22: Dehydration reactor catalyst and conditions, [62]

Catalyst	Ethylene selectivity	Ethanol conversion	Reaction temperature	Pressure	GHSV
Meso-porous silica	99.90%	100%	350°C	1 atm	400 h <sup>-1</sup>

The dehydration reactor was simulated in Aspen Plus<sup>®</sup> using an isothermal stoichiometric reactor, with a fractional conversion of 99.9% of ethanol towards the ethylene by the dehydration reaction shown in Equation 15. The rest of the ethanol is converted to diethyl

ether. As the ethanol dehydration reaction is endothermic, external heating is required to maintain isothermal conditions (this was performed by using hot combustion off-gas).



Although the feed of Haishi et al. did not contain water along with the ethanol, it is assumed, based on literature, that it can handle a small fraction of water (7 wt%  $\text{H}_2\text{O}$ ) without being negatively affected [127], [126].

#### 4.4.6.2 Oligomerization reactor

A two-step oligomerization reactor setup was used to convert the ethylene feed to heavy hydrocarbons. The first oligomerization reactor section converts the ethylene feed to mainly  $\text{C}_4$  and also  $\text{C}_6$  and  $\text{C}_8$  hydrocarbons based on experiments by Mahdaviani et al. [61]. Figure 29 compares the actual PFD (based on [61] and [131]) to the Aspen simulated PFD.

Although the actual PFD consists of solvent and catalyst recycle, this will not be simulated in the Aspen model. The reactor was simulated in a yield reactor with a temperature of  $55^\circ\text{C}$  and a pressure of 22 bar (conditions of Mahdaviani et al.). Although unconverted ethylene recycle has been proposed by [131], it is not employed in the simulation due to the high ethylene conversion (97.8%) achieved by Mahdaviani et al. The yields obtained by Mahdaviani et al. are shown in Table 92 in Appendix B.

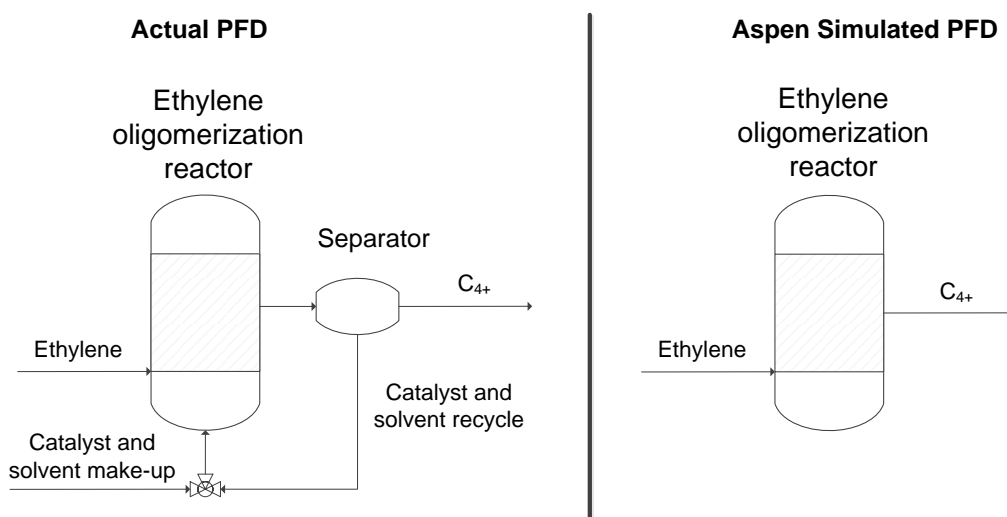


Figure 29: PFD of "actual" and "Aspen simulated" ethylene oligomerization reactor

The second oligomerization reactor section converts the products from the ethylene oligomerization reactor to larger hydrocarbons based on a patent by Keuchler et al. [60]. The product of the ethylene oligomerization reactor and the feed used by Keuchler et al. are

similar (shown in Table 93 in Appendix B) allowing the use of the literature in conjunction. The  $C_{4+}$  oligomerization reactor setup is shown in Figure 30 employing a recycle of  $C_8$ -hydrocarbons for maximization of jet fuel (the product splitter is discussed in section 4.4.4.3). The reactor was modelled isothermally (by steam generation) using a yield reactor in Aspen Plus<sup>®</sup> at a temperature of 235°C and a pressure of 7000 kPa (conditions of Keuchler et al.). The yields of the  $C_{4+}$  oligomerization reactor based on Keuchler et al. are also shown in Table 93 in Appendix B.

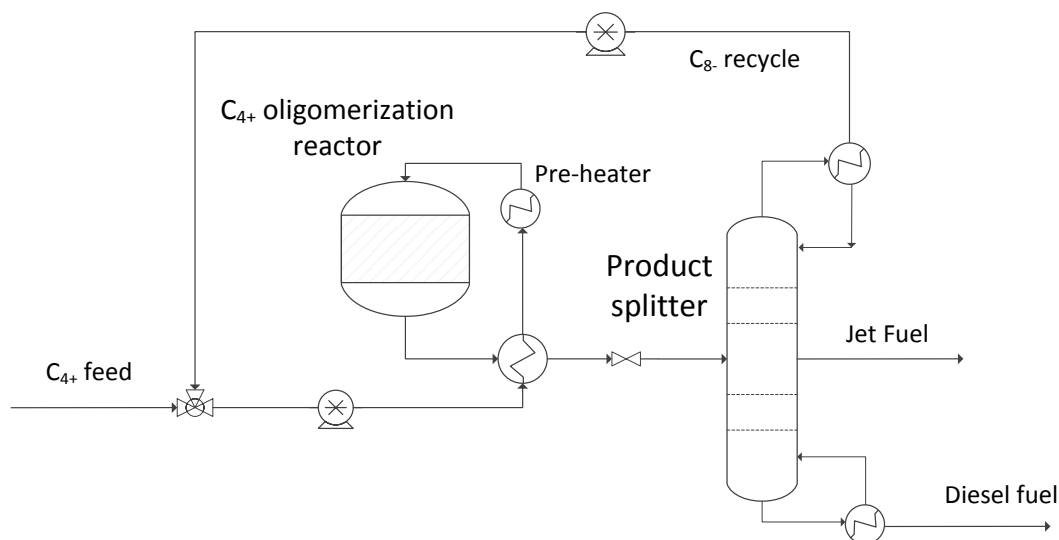


Figure 30:  $C_{4+}$  oligomerization reactor setup with  $C_8$ - recycle

#### 4.4.6.3 Hydroprocessing

A simplified process flow diagram of the hydrogenation reactor section (used for the jet and diesel fuel) is shown in Figure 31.

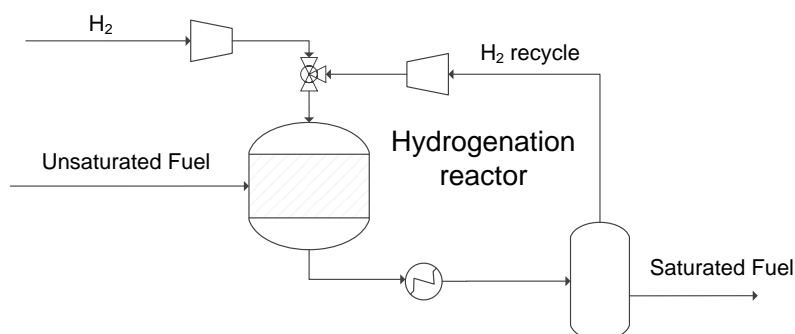


Figure 31: Hydrogenation reactor process flow diagram

The hydroprocessing of the fuels were simulated in Aspen Plus<sup>®</sup> using stoichiometric reactors, assuming total saturation of the fuel with no carbon number distribution change [60]. The reactors were simulated at a pressure of 34.5 bar and a temperature of 185°C

(conditions proposed by Keuchler et al. [60]). As seen in Figure 31, excess hydrogen is fed to the hydrogenation reactor, whilst recycling of the hydrogen is performed.

#### 4.4.7 Thermochemical reactors

As significant overlapping of thermochemical reactors occur between processes, the reactors will be discussed individually.

##### 4.4.7.1 Gasification reactor

The GFT-J and SYN-FER-J processes employ a DFB gasifier reactor. As the reactor was modelled by Petersen et al. [102] in Aspen Plus<sup>®</sup>, the method by Petersen et al. is referenced. The main assumptions are discussed in the *gasification section* in section 3.6.2.

The optimized variables determined by Petersen et al. for the DFB gasification reactor of the GFT-J process is shown in Table 7 in section 3.6.2.

Although the same simulation of the DFB gasifier reactor was employed for the SYN-FER-J process, the optimized variables needed for the downstream fermentation were different. Similar to the study by Petersen et al., no downstream compositional adjustment is considered. The gas composition used by Gaddy et al. [116] for the fermentation is shown in Table 19 in section 4.4.5. It is assumed that the fermentation data by Gaddy et al. can be used if the produced syngas has the same H<sub>2</sub>:CO ratio, has at least the same or higher molar concentration of syngas (%H<sub>2</sub> + %CO) and has at least less impurities than the gas by Gaddy et al.

By performing a sensitivity analysis on the DFB gasifier reactor in Aspen Plus<sup>®</sup>, the three main variables, shown in Table 23, were investigated across their full range (steam to biomass ratio between 0 and 1, moisture content between 0% and 100% and biomass split between 0% and 100%). Restraints were set on the gasifier temperature (required to be above 900°C for tar-free syngas [107], [102]) and on the scenario specific H<sub>2</sub>:CO ratio. For the sets of variables which met both restraints, the set with the maximum syngas flowrate were chosen. The scenario selected variables are shown in Table 23.

Table 23: SYN-FER-J process DFB gasifier selected variables

Scenario	Steam to biomass ratio <sup>1</sup>	Moisture content (%) <sup>2</sup>	Biomass split (%) <sup>3</sup>
A.1	0.2	10	41
A.2			
B	0.8	13	42

<sup>1</sup> Ratio of steam to biomass to the gasification section of the DFB gasifier; <sup>2</sup> Moisture content of biomass to the DFB gasifier; <sup>3</sup> Fraction of biomass split to the combustor section of the DFB gasifier.

Both chosen sets for scenario A and B have a higher concentration of syngas ( $\%H_2 + \%CO$ ) than specified by the downstream fermentation data (larger than 95% for scenario A and larger than 85% for scenario B).

#### 4.4.7.2 Hydrotreater

A hydrotreater is used by both the HEFA and FP-J process. As the hydrotreater in the FP-J process was modelled by the study of McLaren [97] in Aspen Plus<sup>®</sup>, its method is referenced. The main assumptions are discussed in section 3.5.2.

The simulation of the hydrotreater reactor employed by the HEFA process was constructed in this project based on experiments performed by Gong et al. [74] using jatropha oil (experimental yields are shown in Table 89 and Table 90 in Appendix B). The reactor conditions were 350°C, 3 MPa in a fixed bed reactor with a LHSV of  $2h^{-1}$  and a  $H_2$ /feed volume ratio (v/v) of 600. A simplified flow diagram of the hydrotreater reactor is illustrated in Figure 32. The hydrotreater reactor was simulated in Aspen Plus<sup>®</sup> using an isothermal yield reactor with cooling of the exothermic reactions performed by hydrogen feed and steam generation. Only straight-chain alkanes were modelled in Aspen Plus<sup>®</sup>. As shown in Figure 10 in section 3.1.2, the deoxygenation reaction follows various pathways. Using the experimental yields by Gong et al. [74], a mass and molar balance was performed to determine the extents of each reaction pathway. Based on the extents of each pathway, the hydrogen used and the by-products in the gas phase were calculated. As the oil composition used in the HEFA process was based on Gong et al. [74] (shown in section 4.2.3), the insertion of the calculated reactor yield into the Aspen simulation delivers a balanced carbon, hydrogen and oxygen balance.

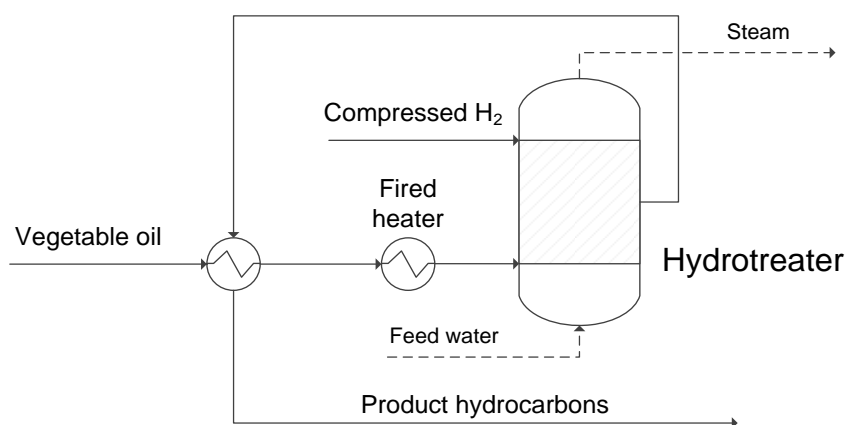


Figure 32: Simplified flow diagram of HEFA process hydrotreater

#### 4.4.7.3 Fischer-Tropsch reactor

The GFT-J process employs a FT reactor to convert the syngas in the feed to hydrocarbons. A flow diagram of the FT reactor is shown in Figure 33. The feed syngas is preheated by the FT product. The reactor is based on a fixed-bed type reactor with temperature kept at 195°C by steam generation, at a pressure of 40 bar and using a cobalt catalyst. Only straight-chain alkanes were modelled for C<sub>1</sub> - C<sub>20</sub> hydrocarbons, with C<sub>20+</sub> waxes being modelled as C<sub>30</sub> (the same approach was taken by Swanson et al. [69]). FT reactions, following the reaction mechanism of Equation 2 in section 1.1.4, were constructed for all the modelled hydrocarbons. It was proposed in section 3.6.2 that the reactions in the FT reactor can be described by the Anderson-Schultz-Flory model. The chain growth probability was calculated using Equation 4 in section 3.6.2 based on the specified reactor temperature and the partial pressures of syngas components in the feed (partial pressures are derived from the Aspen model). The mole fractions of the product hydrocarbons were calculated based on Equation 3 in section 3.6.2. The extents of reaction of the individual reactions were subsequently determined which result in the calculated mole fraction in the hydrocarbon product. The extents of reactions were inserted into the stoichiometric reactor with an assumed conversion of 40% of the carbon dioxide in the feed [69].

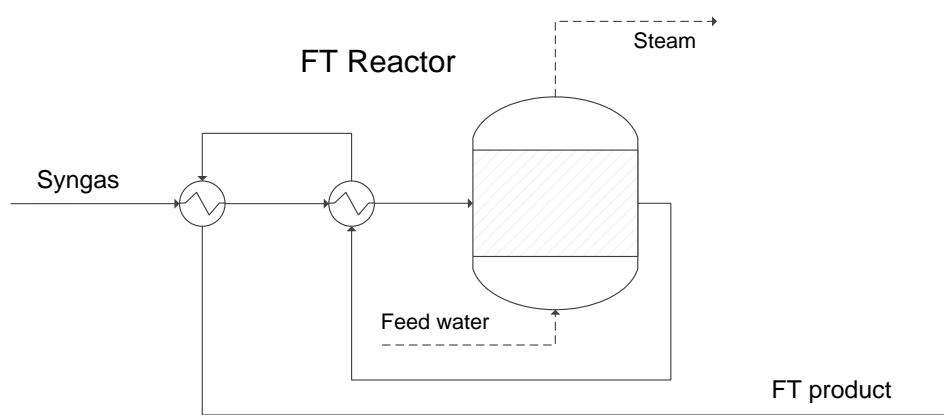


Figure 33: Simplified flow diagram of FT reactor for the GFT-J process

#### 4.4.7.4 Hydrocracker

The GFT-J, HEFA and FP-J processes all use a hydrocracker. As the hydrocracker in the FP-J process was modelled in Aspen Plus<sup>®</sup> by the study of McLaren [97], its method is referenced. The main assumptions for the simulation by McLaren are discussed in section 3.5.2.

Different approaches were followed to simulate the hydrocrackers in the HEFA and GFT-J processes. They will therefore be discussed separately. A simplified flow diagram of the hydrocracker is illustrated in Figure 34.

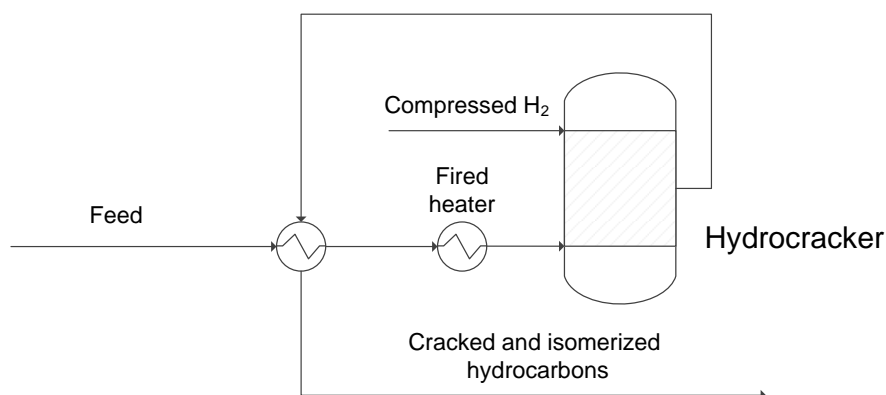


Figure 34: Simplified flow diagram of hydrocracker for HEFA and GFT-J process

The simulation of the hydrocracker reactor employed by the HEFA process was based on experiments performed by Robota et al. [73] (experimental yields are shown in Table 91 in Appendix B). Robota et al. used a very similar feed to the liquid products of Gong et al. [74] for the hydrodeoxygenation reactor system; such that the liquid products from the hydrotreater can be upgraded using the experiments by Robota et al. The selected reactor conditions of Robota et al. were 278°C, 55.16 bar, a LHSV of 1h<sup>-1</sup> and a H<sub>2</sub>/feed volume ratio (v/v) of 850. The hydrocracker was simulated in Aspen Plus<sup>®</sup> using a yield reactor. Only straight-chain alkanes were simulated in Aspen Plus<sup>®</sup>. The temperature of 278°C was achieved, despite of the exothermic reactions, by feeding part of the hydrogen directly to the hydrocracker. Using the experimental yields by Robota et al., a mass and molar balance was performed to determine the hydrogen usage. The reactor yield, that delivers a balanced carbon, hydrogen and oxygen balance in Aspen Plus<sup>®</sup>, was subsequently calculated.

The GFT-J process employed a hydrocracker after the FT reactor. Most of the light components (C<sub>1</sub> - C<sub>4</sub>) are removed from the FT product, whilst a large fraction of the feed also constitutes of recycled waxes. As no literature is available with the precise feed received by the GFT-J process hydrocracker, a cracking function was developed on Microsoft Excel which is based on the feed composition. It was assumed that ideal hydrocracking occurs, as proposed by Regalli [110] for a platinum catalyst, such that hydrocarbon C<sub>(x)</sub>'s cracked product distribution is normal surrounding hydrocarbon C<sub>(x/2)</sub>. An illustration of ideal hydrocracking of C<sub>16</sub>, based on Regalli, is shown in Figure 35.

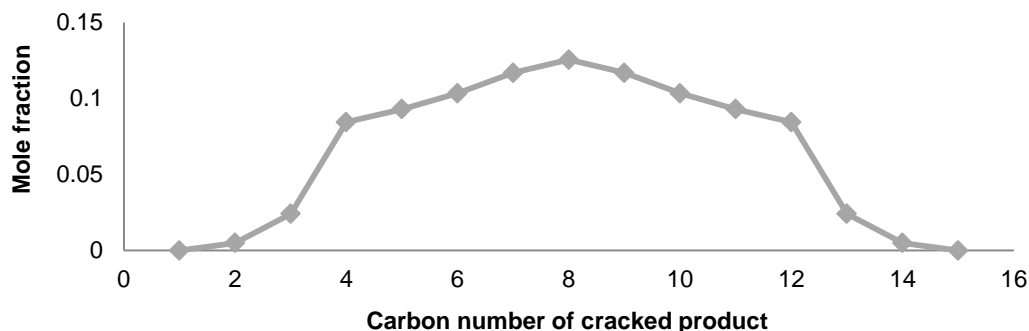


Figure 35: Ideal hydrocracking of C<sub>16</sub>, based on [110]

Further, the extent of hydrocracking was made to increase with increasing carbon number [73] (described by a cumulative normal distribution). The standard deviation for both distributions and mean for the extent of hydrocracking distribution were subsequently manipulated in order that the cracking function accurately described experimental hydrocracker yields of Ekbom et al. [48]; which were based on high severity cracking of a FT product, shown in Figure 54 in Appendix B. The conditions for the hydrocracker of the GFT-J process are as specified by Ekbom et al. – a pressure of 35 bar, temperature of 350°C and a platinum catalyst. The hydrocracker was simulated in Aspen Plus<sup>®</sup> using a yield reactor with simulation of only straight-chain alkanes in Aspen Plus<sup>®</sup>. The hydrocracker temperature was maintained, despite of the exothermic reactions, by feeding part of the hydrogen directly to the hydrocracker. Convergence using the Microsoft Excel cracking function is iterative as the feed to the hydrocracker is based on the cracking, which in turn is a function of the feed.

#### 4.4.7.5 Auto-thermal reformer

The GFT-J process employs an auto-thermal reformer. As the auto-thermal reformer was modelled by Petersen et al. [102] in Aspen Plus<sup>®</sup>, the method by Petersen et al. is referenced. The main assumptions are discussed in section 3.6.2.

#### 4.4.7.6 Pyrolysis

The FP-J process utilizes a pyrolysis reactor. As the pyrolysis reactor in the FP-J process was modelled in Aspen Plus<sup>®</sup> by McLaren [97], the method is referenced. The main assumptions are discussed in section 3.5.2.

### 4.4.8 Utilities and waste water plant

#### 4.4.8.1 Cooling utilities

The process cooling utilities include cooling water, chilled water and refrigeration.

The cooling tower was simulated in Aspen Plus<sup>®</sup>, as prescribed by Petersen [93], using a flash vessel and specifying the outlet temperature (25°C) and the evaporative loss. The subsequent heat duty is divided by the coefficient of performance (COP) to determine the electrical requirements of the cooling tower [93]. A COP of 11.9 was assumed for the cooling tower. For all the processes, a cooling water temperature range of 25°C to 35°C was used (except for the FP-J process, which had a temperature range of 27°C to 45°C as simulated by McLaren [97]). The make-up water to the cooling tower was suggested by Castro et al. [132] to be the sum of the mass of evaporated water, purge water and entrained water. The equations used for evaporative loss and make-up water calculations (based on [132], [32] and [93]) are shown in Appendix B.

No in-depth modelling of the chilling or refrigeration equipment is performed. The COP values for the chilling and refrigeration equipment were taken as 7.2 and 5 respectively.

#### 4.4.8.2 Heating utilities

For all the processes, heating utilities are met within the plant. This was discussed in section 4.4.1.4 and 4.4.1.5.

#### 4.4.8.3 Waste water plant

WWT plants are essential for all the processes to ensure discharge of sufficiently clean water and for recycling of water. The type of WWT plants employed by the various processes is shown in the Table 24. Although all the wastewater was sent through aerobic WWT, anaerobic WWT is only useful if significant organic material is in the wastewater (the case for the SYN-FER-J, S-ETH-J and L-ETH-J process). No anaerobic WWT was, however, performed for the S-ETH-J process as the vinasse product (containing most of the organic material) was regarded as a neutral product. Whether recycling of the wastewater is performed is also indicated in Table 24.

Table 24: Waste water treatment processes

Process	Anaerobic WWT	Aerobic WWT	Wastewater recycling
HEFA	×	✓	×
SYN-FER-J	✓	✓	✓
S-ETH-J	×	✓	✓
L-ETH-J	✓	✓	✓
FP-J	×	✓	×
GFT-J	×	✓	✓

No modelling of the WWT plant was performed on Aspen Plus<sup>®</sup>. The investigation by Humbird et al. [32] was used to determine the overall energy requirements of the WWT

plants. The anaerobic WWT employed by the SYN-FER-J and L-ETH-J processes, produce some biogas which is used in the individual processes (based on [32]).

#### 4.4.9 Biomass drying and grinding

The moisture content (MC) of the feed biomass is given in section 4.2. No biomass drying was required by the S-ETH-J, HEFA or L-ETH-J processes.

The drying of the respective feeds to the GFT-J and SYN-FER-J processes were performed as specified in Table 7 in section 3.6.2 and in Table 23 in section 4.4.7.1. For the GFT-J process, an initial drying MC of 25% was assumed, whilst a MC to the gasification section of the DFB gasifier of 9.5% was chosen for the SYN-FER-J process. The drying was based on the investigation of Petersen et al. [102]; assuming that the biomass drying can be achieved by using the DFB gasifier stack gas and the process combustion off-gas.<sup>M</sup> Drying was also performed by the FP-J process. This was modelled in Aspen Plus<sup>®</sup> by McLaren [97] using process off-gas in a flash vessel (the method by McLaren [97] is referenced).

Grinding was not explicitly modelled in Aspen Plus<sup>®</sup>. According to Ringer et al. [133], significant grinding is required by the FP-J process to reduce fed lignocellulose to sizes smaller than 2 mm. An electrical requirement of 50 kWh per ton of dry feed was assumed [133]. Some grinding of lignocellulose fed to the SYN-FER-J and GFT-J processes are also required to sizes smaller than 50 mm [134]. A lumped electrical requirement for gasification and drying was derived from Phillips et al. [134]. No grinding was required by the S-ETH-J, HEFA or L-ETH-J processes.

#### 4.4.10 Hydrogen production

The process scenarios were constructed such that the processes are hydrogen self-sufficient. As discussed in section 4.4.1.3, hydrogen is recovered from either process off-gas (SYN-FER-J process and GFT-J process) or it is recovered from the products of steam reforming (the other processes). The only process that uses fossil fuel as the source for hydrogen is the FP-J process.

Pressure-swing adsorption (PSA) will mainly be used to recover the hydrogen [135]. According to Spath et al. [135], a hydrogen recovery rate of 85% and product purity of 99.9 volume% can generally be maintained for a 70 mol% hydrogen PSA feed. PSA units were

---

<sup>M</sup> This assumption is supported by an investigation by Dutta et al. who also performed biomass drying in a DFB biomass gasification plant using process off-gas. The investigation by Dutta et al. reduced the MC of the total feed lignocellulose from 50% to 10%.

modelled in Aspen Plus<sup>®</sup> using separator blocks. For feed gasses containing 70 or more mol% hydrogen, an 85% recovery was specified along with absolute purity. For feed gasses containing slightly less than 70 mol% hydrogen, the pure hydrogen product stream is recycled to the PSA feed to ensure a 70 mol% hydrogen feed to the PSA. According to Spath et al., installation of knock-out drums before PSA units is essential to prevent damage of adsorbents by entrained liquids. The energy requirements associated with the PSA were determined from Spath et al.

A different hydrogen recovery approach was taken for the SYN-FER-J process scenarios, based on a patent by Behling et al. [136], as the process off-gas had very low hydrogen concentrations (30-50 mol% hydrogen). The patent described a process (shown in Figure 36) that was able to recover hydrogen from off-gas containing around 20 mol% hydrogen with an overall recovery of 64 mol% hydrogen [136]. Initial concentration of hydrogen from off-gas is first achieved using a selective permeable membrane, whilst final recovery is performed using a PSA unit. An overall hydrogen recovery of 64 mol% was specified for the SYN-FER-J process scenarios in Aspen Plus<sup>®</sup>.

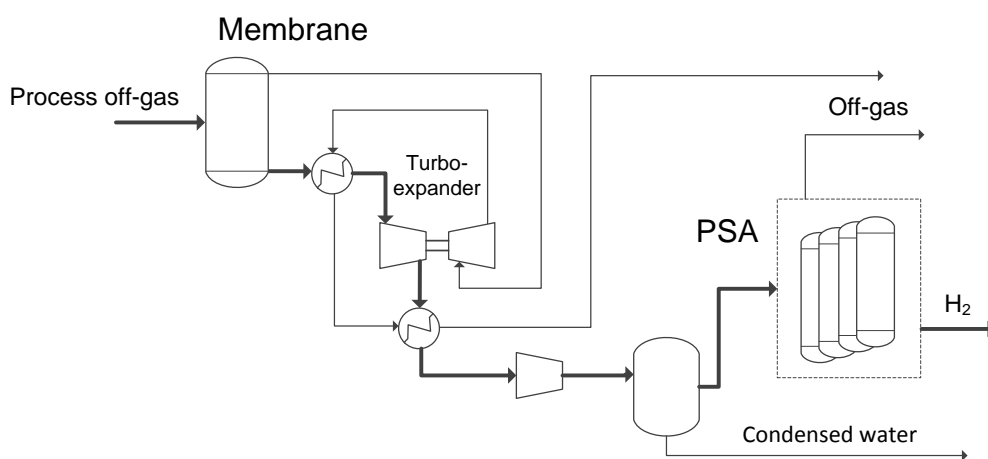


Figure 36: Simplified flow diagram of hydrogen recovery section of the SYN-FER-J process

Steam reforming will be employed by the S-ETH-J and L-ETH-J processes using a part of the ethanol product, by the FP-J process using natural gas and by the HEFA process using off-gas and part of the naphtha product. A simplified process flow diagram of the steam reforming section is shown in Figure 37. After steam reforming of the reformer fuel, the syngas hydrogen content is increased by a high temperature shift reactor. Water is condensed out of the shift reactor product, followed by hydrogen recovery in a PSA unit. Heat is provided to the reforming reactor by combustion in the burner section of the steam reformer.

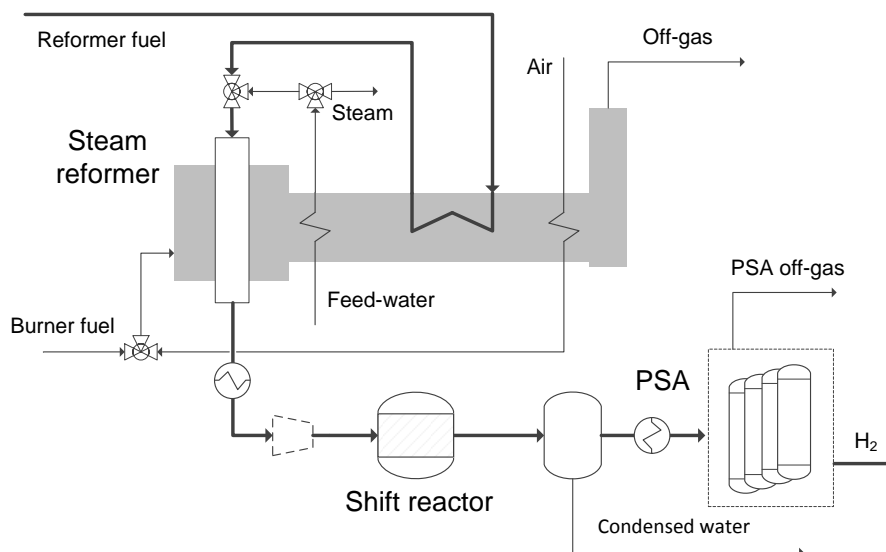


Figure 37: Simplified flow diagram of the steam reforming section, based on [98]

The steam reforming and shift reactor of the FP-J process were modelled by McLaren [97] using yield data of Parkash [137]. The steam reforming reactions of the other processes were modelled in Aspen Plus<sup>®</sup> using Gibbs minimization reactors (similarly to the study by Jones et al. [98]). Steam reforming of ethanol will be performed at atmospheric pressure as Goula et al. [138] found reforming of ethanol to also exhibit close to equilibrium behaviour at atmospheric pressures. The ethanol reforming scenarios consequently have a compressor before the shift reactor. The shift reactor was also modelled in Aspen Plus<sup>®</sup> using a Gibbs minimization reactor. A stoichiometric reactor with complete combustion was used to model the burner section of the steam reformer in Aspen Plus<sup>®</sup>. Table 25 shows the conditions which were used for the steam reforming sections.

Table 25: Steam reforming conditions for the processes

Process	Steam-to-carbon (or -ethanol*) ratio	Steam reformer reactor		Shift reactor	
		Outlet temperature (°C)	Outlet pressure (bar)	Outlet temperature (°C)	Outlet pressure (bar)
HEFA	4.5	850	25.8	353	24.8
FP-J	4.45	857	23.8	390	22.7
L-ETH-J	3*	800	atmospheric	353	24.8
S-ETH-J	3*	800	atmospheric	353	24.8

#### 4.4.11 Power generation

Superheated high pressure steam is required for production of electrical power. Steam generation were performed by all processes using various sources of energy. As discussed

in section 4.4.1.4, the only processes which are in case 2 (i.e. require alternative sources of fuel from the process to meet the process' energy and electrical power requirements) are the HEFA and the SYN-FER-J processes.

Steam generation was performed by the HEFA process from the hydrogen recovery section cooling, the burner section of the steam reformer and the hydrotreatment reactor cooling. The fuel used in the burner section was off-gas and a fraction of the naphtha product. The fraction of the naphtha product sent to the reformer was manipulated to meet the process' energy and electrical power demand. Steam generation for the SYN-FER-J process is mainly from the cooling of the gasification product streams and the combustion of the split fraction of syngas and biogas produced in the anaerobic WWT plant. The fraction of the syngas from the gasification section sent to the combustor is manipulated in order to meet the process' energy and electrical power demand. For the S-ETH-J process, steam is mainly generated from the combustion of the dewatered bagasse and additional trash fed. For the L-ETH-J process, the steam is mainly generated from the combustion of the syrup and lignin from the evaporator section and biogas produced in the anaerobic WWT plant. The steam for the FP-J process is mainly generated from cooling in the quench, hydrotreating, hydrocracking and hydrogen plant sections and from the combustion of char, off-gas, and a fraction of the bio-oil. Some natural gas is also co-fed to the FP-J process as an energy source to the steam reforming section. Steam is mainly generated for the GFT-J process from the cooling of the gasification and FT reactor product streams and the combustion of the upgrading section off-gas, PSA off-gas and a purge stream from the recycle gas to the ATR section.

Biomass boilers were used by the S-ETH-J and L-ETH-J processes (similarly to the study by Humbird et al. [32]). Based on Humbird et al., the boiler efficiencies<sup>N</sup> were specified to be 80% (LHV<sup>O</sup> basis) for the biomass boilers. Incinerators with heat recovery steam generators (HRSG) were used for the FP-J, GFT-J and SYN-FER-J processes. Similarly, an 85% (LHV basis) incineration-steam efficiency was specified for the incineration and HRSG sections of the GFT-J and SYN-FER-J processes. The power generation of the FP-J process simulated by McLaren [97] (which was not available for updating) consisted of an incineration-steam efficiency of around 95%.

---

<sup>N</sup> Boiler efficiency refers to the percentage of fuel heating value which is converted to steam.

<sup>O</sup> Lower heating value

The biomass boilers were modelled, similarly to Humbird et al., as a combustion section and a boiler section. The biomass combustion section was modelled in Aspen Plus<sup>®</sup> as a stoichiometric reactor with 99% conversion specified for all the combustible components in the feed. 20% excess air was sent to the combustor section, whilst the off-gas was assumed to be cooled (by preheating of air) to 180°C. An arbitrary heat loss was specified for the combustion section. The boiler section was modelled in Aspen Plus<sup>®</sup> in a flash vessel with heat flow from the combustion section, whilst a specific flow rate of high pressure water was sent to the boiler to achieve the desired high pressure steam. The assumed boiler efficiency of 80% was achieved by manipulating the heat loss from the combustion section.

The incinerator with HRSG was modelled as a combustion section with down-stream heat exchangers. The incinerator was modelled in Aspen Plus<sup>®</sup> using a Gibbs minimization reactor with 20% excess air and an arbitrary heat loss. Heat recovery from the hot gas is then performed by cooling of gas to 160°C (by HRSG and preheating of air and feedstock). The assumed efficiency of 85% was achieved by manipulating the heat loss from the incinerator. The heat-exchangers used to model the HRSG produce a range of types of steam.

Turbine power generators were used to generate electrical power from superheated high pressure steam. A condensing turbine was employed by all the processes. The number of stages and maximum and minimum pressures used by the investigated processes' turbines are given in Table 26.

Table 26: Turbine number of stages and conditions for investigated processes

Process	Number of Stages	Maximum Pressure (bar)	Minimum Pressure (bar)
HEFA	3	86	0.2 (vacuum)
SYN-FER-J	3	87	0.2 (vacuum)
S-ETH-J	4	90	0.2 (vacuum)
L-ETH-J	4	87	0.2 (vacuum)
FP-J	4	105	0.2 (vacuum)
GFT-J	3	124	0.2 (vacuum)

The specifications used in Aspen Plus<sup>®</sup> to simulate the turbines are shown in Table 27.

Table 27: Turbine specifications

Specification	
Type	Isentropic
Discharge pressure	Process specific
Isentropic efficiency	0.85
Mechanical efficiency	0.96

## 4.5 Equipment Sizing and Cost Estimation

After complete mass and energy balances were constructed for all the investigated processes on Aspen Plus<sup>®</sup>, sizing and costing of equipment commenced.

### 4.5.1 General

The sizing and costing of equipment was performed using literature sources and Aspen Icarus<sup>®</sup>, based on the mass and energy balances in Aspen Plus<sup>®</sup>. An expression was required to cost simulated equipment from literature sources or to update equipment costs (for equipment costed in Aspen Icarus<sup>®</sup>) if size of equipment changed due to process change. Equation 16 was used to determine the new cost based on the new size [139] (or other size related characteristic). The value for the scaling factor (exp) was determined from literature sources (given in Appendix C).

$$New\ Cost = Base\ Cost \times \left( \frac{New\ Size}{Base\ Size} \right)^{exp} \quad \text{Equation 16}$$

As the costing of equipment was done using various sources based on different years, Equation 17 was used to update the costs to the base year of the assessment [139]. The Chemical Engineering Plant Cost Index (given in Table 155 in Appendix I) was used to adjust the capital costs.

$$New\ Cost = Base\ Cost \times \left( \frac{Cost\ Index\ in\ New\ Year}{Cost\ Index\ in\ Base\ Year} \right) \quad \text{Equation 17}$$

Installed costs were determined for the equipment by multiplying the purchased equipment costs by an installation factor. For equipment costed in Aspen Icarus<sup>®</sup>, the installation factor were determined from Aspen Icarus<sup>®</sup>. For the equipment costs derived from literature sources, the accompanying installation factors prescribed by the literature were used. For literature costs not accompanied by installation factors, alternative sources of literature were used [98], [36], [69], [32]. The installation factors of the main equipment derived from literature sources are given in Appendix C.

### 4.5.2 Aspen Icarus

The size and cost of common equipment are accurately predicted using Aspen Icarus<sup>®</sup> software. Aspen Icarus<sup>®</sup> was used for most compressors, turbo-expanders, flash drums, liquid-liquid separators and distillation columns. The dehydration reactor, used for upgrading of the ethanol, was also costed in Aspen Icarus<sup>®</sup>. The simulation of processes in Aspen Plus<sup>®</sup> was imported into Aspen Icarus<sup>®</sup>. For accurate costing of equipment, additional

equipment specific information needs to be entered. A summary of the information used to cost the equipment in Aspen Icarus<sup>®</sup> is given in Table 100 in Appendix C.

#### 4.5.3 Capital costs from literature

Capital costs of the major equipment were generally based on literature. The literature, along with the costing data used to determine the capital costs are displayed for the main equipment in Appendix C. The capital costing data in Appendix C are divided up into various tables for the individually investigated process. The total capital costs for the ethanol production sections of the S-ETH-J and L-ETH-J processes were derived from literature (displayed in Table 103 and Table 105 in Appendix C).

### 4.6 Economic Analysis

An economic analysis is a crucial tool for comparison of various processes [130]. The economics of investigated processes could be used to determine the potential of these processes on the marketplace. According to Kazi et al. [58], it would, however, be more useful in determining the relative potential of the various processes in the future. The economic investigation for each process will be based on the complete mass and energy balances on Aspen Plus<sup>®</sup>.

The cost analysis will be performed assuming an  $n^{\text{th}}$  plant design as described by Jones et al. [98]:

“These assumptions do not account for additional first of a kind plant costs, including special financing, equipment redundancies, large contingencies and longer start-up times necessary for the first few plants. For  $n^{\text{th}}$  plant designs, it is assumed that the costs reflect a future time when the technology is mature and several plants have already been built and are operating.”

The economic investigation will be performed in this study based on an international estimate basis in 2007 US dollars. <sup>P</sup>

#### 4.6.1 Capital Investment

A preliminary estimate of the plant cost will be done for the processes, for which an estimated accuracy range of  $\pm 30\%$  is expected [125], [130]. The method used to determine

---

<sup>P</sup> As this investigation was performed based on costing in the year 2007, direct comparison of economic outputs (such as minimum jet selling prices) with current values should not be done. This assessment is, however, useful to compare the economic outputs of different processes with each other.

the FCI and the total capital investment (TCI) from total installed cost was derived from studies by Jones et al. [98], Dutta et al. [36], Swanson et al. [69] and Humbird et al. [32]. The method to determine the FCI and TCI is given in Table 28. Once the purchased and installed costs are determined (method is discussed in section 4.5), additional direct costs and indirect costs are added to determine the FCI. Additional direct costs are determined relative to the total installed costs. Indirect costs (such as project contingency, field expenses, home office and construction costs and other costs related to construction) are computed as a function of the total direct costs. The sum of the FCI, working capital and land cost is the TCI. The capital investments of all the processes are given and discussed in section 6.

Table 28: FCI and TCI calculation assumptions

Process Area	Purchases Cost (PC)	Installed cost (IC)
Area A	PC (Process Area A)	IC (Process Area A)
Area B	PC (Process Area B)	IC (Process Area B)
.	.	.
.	.	.
.	.	.
<b>Totals</b>	<b>Sum of PC (<math>\sum PC</math>)</b>	<b>Sum of IC (<math>\sum IC</math>)</b>
Additional Direct Costs	10% of total IC <sup>1</sup>	<b>0.1 x <math>\sum IC</math></b>
<b>Total Direct Costs (TDC)</b>		<b>1.1 x <math>\sum IC</math></b>
Prorated Expenses	10% of TDC	<b>0.1 x TDC</b>
Field Expenses	10% of TDC	<b>0.1 x TDC</b>
Home Office & Construction Fee	20% of TDC	<b>0.2 x TDC</b>
Project Contingency	10% of TDC	<b>0.1 x TDC</b>
Other Costs	10% of TDC	<b>0.1 x TDC</b>
<b>Total Indirect Costs (TIC)</b>		<b>0.6 x TDC (or 0.66 x <math>\sum IC</math>)</b>
<b>Fixed Capital Investment (FCI)</b>	TDC + TIC	<b>1.76 x <math>\sum IC</math></b>
Land		<b>Land Cost</b>
Working Capital	10% of FCI	<b>0.1 x FCI</b>
<b>Total Capital Investment (TCI)</b>		<b>1.936 x <math>\sum IC</math> + Land Cost</b>

<sup>1</sup> A relatively low additional direct cost factor is justified as major balance of plant costs (such as cooling towers and waste water treatment plants) are costed explicitly.

#### 4.6.2 Variable operating cost

Variable operating costs are costs that vary with production rate and include raw materials, waste disposal costs, by-product credits and periodic costs. The variable operating costs will be determined using the mass and energy balances and the latest available information of costs. The main variable operating costs for the processes are generally the feedstock cost and by-product credits. Table 29 gives the base feedstock cost assumed for the processes. Table 30 gives the base values for the other main variable operating costs. Natural gas,

enzymes and trash are feed that constitute of a large fraction of the variable operating costs for the FP-J, L-ETH-J and S-ETH-J processes respectively.

Table 29: Base feedstock cost

Feedstock	Process	Cost (2007\$)	Literature Source
Lignocellulose	L-ETH-J, GFT-J, SYN-FER-J	\$70 per dry MT	Based on in-house information, [32], [98] and [36].
Lignocellulose	FP-J	\$71.97 per dry MT <sup>1</sup>	
Vegetable oil	HEFA	\$700 per dry MT <sup>2</sup>	[140]
Sugarcane	S-ETH-J	\$30 per wet MT <sup>3</sup>	[141]

<sup>1</sup> Adjusted cost for lignocellulose due to decreased assumed ash content of FP-J process (0.99 wt%) versus the other processes (3.7 wt%); <sup>2</sup> Based on linear regression of vegetable oil data by [140] (average of soybean and palm oil); <sup>3</sup> Based on linear regression of sugarcane data by [141].

Table 30: Other main variable operating base costs

Feed	Cost (2007\$)	Literature Source
Natural gas	\$200 per MT <sup>1</sup>	[140]
Enzyme	\$507 per MT broth <sup>2</sup>	[58]
Trash	\$70 per dry MT	- <sup>3</sup>
Product	Cost (2007\$)	Literature Source
Naphtha	\$0.79 per litre <sup>4,5</sup>	[140]
Diesel	\$0.88 per litre <sup>5</sup>	[140]
Grid electricity	\$0.08 per kWh	In-house information

<sup>1</sup> Based on linear regression of natural gas cost data by [140]; <sup>2</sup> 10% broth as specified by [58]; <sup>3</sup> Based on the lignocellulose cost; <sup>4</sup> For the FP-J process (which produces jet fuel along with naphtha, diesel and gas oil), the diesel and gas oil is fixed to the naphtha price; <sup>5</sup> Based on linear regression of fuel data by [140] with an assumed 50% increase for fuel product cost due to green premium (in-house-information).

A summary of all the cost information derived from literature sources, used to determine the total variable operating cost, is given in Table 127 and Table 128 in Appendix G. Although a variety of operating cost indices are available, the Inorganic Chemical Index was commonly used by literature investigating similar processes [32], [98], [69], [36]. The Inorganic Chemical Index (given in Table 156 in Appendix I) will be used to adjust the literature sourced variable operating costs to 2007 US dollars (using Equation 17 in section 4.5.1). The variable operating costs associated with all the processes are given section 6.

#### 4.6.3 Fixed operating cost

Fixed operating costs are costs that are not a function of plant operation rate and are thus incurred regardless of whether the plant is producing at full capacity or not [32]. Fixed operating costs include labour and various overhead items. The method used to determine the fixed operating costs of the processes were based on studies by Jones et al. [98], Dutta et al. [36], and Humbird et al. [32]. The method, shown in Table 31, determines the labour and supervision costs based on literature salaries, whilst adding a 90% labour burden [32].

The additional fixed operating costs of maintenance and property insurance & tax are determined based on the FCI. As no in-depth investigation surrounding the fixed operating costs were performed, the same number of employees were assumed for all processes except the HEFA process (which is significantly simpler). The Labour Index (given in Table 157 in Appendix I) will be used to adjust the literature sourced labour costs to 2007 US dollars (using Equation 17 in section 4.5.1). The fixed operating costs associated with all the processes are given section 6.

Table 31: Fixed operating cost assumptions

<b>Labour and supervision</b>		
<u>Position</u>	<u>Number required</u> <sup>1</sup>	<u>Salaries (2009\$)</u> <sup>2</sup>
Plant manager	1	147 000
Plant engineer	2	70 000
Maintenance supervisor	1	57 000
Maintenance technician	16 (12)	40 000
Lab manager	1	56 000
Lab technician	3	40 000
Shift supervisor	5	48 000
Shift operators	40 (20)	40 000
Yard employees	12 (4)	28 000
Clerks & secretaries	3	36 000
Total salaries		Sum of salaries ( $\sum$ Salaries)
Labour burden		90% of sum of salaries
<b>Other overhead</b>		
Maintenance		3.0% of FCI
Property insurance & tax		0.7% of FCI
<b>Total fixed operating costs</b>		$1.9 \times (\sum \text{Salaries}) + 0.037 \times \text{FCI}$

<sup>1</sup> Values for the HEFA process are given in brackets; <sup>2</sup> Salaries are taken from [36].

#### 4.6.4 Discounted cash flow analysis

To determine the economics of projects, the time value of money needs to be taken into account [139]. After the capital investment, variable operating costs and fixed operating costs were determined, a cash flow analysis was performed in Microsoft Excel based on the study by Humbird et al. [32].

Figure 38 shows the significant variability in the market jet fuel price (specifically for the US Gulf Coast). As the future cost of jet fuel (and biojet fuel) is uncertain [5], the method which will be used to compare projects in conjunction with the cash flow analysis is calculation of the minimum jet selling price (MJSP). The MJSP is determined by changing the jet fuel product cost to obtain a NPV of zero at a specific discount rate (equal to the minimum

acceptable IRR). MJSP can be used to compare the processes with each other as well as determining the economic feasibility of the processes (comparing the MJSP to market jet fuel prices). As the MJSP of the processes are significantly higher than market jet fuel prices, calculation of economic criterion (such as NPV or DCFROR) were not deemed worthwhile.

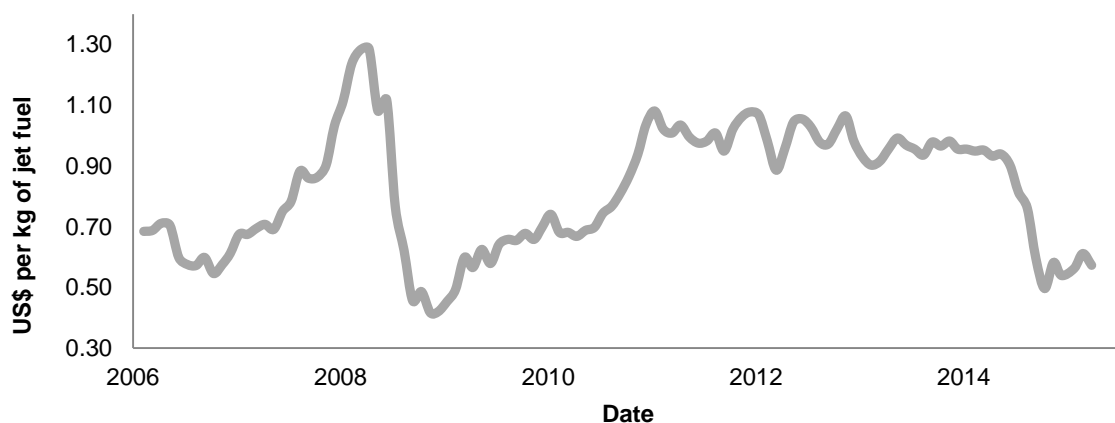


Figure 38: U.S. Gulf Coast Kerosene-Type Jet Fuel Spot Price, [140]

In order to make comparisons of various processes possible, similar economic assumptions need to be made. The economic assumptions used for economic analysis (based on in-house information and studies by Jones et al. [98], Dutta et al. [36] and Humbird et al. [32]) are given in Table 32.

Table 32: Economic assumptions (n<sup>th</sup> plant)

Assumption description	Assumed value
Minimum acceptable internal rate of return	9.3% <sup>1</sup>
Plant financing debt / equity	60% / 40% of total capital investment
Plant life	20 years <sup>2</sup>
Income tax rate	28% <sup>1</sup>
Interest rate for debt financing	6.3% annually <sup>1</sup>
Term for debt financing	20 years
Working capital cost	10% of fixed capital investment
Depreciation schedule	7-years MACRS <sup>3</sup> schedule
Construction period	3 years (8% 1 <sup>st</sup> year, 60% 2 <sup>nd</sup> year, 32% 3 <sup>rd</sup> year) <sup>4</sup>
Plant salvage value	No value
Start-up time	6 months
Revenue and costs during start-up	Revenue = 50% of normal Variable costs = 75% of normal Fixed costs = 100% of normal
On-stream factor	90% (7884 operating hours per year) <sup>5</sup>

<sup>1</sup> In-house information; <sup>2</sup> Same plant life for all the processes, no obvious justification to have different plant life; <sup>3</sup> Modified Accelerated Cost Recovery System; <sup>4</sup> The percent expenditure of the project cost during each construction year; <sup>5</sup> The only exception is the S-ETH-J process with an on-stream factor of 75% due to sugarcane feedstock availability considerations.

#### 4.6.5 Economic sensitivity analysis

As a large amount of uncertainty is associated with the economic parameters used in the economic analysis, a sensitivity analysis will be used to determine the effects of changing economic parameters on the MJSP. The chosen sensitivity analysis parameters, shown in Table 33, consist of the baseline values along with favourable and unfavourable parameter values.

Table 33: Sensitivity analysis parameters

Parameter	Favourable	Baseline	Unfavourable
Stream factor <sup>1</sup>	0.95	0.9	0.85
FCI (% of baseline) <sup>2</sup>	70%	100%	130%
Lignocellulose cost (\$ per dry MT) <sup>3</sup>	40	70	120
Vegetable oil cost (\$ per MT)	400	700	1100
Sugarcane cost (\$ per wet <sup>4</sup> MT)	22	30	40
Selling price of electricity product (\$ per kWh)	0.1	0.08	0.05
Price of naphtha product (\$ per litre) <sup>5</sup>	1.10	0.79	0.55
Price of natural gas feed (\$ per kg) <sup>6</sup>	0.1	0.2	0.4
Enzyme cost (\$ per MT broth) <sup>7</sup>	254	507	1014
Catalyst cost (% of baseline)	50%	100%	150%
Internal rate of return (%)	6%	9.3%	14%
Income tax rate	24%	28%	32%
Interest rate for debt financing	4%	6.3%	9%
Working capital (% of FCI)	5%	10%	15%
Maintenance (% of FCI)	2%	3%	4%

<sup>1</sup> The sensitivity analysis of the stream factor for the S-ETH-J process is performed around the base of 0.75 (0.85, 0.75 & 0.65); <sup>2</sup> The unfavourable scenario for the HEFA process will be taken as 150% of the baseline FCI; <sup>3</sup> For lignocellulose with 3.7 wt% ash, cost is adjusted with same ratio for the FP-J process lignocellulose and sugarcane trash; <sup>4</sup> Composition as specified in 4.2.2.; <sup>5</sup> For the FP-J process, the diesel and gas oil is changed relative to the naphtha price; <sup>6</sup> Only employed by the FP-J process; <sup>7</sup> Only employed by the L-ETH-J process.

During the screening assessment (section 2) it became apparent that the extent to which the processes were optimized for jet fuel had a significant effect on the MJSP. This is because the calculated MJSP's for the investigated processes are generally much larger than the price used for the other fuel products. Although most of the processes were aimed for maximum possible jet fuel (except for the FP-J process), complete maximization of jet fuel was not done for the processes. To investigate the effect of the different extents of maximization for jet fuel between the processes, a theoretical process sensitivity analysis, adjusting the overall jet-to-fuel mass ratios, will be done.

## 5 Process Mass and Energy Overview

This section will give an overview of the mass and energy flows of the investigated processes. An overview of the hydrogen, power and water usage will also be given.

Tables consisting of the processes' power generation and usage and make-up water calculations are given in Appendix D.

### 5.1 HEFA Process

A process description of the HEFA process is performed in section 4.3.1. The summary of the energy balances of the HEFA process is given in Table 34.

Table 34: Summary of energy balance of the HEFA process

Major Inputs			
		Mass flow (kg/h)	Energy (MW) <sup>1</sup>
<b>FEEDSTOCK</b>	Vegetable oil <sup>2</sup>	14 873	161.1
<b>FOSSIL SOURCE</b>	-	-	-
Major Outputs			
		Mass flow (kg/h)	Energy (MW) <sup>1</sup>
<b>FUEL</b>	Jet fuel	7 139	94.4
	Naphtha fuel <sup>3</sup>	1 705	22.8
	Diesel fuel	305	4.0
<b>OTHER</b>	Electrical export	-	0
	Energy Losses <sup>4</sup>	-	39.9

<sup>1</sup> Energy based on HHV of input or output (calculated in Aspen Plus®); <sup>2</sup> Composition is discussed in section 4.2.3; <sup>3</sup> Of the total naphtha produced (3867 kg/h), 56% is used to satisfy the process' hydrogen and electrical power requirement; <sup>4</sup> Energy losses include cooling water, heat and power generation losses.

Table 35 compares the jet fuel mass ratio of the HEFA process to literature which also aimed for maximum jet fuel. There is good agreement between the three studies.

Table 35: Vegetable oil hydroprocessing process jet fuel mass ratios

	HEFA process	Pearlson [15]	Klein-Marcuschamer et al. [5]
Jet fuel mass ratio <sup>1</sup>	0.480	0.494	0.480

<sup>1</sup> Jet fuel mass divided by the mass of the vegetable oil in the feed.

The HEFA process' hydrogen usage, as well as its source, is given in Table 36. Light gasses from the separation section and a fraction of the naphtha product were used to meet the process' hydrogen demand.

Table 36: The HEFA process hydrogen usage and source

Process section	Hydrogen used (kg/h)	Specific hydrogen usage <sup>1</sup>	Source of hydrogen
Hydrotreating	493.8	65.3	Light gasses (C <sub>6</sub> -) from the separation section and 29% of the naphtha product (C <sub>6</sub> -C <sub>8</sub> )
Hydrocracking	103.7		

<sup>1</sup> kg Hydrogen usage per MT of total fuel produced.

The power generation and usage of the HEFA process is shown in Table 37. The HEFA process only produces sufficient electricity to be electrical power self-sufficient. Gas compression accounts for over 72% of the total power usage.

Table 37: Power generation and usage of the HEFA process

<b>Net export</b>	<b>0.00 MW</b>
Total usage	2.60 MW
Total generated	2.60 MW

The HEFA process requires only 28.9 MT/h of make-up water. The boiler feed to the steam reformer requires 6.9 MT/h of make-up water, whilst the cooling tower water losses amount to 18.2 MT/h. All the wastewater (3.6 MT/h) is treated and discarded.

## 5.2 SYN-FER-J Process

A process description of the SYN-FER-J process is given in section 4.3.2. A summary of the energy balances for the three scenarios of the SYN-FER-J process is given in Table 38.

Table 38: Summary of energy balances of the SYN-FER-J process scenarios

Scenario		A.1	A.2	B	A.1	A.2	B
<b>Major Input</b>							
		<b>Mass flow (dry, kg/h)</b>			<b>Energy (MW)<sup>2</sup></b>		
<b>FEEDSTOCK</b>	Lignocellulose <sup>1</sup>	77 882			400.5		
<b>FOSSIL SOURCE</b>	-	-	-	-	-	-	-
<b>Major Outputs</b>							
		<b>Mass flow (dry, kg/h)</b>			<b>Energy (MW)<sup>2</sup></b>		
<b>FUEL</b>	Jet fuel	7 412	7 937	7 847	97.9	104.8	103.6
	Diesel fuel	966	1 035	1 023	12.7	13.6	13.4
<b>OTHER</b>	Electrical export	-	-	-	0	0	0
	Energy Losses <sup>3</sup>	-	-	-	289.9	282.1	283.5

<sup>1</sup> Composition is discussed in section 4.2.1; <sup>2</sup> Energy based on HHV of input or output (calculated in Aspen Plus®); <sup>3</sup> Energy losses include cooling water, heat and power generation losses.

The intermediate product of the SYN-FER-J process is ethanol. Although a fraction of syngas is sent to the steam & power plant, if all the syngas was used for ethanol production by the three scenarios (A.1, A.2 and B), respective yields of 270, 217 and 243 kg ethanol per dry MT lignocellulose are possible. These overall yields compare relatively well to yields proposed by syngas fermentation companies Ineos Bio (245 – 330 kg ethanol per dry MT lignocellulose) and Coskata (330 kg ethanol per dry MT lignocellulose) [37].

The hydrogen usage and source of the SYN-FER-J process is given in Table 39. This excludes the hydrogen in the syngas which is used for syngas fermentation. The SYN-FER-J process uses unconverted syngas for hydrogen recovery.

Table 39: The SYN-FER-J process hydrogen usage and source

Process section	Scenario	Hydrogen used (kg/h)	Specific hydrogen usage <sup>1</sup>	Source of hydrogen (% of the off-gas from the separation section) <sup>2</sup>
Hydroprocessing	A.1	101.6	12.1	33.4
	A.2	108.8	12.1	11.9
	B	107.6	12.1	11.6

<sup>1</sup> kg Hydrogen usage per MT of total fuel produced; <sup>2</sup> Other off-gas is sent to the steam & power plant.

The process scenarios only produce enough electricity to be electrical power self-sufficient. The split fraction of syngas from the gasification plant, which is sent to the steam & power plant to meet processes' energy and electrical power requirements, is shown in Table 40.

Table 40: Syngas fraction of SYN-FER-J processes sent to steam & power plant

Scenario	A.1	A.2	B
Fraction	0.350	0.132	0.233

The power generation and usage of the SYN-FER-J process scenarios is shown in Table 41.

Table 41: Power generation and usage of SYN-FER-J process

Scenario	A.1	A.2	B
Net export (MW)	0.00	0.00	0.00
Total usage (MW)	28.53	25.94	29.64
Total generated (MW)	28.65	26.23	30.7

For the SYN-FER-J scenarios, the plant sections that have the highest power usage are the WWT plant (26% - 33%), the gasification plant (17% - 36%) and the utilities consisting mainly of the cooling tower (19% - 21%). In comparison to scenario A.2, scenario B has a

higher power usage due to compressors in the gasification plant, whilst scenario A.1 has a higher power usage due to a higher syngas recycle flow rate in the fermentation section.

Gaddy et al. [116] proposed a scenario where the separation section bottoms are recycled to the fermenters without wastewater treatment.<sup>Q</sup> This would significantly reduce the power usage of the WWT plant and possibly enable the SYN-FER-J scenarios to be electricity self-sufficient without diverting syngas to the steam & power plant. Gaddy et al. found that the acetic acid in the recycle water could also increase the ethanol yield from the syngas by shifting the reactions to ethanol. Recycling the separation section bottoms will, however, significantly reduce the biogas produced by the anaerobic digestion from the organics in the wastewater. Further investigation into water recycle is recommended.

The make-up water required by the SYN-FER-J process scenario A.1, A.2 and B are 343.2 MT/h, 333.7 MT/h and 337.8 MT/h respectively. For all the scenarios the cooling tower water loss accounts for over 85% of the process water loss.

The main contributors of the cooling water duty (and therefore cooling water loss) are illustrated in Table 42. The high cooling water duty for the separation section (especially the beer column condenser) is due to the low ethanol concentration achieved by the fermentation section of the SYN-FER-J process scenarios (2-2.5 wt% ethanol in comparison to 3.9 wt% and 12.3 wt% achieved by the L-ETH-J and S-ETH-J processes respectively).

Table 42: Main contributors to cooling water duty of SYN-FER-J process scenarios (% of total duty)

Scenario	A.1	A.2	B
Separation section	45.6%	45.1%	41.0%
Condensing turbine	27.0%	26.4%	29.2%
Fermentation section	18.1%	18.2%	15.9%

### 5.3 S-ETH-J Process

The process description of the S-ETH-J process is given in section 4.3.3. The summary of energy balance of the S-ETH-J process is given in Table 43. Apart from the sugarcane, significant amounts of trash are also fed to the S-ETH-J process accounting for over 36% of the energy in the feed.

---

<sup>Q</sup> The specific experimental data of Gaddy et al. unfortunately consisted of transient data, whereas steady-state data was required for this investigation.

Table 43: Summary of the energy balance of the S-ETH-J process

Major Inputs			
		Mass flow (dry, kg/h)	Energy (MW) <sup>2</sup>
FEEDSTOCK	Sugarcane <sup>1</sup>	63 272	288.6
	Trash <sup>1</sup>	31 158	165.3
FOSSIL SOURCE	-	-	-
Major Outputs			
		Mass flow (kg/h)	Energy (MW) <sup>2</sup>
FUEL	Jet fuel	7 763	102.6
	Diesel fuel	1 012	13.3
OTHER	Electrical export	-	52.6 <sup>3</sup>
	Energy Losses <sup>4</sup>	-	285.4

<sup>1</sup> Composition is discussed in section 4.2.2; <sup>2</sup> Energy based on HHV of input or output (calculated in Aspen Plus<sup>®</sup>); <sup>3</sup> Net electrical power produced, in MW; <sup>4</sup> Energy losses include cooling water, heat and power generation losses.

The hydrogen usage and source of the S-ETH-J process, is given in Table 44. A small fraction of the ethanol intermediate product is used for hydrogen production.

Table 44: The S-ETH-J process hydrogen usage and source

Process section	Hydrogen used (kg/h)	Specific hydrogen usage <sup>1</sup>	Source of hydrogen
Hydroprocessing	106.4	12.1	3.8% of the ethanol intermediate product

<sup>1</sup> kg Hydrogen usage per MT of total fuel produced.

The power generation and usage of the S-ETH-J process is shown in Table 45. The process produces significant excess amounts of electricity mainly due to the additional trash fed to the process. It was determined that apart from the trash fed, the process can still obtain electricity self-sufficiency, but with considerable less power generation (a net export of less than 10 MW). The sugarcane to ethanol plant and the utilities (mainly cooling tower) account for 4.9 MW and 4.2 MW of the power usage respectively.

Table 45: Power generation and usage of S-ETH-J process

<b>Net export</b>	<b>52.62 MW</b>
Total usage	15.46 MW
Total generated	68.07 MW

Although the wet sugarcane fed to the S-ETH-J process contains large amounts of water, the S-ETH-J process requires 227.6 MT/h of make-up water. Around 108 MT/h water is lost along with the vinasse as the S-ETH-J process regards the vinasse as a neutral product.

The water loss in the WWT plant was chosen to be 15.8% of the total wastewater (a loss of 21.8 MT/h) such that the make-up water can meet the cooling water make-up (227.6 MT/h). Over 60% of the cooling water duty (and hence cooling water loss) is attributed to the condensing turbine which aids at the production significant surplus electricity. The second largest cooling water duty contributor was the separation section (16.2% of the total duty).

## 5.4 L-ETH-J Process

A process description of the L-ETH-J process is given in section 4.3.4. The summary of the energy balance of the L-ETH-J process is given in Table 46.

Table 46: Summary of energy balance of the L-ETH-J process

Major Inputs			
		Mass flow (dry, kg/h)	Energy (MW) <sup>2</sup>
<b>FEEDSTOCK</b>	Lignocellulose <sup>1</sup>	77 882	404.2
<b>FOSSIL SOURCE</b>	-	-	-
Major Outputs			
		Mass flow (kg/h)	Energy (MW) <sup>2</sup>
<b>FUEL</b>	Jet fuel	7 751	102.4
	Diesel fuel	1 011	13.3
<b>OTHER</b>	Electrical export	-	19.1 <sup>3</sup>
	Energy Losses <sup>4</sup>	-	269.4

<sup>1</sup> Composition is discussed in section 4.2.1; <sup>2</sup> Energy based on HHV of input or output (calculated in Aspen Plus<sup>®</sup>); <sup>3</sup> Net electrical power produced, in MW; <sup>4</sup> Energy losses include cooling water, heat and power generation losses.

The L-ETH-J process produces around 200 kg ethanol per MT lignocellulose fed (dry and ash-free), which is considerably less than what is proposed by Humbird et al. [32] (between 240 to 270 kg ethanol per MT dry & ash-free lignocellulose<sup>R</sup>). In contrast to the other 2G fed processes investigated in this study, the L-ETH-J process does not have the ability to produce fuels from the carbon in the lignin fraction. For the L-ETH-J process the lignin fraction (and unconverted xylose) is combusted for steam and electricity production.

The hydrogen usage and source of the L-ETH-J process, is given in Table 47. The L-ETH-J process uses a fraction of the ethanol intermediate product for hydrogen production.

---

<sup>R</sup> The major difference is the xylose yield to ethanol. Humbird et al. assumes a yield of 85%, whilst the L-ETH-J process (based on Petersen) uses a yield of 44%.

Table 47: The L-ETH-J process hydrogen usage and source

Process section	Hydrogen used (kg/h)	Specific hydrogen usage <sup>1</sup>	Source of hydrogen
Hydroprocessing	105.7	12.1	3.8% of the ethanol intermediate product

<sup>1</sup> kg Hydrogen usage per MT of total fuel produced.

The power generation and usage of the L-ETH-J process is shown in Table 48. The L-ETH-J process produces excess electricity. The sections that consume the most power are the pretreatment & conditioning section with 5.3 MW and the WWT plant with 7.2 MW.

Table 48: Power generation and usage of the L-ETH-J process

<b>Net export</b>	<b>19.05 MW</b>
Total usage	23.79 MW
Total generated	42.84 MW

The L-ETH-J process requires 212.2 MT/h of make-up water. The water purge of the boiler water and wastewater flow was chosen to be 8.2% (a loss of 30.7MT/h), such that the make-up water can meet the cooling water make-up (212.2 MT/h). The cooling tower water loss was about 87% of the total water loss (243 MT/h); similar to the 90% suffered by the study of Humbird et al [32]. According to Humbird et al., a significant reduction of water usage can be achieved if air cooling is used across the process.

## 5.5 FP-J Process

A process description of the FP-J process is given in section 4.3.5. The summary of the energy balance of the FP-J process is given in Table 49. Along with the lignocellulose, a substantial amount of natural gas was also fed to the FP-J process accounting for over 28% of the energy in the feed (for every 100 carbon atoms of lignocellulose fed, 17.4 carbon atoms are fed from natural gas). The FP-J process was the only process that used fossil sources in the feed.

Table 49: Summary of energy balance of the FP-J process

Major Inputs			
		Mass flow (dry, kg/h)	Energy (MW) <sup>2</sup>
<b>FEEDSTOCK</b>	Lignocellulose <sup>1</sup>	83 461	453.5
<b>FOSSIL SOURCE</b>	Natural gas	11 812	182.1
Major Outputs			
		Mass flow (kg/h)	Energy (MW) <sup>2</sup>
<b>FUEL</b>	Jet fuel	4 412	54.2
	Naphtha fuel	4 019	51.6
	Diesel fuel	1 878	23.4
	Gas oil	1 711	21.3
<b>OTHER</b>	Electrical export	-	63.5 <sup>3</sup>
	Energy Losses <sup>4</sup>	-	421.6

<sup>1</sup> Composition is discussed in section 4.2.1; <sup>2</sup> Energy based on HHV of input or output (all calculated in Aspen Plus®, except lignocellulose which is based on the study by McLaren [97]); <sup>3</sup> Net electrical power produced, in MW; <sup>4</sup> Energy losses include cooling water, heat and power generation losses.

In contrast to the other processes investigated in this study, the FP-J process did not aim for maximum jet fuel, with jet fuel only accounting for 36% of the energy in the fuel products. Table 50 compares the overall process fuel mass ratio for the FP-J process to literature. The low fuel yield of the FP-J process is attributed due to the use of a fraction of bio-oil for energy generation as well as the lower heavy hydrocarbon yield in comparison to Jones et al. [98] and Brown et al. [51].

Table 50: Fast pyrolysis with upgrading fuel mass ratios

	FP-J process	Jones et al. [98]	Brown et al. [51]
Fuel mass ratio <sup>1</sup>	0.15	0.28	0.26

<sup>1</sup> Mass of fuel divided by the mass of dry lignocellulose in the feed.

Hydrogen considerations play a critical role in the fast pyrolysis with upgrading process pathway [54]. The FP-J process' hydrogen usage, as well as its source, is given in Table 51. The hydrogen usage of the FP-J process is very high with 128.2 kg hydrogen consumed per MT of total fuel produced. Natural gas was used as the source for hydrogen. In comparison to literature, the make-up hydrogen for both the FP-J process and Jones et al. [98] were around 44 kg per MT biomass fed, whereas Brown et al. only required around 24 kg per MT biomass fed. The hydrogen use per fuel produced of the FP-J process is, however, much more compared to Jones et al. [98] and Brown et al. as the FP-J process produced much less fuel.

Table 51: The FP-J process hydrogen usage and source

Process section	Hydrogen used (kg/h)	Specific hydrogen usage <sup>1</sup>	Source of hydrogen
Hydrotreating	792.0	128.2	8319 kg/h of natural gas
Hydrocracking & Separation <sup>2</sup>	748.4		

<sup>1</sup> kg Hydrogen usage per MT of total fuel produced; <sup>2</sup> Specifically for the hydrocracker.

The power generation and usage of the FP-J process is shown in Table 52. A significant fraction of the intermediate bio-oil (23%) is sent to the steam & power plant. The FP-J process produces significant surplus electricity. The major power usage sections were feedstock grinding, the pyrolysis section and the hydrogen plant accounting for 5.0 MW, 5.8 MW and 10.7 MW respectively.

Table 52: Power generation and usage of the FP-J process

<b>Net export</b>	<b>63.48 MW</b>
Total usage	29.55 MW
Total generated	93.03 MW

The FP-J process requires 253.7 MT/h of water make-up. 41.5 MT/h of steam is sent to the hydrogen plant, whilst cooling tower water loss amounted to 207.3 MT/h. Over 98% of the cooling water duty is attributed to the condensing turbine which aids at the significant surplus electricity production. The FP-J process produced 44.7 MT/h of wastewater (mainly from the hydrotreater section and hydrogen plant) which was treated and discarded.

## 5.6 GFT-J Process

A process description of the GFT-J process is performed in section 4.3.6. The summarized energy balance of the GFT-J process is given in Table 53.

Table 53: Summary of energy balance of the GFT-J process

Major Inputs			
		Mass flow (dry, kg/h)	Energy (MW) <sup>2</sup>
<b>FEEDSTOCK</b>	Lignocellulose <sup>1</sup>	77 882	399.1
<b>FOSSIL SOURCE</b>	-	-	-
Major Outputs			
		Mass flow (kg/h)	Energy (MW) <sup>2</sup>
<b>FUEL</b>	Jet fuel	7 926	104.3
	Naphtha fuel	2 388	31.8
<b>OTHER</b>	Electrical export	-	12.5 <sup>3</sup>
	Energy Losses <sup>4</sup>	-	250.5

<sup>1</sup> Composition is discussed in section 4.2.1; <sup>2</sup> Energy based on HHV of input or output (calculated in Aspen Plus<sup>®</sup>); <sup>3</sup> Net electrical power produced, in MW; <sup>4</sup> Energy losses include cooling water, heat and power generation losses.

Table 54 compares the overall process fuel mass ratio and gasifier conditions of the GFT-J process to literature. Table 54 shows that the differences in fuel mass ratios are strongly influenced by the gasifier conditions employed by the various studies. According to [142], using oxygen as the gasification medium can increase conversion efficiency, whilst Swanson et al. [69] found that higher conversion efficiencies were achieved at higher temperatures.<sup>5</sup>

Table 54: Mass ratios and gasifier conditions of GFT processes

	GFT-J process	Ekbohm et al. [48]	Yamashita et al. [143]	Swanson et al. [69]	
				LT scenario <sup>3</sup>	HT scenario <sup>4</sup>
Fuel mass ratio <sup>1</sup>	0.13	0.21	0.14	0.15	0.19
Pressure (bar)	Atmospheric	10 – 20	Atmospheric	27.6	26.6
Gasification medium	Air	Oxygen	Air	Oxygen	
Temperature (°C)	900	900	- <sup>2</sup>	870	1 300

<sup>1</sup> Mass of fuel divided by the mass of dry lignocellulose in the feed; <sup>2</sup> Not specified by [143]; <sup>3</sup> Low-temperature gasification scenario; <sup>4</sup> High-temperature gasification scenario.

The hydrogen usage and source of the GFT-J process, is given in Table 55 (this excludes the hydrogen in the syngas which is used for FT liquid synthesis). A fraction of the cleaned syngas is used for hydrogen make-up required by the hydrocracker.

<sup>5</sup> This is evident in the fuel mass ratios of the LT and HT gasification scenario of the study by Swanson et al.

Table 55: The GFT-J process hydrogen usage and source

Process section	Hydrogen used (kg/h)	Specific hydrogen usage <sup>1</sup>	Source of hydrogen
Upgrading and Separation <sup>2</sup>	239.5	23.2	4.5% of the cleaned, compressed syngas

<sup>1</sup> kg Hydrogen usage per MT of total fuel produced; <sup>2</sup> Specifically for the hydrocracker.

The power generation and usage of the GFT-J process is shown in Table 56. The GFT-J process produces excess electricity even though over 20 MW of the power produced is used for syngas compression. According to [144], the power required for syngas compression can be reduced significantly when using a pressurized gasifier.

Table 56: Power generation and usage of the GFT-J process

<b>Net export</b>	<b>12.53 MW</b>
Total usage	42.11 MW
Total generated	54.65 MW

The GFT-J process requires 275 MT/h of make-up water. The cooling tower accounted for most of the water loss. The main contributors of the cooling water duty (and therefore cooling water loss) were the condensing turbine and the syngas cooling section amounting to 74.0% and 15.2% of the total cooling water duty respectively. The wastewater amounted to 49.7 MT/h. All the wastewater was treated, whilst 40% was discarded.

## 6 Process Economics

This section contains the capital and operating costs of the investigated processes as well as the results of the discounted cash flow and sensitivity analyses. The methodology followed to determine the process economics is discussed in section 4.6. The costing data used to determine the capital costs are displayed for the main equipment in Appendix C. A summary of all the cost information derived from literature sources, used to determine the total variable operating cost, is given in Table 127 and Table 128 in Appendix G.

### 6.1 HEFA Process

#### 6.1.1 Project Capital and Operating Cost

The capital costs of the HEFA process are summarized in Table 57.

Table 57: Summary of the capital costs of the HEFA process (n<sup>th</sup> plant)

Process Area	Purchased Cost (PC)	Installed cost (IC)
Hydrotreating	\$ 2 100 000	\$ 5 500 000
Hydrocracking	\$ 9 600 000	\$ 28 600 000
Hydrogen plant	\$ 23 300 000	\$ 42 600 000
Separation	\$ 800 000	\$ 2 200 000
Steam & power plant	\$ 1 200 000	\$ 2 900 000
WWT & utilities	\$ 700 000	\$ 1 800 000
<b>Totals</b>	<b>\$ 37 700 000</b>	<b>\$ 83 600 000</b>
Additional Direct Costs	10% of total IC	\$ 8 400 000
<b>Total Direct Costs (TDC)</b>		<b>\$ 92 000 000</b>
Prorated Expenses	10% of TDC	\$ 9 200 000
Field Expenses	10% of TDC	\$ 9 200 000
Home Office & Construction Fee	20% of TDC	\$ 18 400 000
Project Contingency	10% of TDC	\$ 9 200 000
Other Costs	10% of TDC	\$ 9 200 000
<b>Total Indirect Costs (TIC)</b>		<b>\$ 55 200 000</b>
<b>Fixed Capital Investment (FCI)</b>		<b>\$ 147 200 000</b>
Land		\$ 1 800 000
Working Capital	10% of FCI	\$ 14 700 000
<b>Total Capital Investment (TCI)</b>		<b>\$ 163 700 000</b>
Lang Factor (FCI / total purchased cost)		3.90

The main variable operating costs and the fixed operating costs of the HEFA process are given in Table 58 and Table 59. Table 58 illustrates that the vegetable oil in the feed

accounts for almost all the variable operating cost. The complete variable operating costs (including periodic costs) are given in Table 129 and Table 130 in Appendix G.

Table 58: Summary of main variable operating costs of the HEFA process <sup>1</sup>

Stream description	\$/hour (2007\$)	MM\$/year (2007\$)	% of total raw material cost
<b>Raw materials</b>			
Vegetable oil	10 411.19	82.08	99.6%
<b>Subtotal</b>	10 448.70	82.38	
<b>Waste disposal</b>			
<b>Subtotal</b>	5.91	0.05	
<b>By-product credits</b>			
Naphtha	2 005.26	15.81	19.2%
Diesel	356.40	2.81	3.4%
<b>Subtotal</b>	2 361.66	18.62	
<b>Total variable operating costs</b>	8 092.95	63.80	

<sup>1</sup> Only the variable operating costs which are larger than 1% of total raw material cost are included in the table.

Table 59: Fixed operating costs of the HEFA process

Description	MM\$/yr (2007\$)
<b>Labour &amp; Supervision</b>	
Total salaries	2.18
Labour burden	1.96
<b>Other Overhead</b>	
Maintenance	4.42
Property insurance & tax	1.03
<b>Subtotal</b>	9.58

### 6.1.2 Discounted Cash Flow and Sensitivity Analyses

Based on a discounted cash flow analysis of the HEFA process (shown in Appendix H), the base minimum jet selling price (MJSP) was found to be \$1.67 per kg jet fuel. As discussed in section 4.6.4, the MJSP of the investigated processes were determined by changing the jet fuel product cost to obtain a NPV of zero at a specific discount rate (equal to the minimum acceptable IRR). A summary of the costs contributing to the MJSP are shown in Table 60.

Table 60: MJSP breakdown for the HEFA process

<b>Operating Costs (cents per kg jet fuel)</b>	
Vegetable oil	145.8
Catalysts	1.3
Other raw materials	0.1
Waste disposal	0.1
Grid electricity	0.0
Fuel by-products	-33.1
Fixed costs	17.0
Capital depreciation	13.1
Average income tax	2.5
Average return on investment	20.0

A sensitivity analysis was performed for the investigated processes to determine the effects of changing economic parameters on the resulting MJSP; calculating the percent change of the MJSP from the base MJSP. The results of the sensitivity analysis for the HEFA process are summarized in Figure 39. For the HEFA process, feedstock cost change causes the greatest change in MJSP, ranging from \$1.04 to \$2.50 per kg jet fuel.

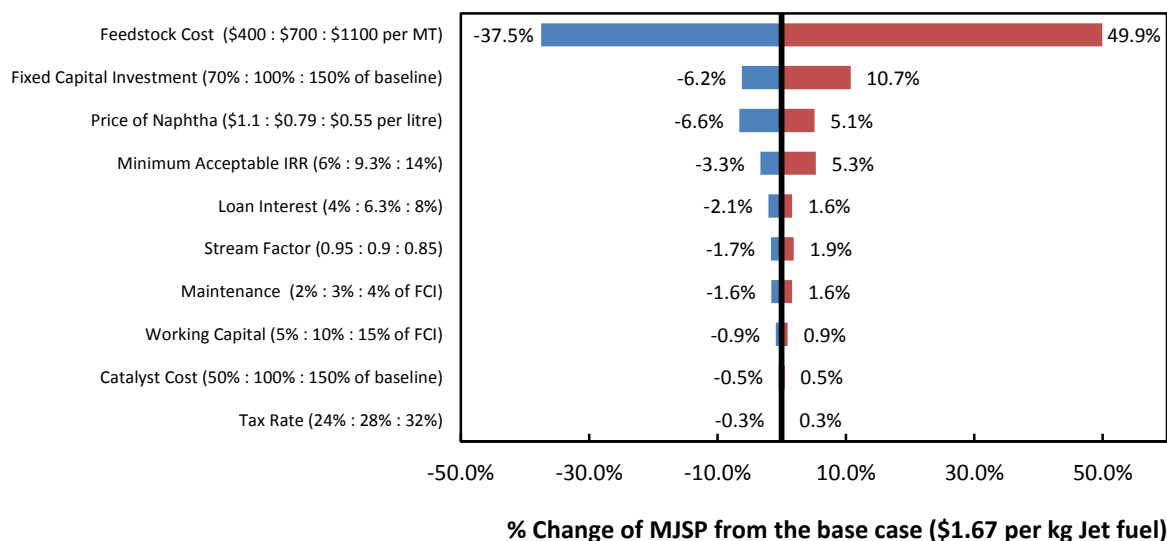


Figure 39: Results of HEFA process sensitivity analysis

## 6.2 SYN-FER-J Process

### 6.2.1 Project Capital and Operating Cost

The capital costs of the SYN-FER-J process (scenario A.1) are summarized in Table 61. The capital costs of the other two scenarios (A.2 and B) are given in Table 121 in Appendix E.

Similar base FCI were determined for the A.1, A.2 and B scenarios at \$378 million, \$374 million and \$368 million respectively.

Table 61: Summary of the capital costs of the SYN-FER-J (A.1) process (n<sup>th</sup> plant)

Process Area	Purchased Cost (PC)	Installed cost (IC)
Feedstock handling	\$ 9 600 000	\$ 23 800 000
Gasification plant	\$ 18 800 000	\$ 43 300 000
Fermentation	\$ 8 500 000	\$ 22 100 000
Separation	\$ 3 800 000	\$ 7 200 000
Hydrogen recovery	\$ 5 500 000	\$ 7 700 000
Steam & power plant	\$ 9 000 000	\$ 18 100 000
Dehydration	\$ 10 700 000	\$ 17 800 000
Oligomerization	\$ 15 500 000	\$ 38 100 000
Hydroprocessing	\$ 1 800 000	\$ 4 400 000
Utilities	\$ 3 000 000	\$ 7 400 000
WWT	\$ 10 100 000	\$ 24 900 000
<b>Totals</b>	<b>\$ 96 400 000</b>	<b>\$ 214 800 000</b>
Additional Direct Costs	10% of total IC	\$ 21 480 000
<b>Total Direct Costs (TDC)</b>		<b>\$ 236 300 000</b>
Prorated Expenses	10% of TDC	\$ 23 600 000
Field Expenses	10% of TDC	\$ 23 600 000
Home Office & Construction Fee	20% of TDC	\$ 47 300 000
Project Contingency	10% of TDC	\$ 23 600 000
Other Costs	10% of TDC	\$ 23 600 000
<b>Total Indirect Costs (TIC)</b>		<b>\$ 141 800 000</b>
<b>Fixed Capital Investment (FCI)</b>		<b>\$ 378 000 000</b>
Land		\$ 1 800 000
Working Capital	10% of FCI	\$ 37 800 000
<b>Total Capital Investment (TCI)</b>		<b>\$ 417 700 000</b>
Lang Factor (FCI / total purchased cost)		4.09

Table 62 gives the main variable operating costs of the SYN-FER-J process (scenario A.1), whilst Table 63 gives the fixed operating costs of the three SYN-FER-J process scenarios. The complete variable operating costs of all three scenarios (including periodic costs) are given in Appendix G.

Table 62: Summary of main variable operating costs of the SYN-FER-J (A.1) process <sup>1</sup>

Stream description	\$/hour (2007\$)	MM\$/year (2007\$)	% of total raw material cost
<b>Raw materials</b>			
Lignocellulose feedstock	5 451.71	42.98	86.8%
Water (make-up)	88.71	0.70	1.4%
Nutrients	272.59	2.15	4.3%
Solvent make-up <sup>2</sup>	202.49	1.60	3.2%
Oligomerization catalyst <sup>3</sup>	202.49	1.60	3.2%
<b>Subtotal</b>	<b>6 279.81</b>	<b>49.51</b>	
<b>Waste disposal</b>			
Wastewater	80.63	0.64	1.28%
Solids disposal	90.87	0.72	1.45%
<b>Subtotal</b>	<b>171.50</b>	<b>1.35</b>	
<b>By-product credits</b>			
Diesel	1 129.95	8.91	18.0%
<b>Subtotal</b>	<b>1 129.95</b>	<b>8.91</b>	
<b>Total variable operating costs</b>	<b>5 321.35</b>	<b>41.95</b>	

<sup>1</sup> Only the variable operating costs which are larger than 1% of total raw material costs are included in the table; <sup>2</sup> Solvent make-up of ethylene oligomerization reactor (n-heptane); <sup>3</sup> Ethylene oligomerization reactor catalyst.

Table 63: Fixed operating costs of the SYN-FER-J process

Description	MM\$/yr (2007\$)		
Scenario	A.1	A.2	B
<b>Labour &amp; Supervision</b>			
Total salaries	3.32	3.32	3.32
Labour burden	2.99	2.99	2.99
<b>Other Overhead</b>			
Maintenance	11.34	11.21	11.04
Property insurance & tax	2.65	2.62	2.58
<b>Subtotal</b>	<b>20.29</b>	<b>20.13</b>	<b>19.92</b>

### 6.2.2 Discounted Cash Flow and Sensitivity Analyses

A discounted cash flow analysis was done for all three SYN-FER-J process scenarios (scenario A.1 is presented in Appendix H). The base MJSP was determined for the scenario A.1, A.2 and B to be \$2.05, \$1.90 and \$1.91 per kg jet fuel respectively. A summary of the costs contributing to the MJSP are shown in Table 64. The three scenarios were investigated for the SYN-FER-J process based on different fermentation data by Gaddy et al. [116] as the interplay between fermentation output parameters on the process promise

was unclear. However, the ultimate MJSP of the three scenarios were very similar. One reason is because the scenarios all required diversion of syngas for electricity production (therefore processes with a higher conversion in the fermentation section, subsequently just requiring larger amounts of syngas to be diverted for electricity generation). Under these conditions, conversion is therefore not so important, but targeting increased ethanol concentration or productivity would be more worthwhile.

Table 64: MJSP breakdown for the SYN-FER-J process scenarios

Operating Costs (cents per kg jet fuel)			
Scenario	A.1	A.2	B
Lignocellulose feedstock	73.6	68.7	69.5
Catalysts	12.9	12.9	12.9
Other raw materials	8.4	8.0	8.1
Waste disposal	2.3	2.1	2.1
Grid electricity	0.0	0.0	0.0
Fuel by-products	-15.2	-15.2	-15.2
Fixed costs	34.7	32.2	32.2
Capital depreciation	12.6	11.8	11.9
Average income tax	6.3	5.9	5.9
Average return on investment	69.5	64.1	63.7

The results of the sensitivity analysis for the SYN-FER-J process scenario A.1 are summarized in Figure 40.

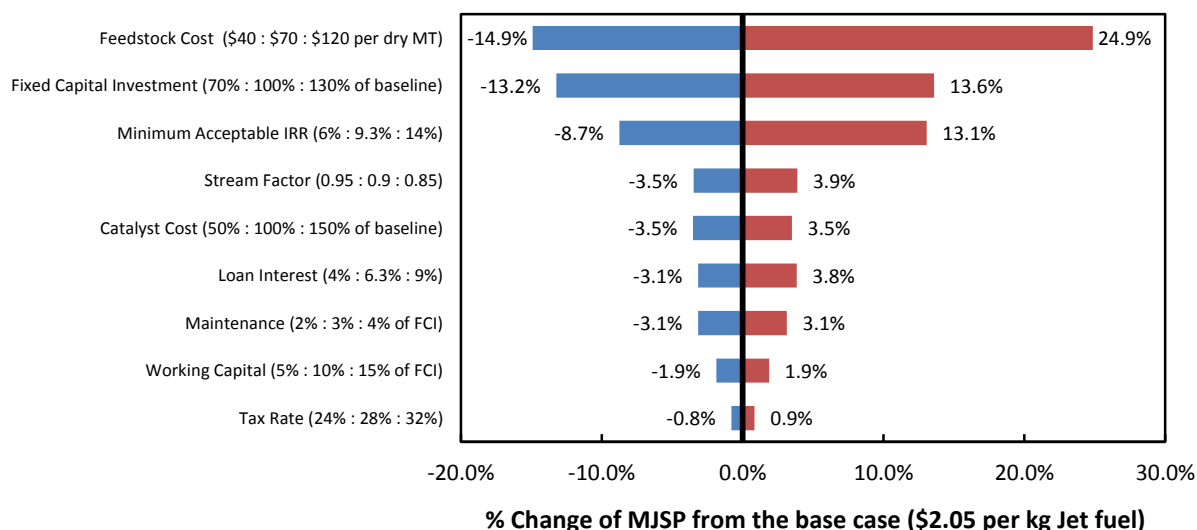


Figure 40: Results of SYN-FER-J (scenario A.1) process sensitivity analysis

Feedstock cost and FCI cost change had the largest effect on the MJSP of the SYN-FER-J process scenario A.1, whilst the minimum acceptable IRR also had a significant effect on the

MJSP. Although the MJSP for the SYN-FER-J scenarios differ somewhat, the sensitivity analysis outcomes are very similar (with regards to % change of MJSP from base case).

## 6.3 S-ETH-J Process

### 6.3.1 Project Capital and Operating Cost

The capital costs of the S-ETH-J process are summarized in Table 65. The ethanol production section consists of around half of the total installed cost, whilst the remaining cost is for ethanol upgrading, the hydrogen plant, utilities and WWT.

Table 65: Summary of the capital costs of the S-ETH-J process (n<sup>th</sup> plant)

Process Area	Purchased Cost (PC)	Installed cost (IC)
Ethanol production <sup>1</sup>	\$ 55 200 000	\$ 82 900 000
Hydrogen plant	\$ 5 500 000	\$ 8 200 000
Dehydration	\$ 11 000 000	\$ 18 300 000
Oligomerization	\$ 16 100 000	\$ 39 400 000
Hydroprocessing	\$ 1 800 000	\$ 4 500 000
Utilities	\$ 2 400 000	\$ 5 800 000
WWT	\$ 3 600 000	\$ 8 800 000
<b>Totals</b>	<b>\$ 95 600 000</b>	<b>\$ 167 900 000</b>
Additional Direct Costs	10% of total IC	\$ 16 790 000
<b>Total Direct Costs (TDC)</b>		<b>\$ 184 700 000</b>
Prorated Expenses	10% of TDC	\$ 18 500 000
Field Expenses	10% of TDC	\$ 18 500 000
Home Office & Construction Fee	20% of TDC	\$ 36 900 000
Project Contingency	10% of TDC	\$ 18 500 000
Other Costs	10% of TDC	\$ 18 500 000
<b>Total Indirect Costs (TIC)</b>		<b>\$ 110 800 000</b>
<b>Fixed Capital Investment (FCI)</b>		<b>\$ 295 500 000</b>
Land		\$ 1 800 000
Working Capital		\$ 29 500 000
<b>Total Capital Investment (TCI)</b>		<b>\$ 326 900 000</b>
Lang Factor (FCI / total purchased cost)		4.08

<sup>1</sup> Ethanol production section consists of sugarcane cleaning, sucrose extraction, juice treatment, clarification, juice concentration, sterilization, fermentation, separation and cogeneration.

Table 66 and Table 67 give the main variable operating costs and fixed operating costs of the S-ETH-J process. The complete variable operating costs are given in Table 135 and Table 136 in Appendix G. The two main raw material costs are sugarcane and trash while the grid electricity by-product credit almost amounts to 50% of the total raw material cost.

Table 66: Summary of main variable operating costs of the S-ETH-J process <sup>1</sup>

Stream description	\$/hour (2007\$)	MM\$/year (2007\$)	% of total raw material cost
<b>Raw materials</b>			
Sugarcane	6 676.61	43.87	72.11%
Trash	2 181.03	14.33	23.56%
Solvent make-up <sup>2</sup>	140.33	0.92	1.52%
Oligomerization catalyst <sup>3</sup>	140.33	0.92	1.52%
<b>Subtotal</b>	<b>9 259.28</b>	<b>60.83</b>	
<b>Waste disposal</b>			
Solids disposal	196.96	1.29	2.13%
<b>Subtotal</b>	<b>252.06</b>	<b>1.66</b>	
<b>By-product credits</b>			
Grid electricity	4 209.33	27.66	45.46%
Diesel	1 183.44	7.78	12.78%
<b>Subtotal</b>	<b>5 392.77</b>	<b>35.43</b>	
<b>Total variable operating costs</b>	<b>4 118.57</b>	<b>27.06</b>	

<sup>1</sup> Only the variable operating costs which are larger than 1% of total raw material costs are included in the table; <sup>2</sup> Solvent make-up of ethylene oligomerization reactor (n-heptane); <sup>3</sup> Ethylene oligomerization reactor catalyst.

Table 67: Fixed operating costs of the S-ETH-J process

Description	MM\$/yr (2007\$)
<b>Labour &amp; Supervision</b>	
Total salaries	3.32
Labour burden	2.99
<b>Other Overhead</b>	
Maintenance	8.86
Property insurance & tax	2.07
<b>Subtotal</b>	<b>17.24</b>

### 6.3.2 Discounted Cash Flow and Sensitivity Analyses

Based on a discounted cash flow analysis for the S-ETH-J process (presented in Appendix H), the base MJSP was found to be \$1.79 per kg jet fuel. A summary of the costs contributing to the MJSP are shown in Table 68.

Table 68: MJSP breakdown for the S-ETH-J process

Operating Costs (cents per kg jet fuel)	
Sugarcane	86.0
Trash	28.1
Catalysts	14.0
Other raw materials	3.3
Waste disposal	3.2
Grid electricity	-54.2
Fuel by-products	-15.2
Fixed costs	33.8
Capital depreciation	14.4
Average income tax	5.8
Average return on investment	60.1

The results of the sensitivity analysis for the S-ETH-J process are summarized in Figure 41. Although the MJSP of the S-ETH-J process does not change greatly for one sensitivity parameter, the S-ETH-J process has a few sensitivity parameters that cause a noteworthy change in the MJSP including sugarcane cost, FCI, stream factor, price of electricity, minimum acceptable IRR and trash cost.

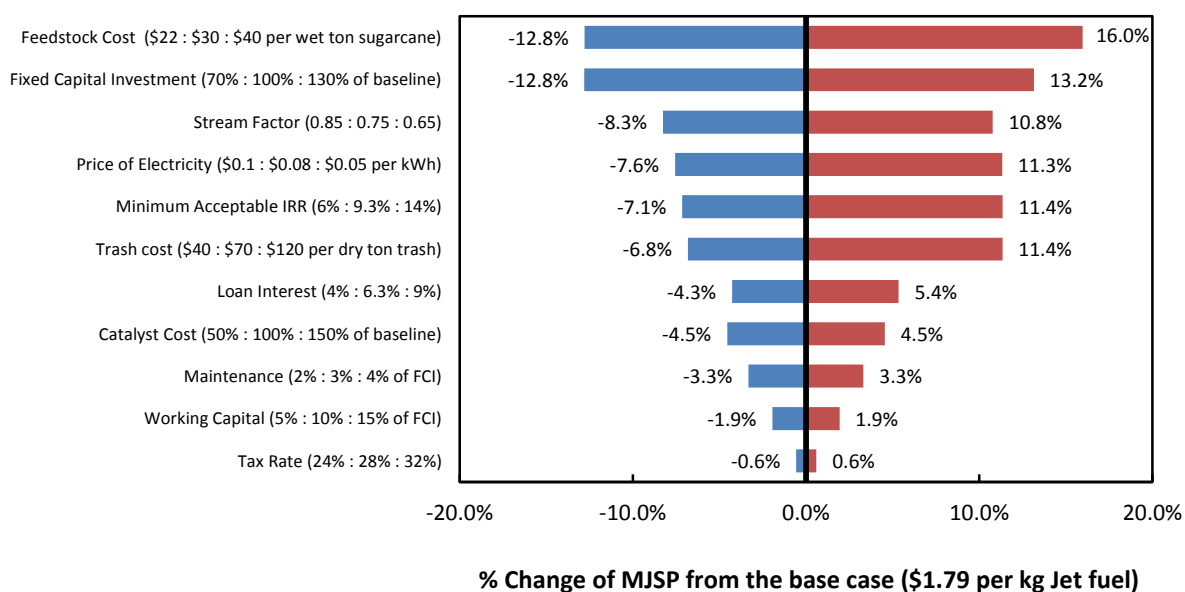


Figure 41: Results of S-ETH-J process sensitivity analysis

## 6.4 L-ETH-J Process

### 6.4.1 Project Capital and Operating Cost

The capital costs of the L-ETH-J process are summarized in Table 69. The ethanol production section consists of almost 60% of the total installed cost, whilst the remaining cost is for ethanol upgrading, the hydrogen plant, utilities and WWT.

Table 69: Summary of the capital costs of the L-ETH-J process (n<sup>th</sup> plant)

Process Area	Purchased Cost (PC)	Installed cost (IC)
Ethanol production <sup>1</sup>	\$ 59 000 000	\$ 145 800 000
Hydrogen plant	\$ 5 500 000	\$ 8 200 000
Dehydration	\$ 11 100 000	\$ 18 300 000
Oligomerization	\$ 16 100 000	\$ 39 500 000
Hydroprocessing	\$ 1 800 000	\$ 4 500 000
Utilities	\$ 2 200 000	\$ 5 500 000
WWT	\$ 10 800 000	\$ 28 300 000
<b>Totals</b>	<b>\$ 106 500 000</b>	<b>\$ 250 100 000</b>
Additional Direct Costs	10% of total IC	\$ 25 010 000
<b>Total Direct Costs (TDC)</b>		<b>\$ 275 100 000</b>
Prorated Expenses	10% of TDC	\$ 27 500 000
Field Expenses	10% of TDC	\$ 27 500 000
Home Office & Construction Fee	20% of TDC	\$ 55 000 000
Project Contingency	10% of TDC	\$ 27 500 000
Other Costs	10% of TDC	\$ 27 500 000
<b>Total Indirect Costs (TIC)</b>		<b>\$ 165 000 000</b>
<b>Fixed Capital Investment (FCI)</b>		<b>\$ 440 100 000</b>
Land		\$ 1 800 000
Working Capital		\$ 44 000 000
<b>Total Capital Investment (TCI)</b>		<b>\$ 486 000 000</b>
Lang Factor (FCI / total purchased cost)		4.30

<sup>1</sup> Ethanol production section consists of feedstock handling, pretreatment, a seed train, enzymatic hydrolysis and fermentation, ethanol recovery, evaporation and cogeneration.

Table 70 and Table 71 gives the main variable operating costs and fixed operating costs of the L-ETH-J process. The complete variable operating costs are given in Table 137 and Table 138 in Appendix G. Along with the lignocellulose feedstock cost, the enzyme cost contributes substantially to the total raw material cost of the L-ETH-J process.

Table 70: Summary of main variable operating costs of the L-ETH-J process <sup>1</sup>

Stream description	\$/hour (2007\$)	MM\$/year (2007\$)	% of total raw material cost
<b>Raw materials</b>			
Lignocellulose feedstock	5 451.71	42.98	49.5%
Sulphur dioxide	441.65	3.48	4.0%
Glucose	180.43	1.42	1.6%
Nutrients	254.86	2.01	2.3%
Enzymes	4 126.28	32.53	37.5%
Solvent make-up <sup>2</sup>	212.15	1.67	1.9%
Oligomerization catalyst <sup>3</sup>	212.15	1.67	1.9%
<b>Subtotal</b>	<b>11011.87</b>	<b>86.82</b>	
<b>Waste disposal</b>			
<b>Subtotal</b>	<b>151.51</b>	<b>1.19</b>	
<b>By-product credits</b>			
Grid electricity	1 526.22	12.03	13.9%
Diesel	1 182.94	9.33	10.7%
<b>Subtotal</b>	<b>2 709.16</b>	<b>21.36</b>	
<b>Total variable operating costs</b>	<b>8 454.23</b>	<b>66.65</b>	

<sup>1</sup> Only the variable operating costs which are larger than 1% of total raw material costs are included in the table; <sup>2</sup> Solvent make-up of ethylene oligomerization reactor (n-heptane); <sup>3</sup> Ethylene oligomerization reactor catalyst.

Table 71: Fixed operating costs of the L-ETH-J process

Description	MM\$/yr (2007\$)
<b>Labour &amp; Supervision</b>	
Total salaries	3.32
Labour burden	2.99
<b>Other Overhead</b>	
Maintenance	13.20
Property insurance & tax	3.08
<b>Subtotal</b>	<b>22.59</b>

#### 6.4.2 Discounted Cash Flow and Sensitivity Analyses

After completion of a discounted cash flow analysis for the L-ETH-J process (shown in Appendix H), the base MJSP of \$2.55 per kg jet fuel was determined. A summary of the costs contributing to the MJSP are shown in Table 72.

Table 72: MJSP breakdown for the L-ETH-J process

Operating Costs (cents per kg jet fuel)	
Lignocellulose feedstock	70.3
Enzymes	53.2
Catalysts	13.0
Other raw materials	15.7
Waste disposal	2.0
Grid electricity	-19.7
Fuel by-products	-15.3
Fixed costs	37.0
Capital depreciation	12.0
Average income tax	7.1
Average return on investment	79.8

The sensitivity analysis results for the L-ETH-J process are summarized in Figure 42. For the sensitivity parameter ranges the enzyme cost, feedstock cost and FCI change had the largest effect on the MJSP of the L-ETH-J process.

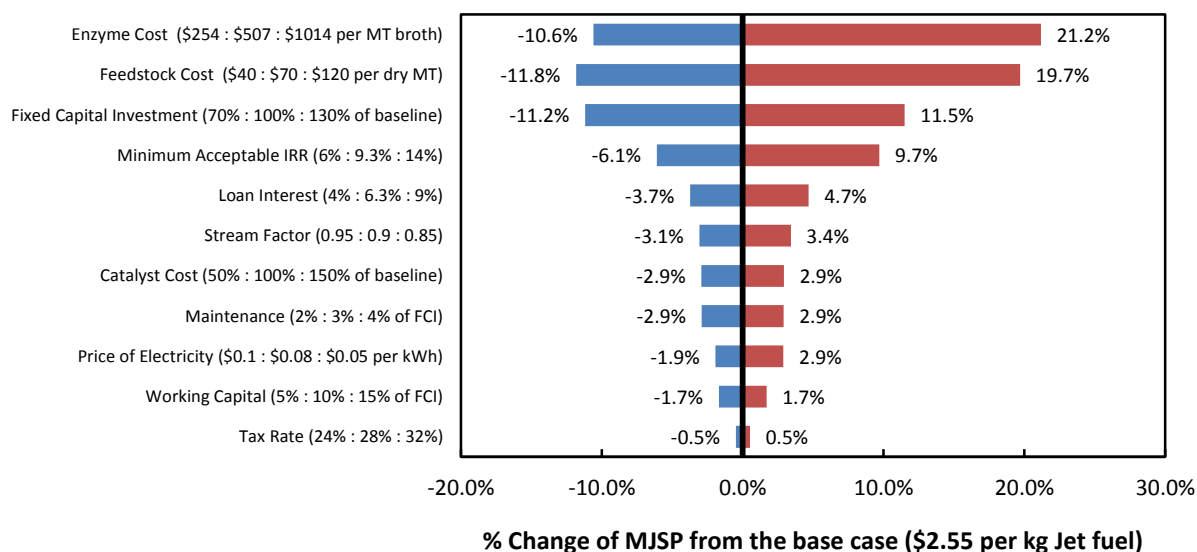


Figure 42: Results of L-ETH-J process sensitivity analysis

## 6.5 FP-J Process

### 6.5.1 Project Capital and Operating Cost

The capital costs of the FP-J process are summarized in Table 73. The main installed costs of the FP-J process are the pyrolysis section, hydroprocessing sections and hydrogen plant consisting of 35.6%, 20.0% and 17.7% of the total installed costs respectively.

Table 73: Summary of the capital costs of the FP-J process (n<sup>th</sup> plant)

Process Area	Purchases Cost (PC)	Installed cost (IC)
Feedstock handling	\$ 10 100 000	\$ 25 100 000
Pyrolysis <sup>1</sup>	\$ 58 900 000	\$ 145 500 000
Heat recovery	\$ 17 500 000	\$ 28 200 000
Oil filter	\$ 5 500 000	\$ 7 700 000
Steam & power plant	\$ 15 200 000	\$ 37 600 000
WWT & utilities	\$ 4 400 000	\$ 11 000 000
Hydrotreating	\$ 15 400 000	\$ 40 000 000
Hydrocracking & separation	\$ 14 000 000	\$ 41 600 000
Hydrogen plant	\$ 38 600 000	\$ 72 100 000
<b>Totals</b>	<b>\$ 179 800 000</b>	<b>\$ 408 600 000</b>
Additional Direct Costs	10% of total IC	\$ 40 900 000
<b>Total Direct Costs (TDC)</b>		<b>\$ 449 500 000</b>
Prorated Expenses	10% of TDC	\$ 45 000 000
Field Expenses	10% of TDC	\$ 45 000 000
Home Office & Construction Fee	20% of TDC	\$ 89 900 000
Project Contingency	10% of TDC	\$ 45 000 000
Other Costs	10% of TDC	\$ 45 000 000
<b>Total Indirect Costs (TIC)</b>		<b>\$ 269 700 000</b>
<b>Fixed Capital Investment (FCI)</b>		<b>\$ 719 200 000</b>
Land		\$ 1 800 000
Working Capital	10% of FCI	\$ 71 900 000
<b>Total Capital Investment (TCI)</b>		<b>\$ 793 000 000</b>
Lang Factor (FCI / total purchased cost)		4.00

<sup>1</sup> The pyrolysis section includes a pyrolysis reactor section, quench section and a heat recovery section.

Table 74 and Table 75 give the main variable operating costs and fixed operating costs of the FP-J process. The complete variable operating costs of the FP-J process are given in Appendix G. Along with the lignocellulose feedstock cost, the natural gas cost contributes considerably to the total raw material cost of the FP-J process. The combined by-product credits of the FP-J process consist of more than the total raw material cost.

Table 74: Summary of main variable operating costs of the FP-J process <sup>1</sup>

Stream description	\$/hour (2007\$)	MM\$/year (2007\$)	% of total raw material cost
<b>Raw materials</b>			
Lignocellulose feedstock	6 006.69	47.36	70.59%
Natural gas	2 362.40	18.63	27.76%
<b>Subtotal</b>	<b>8 509.04</b>	<b>67.09</b>	
<b>Waste disposal</b>			
Solids disposal	152.66	1.20	1.79%
<b>Subtotal</b>	<b>220.30</b>	<b>1.74</b>	
<b>By-product credits</b>			
Grid electricity	5 078.37	40.04	59.68%
Naphtha	4 726.79	37.27	55.55%
Diesel	2 195.71	17.31	25.80%
Gas oil	1 987.57	15.67	23.36%
<b>Subtotal</b>	<b>13 998.45</b>	<b>110.28</b>	
<b>Total variable operating costs</b>	<b>-5 259.11</b>	<b>-41.46</b>	

<sup>1</sup> Only the variable operating costs which are larger than 1% of total raw material costs are included in the table.

Table 75: Fixed operating costs of the FP-J process

Description	MM\$/yr (2007\$)
<b>Labour &amp; Supervision</b>	
Total salaries	3.32
Labour burden	2.99
<b>Other Overhead</b>	
Maintenance	21.58
Property insurance & tax	5.03
<b>Subtotal</b>	<b>32.91</b>

### 6.5.2 Discounted Cash Flow and Sensitivity Analyses

Based on a discounted cash flow analysis for the FP-J process (presented in Appendix H), the base MJSP of \$2.58 per kg jet fuel was determined. A summary of the costs contributing to the MJSP are shown in Table 76.

Table 76: MJSP breakdown for the FP-J process

<b>Operating Costs (cents per kg jet fuel)</b>	
Lignocellulose feedstock	136.2
Natural gas	53.5
Catalysts	9.0
Other raw materials	1.9
Waste disposal	5.0
Grid electricity	-115.1
Fuel by-products	-202.0
Fixed costs	94.6
Capital depreciation	21.2
Average income tax	19.1
Average return on investment	235.4

The sensitivity analysis results for the FP-J process are summarized in Figure 43. The FP-J process has a few sensitivity parameters that cause a substantial change in the MJSP including FCI, feedstock cost, minimum acceptable IRR, price of naphtha, price of natural gas and price of electricity. The large variability of the MJSP of the FP-J process is mainly because the FP-J process was not aimed at maximum jet fuel.

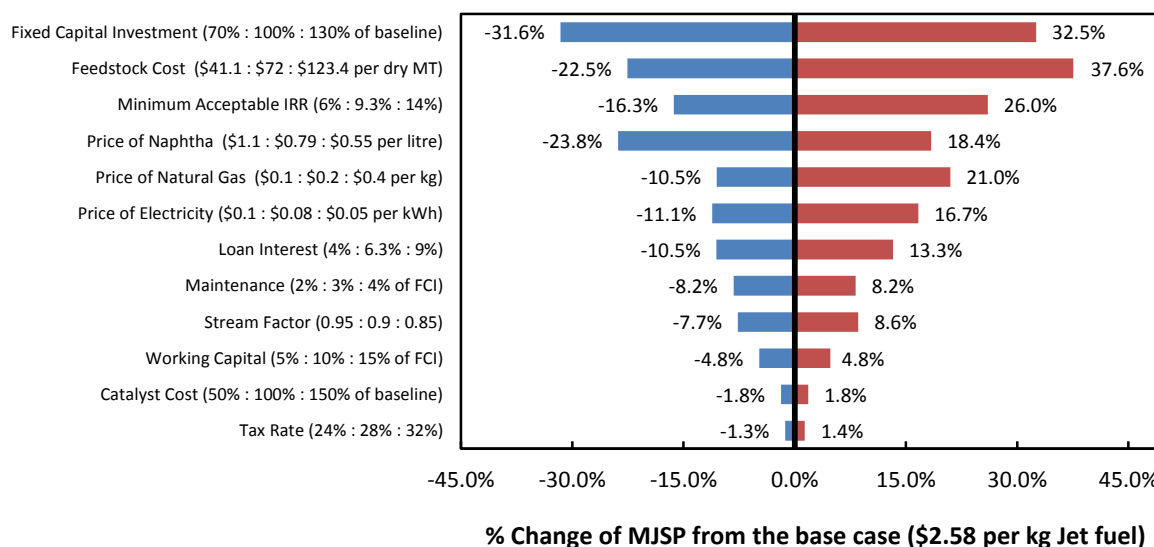


Figure 43: Results of the FP-J process sensitivity analysis

## 6.6 GFT-J Process

### 6.6.1 Project Capital and Operating Cost

The capital costs of the GFT-J process are summarized in Table 77. Sections that contribute significantly to the installed costs of the GFT-J process are the gasification plant, gas

cleaning section, upgrading and separation section and ATR consisting of 14.9%, 17.8%, 13.5% and 18.6% of the total installed costs respectively.

Table 77: Summary of the capital costs of the GFT-J process (n<sup>th</sup> plant)

Process Area	Purchases Cost (PC)	Installed cost (IC)
Feedstock handling	\$ 9 600 000	\$ 23 800 000
Gasification plant	\$ 18 800 000	\$ 43 700 000
Gas cleaning	\$ 41 200 000	\$ 52 200 000
FT-plant	\$ 11 200 000	\$ 26 300 000
Hydrogen recovery plant	\$ 8 200 000	\$ 14 600 000
Upgrading & separation	\$ 13 400 000	\$ 39 700 000
Steam & power plant	\$ 10 400 000	\$ 24 400 000
Auto-thermal reformer <sup>1</sup>	\$ 24 700 000	\$ 54 600 000
WWT & utilities	\$ 5 600 000	\$ 13 700 000
<b>Totals</b>	<b>\$ 143 200 000</b>	<b>\$ 293 000 000</b>
Additional Direct Costs	10% of total IC	\$ 29 300 000
<b>Total Direct Costs (TDC)</b>		<b>\$ 322 300 000</b>
Prorated Expenses	10% of TDC	\$ 32 200 000
Field Expenses	10% of TDC	\$ 32 200 000
Home Office & Construction Fee	20% of TDC	\$ 64 500 000
Project Contingency	10% of TDC	\$ 32 200 000
Other Costs	10% of TDC	\$ 32 200 000
<b>Total Indirect Costs (TIC)</b>		<b>\$ 193 400 000</b>
<b>Fixed Capital Investment (FCI)</b>		<b>\$ 515 700 000</b>
Land		\$ 1 800 000
Working Capital	10% of FCI	\$ 51 600 000
<b>Total Capital Investment (TCI)</b>		<b>\$ 569 100 000</b>
Lang Factor (FCI / total purchased cost)		3.60 <sup>2</sup>

<sup>1</sup> The ATR section includes an ASU; <sup>2</sup> The low Lang factor of the GFT-J process is mainly due to the low installation cost of the Rectisol unit, in the gas-cleaning section.

Table 78 and Table 79 give the main variable operating costs and fixed operating costs of the GFT-J process. The complete variable operating costs of the GFT-J process are given in Table 141 and Table 142 in Appendix G. The total raw material cost consists mainly of lignocellulose cost while the naphtha by-product credit amounts to almost 50% of the total raw material cost.

Table 78: Summary of main variable operating costs of the GFT-J process <sup>1</sup>

Stream description	\$/hour (2007\$)	MM\$/year (2007\$)	% of total raw material cost
<b>Raw materials</b>			
Lignocellulose feedstock	5 451.71	42.98	96.43%
Water (make-up)	71.06	0.56	1.26%
Auto-thermal reformer catalyst	69.13	0.55	1.22%
<b>Subtotal</b>	<b>5 653.38</b>	<b>44.57</b>	
<b>Waste disposal</b>			
Wastewater	58.92	0.46	1.04%
Solids disposal	90.87	0.72	1.61%
<b>Subtotal</b>	<b>149.79</b>	<b>1.18</b>	
<b>By-product credits</b>			
Grid electricity	1 002.65	7.90	17.74%
Naphtha	2 808.84	22.14	49.68%
<b>Subtotal</b>	<b>3 811.49</b>	<b>30.05</b>	
<b>Total variable operating costs</b>	<b>1 991.69</b>	<b>15.70</b>	

<sup>1</sup> Only the variable operating costs which are larger than 1% of total raw material costs are included in the table.

Table 79: Fixed operating costs of the GFT-J process

Description	MM\$/yr (2007\$)
<b>Labour &amp; Supervision</b>	
Total salaries	3.32
Labour burden	2.99
<b>Other Overhead</b>	
Maintenance	15.47
Property insurance & tax	3.61
<b>Subtotal</b>	<b>25.38</b>

## 6.6.2 Discounted Cash Flow and Sensitivity Analyses

After completion of the discounted cash flow analysis of the GFT-J process (presented in Appendix H), the base MJSP of \$1.86 per kg jet fuel was determined. A summary of the costs contributing to the MJSP are shown in Table 80.

Table 80: MJSP breakdown for the GFT-J process

Operating Costs (cents per kg jet fuel)	
Lignocellulose feedstock	68.8
Catalysts	10.0
Other raw materials	1.7
Waste disposal	1.9
Grid electricity	-12.6
Fuel by-products	-35.4
Fixed costs	40.6
Capital depreciation	11.8
Average income tax	7.8
Average return on investment	91.2

The sensitivity analysis results for the GFT-J process are summarized in Figure 44. Feedstock cost and FCI cost change had the largest effect on the MJSP of the GFT-J process, whereas the minimum acceptable IRR also had a significant effect on the MJSP.

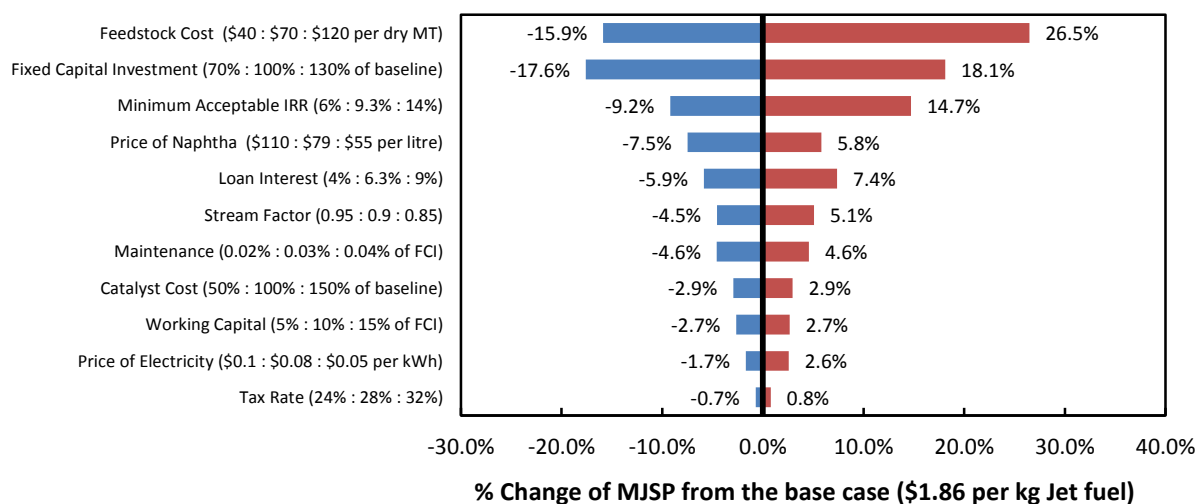


Figure 44: Results of the GFT-J process sensitivity analysis

## 7 Comparisons of Processes

This section compares the investigated processes with each other and to literature based on process properties and economics.

### 7.1 Process Properties

#### 7.1.1 Process properties of processes in this study

Table 81 illustrates the various mass ratios of the 2G and 1G fed processes investigated in this study. Except for the FP-J process (that uses significant amounts of natural gas) all the processes are hydrogen and electricity self-sufficient; independent of fossil sources. The highest total fuel mass ratios for the 2G fed processes were achieved by the thermochemical processes; the FP-J process<sup>T</sup> and the GFT-J process. The highest jet fuel mass ratios for the 2G fed processes were obtained by the GFT-J process and the SYN-FER-J process.

Table 81: Comparison of mass ratios of the investigated processes

	FP-J <sup>1</sup>	GFT-J <sup>1</sup>	L-ETH-J <sup>1</sup>	SYN-FER-J <sup>1</sup>			HEFA <sup>2</sup>	S-ETH-J <sup>3</sup>
				A.1	A.2	B		
<b>Total fuel</b>	0.15	0.14	0.12	0.11	0.12	0.12	0.62	0.14 (0.30) <sup>4</sup>
<b>Jet fuel</b>	0.05	0.11	0.10	0.10	0.11	0.10	0.48	0.12 (0.26) <sup>4</sup>

<sup>1</sup> Based on dry, ash-free lignocellulose in the feed; <sup>2</sup> Based on vegetable oil in the feed; <sup>3</sup> Based on dry sugarcane in the feed; <sup>4</sup> Values in brackets are based on sucrose in the feed.

As the 1G fed processes (HEFA and S-ETH-J) have different feeds, the mass ratios are not directly comparable. The HEFA process almost achieved a jet fuel mass ratio of 0.5 based on the vegetable oil feed, whilst the S-ETH-J process produced 262 kg of jet fuel per MT sucrose in the sugarcane fed. Except for the FP-J process, all the processes had the total fuel consist of over 75% of jet fuel.

Table 82 compares the specific hydrogen usage (kg hydrogen usage per MT fuel produced) of the investigated processes. The FP-J and HEFA processes had the highest specific hydrogen usage mainly for oxygen removal, requiring a significant fraction of energy for hydrogen production. In contrast, the biochemical processes with ethanol as an intermediate product (S-ETH-J, L-ETH-J and SYN-FER-J processes) had the lowest hydrogen usage (no hydrogen is needed for oxygen removal from ethanol).

<sup>T</sup> According to Wright et al., a fast pyrolysis with upgrading process (like the FP-J process) that produces hydrogen from natural gas has up to 1.6 times larger fuel mass ratios in comparison to a process that produces the hydrogen from the bio-oil intermediate.

Table 82: Specific hydrogen usage of the investigated processes

	FP-J	GFT-J	L-ETH-J <sup>2</sup>	SYN-FER-J <sup>2</sup>	HEFA	S-ETH-J <sup>2</sup>
<b>Specific hydrogen usage <sup>1</sup></b>	128.2	23.2	12.1	12.1	65.3	12.1

<sup>1</sup> kg Hydrogen usage per MT of total fuel produced; <sup>2</sup> The L-ETH-J, SYN-FER-J and S-ETH-J have the same specific hydrogen usage as the same ethanol upgrading section was employed.

The specific water usage (kg water usage per kg fuel produced) of the investigated processes are compared in Table 83. The highest water usage was experienced by the SYN-FER-J process, which attributed close to 40% of the water usage to the high cooling water duty of its separation section. Cooling water usage for the condensing turbine was the main contributor of water usage for the FP-J, GFT-J and S-ETH-J processes. The water usage of the S-ETH-J process could be reduced significantly if the vinasse was treated in a WWT plant with recycling of the water. The HEFA process obtained the lowest specific water usage due to its low cooling water requirement.

Table 83: Specific water usage of the investigated processes

	FP-J	GFT-J	L-ETH-J	SYN-FER-J	HEFA	S-ETH-J
<b>Specific water usage <sup>1</sup></b>	21.1	26.7	24.2	37.2 – 41.0	3.2	25.9

<sup>1</sup> kg Water usage per kg of total fuel produced.

For the investigated processes, the fraction of energy in the feed which is converted to products is illustrated in Figure 45<sup>U</sup>. Table 84 compares the energy ratios and energy efficiencies of the investigated processes.

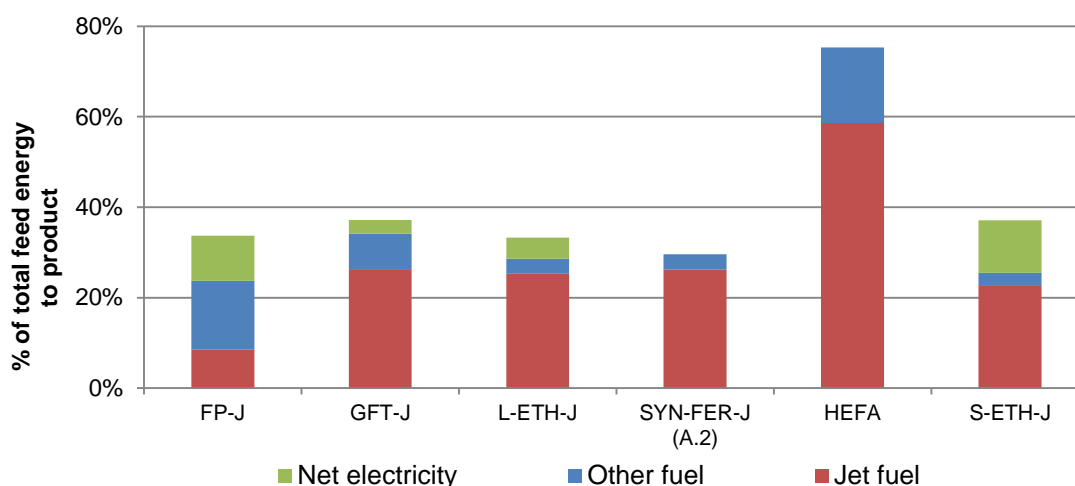


Figure 45: Energy conversion from total feed to product for investigated processes

<sup>U</sup> Only the SYN-FER-J process scenario A.2 is shown; the scenario with the highest conversion efficiency.

Table 84: Comparison of energy ratios and energy efficiencies of the investigated processes

		FP-J	GFT-J	L-ETH-J	SYN-FER-J			HEFA <sup>1</sup>	S-ETH-J <sup>2</sup>
					A.1	A.2	B		
<b>Energy ratios</b>									
<b>Liquid fuel</b>	$\left[ \frac{MW_{thermal\ product}}{MW_{thermal\ biomass\ input}} \right]$	33.2% (23.7%) <sup>3</sup>	34.1%	28.6%	27.6%	29.6%	29.2%	75.3%	25.5% (40.1%) <sup>4</sup>
<b>Jet fuel</b>	$\left[ \frac{MW_{thermal\ product}}{MW_{thermal\ biomass\ input}} \right]$	12.0% (8.5%) <sup>3</sup>	26.1%	25.3%	24.4%	26.2%	25.9%	58.6%	22.6% (35.5%) <sup>4</sup>
<b>Electricity</b>	$\left[ \frac{MW_{electricity\ product}}{MW_{thermal\ biomass\ input}} \right]$	14.0% (10.0%) <sup>5</sup>	3.1%	4.7%	0.0% <sup>6</sup>	0.0% <sup>6</sup>	0.0% <sup>6</sup>	0.0% <sup>6</sup>	11.6%
<b>Process energy efficiencies<sup>7</sup></b>									
<b>Liquid fuel</b>		48.2%	36.7%	32.0%	27.6%	29.6%	29.2%	75.3%	34.4%
<b>Overall</b>		33.7%	37.2%	33.3%	27.6%	29.6%	29.2%	75.3%	37.1%

<sup>1</sup> Based on vegetable oil in the feed; <sup>2</sup> Based on sugarcane and trash in the feed; <sup>3</sup> Value in bracket is  $[MW_{thermal\ product} / (MW_{thermal\ biomass\ input} + MW_{thermal\ fossil\ input})]$ ; <sup>4</sup> Value in brackets is based on feed sugarcane; <sup>5</sup> Value in bracket is  $[MW_{electricity\ product} / (MW_{thermal\ biomass\ input} + MW_{thermal\ fossil\ input})]$ ; <sup>6</sup> No net electricity export by process; <sup>7</sup> The definitions for the liquid fuel and overall process energy efficiencies are given in section 4.4.1.2.

All the 2G fed processes (except for the FP-J process) obtained similar jet fuel energy ratios; between 0.244 and 0.262 based on biomass input. The GFT-J process obtained the highest liquid fuel energy ratio of the 2G fed processes of 34.1%. Although the FP-J process obtained a high liquid fuel energy ratio based on biomass (33.2%), the liquid fuel energy ratio based on biomass and fossil input was only 23.7%.

It can be seen in Figure 45 and Table 84 that the HEFA process converted approximately 75% of the energy from the vegetable oil to liquid fuel product. The S-ETH-J process obtained low liquid fuel energy ratios based on the total feed (25.5%) as the feed consisted of sugarcane and significant amounts of trash<sup>V</sup>; however, based on sugarcane in the feed it achieved liquid fuel energy ratios of 40.1%.

It is evident in Figure 45 and Table 84 that a large amount of the energy in the feed was converted to excess electricity by the FP-J and S-ETH-J process (14.0% and 11.6% respectively), whilst a lesser amount of surplus electricity was also produced by the GFT-J and L-ETH-J process. The HEFA and SYN-FER-J processes only produced sufficient electricity to be electricity self-sufficient.

The only significant difference between the liquid fuel and overall process energy efficiencies are for the FP-J process (due to fossil feed and significant electricity production) and the S-ETH-J process (due to significant electricity production). The 2G fed process with the highest overall process energy efficiency was the GFT-J process with 37.2%, whilst the SYN-FER-J scenarios obtained the lowest overall process energy efficiencies (all below 30%).

The process with 1G feed that had the highest overall process energy efficiency was the HEFA process with 75.3%. The high overall energy efficiency achieved by the HEFA process is because the vegetable oil feed is much more similar to the final product than the feed of the other processes (lignocellulose or sugarcane).

### 7.1.2 Comparison of process properties of this study with literature

In this section the overall energy efficiencies of the investigated processes in this study are compared to literature studies. Figure 46 compares overall energy efficiencies for thermochemical processes from this study (blue bars) and literature (orange bars). Although all the processes in Figure 46 produce fuels (generally gasoline and diesel), the *Ekbom study* and the GFT-J process aim for mainly jet fuel while the FP-J process also produces some jet fuel.

---

<sup>V</sup> For each MW of sugarcane fed, 0.57 MW of trash was fed; trash was used for production of excess electricity.

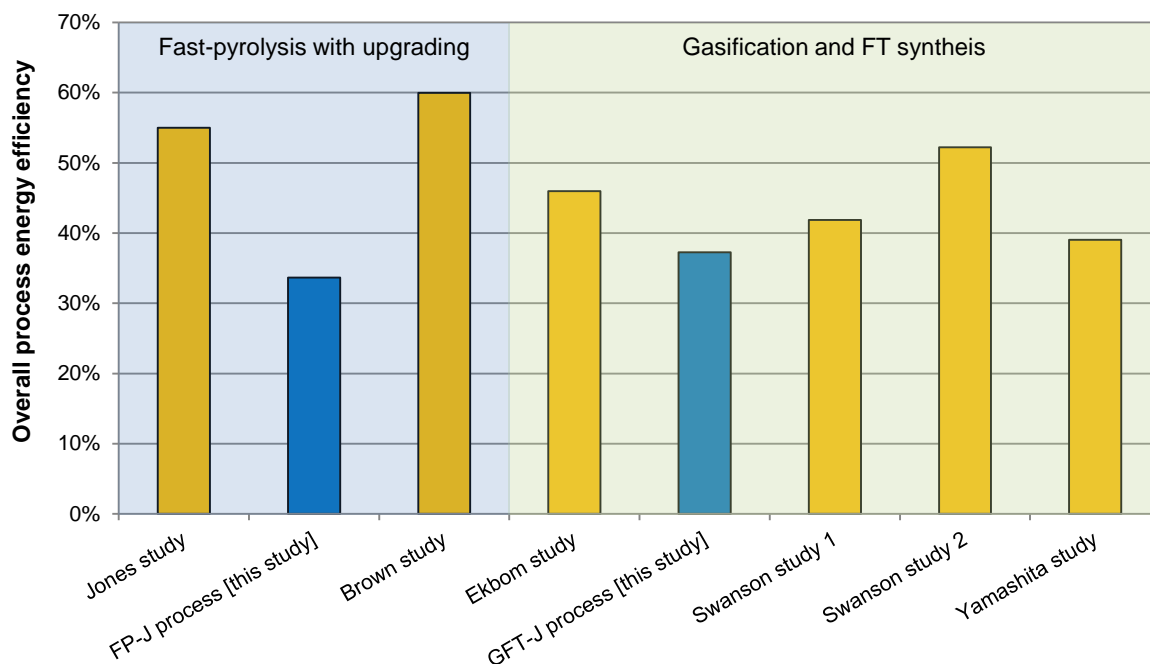


Figure 46: Typical process energy efficiencies of thermochemical processes

*Jones study* – study by Jones et al. [98]; *Brown study* – study by Brown et al. [51]; *Ekbom study* – study by Ekbom et al. [48], (district heating is excluded in calculation); *Swanson study 1* – Low-temperature gasification scenario in study by Swanson et al. [69]; *Swanson study 2* – High-temperature gasification scenario in study by Swanson et al. [69]; *Yamashita study* – study by Yamashita et al. [143].

Fast pyrolysis with upgrading to fuels was investigated by the *Jones study*, the FP-J process and the *Brown study* with varying process energy efficiencies (34% - 60%) being obtained. The relatively low process efficiency by the FP-J process can be attributed to a relatively low fuel yield, high hydrogen requirement (in comparison to *Brown study*) and its aim for significant surplus power. Furthermore, the use of a gas turbine would have increased the power production over a standard steam turbine used by the FP-J process [48], [143].

The *Ekbom study*, *Swanson studies*, *Yamashita study* and the GFT-J process convert lignocellulose to fuels, via gasification and FT synthesis, with overall process energy efficiencies from 37% up to 52% (shown in Figure 46). The type of gasifier and conditions plays an important role in determining the overall energy efficiency of this process [69]. Although more capital intensive, the overall process energy efficiencies can generally be increased by using pressurized gasifiers [144], using oxygen as the gasification medium [142] and employing increased operating temperatures (gasifier conditions of studies are shown in Table 54, section 5.6). A gas-turbine was employed by all the processes except the GFT-J process and the *Ekbom study*. The lower energy efficiency of the GFT-J process can mainly be attributed to the type and conditions of the gasifier employed and to the use of a standard steam turbine.

Figure 47 compares the overall energy efficiencies for the biochemical and hybrid<sup>w</sup> processes from this study (blue bars) and literature (orange bars). The *Petersen study*, *Humbird study* and *Piccolo study* produce ethanol, whilst the other processes in Figure 47 aim for mainly jet fuel. Figure 47 shows that, based on current technology, the biochemical processes have higher overall process energy efficiencies in comparison to the hybrid processes.

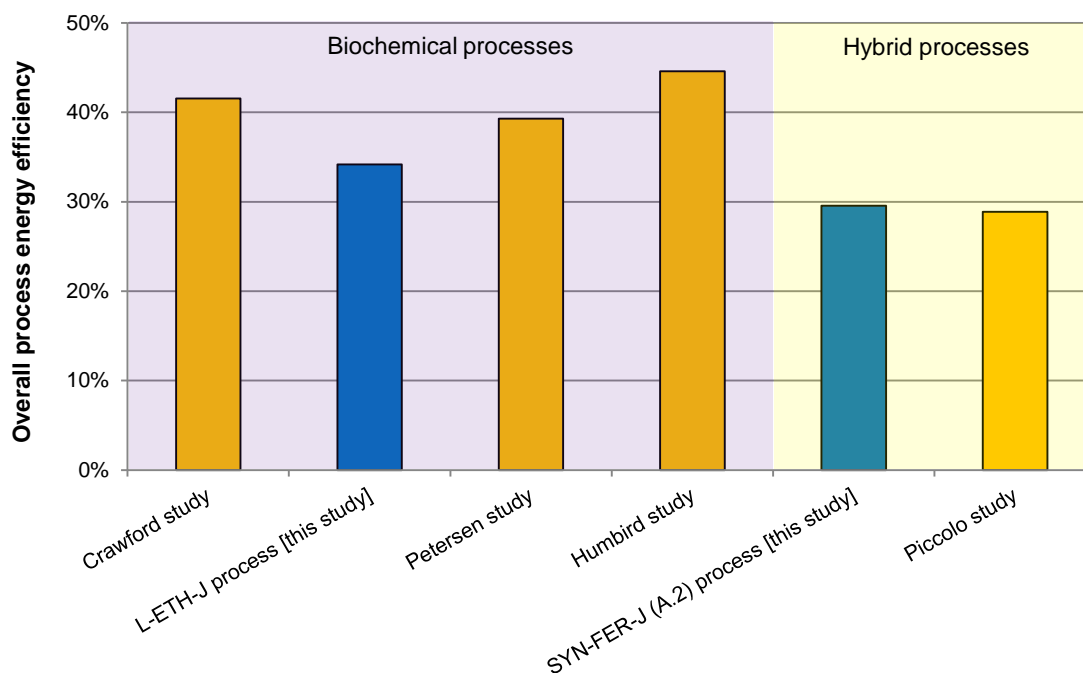


Figure 47: Typical process energy efficiencies of biochemical and hybrid processes

*Crawford study* – study by Crawford [49], scenario that produces hydrogen by natural gas reforming; *Petersen study* – study by Petersen [93]; *Humbird study* – study by Humbird et al. [32]; *Piccolo study* – study by Piccolo et al. [6], base scenario.

The L-ETH-J process updated the *Petersen study* by converting its ethanol product to mainly jet fuel resulting in a reduction in overall process energy efficiency (39% to 33%). The lower overall process energy efficiency of the *Petersen study* in comparison to the *Humbird study* (both utilized biochemical conversion of lignocellulose to ethanol) can largely be ascribed to the lower ethanol yield obtained by the *Petersen study*.<sup>x</sup>

The *Crawford study* performed lignocellulose fermentation to acetic acid, catalytic conversion to ethanol, followed by upgrading to jet fuel. The significant hydrogen required by

<sup>w</sup> The hybrid processes utilized the thermochemical and biochemical pathway.

<sup>x</sup> The L-ETH-J process produces around 200 kg ethanol per MT lignocellulose fed (dry and ash-free) which is considerably less than what is proposed by Humbird et al. (between 240 to 270 kg ethanol per MT dry & ash-free lignocellulose).

the *Crawford study* process was obtained from natural gas reforming (in contrast to the use of ethanol by the L-ETH-J process for hydrogen production). The high process energy efficiency obtained by the *Crawford study* is due to optimistic yields (250 kg jet fuel per dry MT lignocellulose) and the use of fossil-sourced hydrogen.

The two hybrid processes in Figure 47 (utilizing gasification followed by syngas fermentation) both achieved process efficiencies just below 30%. The SYN-FER-J process also performed upgrading of the ethanol to jet fuel. Piccolo et al. [6] predicted future process energy efficiencies of up to 36%.

The typical overall process energy efficiencies of 1G conversion processes based on vegetable oil and sugarcane (or molasses) feed are compared in Figure 48.

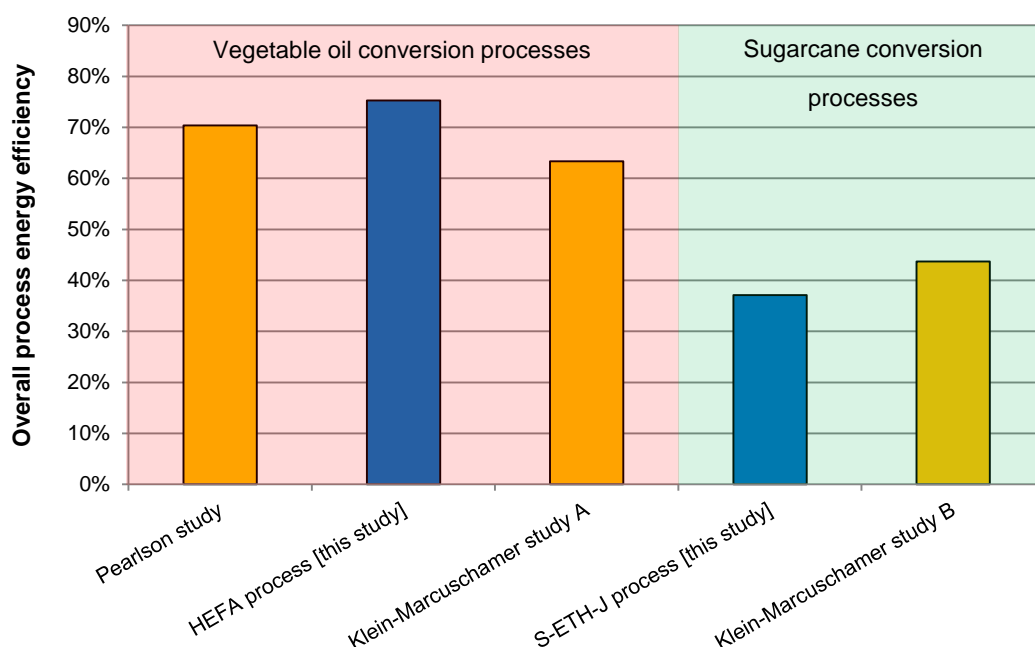


Figure 48: Typical process energy efficiencies of 1G conversion processes

*Klein-Marcuschamer study A* – study by Klein-Marcuschamer et al. [5], scenario that converts pongomia oil to mainly jet fuel; *Pearlson study* – study by Pearlson [15], hydrogen production scenario; *Klein-Marcuschamer study B* – study by Klein-Marcuschamer et al. [5], scenario that converts molasses to mainly jet fuel.

The *Pearlson study* [15], the *Klein-Marcuschamer study A* [5] and the HEFA process from this study all convert vegetable oil to fuels (mainly jet fuel) with process energy efficiencies between 63% and 75%. The HEFA process is the only study that produces hydrogen from the process by-products, whilst the *Pearlson study* produces hydrogen from natural gas and the *Klein-Marcuschamer study A* purchased hydrogen.

The *Klein-Marcuschamer study B* [5] converts sugarcane molasses via fermentation to farnesene which is upgraded to fuels (mainly jet fuel). Although the S-ETH-J process from this study converts sugarcane and trash to mainly jet fuel via ethanol (with significant electricity surplus,) similar overall process energy efficiencies (37% and 44%) were achieved.

## 7.2 Process Economics

### 7.2.1 Capital and operating costs of processes in this study

The investigated processes' base FCI and total raw material base cost are compared in Figure 49. The total raw material costs consist mainly of the main feedstock cost (lignocellulose, vegetable oil and sugarcane), whilst the major additional raw material costs are natural gas for the FP-J process, enzymes for the L-ETH-J process and trash for the S-ETH-J process.

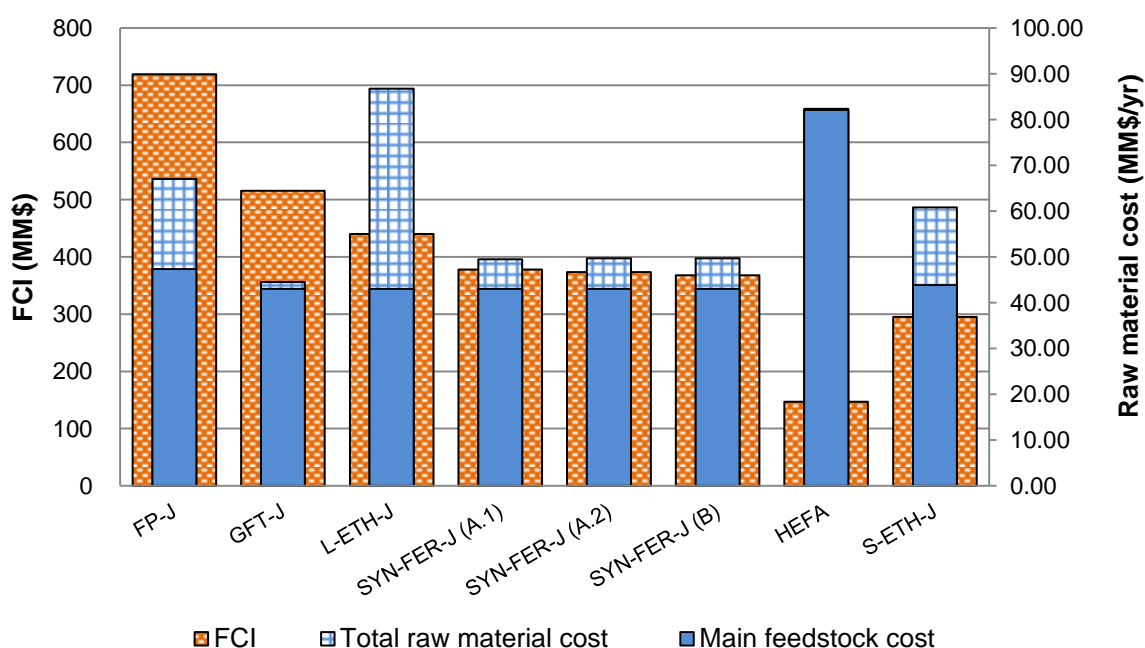


Figure 49: FCI, feedstock and total raw material cost of the investigated processes

It can be seen in Figure 49 that processes using 1G feedstock (HEFA and S-ETH-J) have smaller FCI in comparison to the 2G fed processes, whilst the raw material costs of the 2G fed processes are generally smaller than the 1G fed processes (with exception to the FP-J process due to natural gas costs and the L-ETH-J process due to enzyme costs).

For the 2G fed processes, the pure thermochemical processes have the highest FCI with the \$719 million for the FP-J process and \$516 million for the GFT-J process. There is

considerable uncertainty surrounding the future cost of enzymes accounting for around 37% of the total raw material cost of the L-ETH-J process [58]. The HEFA process with a low FCI of \$147 million has annual total raw material cost of over \$80 million primarily due to the vegetable oil feed. Around 25% of the raw material cost of the S-ETH-J is devoted to buying of trash for surplus power generation.

Furthermore, the fixed operating costs of the processes are compared in Table 85. The labour related fixed operating costs are the same for all the processes except for the HEFA process.<sup>Y</sup> The additional fixed operating costs (maintenance and property insurance & tax) were taken to be directly proportional to the FCI (see section 4.6.3).

Table 85: Fixed operating costs of the investigated processes, costs are in MM\$

FP-J	GFT-J	L-ETH-J	SYN-FER-J			HEFA	S-ETH-J
			A.1	A.2	B		
32.9	25.4	22.6	20.3	20.1	19.9	9.6	17.2

## 7.2.2 Capital cost comparison with previous studies

As the capital costs of the processes had a significant effect on the resulting MJSP, a thorough comparison between the capital costs in this study and capital costs in literature was performed. The comparison will only be briefly discussed below, whilst the comprehensive comparison is shown in Appendix F.

The capital cost of the HEFA process was compared in Appendix F to the vegetable oil upgrading process by Klein-Marcuschamer et al. [5]. The HEFA process obtained a considerably lower total installed equipment cost of \$92 million versus the \$220 million<sup>Z</sup> determined by Klein-Marcuschamer et al. The main difference is in the hydrocracker capital cost (\$27 million versus \$120 million). The use of three sequential hydrotreaters by the study of Klein-Marcuschamer et al., in comparison to only one by the HEFA process, also increased the capital costs for the hydrotreater section (as well as increasing the capital costs of the compressors).

The only literature capital cost available for the ethanol to jet fuel (ETH-J) process section was from a study by Crawford [49]. The lower FCI of the study by Crawford of \$41 million

<sup>Y</sup> The labour related costs for the HEFA process are less as it comprises of a simpler process.

<sup>Z</sup> Based on this project's vegetable oil feed rate (14.9 MT/h) and 2007 dollars.

versus this project's \$101 million<sup>AA</sup> is possibly due to the use of a single step oligomerization process (instead of a two-step used by this study).

The capital cost of the SYN-FER process section (scenario A.1) was compared in Appendix F to the study by Piccolo et al. [6], whom also investigated the gasification followed by syngas fermentation process. The higher total installed equipment cost of Piccolo et al. of \$271 million<sup>BB</sup> versus this project's \$162 million is mainly due to the use of an oxygen-blown gasifier (that also requires an ASU) in comparison to a DFB gasifier used by this study. The power generation of the study by Piccolo et al. is also more expensive.

No comparison of the S-ETH process section was performed. A superficial comparison to the study by Humbird et al. [32] was made for the L-ETH process section in Appendix F. The total installed cost for the L-ETH process section of \$196 million compares well to the total installed cost by Humbird et al. of \$207 million<sup>CC</sup>.

In Appendix F, the capital cost of the FP-J process is compared to other fast pyrolysis with upgrading to fuels studies by Brown et al. [51] and Jones et al. [98]. The total installed costs for the FP-J process and studies by Brown et al. and Jones et al. [98] are \$450, \$347 and \$213 million respectively.<sup>DD</sup> The difference in cost obtained between the FP-J process and the study by Jones et al. [98] is mainly because of process difference (the FP-J process additionally consisted of a feedstock handling and power generation section). The much lower total installed cost by the study of Brown et al. is attributed to the purchase of hydrogen (the other two studies produced hydrogen on site) and due to the much lower capital costs predicted for the pyrolysis and hydroprocessing sections.

Studies by Ekbom et al. [48] and Swanson et al. [69] were included in the detailed capital costs comparison of the GFT-J process (see Appendix F). The GFT-J process in this study predicted a total installed cost of \$322 million which is in between the total installed costs of the studies by Ekbom et al. and Swanson et al. (\$479 million and \$226 million respectively<sup>EE</sup>). The main reason why the study by Ekbom et al. has higher capital cost in comparison to the GFT-J process is because it uses an expensive pressurized oxygen-blown gasifier (the study by Ekbom et al. also therefore requires a larger ASU) in

---

<sup>AA</sup> Both capital costs are based on an ethanol feed rate of 10<sup>6</sup> MT per year and 2007 dollars.

<sup>BB</sup> Based on this project's lignocellulose feed rate (77.9 MT/h) and 2007 dollars.

<sup>CC</sup> After removing the cost of the enzyme production section for the study by Humbird et al. as the L-ETH process bought enzymes. The cost is based on this project's lignocellulose feed rate (77.9 MT/h) and 2007 dollars.

<sup>DD</sup> The costs are based on the FP-J process' lignocellulose feed rate (83.5 MT/h) and 2007 dollars.

<sup>EE</sup> The cost is based on this project's lignocellulose feed rate (77.9 MT/h) and 2007 dollars.

comparison to an atmospheric DFB gasifier used by the GFT-J process. The less expensive installed cost by Swanson et al. can somewhat be attributed to the use of amine scrubbing for acid gas removal (the other two studies used a Rectisol unit) and to the absence of an ATR section.

### 7.2.3 Minimum jet selling prices

At the base economic parameters the HEFA process attained the lowest MJSP of all the investigated processes of \$1.67 per kg of jet fuel. The 2G fed process with the lowest MJSP was the GFT-J process with \$1.86 per kg of jet fuel; only slightly higher than the \$1.79 per kg of jet fuel of the S-ETH-J process. The MJSP of the FP-J process and the L-ETH-J process was \$2.57 and \$2.55 per kg jet fuel respectively, whereas the SYN-FER-J process scenarios obtained MJSP between \$1.90 and \$2.05 per kg jet fuel.

The MJSP of this study (blue bars) are compared in Figure 50 to MJSP of similar processes investigated by IATA [7] (red bars).<sup>FF</sup>

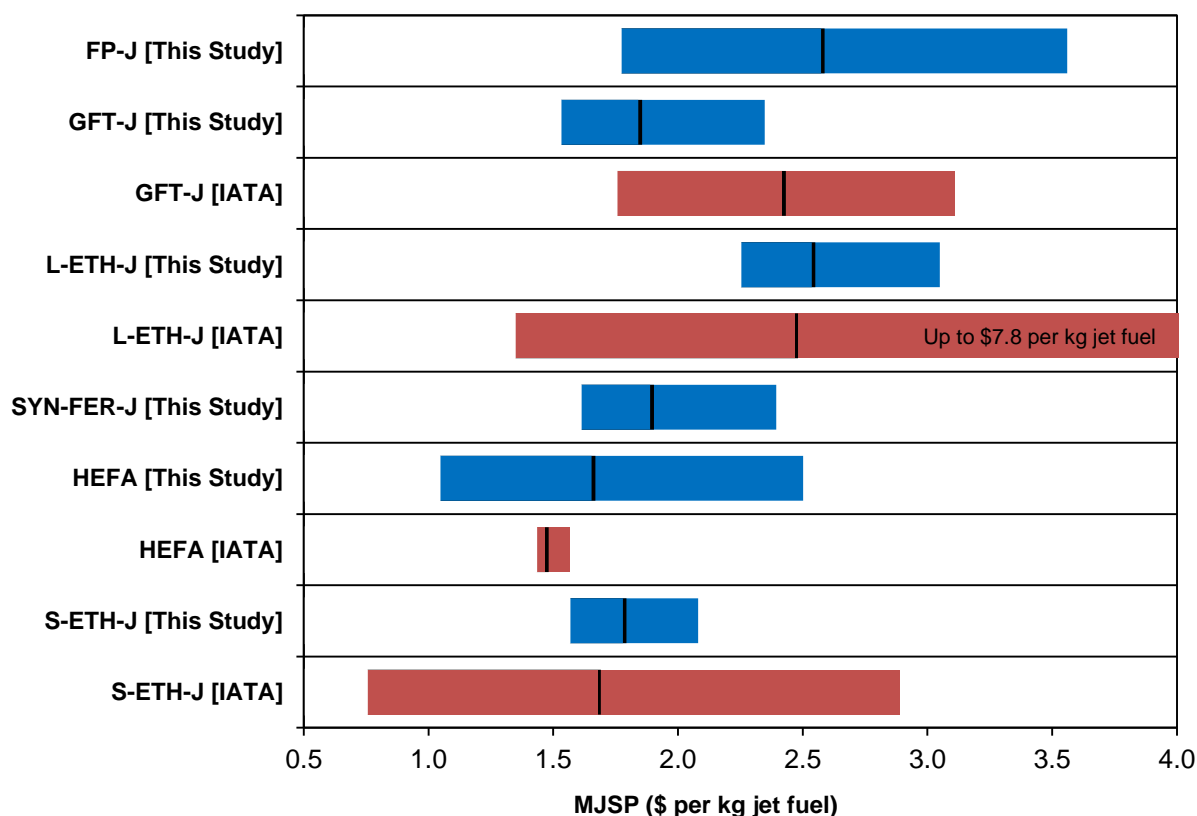


Figure 50: MJSP of processes in this study, compared to literature [7]

<sup>FF</sup> Note that the minimum fuel selling prices are a strong function of the various economic assumptions made by each investigation.

In Figure 50, the base MJSP are indicated by the black vertical lines on the bars. The low and high MJSP values of this study are the maximum variation of MJSP due to a *single parameter sensitivity analysis*, whilst the larger variability generally experienced by IATA MJSP is probably due to the calculation of a *multivariable sensitivity analysis*. Except for the GFT-J process, the base MJSP's of the L-ETH-J, HEFA and S-ETH-J processes in this study compare well to IATA's MJSP. It was determined by both this study and IATA that the base MJSP of the 1G fed processes currently have lower MJSP than 2G fed processes.

Table 86 compares the breakdown of the MJSP for the investigated processes. For all the processes, the main feedstock cost and average return on investment cost are generally responsible for the major share of the resulting MJSP. The resulting MJSP is also largely influenced by major additional feedstock costs (trash, enzymes and natural gas) and by-products such as grid electricity and fuels. Fixed costs also have a large influence on the MJSP for all the processes.

Table 86: MJSP breakdown for the investigated processes

Process	Operating Costs (percentage of MJSP)					
	HEFA	SYN-FER-J (A.2)	S-ETH-J	L-ETH-J	FP-J	GFT-J
Main feedstock <sup>1</sup>	87.4%	36.1%	48.0%	27.6%	52.6%	37.0%
Trash	-	-	15.7%	-	-	-
Enzymes	-	-	-	20.9%	-	-
Natural gas	-	-	-	-	20.7%	-
Catalysts	0.8%	6.8%	7.8%	5.1%	3.5%	5.4%
Other raw materials	0.1%	4.2%	1.8%	6.2%	0.7%	0.9%
Waste disposal	0.1%	1.1%	1.8%	0.8%	1.9%	1.0%
Grid electricity	0.0%	0.0%	-30.2%	-7.7%	-44.5%	-6.8%
Fuel by-products	-19.8%	-8.0%	-8.5%	-6.0%	-78.1%	-19.1%
Fixed costs	10.2%	16.9%	18.9%	14.5%	36.6%	21.9%
Capital depreciation	7.9%	6.2%	8.0%	4.7%	8.2%	6.4%
Average income tax	1.5%	3.1%	3.2%	2.8%	7.4%	4.2%
Average return on investment	12.0%	33.6%	33.5%	31.3%	91.0%	49.1%

<sup>1</sup> Consisting of lignocellulose, vegetable oil and sugarcane, respectively.

Figure 51 compares the effect of lignocellulose feedstock cost on the MJSP of the 2G fed processes with a base feedstock cost of \$70 per dry MT lignocellulose. Except for the FP-J process, similar changes in MJSP are experienced based on feedstock cost change for the processes (changes of MJSP ranged from \$0.78 to \$0.84 per kg jet fuel). The large MJSP cost change of \$1.56 per kg jet fuel shown by the FP-J process is mainly because the FP-J process was not aimed at maximum jet fuel.

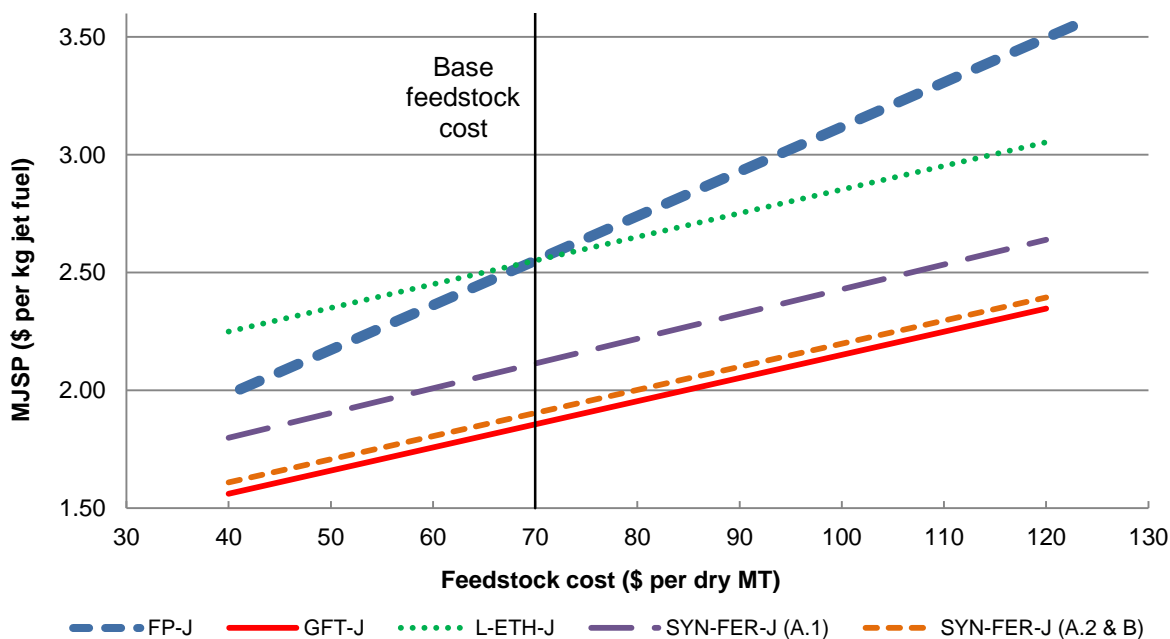


Figure 51: Effect of changing lignocellulose feedstock cost on 2G processes' MJSP

The effects of feedstock cost on the MJSP of the 1G fed processes are shown in Figure 52. The base feedstock cost of the HEFA process was \$700 per MT vegetable oil and the S-ETH-J process was \$30 per wet MT sugarcane. The HEFA process experienced significant changes in final MJSP ranging from \$1.04 to \$2.50 per kg jet fuel for vegetable oil costs between \$400 and \$1100 per MT vegetable oil. The S-ETH-J process showed smaller changes of MJSP based on changing sugarcane feedstock cost. For sugarcane costs between \$22 and \$40 per wet MT the S-ETH-J process displayed MJSP ranging from \$1.56 to \$2.08 per kg jet fuel.

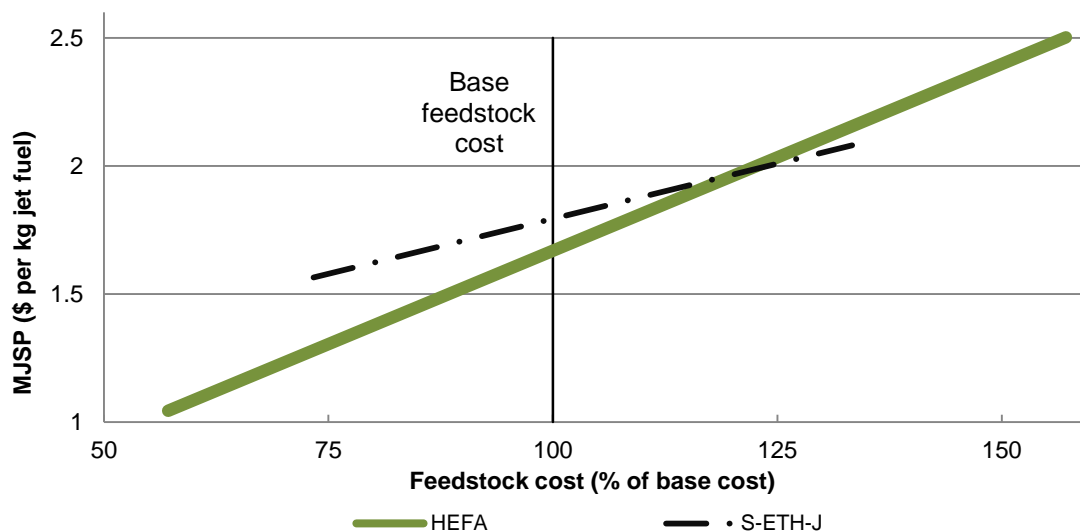


Figure 52: Effect of changing feedstock cost on 1G processes' MJSP

The effects of changing FCI on the MJSP of the investigated processes are demonstrated in Figure 53. The FCI were changed for the processes ranging from 70% of the base FCI up to 130% of the base FCI.<sup>GG</sup> The large MJSP cost change shown by the FP-J process is mainly because the FP-J process was not aimed at maximum jet fuel and because the process has a very large base FCI. Similarly, the GFT-J process with a large base FCI experienced a significant change in MJSP with changing FCI, whilst the HEFA process with a low base FCI experienced little change in MJSP with changing FCI.

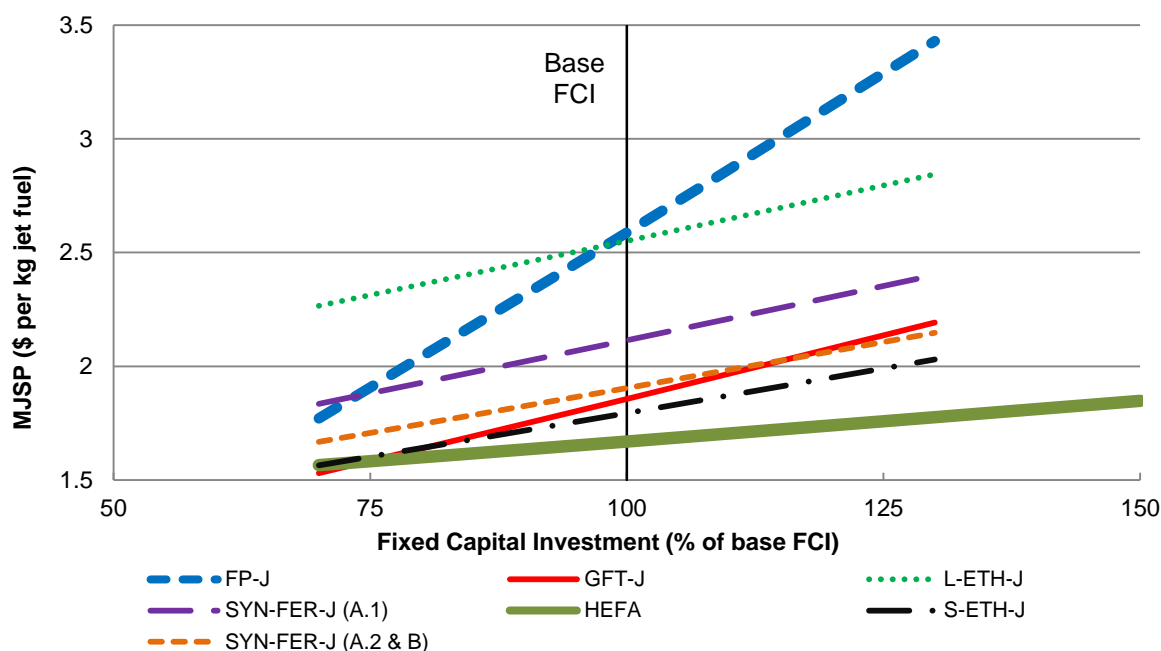


Figure 53: Effect of changing FCI cost on processes' MJSP

As discussed in section 4.6.5, a theoretical sensitivity analysis was done to determine the effects of the jet-to-fuel (JTF) ratios of the processes on the resulting MJSP.<sup>HH</sup> The JTF ratios and related MJSP of the processes are given in Table 87 for the base and sensitivity cases. From Table 87 it is apparent that the extent to which the processes were optimized for jet fuel had a substantial effect on the resulting MJSP. At an increased JTF ratio of 0.85, the MJSP of the FP-J process is reduced to about 70% of its base MJSP. For an increased JTF ratio of 0.85, the MJSP of the GFT-J and HEFA processes also reduced by \$0.07 and \$0.04 per kg jet fuel respectively.

<sup>GG</sup> The HEFA process was changed up to 150% of base FCI as it had a small base FCI.

<sup>HH</sup> The sensitivity analysis was performed by simply adjusting the final fuel mass ratios. This therefore does not take into account the process changes (and associated capital and operating cost changes) required to achieve the JTF ratios.

Table 87: Effect of JTF ratios on MJSP

Process	Base JTF ratio	Base MJSP (\$ per kg jet fuel)	Sensitivity values for JTF ratio	Sensitivity MJSP (\$ per kg jet fuel)
HEFA	0.78	1.67	0.85	1.63
SYN-FER-J	0.88 <sup>1</sup>	1.90 – 2.05	-	-
S-ETH-J	0.88 <sup>1</sup>	1.79	-	-
L-ETH-J	0.88 <sup>1</sup>	2.55	-	-
FP-J	0.37	2.57	0.7; 0.85	1.91; 1.78
GFT-J	0.77	1.86	0.85	1.79

<sup>1</sup> The same jet-to-fuel ratios are achieved by the SYN-FER-J, S-ETH-J and L-ETH-J processes as the upgrading section (from ethanol to jet fuel) is the same for all three processes.

However, the extents to which the processes can be optimized for jet fuel are in reality governed by certain theoretical and practical limits. Although the prospective and practicality of increasing the JTF ratio of the GFT-J and HEFA processes are doubtful, it would certainly be worthwhile to investigate the extent of maximization of jet fuel for the FP-J process. The use of a hydrocracker to convert the diesel and gas oil fractions of the FP-J process to mainly jet fuel is one possibility.

### 7.3 Concluding remarks

Based on current technology and the base assumptions, this study found that the 1G fed processes have lower MJSP in comparison to 2G fed processes. There was, however, significant overlap between the MJSP of the 1G fed processes and certain 2G fed processes (especially GFT-J and SYN-FER-J processes) based on the economic sensitivity analysis.

Although the HEFA process is attractive as it attained the lowest MJSP and required a low FCI, it is very sensitive to its vegetable oil feedstock cost which has shown significant variability in the last 10 years (from below \$400 up to \$1400 per MT vegetable oil) [140]. As lignocellulosic biomass is an abundant feedstock [24] with a relatively low cost [18], processes utilizing lignocellulose are less susceptible and influenced to large fluctuations in feedstock cost (this is evident in the relatively lower sensitivity to feedstock cost experienced by the GFT-J, SYN-FER-J and L-ETH-J processes). Even though the S-ETH-J process does not have one sensitivity parameter which significantly changes its MJSP, the cumulative effect of a few parameters with noteworthy effect on its MJSP (sugarcane cost, FCI, stream factor, price of electricity, minimum acceptable IRR and trash cost) also causes uncertainty in its MJSP.

The FP-J process had the highest MJSP due to its low JTF ratio. At an increased JTF ratio (theoretical analysis) the prospect of the FP-J process increased significantly, validating

future investigation. The “environmental setback” due to the use of natural gas by the FP-J process will, however, need to be quantified in future study to enable adequate comparison to other processes. The high additional costs of the L-ETH-J process (especially enzyme cost) render it unpromising. According to Kazi et al. [58], there is significant uncertainty surrounding the future cost for enzymes. Reduced costs for enzymes, increased yields from especially the xylose fraction (as described by Humbird et al. [32]) and increased ethanol concentrations could, however, significantly increase the future promise of the L-ETH-J process.

Based on current technology, the GFT-J process and SYN-FER-J process scenarios obtained the lowest MJSP of all the 2G fed processes. The SYN-FER-J process scenarios performed well attaining slightly higher MJSP to the GFT-J process despite having the lowest energy efficiencies. The promising MJSP of the SYN-FER-J process scenarios are attributed to its high jet fuel ratios, low additional raw material costs and its relatively low FCI (in comparison to the 2G fed processes). In contrast to the SYN-FER-J process, the GFT-J process required a very high FCI, but had the highest energy efficiency of all the 2G fed process. Higher fuel mass ratios obtained for the GFT processes by literature [69], [48] suggest that alternative process configurations for the GFT-J process could further decrease its MJSP.

Although the 1G fed processes achieved the lowest MJSP, sufficient 1G feedstock to substantially reduce GHG emissions of the aviation industry, without negatively affecting food prices, is unlikely [145]. In contrast, lignocellulose is plentiful, whilst not competing with food crops [145]. It is therefore believed that 2G fed processes are essential for the sustainable mitigation of GHG emissions of the aviation industry in the future.

## 8 Conclusions

This study consisted of comprehensive assessments on jet fuel production processes from plant-derived sources. Mass and energy balances were derived for the investigated processes based on detailed process models. Furthermore, the process economics of the processes were investigated on the same basis. Based on the results, the following conclusions were drawn.

All the investigated processes obtained electricity and hydrogen self-sufficiency independent of fossil fuels except for the FP-J process.<sup>II</sup> The HEFA and SYN-FER-J processes, however, required the combustion of intermediate products to be electricity self-sufficient.

For the 2G fed processes, the two thermochemical processes (FP-J and GFT-J processes) obtained the highest fuel mass ratios of around 0.14. The processes with an ethanol intermediate (L-ETH-J, S-ETH-J and SYN-FER-J processes) were able to obtain the highest jet-to-fuel ratios of 0.88, whilst the GFT-J and HEFA processes which aimed for jet fuel, only obtained jet-to-fuel ratios slightly below 0.8. The FP-J and HEFA processes required the largest amount of hydrogen (128.2 kg and 65.3 kg per MT of fuel produced respectively).

The highest overall process energy efficiency for the 2G and 1G fed processes was 37.2% for the GFT-J process and 75.3% for the HEFA process. The SYN-FER-J process scenarios obtained the lowest overall process energy efficiency (between 27.6% and 29.6%).

The overall energy efficiencies of the 1G fed processes compared well to literature, but the overall energy efficiencies of the 2G fed processes were irregular compared to literature. The varying overall energy efficiencies of the 2G fed processes with a biochemical conversion section (L-ETH-J and SYN-FER-J processes) are mainly attributed to the assumed SOT; which is significantly different between studies as the SOT for the biochemical conversion sections are continually improving.<sup>JJ</sup> The different process configurations of the gasification and FT synthesis process resulted in varying overall energy efficiencies between literature and the GFT-J process, whereas the low overall efficiency of the FP-J process compared to previous studies can mainly be ascribed to its low overall fuel yield and its aim for substantial surplus power production.

---

<sup>II</sup> The FP-J process fed natural gas for hydrogen production. The process can attain hydrogen self-sufficiency, but at a significant reduction in fuel production.

<sup>JJ</sup> The conversion yields of the SYN-FER-J process were up to date, but the conversion yields of the L-ETH-J process were somewhat outdated.

For the investigated processes, the FCI of the thermochemical processes were determined to be the highest at \$719 million for the FP-J process and \$516 million for the GFT-J process. The L-ETH-J process and SYN-FER-J process scenarios obtained FCI of \$440 million and between \$368 and \$378 million respectively. The FCI of both 1G fed processes were lower than all the FCI of the 2G fed processes with \$147 million for the HEFA process and \$295 million for the S-ETH-J process. Although the total raw material costs consisted largely of the main feedstock cost (lignocellulose, vegetable oil or sugarcane), major additional raw material costs included enzymes for the L-ETH-J process, natural gas for the FP-J process and trash for the S-ETH-J process.

For the 2G fed processes at the base economic parameters, the FP-J and L-ETH-J processes obtained the higher MJSP of \$2.57 and \$2.55 per kg jet fuel respectively, whilst the GFT-J process and SYN-FER-J processes obtained the lower MJSP of \$1.86 and \$1.90 per kg jet fuel respectively. The HEFA process obtained the lowest base MJSP of all the investigated processes at \$1.67 per kg of jet fuel while the S-ETH-J process obtained a base MJSP of \$1.79 per kg of jet fuel.

Based on the economic sensitivity analysis performed for the processes, it was found that the main feedstock cost and FCI generally had the largest effect on the resulting MJSP. Except for the FP-J process, all the 2G fed processes experienced similar changes in MJSP due to changing feedstock cost. The MJSP of the HEFA process has uncertainty as it is considerably influenced by changing feedstock cost. Changing FCI had large effects on the MJSP of the processes with a large FCI (FP-J and GFT-J processes), whilst it had much smaller effects on the MJSP of the 1G fed processes with a smaller FCI. Another factor that also influenced the MJSP of the 2G fed processes significantly was the minimum acceptable IRR. It was found that the MJSP of the FP-J process can be decreased significantly by increasing of its jet-to-fuel ratios (theoretical analysis), validating future investigation.

As the economic sensitivity analysis showed that there was significant overlap between the MJSP of the 1G fed processes and certain 2G fed processes (especially GFT-J and SYN-FER-J processes) along with the abundance of lignocellulose whilst not competing with food crops, suggests that 2G fed processes have large potential for the sustainable mitigation of GHG emissions of the aviation industry in the future [145].

## 9 Recommendations for Future Work

Recommendations for enhancement of existing process designs:

- Validating of the used physical property methods.
- The ethylene oligomerization reactor was simulated in Aspen Plus® without considerations of the catalyst or solvent recycle which is recommended for future study. Investigation on the type of solvent which would be most applicable may also prove useful.
- The ethylene oligomerization to jet fuel was performed in a two-step arrangement based on two sets of literature. It is recommended that one set of literature be obtained that optimizes the total ethylene oligomerization to jet fuel section. It is also recommended that the use of a one-step arrangement for ethylene oligomerization to jet fuel must be investigated (this could decrease the capital cost).
- Investigate the use of a high pressure gasifier for the high pressure syngas fermentation scenario of the SYN-FER-J process (scenario B).
- The bubble column reactors for the SYN-FER-J process were based on CSTR fermentation data. It is recommended that promising syngas fermentation data for reactors other than CSTR be obtained (e.g. bubble column or trickle-bed reactors).
- For the SYN-FER-J process, investigate the possibility of recycling a significant fraction of the separation section bottoms to the fermentation section. This could significantly reduce the process' wastewater (and associated power usage), whilst also possibly increasing the ethanol production by reducing the acetic acid by-product production.
- As the L-ETH-J process produced considerably less ethanol per MT lignocellulose than what was proposed by Humbird et al. [32], it is recommended that the conversion yields of the L-ETH-J process be updated with newer experimental data.
- For the GFT-J process, determine the effect of different process configurations (e.g. different types of gasifiers, the use of an ATR, different types of FT reactor etc.) on the process efficiencies and economics.
- For the FP-J process, explore the various possibilities for maximization of the jet fuel fraction based on the fast pyrolysis process section as well as the hydroprocessing and separation section.
- Adjust the FP-J process so that it does not aim for significant surplus electricity generation.
- Further investigate the hydrogen requirements of the FP-J process.

- For the processes producing substantial amounts of electricity, investigate different power generation scenarios (e.g. gas turbine versus standard steam turbine).
- Investigate the S-ETH-J process without feeding of additional trash.
- Explicitly simulate the drying of the biomass.
- Investigate the possible reduction in water make-up required by the processes when using air cooling instead of cooling water.

Additionally to the process designs, the following is recommended:

- Along with further investigation of the processes chosen in this study, it is recommended that the following 2G fed processes also be investigated (it is believed that sufficient literature is available in literature for their process simulation): L-ACID-J process, the SEP-CAT process, the L-BUT-J process and the SYN-CAT-J process.
- It is recommended that the effect of changing lignocellulose composition on the ultimate process outcomes be investigated (e.g. determining which type of lignocellulose composition favours which process pathway).
- A life-cycle assessment of the investigated processes is strongly recommended in a future study. Investigation of especially GHG emissions will be useful as this study aims to address the GHG emissions associated with the aviation industry. This will enable the comparison of the GHG emission reduction of different processes. It will also enable the comparison of different process scenarios for each process pathway (e.g. hydrogen purchase versus hydrogen production or electricity purchase versus electricity production) based on resultant GHG emissions. This can be used to guide decision-making for various process scenarios.
- Except for the SYN-FER-J process, only one process configuration was investigated for each process pathway. Investigation of various process configurations for each process pathway will give a better idea of the promise associated with each process pathway.
- It is recommended that comprehensive process sensitivity analysis be performed on the processes by changing the process conditions or yields in the Aspen Plus<sup>®</sup> simulations and determining their effect on process efficiencies and economics.
- From the literature investigation, it was apparent that there is a high variability in the capital cost of equipment. Further scrutinizing of the main equipment of the investigated processes could increase the accuracy of the final FCI.
- For the investigated processes, it is recommended that the effect of plant size on ultimate process economics be explored (this will include establishing the effect of plant size on feedstock price).

## 10 References

- [1] J. Moavenzadeh, M. Torres-Montoya and T. Gange, "Repowering Transport: Project White Paper," in *World Economic Forum*, Geneva, 2011.
- [2] "IndexMundi," IndexMundi, 2015. [Online]. Available: <http://www.indexmundi.com/energy.aspx?product=jet-fuel>. [Accessed 13 August 2015].
- [3] D. B. Agusdinata, F. Zhao, K. Ileleji and D. DeLaurentis, "Life Cycle Assessment of Potential Biojet Fuel Production in the United States," *Environmental science & technology*, vol. 45, no. 21, pp. 9133-9143, 2011.
- [4] J. Q. Bond et al., "Production of renewable jet fuel range alkanes and commodity chemicals from integrated catalytic processing of biomass," *Energy & Environmental Science*, vol. 7, no. 4, pp. 1500-1523, 2014.
- [5] D. Klein-Marcuschamer, C. Turner, M. Allen, P. Gray, K. Heimann, R. G. Dietzgen, P. M. Gresshoff, B. Hankamer, P. T. Scott, E. Stephens, R. Speights and L. K. Nielsen, "Technoeconomic analysis of renewable aviation fuel from microalgae, *Pongomia pinnata*, and sugarcane," *Biofuels, Bioproducts & Biorefining*, vol. 7, no. 4, pp. 416-428, 2013.
- [6] C. Piccolo and F. Bezzo, "A techno-economic comparison between two technologies for bioethanol production from lignocellulose," *Biomass and bioenergy*, vol. 33, no. 3, pp. 478-491, 2008.
- [7] "IATA 2014 Report on Alternative Fuels," IATA, Montreal, 2014.
- [8] J. Holladay, K. Albrecht and R. Hallen, "Renewable routes to jet fuel," 5 November 2014. [Online]. Available: [http://aviation.u-tokyo.ac.jp/eventcopy/ws2014/20141105\\_07DOE%EF%BC%BFHolladay.pdf](http://aviation.u-tokyo.ac.jp/eventcopy/ws2014/20141105_07DOE%EF%BC%BFHolladay.pdf). [Accessed 13 August 2015].
- [9] G. Heminghaus et al., "Alternative Jet Fuels: A supplement to Chevron's Aviation Fuels Technical Review," Chevron Corporation, 2006.

- [10] J. Sandquist and M. B. Güell, "Overview of Biofuels for Aviation," *Chemical Engineering Transactions*, vol. 29, pp. 1147-1152, 2012.
- [11] G. T. Belot, "An Evaluation and Economic Study of Alternative Jet Fuel from *Jatropha Curcas* Oil," Masters's Dissertation, The Pennsylvania State University, 2009.
- [12] R. W. Stratton, H. M. Wong and J. I. Hileman, "Life Cycle Greenhouse Gas Emissions from Alternative Jet Fuels," The Partnership for Air Transportation Noise and Emissions Reduction, Cambridge, 2010.
- [13] S. Butnark, "Thermally stable coal-based jet fuel: Chemical composition, thermal stability, physical properties and their relationships," Doctoral Dissertation, The Pennsylvania State University, 2003.
- [14] J. Hileman, D. Ortiz, J. Bartis, H. Wong, P. Donohoo, M. A. Weiss and I. Waitz, "Near-Term Feasibility of Alternative Fuels," Rand Corporation, 2009.
- [15] M. N. Pearlson, "A techno-economic and environmental assessment of hydroprocessed renewable distillate fuels," Master's Dissertation, Massachusetts Institute of Technology, 2011.
- [16] A. De Klerk, *Fischer-Tropsch Refining*, John Wiley & Sons, 2012.
- [17] L. M. Balster, E. Corporan, M. J. DeWitt, J. T. Edwards, J. S. Ervin, J. L. Graham and S.-Y. Lee, "Development of an advanced, thermally stable, coal-based jet fuel," *Fuel Processing Technology*, vol. 4, no. 89, pp. 364-378, 2008.
- [18] L. Horta Nogueira, "Flightpath to Aviation Biofuels in Brazil," 2013. [Online]. Available: <http://academic.sun.ac.za/microbiology/Documents/ISAF%20PDF%20for%20web/Session%2015/Luiz%20Horta%20Nogueira%20.pdf> . [Accessed 25 May 2013].
- [19] "IATA 2011 Report on Alternative Fuels," IATA, Montreal, 2011.
- [20] "IATA 2009 Report on Alternative Fuels," IATA, Montreal, 2009.
- [21] "IATA 2012 Report on Alternative Fuels," IATA, Montreal, 2012.

- [22] J. I. Hileman, H. M. Wong, D. Ortiz, N. Brown, L. Maurice and M. Rumizen, "The feasibility and potential environmental benefits of alternative fuels for commercial aviation," in *26th International Congress of the Aeronautical Sciences (ICAS)*, Anchorage, 2008.
- [23] "Energy from waste and wood," Weebly, [Online]. Available: <http://energyfromwasteandwood.weebly.com/generations-of-biofuels.html>. [Accessed 20 May 2012].
- [24] L. A. Lucia, "Lignocellulose biomass: A potential feedstock to replace petroleum," *BioResources*, vol. 3, no. 4, pp. 981-982, 2008.
- [25] A. Demirbas, "Biomass feedstocks," in *Biofuels*, London, Springer, 2009, pp. 45-85.
- [26] P. Kumar, M. B. Diane, M. J. Delwiche and P. Stroeve, "Methods for pretreatment of lignocellulosic biomass for efficient hydrolysis and biofuel production," *Industrial & Engineering Chemistry Research*, vol. 48, no. 8, pp. 3713-3729, 2009.
- [27] K. R. Hakeem, M. Jawaid and U. Rashid, *Biomass and Bioenergy: Processing and Properties*, Springer, 2014.
- [28] "Oilsands," Fuel Chemistry Division, [Online]. Available: [http://www.ems.psu.edu/~pisupati/ACSOutreach/Oil\\_Sands.html](http://www.ems.psu.edu/~pisupati/ACSOutreach/Oil_Sands.html). [Accessed 11 June 2013].
- [29] A. P. Raje and B. Davis, "Fischer-Tropsch synthesis over iron-based catalysts in a slurry reactor. Reaction rates, selectivities and implications for improving hydrocarbon productivity," *Catalysis today*, vol. 36, no. 3, pp. 335-345, 1997.
- [30] S. Bharadwaj and L. Schmidt, "Catalytic partial oxidation of natural gas to syngas," *Fuel Processing Technology*, vol. 42, no. 2, pp. 109-127, 1995.
- [31] I. Saito and J. Shabtai, "Process for the low-temperature depolymerization of coal and its conversion to a hydrocarbon oil". Washington, DC: U.S. Patent and Trademark Office. Patent U.S. No. 4 728 418, 1 March 1988.
- [32] D. Humbird et al., "Process Design and Economics for Biochemical Conversion of Lignocellulosic Biomass to Ethanol," National Renewable Energy Laboratory,

Colorado, 2011.

- [33] M. D. Staples et al., "Lifecycle greenhouse gas footprint and minimum selling price of renewable diesel and jet fuel from fermentation and advanced fermentation production technologies," *Energy & Environmental Science*, vol. 7, no. 5, pp. 1545-1554, 2014.
- [34] S. Kumar, J.-P. Lange, G. van Rossum and S. R. Kersten, "Liquefaction of lignocellulose in fractionated light bio-oil: Proof of concept and techno-economic assessment," *ACS Sustainable Chemistry & Engineering*, 2015.
- [35] Y. Guo, T. Yeh, W. Song, D. Xu and S. Wang, "A review of bio-oil production from hydrothermal liquefaction of algae," *Renewable and Sustainable Energy Reviews*, vol. 48, pp. 776-790, 2015.
- [36] A. Dutta et al., "Process Design and Economics for Conversion of Lignocellulosic Biomass to Ethanol: Thermochemical Pathway by Indirect Gasification and Mixed Alcohol Synthesis," National Renewable Energy Laboratory, Colorado, 2011.
- [37] J. Daniell, M. Köpke and S. D. Simpson, "Commercial Biomass Syngas Fermentation," *Energies*, vol. 5, no. 12, pp. 5372-5417, 2012.
- [38] M. J. Climent, A. Corma and S. Iborra, "Conversion of biomass platform molecules into fuel additives and liquid hydrocarbon fuels," *Green Chemistry*, vol. 16, no. 2, pp. 516-547, 2014.
- [39] J. Kowal, "Boeing and Sustainable Aviation Biofuel Development," May 2015. [Online]. Available:  
[http://www.boeing.com/resources/boeingdotcom/principles/environment/pdf/Background\\_Boeing\\_biofuel.pdf](http://www.boeing.com/resources/boeingdotcom/principles/environment/pdf/Background_Boeing_biofuel.pdf). [Accessed 13 August 2015].
- [40] "Honeywell Green Jet Fuel," Honeywell International Inc., 2015. [Online]. Available:  
<http://www.uop.com/processing-solutions/renewables/green-jet-fuel/>. [Accessed 13 August 2015].
- [41] "Our Process," Fulcrum BioEnergy, 2015. [Online]. Available: <http://fulcrum-bioenergy.com/technology/our-process/>. [Accessed 13 August 2015].

- [42] "The Solena Fuels Solution," Solena Fuels, 2015. [Online]. Available: <http://www.solenafuels.com/index.php/our-solution>. [Accessed 13 August 2015].
- [43] "Jet Fuel," Amyris, 2015. [Online]. Available: <https://amyris.com/products/jet-fuel/>. [Accessed 13 August 2015].
- [44] B. M. Güell, M. Bugge, R. S. Kempegowda, A. G. Paap and M. Scott, "Benchmark of conversion and production technologies for synthetic biofuels for aviation," SINTEF Energy Research, Norway, 2012.
- [45] R. E. Sims, W. Mabee, J. N. Saddler and M. Taylor, "An overview of second generation biofuel technologies," *Bioresource technology*, vol. 101, no. 6, pp. 1570-1580, 2010.
- [46] C. B. Clifford, "Ethanol Production - General Information," The Pennsylvania State University, 2015. [Online]. Available: <https://www.e-education.psu.edu/egee439/node/646>. [Accessed 5 11 2015].
- [47] International Energy Agency, Biofuels for transport: an international perspective, International Energy Agency, OECD, 2004.
- [48] T. Ekbom, C. Hjerpe, M. Hagström and F. Hermann, "Förstudie för biobaserat flygbränsle för Stockholm-Arlanda Flygplats," Varmesfork, Stockholm, 2009.
- [49] J. Crawford, "Techno-economic analysis of hydrocarbon biofuels from poplar biomass," Master's Dissertation, University of Washington, 2013.
- [50] V. Pham, M. Holtzapple and M. El-Halwagi, "Techno-economic analysis of biomass to fuel conversion via the MixAlco process," *Journal of industrial microbiology & biotechnology*, vol. 37, no. 11, pp. 1157-1168, 2010.
- [51] T. Brown, R. Thilakaratne, R. Brown and G. Hu, "Techno-economic analysis of biomass to transportation fuels and electricity via fast pyrolysis and hydroprocessing," *Fuel*, vol. 106, pp. 463-469, 2013.
- [52] B. Gebreslassie, M. Slivinsky, B. Wang and F. You, "Life cycle optimisation for sustainable design and operations of hydrocarbon biorefinery via fast pyrolysis, hydrotreating and hydrocracking," *Computers & Chemical Engineering*, vol. 50, pp. 71-

91, 2013.

- [53] Y. Zhang, T. Brown, G. Hu and R. Brown, "Techno-economic analysis of two bio-oil upgrading pathways," *Chemical Engineering Journal*, vol. 225, pp. 895-904, 2013.
- [54] M. Wright, J. Satrio, R. Brown, D. Daugaard and D. Hsu, "Techno-economic analysis of biomass fast pyrolysis to transportation fuels," National Renewable Energy Laboratory, Colorado, 2010.
- [55] S. Jones, J. Holladay, C. Valkenburg, D. Stevens, C. Walton, C. Kinchin, D. Czernik and S. Elliott, "Production of Gasoline and Diesel from Biomass via Fast Pyrolysis, Hydrotreating and Hydrocracking: A Design Case," Pacific Northwest National Laboratory, Washington, 2009.
- [56] R. Thilakaratne, T. Brown, Y. Li, G. Hud and R. Brown, "Mild catalytic pyrolysis of biomass for production of transportation fuels: a techno-economic analysis," *Green Chemistry*, vol. 16, no. 2, pp. 627-636, 2014.
- [57] E. Voegelé, "KiOR Outlines 2014 plan in operational update call," Biomass Magazine, 2014. [Online]. Available: <http://biomassmagazine.com/articles/9898/kior-outlines-2014-plan-in-operational-update-call>. [Accessed 15 January 2014].
- [58] F. K. Kazi, J. Fortman, R. Anex, G. Kothandaraman, D. Hsu, A. Aden and A. Dutta, "Techno-Economic Analysis of Biochemical Scenarios for Production of Cellulosic Ethanol," National Renewable Energy Laboratory, Colorado, 2010.
- [59] "Synfuels Biofuels," Synfuels International, Inc., [Online]. Available: <http://www.synfuels.com/SynfuelsBiofuelsBasics.pdf>. [Accessed 15 October 2013].
- [60] K. Keuchler, S. Brown and H. Jaenesch, "Olefin oligomerization to produce hydrocarbon compositions useful as fuels". Washington, DC: U.S. Patent and Trademark Office. Patent U.S. No. 7 678 954, 16 March 2010.
- [61] S. H. Mahdavian, D. Soudbar and M. Parvari, "Selective ethylene dimerization toward 1-butene by a new highly efficient catalyst system and determination of its optimum operating conditions in a buchi reactor.," *Int J Chem Eng Applic*, vol. 1, no. 3, pp. 276-281, 2010.

- [62] T. Haishi, K. Kasai and M. Iwamoto, "Fast and Quantitative Dehydration of Lower Alcohols to Corresponding Olefins on Mesoporous Silica Catalyst," *Chemistry Letters*, vol. 40, no. 6, pp. 614-616, 2011.
- [63] M. Kumar, Y. Goyal, A. Sarkar and K. Gayen, "Comparative economic assessment of ABE fermentation based on cellulosic and non-cellulosic feedstocks," *Applied Energy*, vol. 93, pp. 193-204, 2012.
- [64] S. Nahreen and B. Gupta, "Conversion of the Acetone–Butanol–Ethanol (ABE) Mixture to Hydrocarbons by Catalytic Dehydration," *Energy & Fuels*, vol. 27, no. 4, pp. 2116-2125, 2013.
- [65] R. Davis, L. Tao, E. Tan, M. Bidy, G. Beckham and C. Scarlata, "Process Design and Economic for the Conversion of Lignocellulosic biomass to Hydrocarbons: Dilute-Acid and Enzymatic Deconstruction of Biomass to Sugars and Biological Conversion of Sugars to Hydrocarbons," National Renewable Energy Laboratory, Denver, 2013.
- [66] Y. Xiaochen, Z. Jiljao and Z. Yubin, "SSF of lignocellulosic biomass for single cell oil production by oleaginous microorganisms". Patent WO2013006755-A3, 2 May 2013.
- [67] F. Zhang, S. R. Keasling and D. Jay, "Metabolic engineering of microbial pathways for advanced biofuels production," *Chemical biotechnology*, vol. 22, pp. 775-783, 2011.
- [68] R. M. Lennen and B. F. Pfleger, "Engineering Escherichia coli to synthesize free fatty acids," *Trends in Biotechnology*, vol. 30, no. 12, pp. 659-667, 2012.
- [69] R. M. Swanson, J. A. Satrio, R. C. Brown and A. Platon, "Techno-Economic Analysis of Biofuels Production Based on Gasification," National Renewable Energy Laboratory, Colorado, 2010.
- [70] S. LeViness, "Velocys Fischer-Tropsch Synthesis Technology – Comparison to Conventional FT Technologies," in *AIChE 2013 Spring Meeting*, 2013.
- [71] D. Verma, R. Kumar, A. Sinha and B. Rana, "Aviation fuel production from lipids by a single-step route using hierarchical mesoporous zeolites," *Energy & Environmental Science*, vol. 4, no. 5, pp. 1667-1671, 2011.

- [72] M. Mohammad, T. Hari, Z. Yaakob, Y. Sharma and K. Sopian, "Overview on the production of paraffin based-biofuels via catalytic hydrodeoxygenation," *Renewable and Sustainable Energy Reviews*, vol. 22, pp. 121-132, 2013.
- [73] H. J. Robota, J. C. Alger and L. Shafer, "Converting Algal Triglycerides to Diesel and HEFA Jet Fuel Fractions," *Energy & Fuels*, vol. 27, no. 2, pp. 985-966, 2013.
- [74] S. Gong, A. Shinozaki, M. Shi and E. Qian., "Hydrotreating of Jatropha Oil over Alumina Based Catalysts," *Energy & Fuels*, vol. 26, no. 4, pp. 2394-2399, 2011.
- [75] R. Kumar, B. S. Rana, R. Tiwari, D. Verma, R. Kumar, R. K. Joshi, M. O. Garg and A. K. Sinha, "Hydroprocessing of jatropha oil and its mixtures with gas oil," *Green Chemistry*, vol. 12, no. 12, pp. 2232-2239, 2010.
- [76] H. Huo, M. Wang, C. Bloyd and V. Putsche, "Life-Cycle Assessment of Energy and Greenhouse Gas Effects of Soybean-Derived Biodiesel and Renewable Fuels," Argonne National Laboratory, Lemont, IL, 2008.
- [77] P. Kokayeff, T. Marker and J. Petri, "Production of Fuel from Renewable Feedstocks using a Finishing Reactor". Washington, DC: U.S. Patent and Trademark Office. Patent US No. 0 133 144 A1, 3 June 2010.
- [78] S. Gong, N. Chen, S. Nakayama and E. W. Qian, "Isomerization of n-alkanes derived from jatropha oil over bifunctional catalysts," *Journal of Molecular Catalysis*, vol. 370, pp. 14-21, 2012.
- [79] M. McCall, J. Kocal, A. Bhattacharyya, T. Kalnes and T. Brandvold, "Production of Aviation Fuel from Renewable Feedstocks". Washington, DC: U.S. Patent and Trademark Office. Patent U.S. No.0 283 442 A1, 19 November 2009.
- [80] D. Fan, D.-J. Dai and H.-S. Wu, "Ethylene Formation by Catalytic Dehydration of Ethanol with Industrial Considerations," *Materials*, vol. 6, no. 1, pp. 101-115, 2013.
- [81] G. Chen, S. Li, F. Jiao and Q. Yuan, "Catalytic dehydration of bioethanol to ethylene over TiO<sub>2</sub>/γ-Al<sub>2</sub>O<sub>3</sub> catalysts in microchannel reactors.," *Catalysis Today*, vol. 125, no. 1, pp. 111-119, 2007.

- [82] N. Zhan, Y. Hu, H. Li, D. Yu, Y. Han and H. Huang, "Lanthanum-phosphorous modified HZSM-5 catalysts in dehydration of ethanol to ethylene: A comparative analysis," *Catalysis Communications*, vol. 11, no. 7, pp. 633-637, 2010.
- [83] J. Bi, X. Guo, M. Liu and X. Wang, "High effective dehydration of bio-ethanol into ethylene over nanoscale HZSM-5 zeolite catalysts," *Catalysis Today*, vol. 149, no. 1, pp. 143-147, 2010.
- [84] A. W. Al-Sa'doun, "Dimerization of ethylene to butene-1 catalyzed by Ti(OR')<sub>4</sub>-A1R<sub>3</sub>," *Applied Catalysis A: General*, vol. 105, no. 1, pp. 1-40, 1993.
- [85] W. E. Garwood and W. Lee, "Process for separating ethylene from light olefin mixtures while producing both gasoline and fuel oil". Washington, DC: U.S. Patent and Trademark Office. Patent U.S. No. 4 227 992, 10 December 1980.
- [86] M. Leal, "Technological evolution of sugarcane processing for ethanol and electric power generation," *Sugarcane bioethanol - R&D for Productivity and Sustainability*, pp. 561-576, 2010.
- [87] M. O. Dias et al., "Production of bioethanol and bio-based materials from sugarcane bagasse: Integration to conventional bioethanol production process," *Chemical Engineering Research and Design*, vol. 87, no. 9, pp. 1206-1216, 2009.
- [88] M. O. Dias et al., "Simulation of ethanol production from sugarcane in Brazil: economic study of an autonomous distillery," *Computer Aided Chemical Engineering*, vol. 28, pp. 733-738, 2010.
- [89] M. O. Dias et al., "Integrated versus stand-alone second generation ethanol production from sugarcane bagasse and trash," *Bioresource technology*, vol. 103, no. 1, pp. 152-161, 2012.
- [90] S. Macrelli, J. Mogensen and G. Zacchi, "Techno-economic evaluation of 2nd generation bioethanol production from sugar cane bagasse and leaves integrated with the sugar-based ethanol process," *Biotechnology for biofuels*, vol. 5, no. 1, pp. 1-18, 2014.
- [91] W. van der Westhuizen, "A Techno-economic evaluation of integrating first and

- second generation bioethanol production from sugarcane in Sub-Saharan Africa,” Master's Dissertation, University of Stellenbosch, 2013.
- [92] N. H. Leibbrandt, “Techno-economic study for Sugarcane Bagasse to Liquid Biofuels in South Africa: A Comparison between Biological and Thermochemical Process Routes,” Doctoral Dissertation, University of Stellenbosch, 2010.
- [93] A. M. Petersen, “Comparisons of the technical, financial risk and life cycle assessments of various processing options of sugarcane bagasse to biofuels in South Africa,” Master's Dissertation, University of Stellenbosch, 2012.
- [94] J. Sendelius, “Steam Pretreatment Optimisation for Sugarcane Bagasse in Bioethanol Production,” Master's Dissertation, Lund University, 2005.
- [95] C. Carrasco et al., “SO<sub>2</sub> catalyzed steam pretreatment and fermentation of enzymatically hydrolyzed sugarcane bagasse,” *Enzyme and Microbial Technology*, vol. 46, no. 2, pp. 64-73, 2010.
- [96] C. Martín, M. Marcet, O. Almazán and L. Jönsson, “Adaptation of a recombinant xylose-utilizing *Saccharomyces cerevisiae* strain to a sugarcane bagasse hydrolysate with high content of fermentation inhibitors,” *Bioresource Technology*, vol. 98, no. 9, pp. 1767-1773, 2007.
- [97] S. McLaren, “Evaluating the fast pyrolysis and hydrodeoxygenation process for the production of jet fuel and jet-fuel aromatics.,” Master's Dissertation, University of Stellenbosch, 2015.
- [98] S. Jones, P. Meyer, L. Snowden-Swan, A. Padmaperuma, E. Tan, A. Dutta, J. Jacobson and K. Cafferty, “Process Design and Economics for the Conversion of Lignocellulosic Biomass to Hydrocarbon Fuels,” Pacific Northwest National Laboratory & National Renewable Energy Laboratory & Idaho National Laboratory, 2013.
- [99] J. Piskorz, P. Majerski, D. Radlein, D. Scott and A. Bridgewater, “Fast pyrolysis of sweet sorghum and sweet sorghum bagasse,” *Journal of Analytical and Applied Pyrolysis*, vol. 46, no. 1, pp. 15-29, 1998.
- [100] D. C. Elliott, T. R. Hart, G. G. Neuenschwander, L. J. Rotness and A. Zacher,

- “Catalytic Hydroprocessing of Biomass Fast Pyrolysis Bio-oil to Produce Hydrocarbon Products,” *Environmental progress & sustainable energy*, vol. 28, no. 3, pp. 441-449, 2009.
- [101] E. D. Christensen, G. M. Chupka, J. Luecke, T. Smurthwaite, T. L. Alleman, K. Lisa, J. Franz, D. C. Elliott and R. L. McCormick, “Analysis of Oxygenated Compounds in Hydrotreated Biomass Fast Pyrolysis Oil Distillate Fractions,” *Energy & Fuels*, vol. 25, no. 11, pp. 5462-5471, 2011.
- [102] A. Petersen, S. Farzad and J. Görgens, “Techno-economic assessment of integrating methanol or Fischer-Tropsch synthesis in a South African sugar mill,” *Bioresource Technology*, vol. 183, pp. 141-152, 2015.
- [103] F. Trippe, M. Frohling, F. Schultmann, R. Stahl, E. Henrich and A. Dalai, “Comprehensive techno-economic assessment of DME synthesis and Fischer-Tropsch synthesis as alternative process steps within biomass-to-liquid production,” *Fuel Processing Technology*, vol. 106, pp. 577-586, 2012.
- [104] T. G. Kreutz, E. D. Larson, G. Liu and R. William, “Fischer-Tropsch Fuels from Coal and Biomass,” in *25th Annual International Pittsburgh Coal Conference*, Pittsburgh, Pennsylvania, 2008.
- [105] A. de Klerk, “Fischer-Tropsch fuels refinery design,” *Energy & Environmental Science*, vol. 4, no. 4, pp. 1177-1205, 2011.
- [106] K. Mansaray, A. M. Al-Taweel, A. E. Ghaly, F. Hamdullahpur and V. Ugursal, “Mathematical Modeling of a Fluidized Bed Rice Husk Gasifier: Part I-Model Development,” *Energy Sources*, vol. 22, no. 1, pp. 83-98, 2000.
- [107] C. Pfeifer, R. Rauch and H. Hofbauer, “In-Bed Catalytic Tar Reduction in a Dual Fluidized Bed Biomass Steam Gasifier,” *Industrial & engineering chemistry research*, vol. 43, no. 7, pp. 1634-1640, 2004.
- [108] L. Sun and R. Smith, “Rectisol wash process simulation and analysis,” *Journal of Cleaner Production*, vol. 39, pp. 321-328, 2013.
- [109] H. Song, D. Ramkrishna, S. Trinh and H. Wright, “Operating Strategies for Fischer-

- Tropsch Reactors: A Model-Directed Study,” *Korean Journal of Chemical Engineering*, vol. 21, no. 2, pp. 308-317, 2004.
- [110] F. Regalli, “Hydroconversion of model Fischer-Tropsch wax over noble metal/silica-alumina catalysts,” KTH Royal Institute of Technology, Stockholm, 2013.
- [111] Ş. Özkara-Aydınoğlu, “Thermodynamic equilibrium analysis of combined carbon dioxide reforming with steam reforming of methane to synthesis gas,” *International Journal of Hydrogen Energy*, vol. 35, no. 23, pp. 12821-12828, 2010.
- [112] V. Putsche, “Complete Process and Economic Model of Syngas Fermentation to Ethanol,” National Renewable Energy Laboratory, Colorado, 1999.
- [113] M. Martín and I. E. Grossmann, “Energy Optimization of Bioethanol Production via Gasification of Switchgrass,” *AIChE Journal*, vol. 57, no. 12, pp. 3408-3428, 2011.
- [114] J. van Kasteren, D. Dizdarevic, W. van der Waall, J. Guo and R. Verberne, “Bio-ethanol from Syngas,” Technische Universiteit Eindhoven, Eindhoven, 2005.
- [115] M. Mohammadi, G. D. Najafpour, H. Younesi, P. Lahijani, M. H. Uzir and A. R. Mohamed, “Bioconversion of synthesis gas to second generation biofuels: A review,” *Renewable and Sustainable Energy Reviews*, vol. 15, no. 9, pp. 4255-4273, 2011.
- [116] J. L. Gaddy, D. K. Arora, C.-W. Ko, J. R. Phillips, R. Basu, C. V. Wilkstrom and E. C. Clausen, “Methods for increasing the production of ethanol from microbial fermentation”. Washington, DC: U.S. Patent and Trademark Office. Patent U.S. No. 8 642 302 B2, 4 February 2014.
- [117] A. W. Bhutto, K. Qureshi, K. Harijan, G. Zahedi and A. Bahadori, “Strategies for the consolidation of biologically mediated events in the conversion of pre-treated lignocellulose into ethanol,” *RSC Advances*, vol. 4, no. 7, pp. 3392-3412, 2014.
- [118] P. C. Munasinghe and S. K. Khanal, “Biomass-derived syngas fermentation into biofuels: Opportunities and challenges,” *Bioresource technology*, vol. 101, no. 13, pp. 5013-5022, 2010.
- [119] R. Nieves, “Final Report from Mississippi Ethanol LLC to the National Renewable

- Energy Laboratory,” National Renewable Energy Laboratory, Mississippi, 2002.
- [120] A. Dutta, M. Talmadge, J. Hensley, M. Worley, D. Dudgeon, D. Barton, P. Groenendijk, D. Ferrari, B. Stears, E. Searcy, C. Wright and J. Hess, “Process Design and Economics for Conversion of Lignocellulosic Biomass to Ethanol: Thermochemical Pathway by Indirect Gasification and Mixed Alcohol Synthesis,” National Renewable Energy Laboratory, Colorado, 2011.
- [121] A. Morales, “Airlines May Get 1% of Fuel From Biofuels By 2015, Boeing Says,” Bloomberg Business, 22 July 2010. [Online]. Available: <http://www.bloomberg.com/news/articles/2010-07-22/commercial-airlines-may-get-1-of-fuel-from-biofuels-by-2015-boeing-says>. [Accessed 07 November 2015].
- [122] “IATA says too soon for aviation biofuels at scale; aims for 6% switch by 2020,” Biofuels Digest, 13 June 2011. [Online]. Available: <http://www.biofuelsdigest.com/bdigest/2011/06/13/iata-says-too-soon-for-aviation-biofuels-at-scale-aims-for-6-switch-by-2020/>. [Accessed 07 November 2015].
- [123] “Aspen Plus, V8.2,” Aspen Technology, Inc., 2013. [Online]. Available: [www.aspentech.com](http://www.aspentech.com).
- [124] E. C. Carlson, “Don't gamble with physical properties for simulations,” *Chemical Engineering Progress*, vol. 92, no. 10, pp. 35-46, 1996.
- [125] A. B. van der Merwe, “Evaluation of Different Process Designs for Biobutanol Production from Sugarcane Molasses,” Master's Dissertation, University of Stellenbosch, 2011.
- [126] M. Arvidsson and L. Björn, “Process integration study of a biorefinery producing ethylene from lignocellulosic feedstock for a chemical cluster,” Master's Dissertation, Chalmers University of Technology, 2011.
- [127] M. Zhang and Y. Yu, “Dehydration of Ethanol to Ethylene,” *Industrial & Engineering Chemistry Research*, vol. 52, no. 28, pp. 9505-9514, 2013.
- [128] J. Gorawara, “Use of Molecular Sieves and other Adsorbents for Contaminant Removal in Ethylene and Propylene Production,” in *AICHE 2009 Spring National*

*Meeting*, Tampa, Florida, 2009.

- [129] G. Cameron, L. Le, J. Levine and N. Nagulapalli, "Process Design for the Production of Ethylene from Ethanol," University of Pennsylvania, Pennsylvania, 2012.
- [130] R. Sinnott and G. Towler, *Coulson & Richardson's chemical engineering: vol. 6: Chemical Engineering Design*, Oxford: Butterworth-Heinemann, 2009.
- [131] J. A. Moulijn, M. Makkee and A. E. vand Diepen, *Chemical Process Technology*, Delft: John Wiley & Sons, 2013.
- [132] M. Castro, T. Song and J. Pinto, "Operational cost minimization in cooling water systems," *Brazilian Journal of Chemical Engineering*, vol. 17, no. 4, pp. 649-658, 2000.
- [133] M. Ringer, V. Putsche and J. Scahill, "Large-Scale Pyrolysis Oil Production : A Technology Assessment and Economic Analysis," National Renewable Energy Laboratory, Colorado, 2006.
- [134] S. Phillips, A. Aden, J. Jechura and D. Dayton, "Thermochemical Ethanol via Indirect Gasification and Mixed Alcohol Synthesis of Lignocellulosic Biomass," National Renewable Energy Laboratory, Colorado, 2007.
- [135] P. Spath, A. Aden, T. Eggeman, M. Ringer, B. Wallace and J. Jechura, "Biomass to Hydrogen Production Detailed Design and Economics Utilizing the Battelle Columbus Laboratory Indirectly-Heated Gasifier," National Renewable Energy Laboratory, Colorado, 2005.
- [136] R.-D. Behling, K.-V. Peinemann and L. B. da Silva, "Process for the separation/recovery of gasses". Washington, DC: U.S. Patent and Trademark Office. Patent US 6 179 900 B1, 30 January 2001.
- [137] S. Parkash, *Refining Process Handbook*, Burlington: Gulf Professional Publishing, 2003.
- [138] M. A. Goula, S. K. Kontou and P. E. Tsiakaras, "Hydrogen production by ethanol steam reforming over a commercial Pd/ $\gamma$ -Al<sub>2</sub>O<sub>3</sub> catalyst," *Applied Catalysis B*:

*Environmental*, vol. 49, no. 2, pp. 135-144, 2004.

- [139] R. Turton, R. C. Bailie, W. B. Whitling, J. A. Shaeiwitz and D. Bhattacharyya, *Analysis, Synthesis, and Design of Chemical Processes*, New Jersey: Pearson Education, Inc., 2012.
- [140] "IndexMundi," IndexMundi, 2015. [Online]. Available: <http://www.indexmundi.com/commodities/>. [Accessed 20 April 2015].
- [141] "South African Sugar Association," [Online]. Available: [http://www.sasa.org.za/Libraries/facts\\_figures\\_2014-2015/Recoverable\\_Value\\_and\\_Cane\\_Prices.sflb.ashx](http://www.sasa.org.za/Libraries/facts_figures_2014-2015/Recoverable_Value_and_Cane_Prices.sflb.ashx). [Accessed 15 July 2015].
- [142] C. Higman and M. van der Burgt, *Gasification*, Gulf Professional Publishing, 2011.
- [143] K. Yamashita and L. Barreto, "Biomass gasification for the co-production of Fischer-Tropsch liquids and electricity," International Institute for Applied Systems Analysis, Laxenburg, 2004.
- [144] "Renewable Bioenergy: Technologies, Risks and Rewards," in *IMECHE Conference Transactions*, Suffolk, Professional Engineering Publishers, 2003.
- [145] S. N. Naik, V. V. Goud, P. K. Rout and A. K. Dalai, "Production of first and second generation biofuels: a comprehensive review," *Renewable and Sustainable Energy Reviews*, vol. 14, no. 2, pp. 578-597, 2010.
- [146] J. R. Phillips, K. T. Klasson, E. C. Clausen and J. L. Gaddy, "Biological Production of Ethanol from Coal Synthesis Gas – Medium Development Studies," *Applied biochemistry and biotechnology*, vol. 39, no. 1, pp. 559-571, 1993.
- [147] D. Arora, R. Basu, J. R. Phillips, C. V. Wikstrom, E. C. Clausen and J. L. Gaddy, "Production of ethanol from refinery waste gases. Phase 2, technology development, annual report," Bioengineering Resources, Inc., Fayetteville, 1995.
- [148] K. T. Klasson, A. Gupta, E. C. Clausen and J. L. Gaddy, "Evaluation of Mass-Transfer and Kinetic Parameters for *Rhodospirillum rubrum* in a Continuous Stirred Tank Reactor," *Applied biochemistry and biotechnology*, vol. 39, no. 1, pp. 549-557, 1993.

- [149] D. K. Kundiyana, R. L. Huhnke and M. R. Wilkins, "Syngas fermentation in a 100-L pilot scale fermentor: Design and process considerations," *Journal of bioscience and bioengineering*, vol. 109, no. 5, pp. 492-498, 2010.
- [150] "Alibaba," 2015. [Online]. Available: [http://www.alibaba.com/product-detail/China-high-purity-n-Heptane-95\\_1438611978.html](http://www.alibaba.com/product-detail/China-high-purity-n-Heptane-95_1438611978.html). [Accessed 10 June 2015].
- [151] "Alibaba," 2015. [Online]. Available: [http://www.alibaba.com/trade/search?fsb=y&IndexArea=product\\_en&CatId=&SearchText=lime](http://www.alibaba.com/trade/search?fsb=y&IndexArea=product_en&CatId=&SearchText=lime). [Accessed 10 June 2015].
- [152] B. Pennstrom, A. Ibrado and D. Gertenbach, "Hycroft Oxidation Pilot Plant Overview," 21 February 2014. [Online]. Available: <http://www.alliednevada.com/wp-content/uploads/140221-AAO-Pilot-Plant-Presentation.pdf>. [Accessed 9 June 2015].

## Appendix A. Screening Assessment

### Scope of the Screening Assessment

A brief description of each process in the screening assessment is shown in Table 88.

Table 88: Brief description of processes in screening assessment

Process	Description	Sources <sup>1</sup>
FP-J	The FP-J process converts lignocellulose by pyrolysis (without a catalyst) to mainly oil. The bio-oil is upgraded to fuels (mainly jet fuel) using hydrotreating and hydrocracking reactors. Natural gas is used for hydrogen production.	[51], [52], [53], [54], [55]
CFP-J	The CFP-J process converts lignocellulose by pyrolysis and catalytic cracking in a single reactor to mainly oil. The bio-oil is upgraded to fuels (mainly jet fuel) by hydrotreating. Product gasses are used for hydrogen production.	[56], [51], [57], [52].
L-ETH-J	Lignocellulose is pretreated with dilute-acid pretreatment, which is converted to ethanol by saccharification and co-fermentation. Ethanol is concentrated by two distillation columns and a molecular sieve. Cogeneration of steam and electricity occurs from the residual solids. The ethanol is dehydrated to ethylene and oligomerized to hydrocarbons (aimed at maximum jet fuel production). Products are upgraded by hydroprocessing. Hydrogen is produced from part of the alcohol.	[58], [59], [60], [61], [62]
SYN-FER-J	Lignocellulose is gasified to syngas followed by a crude gas clean-up. The syngas is fermented to mainly ethanol. Ethanol is concentrated by two distillation columns and a molecular sieve. The ethanol is dehydrated to ethylene and oligomerized to hydrocarbons (aimed at maximum jet fuel production). Products are upgraded by hydroprocessing. Hydrogen is produced from part of the alcohol.	[6], [59], [60], [61], [62]
SYN-CAT-J	Lignocellulose is gasified to syngas followed by a thorough gas clean-up and heat recovery. The syngas is converted to mainly alcohols (C <sub>2</sub> -C <sub>4</sub> ), CO <sub>2</sub> and methane. The alcohols are separated. The alcohols are dehydrated to alkenes and oligomerized to hydrocarbons (aimed at maximum jet fuel production). Products are upgraded by hydroprocessing. Hydrogen is produced from part of the alcohol.	[36], [59], [60], [61], [62]
L-BUT-J	Lignocellulose is pretreated followed by inhibitor removal by ion exchange. This is converted to butanol, acetone and ethanol (ABE mixture) by saccharification and co-fermentation. The mixture is separated and concentrated by four distillation columns, a decanter and a molecular sieve. Cogeneration of steam and electricity occurs from the residual solids. The ABE mixture is oligomerized to larger hydrocarbons (aimed at maximum jet fuel production). Products are upgraded by hydroprocessing. Hydrogen is produced from part of the alcohol.	[63], [59], [60], [64]
L-LIP-J	Lignocellulose is pretreated with deacetylation and acid-treatment. The slurry is hydrolysed enzymatically. Sugars are converted to lipids in bioreactors. The lipids are separated from the cells. The lipids are hydrodeoxygenated to alkanes and propane. The alkanes are hydrocracked for maximum jet fuel production. Hydrogen is purchased.	[65], [66]
L-FFA-J	Lignocellulose is pretreated with deacetylation and acid-treatment. The slurry is hydrolysed enzymatically. Sugars are converted to FFA in bioreactors (secreted externally). The FFA's are separated from the broth. The FFA's are hydrotreated to alkanes. The alkanes are hydrocracked to maximize the jet fuel fraction. Hydrogen is purchased.	[65], [67], [68]
L-ACID-J	Lignocellulose is pretreated with lime which is fermented to carboxylic salts. The broth is degasified, descummed, dewatered and crystalized. The carboxylic salts are converted to ketones, which are hydrogenated to alcohols. The alcohols are dehydrated to alkenes and oligomerized to hydrocarbons (not maximum jet fuel). Products are upgraded by hydroprocessing. Cogeneration of steam, electricity and hydrogen occurs from the residual solids.	[50]

<b>SEP-CAT</b>	Lignocellulose is pretreated with hot-water extraction. Cellulose and hemicellulose are catalytically treated, separately. The hemicellulose is converted to mainly furfural by dehydration. The furfural is converted to alkanes (mainly jet fuel) by reaction with acetone. The cellulose is dehydrated to produce mainly levulinic acid. This is hydrogenated, decarboxylated to butene and then oligomerized to larger alkenes (mainly jet fuel). Products are upgraded by hydroprocessing. Cogeneration of steam and electricity occurs from the solids. Hydrogen is purchased.	[4]
<b>GFT-J (HT)</b>	Lignocellulose is gasified at relatively high temperatures (1300°C) to syngas followed by a thorough gas clean-up and heat recovery. Fuels are produced by FT synthesis. FT-liquid is upgraded to mainly jet fuel by hydroprocessing. Power generation occurs from unconverted syngas and fuel gas.	[48], [69]
<b>GFT-J (LT)</b>	Lignocellulose is gasified at relatively low temperatures (870°C) to syngas followed by a thorough gas clean-up and heat recovery. Methane is converted by steam-methane reforming and H <sub>2</sub> :CO ratio is adjusted in a water-gas-shift reactor. Fuels are produced by FT synthesis. FT-liquid is upgraded to mainly jet fuel by hydroprocessing. Power generation occurs from unconverted syngas and fuel gas.	[48], [69]
<b>Small GFT-J (HT)</b>	The process description is the same as for GFT-J (HT). The capacity is smaller due to the use of a micro-channel FT reactor.	[48], [69], [70]

<sup>1</sup> The main literature sources are shaded in grey.

## Methods used to Perform Screening of Investigated Processes

The process properties (energy ratios and energy efficiencies) were calculated according to the equations in section 4.4.1.2. For the processes that have a fossil-derived fuel fed to produce hydrogen, the energy ratio takes into account the fossil-input.

The method that was used to compare economic feasibility is determination of MJSP. The operating and capital costs associated with each investigated process were determined using literature (shown in Table 88) and the estimation methods described by Turton et al. [139].<sup>KK</sup> The MJSP were calculated for various capacities, as applicable for each technology.

Assumptions made to determine the MJSP in the screening assessment are shown below:

- Total capital expenditure occurs and full operation starts at year zero
- Straight-line depreciation over 10 years
- A discount rate of 12% and income tax rate of 30%
- The processes have 8000 working hours per year and a 20 year project life time
- Lignocellulosic feedstock cost of \$84 per MT and market prices for all fuels other than jet fuel
- NPV of zero after the project life time
- Year of costing is 2013 (Chemical Engineering Plant Cost Index = 564)

---

<sup>KK</sup> After investigation, it was found that Turton et al. over-predicted the operating costs in comparison to other estimation methods such as described by Sinnott et al.

## Appendix B. Proposed Yields

This appendix provides yields for processes discussed in section 3. This is not a complete set of yields but only a supplementation to the discussion in section 3.

### HEFA Process

Yields for the hydrodeoxygenation reactor section of jatropha oil, performed by Gong et al. [74], are shown in Table 89 and Table 90.

Table 89: Yields based on fed jatropha oil, [74].

Product yields	Wt%
Liquid hydrocarbon	83.9
Gas hydrocarbon	5.6
Water	7.5

Table 90: Liquid hydrocarbon products of hydrodeoxygenated jatropha oil, [74].

Carbon no.	Normal (%C)	Isomeric (%C)
4	0.01	0
5	0.05	0
6	0.11	0
7	0.22	0
8	0.24	0
9	0.31	0
10	0.28	0
11	0.2	0
12	0.14	0
13	0.13	0
14	0.13	0
15	7.61	0.06
16	7.26	0.17
17	37.31	3.19
18	36.49	3.67
18+	2.41	0

Yields for the cracking and isomerization reactor section of hydrodeoxygenated oil, performed by Robota et al. [73], are shown in Table 91.

Table 91: Cracking and isomerization of hydrocarbons, [73].

Alkane composition	Feed composition			Product yield for maximum jet fuel production, (T=278 °C)		
Carbon no.	Total wt%	n-alkanes wt%	iso-alkane wt%	Total wt%	n-alkanes wt%	iso-alkane wt%
4	0	0	0	2.37	0.74	1.63
5	0	0	0	6.06	1.38	4.68
6	0.01	0	0	8.85	1.9	6.95
7	0.04	0.01	0.03	11.72	2.2	9.52
8	0.12	0.03	0.1	14.07	2.17	11.9
9	0.23	0.06	0.17	14.36	1.92	12.44
10	1.03	0.79	0.24	14.75	2.02	12.73
11	0.18	0.07	0.12	11.14	0.99	10.15
12	0.17	0.08	0.09	7.97	0.63	7.34
13	0.62	0.45	0.17	4.64	0.33	4.31
14	2.93	2.03	0.9	2.14	0.12	2.01
15	5.17	5.07	0.1	0.59	0.04	0.56
16	6.08	5.94	0.14	0.3	0.01	0.29
17	38.03	37.43	0.6	0.43	0.02	0.41
18	43.38	42.21	1.16	0.19	0.01	0.18
19	0.82	0.34	0.48	0.02	0	0.02
20	0.51	0.3	0.21	0.02	0	0.02
21	0.17	0.07	0.1	0.02	0	0.02
22	0.1	0.05	0.04	0.02	0	0.02
23	0.09	0.03	0.06	0.01	0	0.01

### Ethanol to Jet Process Section

The yields for the conversion of ethylene to light olefins, described by Mahdaviyani et al. [61] are shown in Table 92.

Table 92: Yields for the ethylene conversion, [61].

Components	Yield (wt%)
C2	0.0222
C4	0.8135
C6	0.1604
C8	0.0039

The actual feed (based on Mahdaviyani et al.), the feed without recycle of Keuchler et al. [60] and the product yields of oligomerization of light olefins with recycle by Keuchler et al. are shown in Table 93.

Table 93: Feed and product of oligomerization reactor with recycle fed to reactor, [60].

Reactor product	Feed of Keuchler et al. (wt%)	Actual feed (wt%) <sup>1</sup>	Product yield of Keuchler et al. based on new feed and recycle fed to reactor (wt%)
C2	0	2.24	0
C3	0	0	0
C4	66.6	81.32	7.5
C5	22.3	0	2.1
C6	11.1	16.08	1.4
C7	0	0	5.2
C8	0	0.352	23.8
C9	0	0	16.3
C10	0	0	6.4
C11	0	0	7.15
C12	0	0	11.4
C13	0	0	5.8
C14	0	0	3.45
C15	0	0	3.85
C16	0	0	2.65
C17	0	0	1.25
C18	0	0	0.85
C19	0	0	0.55
C20	0	0	0.35

<sup>1</sup> Product of ethylene oligomerization reactor, based on [61].

## FP-J Process

The yields proposed by the study of McLaren [97] (and this study) with a comparison with Jones et al. [55] are shown in Table 94.

Table 94: Overall yields of pyrolysis (wt% based on biomass fed)

Components	McLaren [97]	Jones et al. [55]
Organics <sup>1</sup>	59.9 – 64.0	65
Water <sup>1</sup>	10.0 – 10.8	10
Char	12.0 – 16.2	13
Gasses	12.0 – 13.1	12

<sup>1</sup> Organics and water combined are referred to as bio-oil

The conditions of the hydrotreating and hydrocracking reactors proposed by the study of McLaren (and this study) and Jones et al. [55] are compared in Table 95 and Table 96.

Table 95: Hydrotreating reactor conditions and hydrogen use, [100].

Specification	McLaren [97]	Jones et al. [55] <sup>2</sup>
Temperature	340°C	370°C
Pressure	2000 psig	2015 psig
H <sub>2</sub> consumed	1.57 <sup>1</sup>	-

<sup>1</sup> [%wt H<sub>2</sub>/ wt bio-oil fed]; <sup>2</sup> Main hydrotreating reactor

Table 96: Hydrocracking reactor conditions and hydrogen use, [100].

Specification	McLaren [97]	Jones et al. [55]
Temperature	405°C	427°C
Pressure	1500 psig	1280 psig
H <sub>2</sub> consumed	3.07 <sup>1</sup>	-

<sup>1</sup> [%wt H<sub>2</sub>/ wt oily phase from hydrotreating fed]

The overall phase yields and hydrocarbon distillate yields used by the study of McLaren obtained from Elliot et al. [100] and Christensen et al. [101] are given in Table 97 and Table 98.

Table 97: Overall phase yields of hydrotreating and hydrocracking reactors, [100].

Phase	Yields	Yield calculation
Gas	6.02	[wt gas/(wt bio-oil + H <sub>2</sub> consumed)]
Aqueous	57.98	[wt aqueous / (wt bio-oil + H <sub>2</sub> consumed)]
Solids	7.78	[wt solids/(wt bio-oil + H <sub>2</sub> consumed)]
Upgraded Oil	28.22	[wt oil/(wt bio-oil + H <sub>2</sub> consumed)]

Table 98: Overall hydrocarbon distillate yields, [101].

Hydrocarbon	Yields (wt% based on bio-oil fed) <sup>1</sup>
Lights	4.03
Naphtha	8.77
Jet	6.39
Diesel	5.98
Gas oil	3.12

<sup>1</sup> The jet fuel fraction will be increased by apportioning 40% of the diesel fraction to the jet fuel fraction; this is done because there is significant overlap between these fuel fractions and this assessment aimed for jet fuel.

## GFT-J Process

Refining of FT product (with hydrocarbons smaller than C<sub>5</sub> removed) was performed by Shell (shown in Figure 54) and was used by Ekbom et al. [48]. The hydrocracker of the GFT-J process was simulated based on the high-severity cracking in Figure 54.

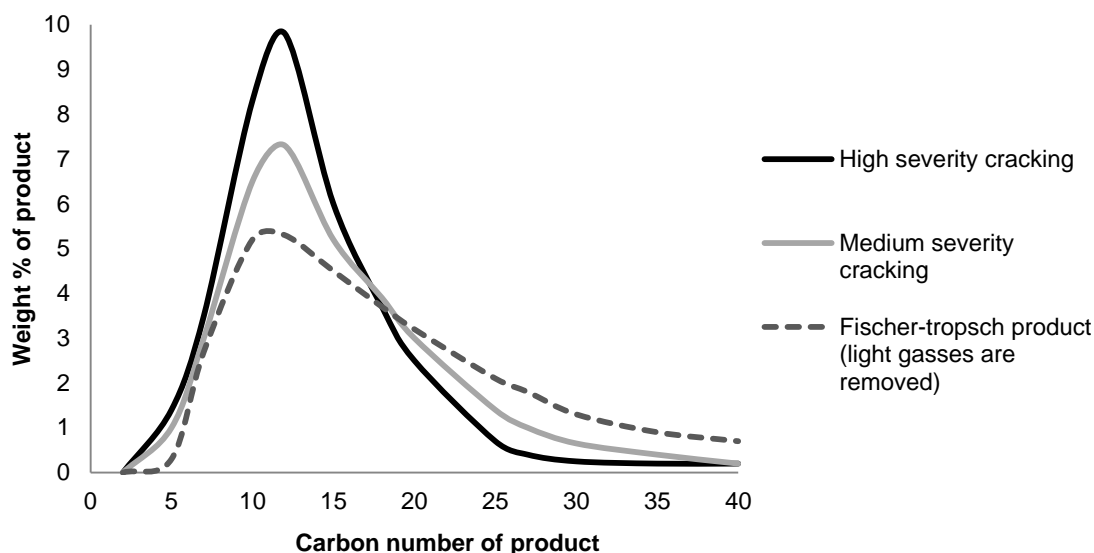


Figure 54 : Varying degrees of hydrocracking that was accomplished by Shell of a FT product, redrawn from [48].

### SYN-FER-J Process

A comparison of promising syngas fermentation experimental literature is given in Table 99, on page 155. Experiment number 3 and 5 are employed in this assessment.

### Cooling Tower Calculations

According to Castro et al. [132], make-up water required for a cooling tower is equal to the sum of the mass of evaporated water ( $m_{evap}$ ), purge water ( $m_{purge}$ ) and entrained water ( $m_{entr}$ ). Below are the equations used for the make-up water calculations [132], [32], [93].

$$m_{evap} = 0.00119 \times m_{CT} \times (\Delta T) \quad \text{Equation 18}$$

$$m_{purge} = \frac{m_{evap}}{n_{cycles} - 1} \quad \text{Equation 19}$$

$$m_{entr} = 0.001 \times m_{CT} \quad \text{Equation 20}$$

With  $m_{CT}$  - Mass of cooling water to tower  
 $\Delta T$  - Temperature change of cooling water (in degrees Celsius)  
 $n_{cycles}$  - Number of cycles; taken to be 4

Table 99: A comparison of promising syngas fermentation experimental literature

Experiment number	Organism	Syngas composition (v/v, %)	Culture mode	Ethanol productivity (g/l.day)	Cell density (g/l)	Conversion efficiency	Product	Reference
1	<i>C. ljungdahlii</i> strain C-01	20% H <sub>2</sub> , 65% CO, 10% CO <sub>2</sub> and 5% CH <sub>4</sub>	CSTR (no cell recycle)	14.4 - 21.1	2.3 - 3.6	xCO – 85 to 94%; xH <sub>2</sub> – 10 to 63%	Ethanol (17.5 - 33 g/l); Acetate (2.5 - 6.1 g/l)	Gaddy et al. [116]
2	<i>C. ljungdahlii</i> strain C-01	16% H <sub>2</sub> , 27% CO, 6% CO <sub>2</sub> , and 51% N <sub>2</sub>	CSTR (no cell recycle)	11.1 - 20.1	2.3 - 4.2	xCO – 80 to 90%; xH <sub>2</sub> – 30 to 64%	Ethanol (11 - 26 g/l) Acetate (2.0 - 5.0 g/l)	Gaddy et al. [116]
3	<i>C. ljungdahlii</i> strain O-52	50% H <sub>2</sub> , 45% CO and 5% CH <sub>4</sub>	CSTR (with cell recycle)	21.1 - 39.0	3.8 - 6	xCO – 81 to 96%; xH <sub>2</sub> – 42 to 81%	Ethanol (18 - 23.5 g/l); Acetate (3.0 - 5.7 g/l)	Gaddy et al. [116]
4	<i>C. ljungdahlii</i> strain C-01	62% H <sub>2</sub> , 31% CO and 5% C <sub>2</sub> H <sub>6</sub>	CSTR (with cell recycle) - High Pressure (30 Psig)	150	8	xCO – 90%; xH <sub>2</sub> – 40%	Ethanol (20 g/l); Acetate (2.75 g/l)	Gaddy et al. [116]
5	<i>C. ljungdahlii</i> strain C-02	55% H <sub>2</sub> , 30% CO, 5% CH <sub>4</sub> and 10% CO <sub>2</sub> .	CSTR (with cell recycle) - High Pressure (75 Psig)	369	2	xCO – 95%; xH <sub>2</sub> – 60%	Ethanol (25 g/l); Acetate (3 g/l)	Gaddy et al. [116]

Experiment number	Organism	Syngas composition (v/v, %)	Culture mode	Ethanol productivity (g/l.day)	Cell density (g/l)	Conversion efficiency	Product	Reference
6	<i>C. ljungdahlii</i>	20% H <sub>2</sub> , 55% CO, 10% CO <sub>2</sub> , and 15% Argon	CSTR (with cell recycle); unsteady-state with 530 hours experimental run	1.04 - 1.96 mmol/g.hr	0.8 - 3.5	xCO – 90%; xH <sub>2</sub> – 70%	Ethanol (6 - 48 g/l); Acetate (3 - 5 g/l)	Phillips et al. [146]
7	<i>C. ljungdahlii</i> strain BRI C-01	34% CO, 32% H <sub>2</sub> , 5% CH <sub>4</sub> , and 29% CO <sub>2</sub>	CSTR (with varying degrees of cell purge)	16.3 - 38.6	- <sup>1</sup>	xCO > 80%; xH <sub>2</sub> – 50 to 60%	Ethanol (19 - 23 g/l); Acetate (4 - 5 g/l)	Arora et al. [147]
8	<i>C. ljungdahlii</i> strain BRI C-02	34% CO, 32% H <sub>2</sub> , 5% CH <sub>4</sub> , and 29% CO <sub>2</sub>	Two stage CSTR (with liquid from first reactor overflowing to second; fresh gas in each reactor)	- <sup>1</sup>	- <sup>1</sup>	xCO – 87%; xH <sub>2</sub> – 62%	Ethanol (30 g/l); Acetate (4 - 5 g/l)	Arora et al. [147]
9	<i>C. ljungdahlii</i>	46.6% H <sub>2</sub> , 28% CO, 7% CH <sub>4</sub> , 15% CO <sub>2</sub> , 2% C <sub>2</sub> H <sub>4</sub> , 0.7% C <sub>6</sub> H <sub>14</sub> and 0.7% C <sub>6</sub> H <sub>6</sub>	CSTR (with cell recycle)	4.0	2.5	xCO – 85.3%; xH <sub>2</sub> – 14.1%	Ethanol (16.9 g/l); Acetate (1.04 g/l)	Nieves et al. [119] based on work by Klasson et al. [148]
10	<i>Clostridium</i> strain P11	5% H <sub>2</sub> , 20% CO, 15% CO <sub>2</sub> , and 60% N <sub>2</sub>	Batch mode with continuous syngas supply; (100 litre fermenter)	- <sup>1,2</sup>	0.44 - 0.84	- <sup>1</sup>	Ethanol (25.26 g/l); Acetate (4.82 g/l); 2-propanol (9.25 g/l); 1-butanol (0.47 g/l)	Kundiyanan et al. [149]

<sup>1</sup> Data not provided by the literature; <sup>2</sup> Experiment ran for 59 days.

## Appendix C. Capital Cost Estimation

As discussed in section 4.5, the sizing and costing of equipment were mainly performed using literature sources, as well as Aspen Icarus®.

### Aspen Icarus

The following table summarizes the information which was used for costing of equipment in Aspen Icarus®.

Table 100: Summary of information used for costing of equipment in Aspen Icarus®

Unit or Section	Process	Literature source <sup>1</sup>	Additional design information
Compressors	SYN-FER-J	Spath et al. [135]	"Centrifugal compressors - horizontal"; Material of construction (MOC) is A285C [135].
	L-ETH-J	Spath et al. [135]	"Centrifugal compressors - horizontal"; MOC is A285C [135].
	S-ETH-J	Spath et al. [135]	"Centrifugal compressors - horizontal"; MOC is A285C [135].
	GFT-J	Spath et al. [135]	All specified as "Centrifugal compressors - horizontal" except for low flow rate oxygen compressors - "Reciprocating compressors"; MOC is A285C [135].
	FP-J	Jones et al. [98]	"Reciprocating compressors" as specified by [98]; MOC is CS [98].
Turbo-expander	SYN-FER-J	-	"Turboexpander"; MOC is A285C [135].
Oligomerization distillation column	SYN-FER-J; L-ETH-J; S-ETH-J	Jones et al. [98]	"Full-Single" configuration specified for distillation column; SS316 cladding [98].
Hydrocarbon Recovery Section	HEFA; GFT-J	Jones et al. [98]	"Full-Single" configuration specified for both distillation columns; SS316 cladding [98].
Ethanol Recovery Section	SYN-FER-J	Humbird et al. [32]	"Full-Single" configuration specified for two distillation columns & "Trayed tower" specified for scrubber; SS316 cladding [32].
Flash in hydrogen recovery section	SYN-FER-J	Spath et al. [135]	"Vertical process vessel"; MOC is CS [135].
	GFT-J process	Spath et al. [135]	"Vertical process vessel"; MOC is CS [135].
Flash in dehydration section	SYN-FER-J; L-ETH-J; S-ETH-J	Cameron et al. [129]	"Vertical process vessel"; MOC is CS [129].
Knock-out drums between syngas compressors	GFT-J process	Spath et al. [135]	"Vertical process vessel"; MOC is CS [135].
FT reactor product separation	GFT-J process	Jones et al. [98]	Flash specified as "Vertical process vessel", Liquid-liquid separator specified as "Horizontal drum"; SS316 cladding [98].
Dehydration reactor	SYN-FER-J; L-ETH-J; S-ETH-J	Cameron et al. [129]	Reactor was specified as a "Fixed tube sheet shell and tube exchanger" as prescribed by Cameron et al.; Shell MOC is SS304, Tube MOC is A213F [129].

<sup>1</sup> Main literature used for specifying equipment in Aspen Icarus®.

## Capital Costs from Literature

Tables including the capital costs derived from literature for the main equipment or process sections were constructed for each process (Table 101 to Table 108). Significant amounts of equipment with relatively low price are not displayed in the tables (including pumps, certain heat-exchangers and separation equipment). For equipment where no scaling factor (exp) or specific installation factor was found in literature, a scaling factor of 0.65 and an average installation factor of 2.47 were assumed [135]. An installation factor of 1 is given to equipment where installed equipment costs were obtained from literature. Standard volume of gas in the tables below (Nm<sup>3</sup>) refers to the standard conditions of 20°C and 1 atm.

Table 101: HEFA process - capital costs for equipment based on literature sources

Unit	Scale Parameter	Base Value	Base Year	Base Price	Scaling Factor	Installation Factor	Literature Source
Hydrotreater	Reactor volume (m <sup>3</sup> )	342	2011	\$ 4 890 600	0.65	2.75	Jones et al. [98]
Hydrocracker	Feed flow (kg/h of Hydrocarbons)	4 355	2011	\$ 5 021 074	0.65	3.00	Jones et al. [98]
Steam Reformer	Flow (Nm <sup>3</sup> /h of H <sub>2</sub> Produced)	52 510	2011	\$ 36 012 778	0.65	1.92	Jones et al. [98]
Compressor for Hydrogen Generation	Work (kW)	297	2007	\$ 1 461 700	0.80	1.20	Swanson et al. [69]
Pressure Swing Adsorption Unit	Flow (kg/h of H <sub>2</sub> Produced)	8 665	2002	\$ 4 855 471	0.60	2.47	Spath et al. [135]
Turbine Power Generator	Net work (MW)	25.6	2002	\$ 4 045 870	0.71	2.47	Spath et al. [135]
Cooling Tower	Cooling water flow (litre/s)	5 000	2007	\$ 2 923 425	0.90	2.47	Sinnott et al. [130]
WWT Plant (Aerobic)	Wastewater flow (kg/h)	32 724	2007	\$ 3 567 191	0.65	1.00	Jones et al. [55]

Table 102: SYN-FER-J process - capital costs for equipment based on literature sources

Unit	Scale Parameter	Base Value	Base Year	Base Price	Scaling Factor	Installation Factor	Literature Source
Biomass Feed Handling & Dryer	Biomass feed (dry MT/h)	41.67	2002	\$ 3 813 728	0.75	2.47	Phillips et al. [134]
Gasifier	Biomass feed (dry MT/h)	20.83	2010	\$ 6 466 667	0.60	2.31	Dutta et al. [36]
Syngas Fermenters	Number of reactors <sup>1</sup>	1	2005	\$ 418 211	1.00	4.00 <sup>2</sup>	van Kasteren et al. [114]
Cell Recycling Membrane	Liquid flow (litre/min)	95	2002	\$ 160 000	0.65	1.50	Nieves [119]
H <sub>2</sub> Selective Membrane	Flow (kg/h of H <sub>2</sub> Produced)	8 665	2002	\$ 4 855 471	0.60	2.47	- <sup>3</sup>
Pressure Swing Adsorption Unit	Flow (kg/h of H <sub>2</sub> Produced)	8 665	2002	\$ 4 855 471	0.60	2.47	Spath et al. [135]
Incinerator & HRSG	Equivalent steam produced <sup>4</sup> (kg/h)	650 000	2011	\$ 11 272 996	0.86	1.02	Klein-Marcuschamer et al. [5]
Molecular Sieve (ethylene drying)	Flow to column (kg/h)	152 107	2012	\$ 110 500	0.65	3.30	Cameron et al. [129]
Ethylene Compressor	Work (kW)	861	2012	\$ 1 403 400	0.65	3.30	Cameron et al. [129]

Unit	Scale Parameter	Base Value	Base Year	Base Price	Scaling Factor	Installation Factor	Literature Source
Ethylene Oligomerization Reactor	Flow to reactor (kg/h)	3 675	2006	\$ 6 320 000	0.60	1.00	Sinnott et al. [130]
C <sub>4+</sub> Oligomerization Reactor	Product flow (kg/h of Hydrocarbons)	6 875	2010	\$ 10 158 545	0.90	1.00	Bond et al. [4]
Hydroprocessing Reactor	Product flow (kg/h of Hydrocarbons)	6 875	2010	\$ 2 223 945	0.90	1.00	Bond et al. [4]
H <sub>2</sub> Compressor to Hydroprocessor	Work (kW)	4 064	2002	\$ 914 235	0.65	2.47	Spath et al. [135]
Turbine Power Generator	Net work (MW)	25.6	2002	\$ 4 045 870	0.71	2.47	Spath et al. [135]
Cooling Tower	Cooling water flow (litre/s)	5 000	2007	\$ 2 923 425	0.90	2.47	Sinnott et al. [130]
Aerobic WWT Plant	Wastewater flow (kg/h)	360 000	2007	\$ 9 757 602	0.60	1.00	Humbird et al. [32]
Anaerobic WWT Plant	Wastewater flow (kg/h)	602 570	2007	\$ 9 809 248	0.60	1.00	Humbird et al. [32]

<sup>1</sup> Volume of each reactor is 2268 m<sup>3</sup>; <sup>2</sup> High installation factor is chosen due to large uncertainty surrounding cost; <sup>3</sup> Uncertainty surrounding cost, assume it is has the same cost as the PSA unit; <sup>4</sup> Based on 32 bar steam.

For the S-ETH-J process, the process section producing ethanol from sugarcane (including the cogeneration section) was costed based on a study by van der Westhuizen [91]. The cost data of this section is given in Table 103.

Table 103: Capital cost of sugarcane to ethanol process section, [91].

Scale Parameter	Base Value	Base Year	Base Price (FCI)	Scaling Factor <sup>1</sup>	FCI/TIC <sup>2</sup>
Wet sugarcane fed (MT/h)	500	2010	\$ 240 000 000	0.6	1.7

<sup>1</sup> Based on [130]; <sup>2</sup> Assumed ratio between Fixed Capital Investment (FCI) and Total Installed Cost (TIC) based on literature [32], [69], [36].

The additional data which was used for determining the total capital cost of the S-ETH-J process is given in Table 104.

Table 104: S-ETH-J process - capital costs for equipment based on literature sources

Unit	Scale Parameter	Base Value	Base Year	Base Price	Scaling Factor	Installation Factor	Literature Source
Aerobic WWT Plant	Wastewater flow (kg/h)	360 000	2007	\$ 15 630 229	0.60	1.00	Humbird et al. [32]
Cooling Tower	Cooling water flow (litre/s)	5 000	2007	\$ 2 923 425	0.90	2.47	Sinnott et al. [130]
Chiller	Duty (kW)	1 000	2007	\$ 1 574 680	0.90	2.47	Sinnott et al. [130]
Ethanol Reformer	Flow (Nm <sup>3</sup> /h of H <sub>2</sub> Produced )	52 510	2011	\$ 36 012 778	0.65	1.92	Jones et al. [98]
Molecular Sieve (ethylene drying)	Flow to column (kg/h)	152 107	2012	\$ 110 500	0.65	3.30	Cameron et al. [129]
Ethylene Compressor	Work (kW)	861	2012	\$ 1 403 400	0.65	3.30	Cameron et al. [129]
Ethylene Oligomerization Reactor	Flow to reactor (kg/h)	3 675	2006	\$ 6 320 000	0.60	1.00	Sinnott et al. [130]
C <sub>4+</sub> Oligomerization Reactor	Product flow (kg/h of Hydrocarbons)	6 875	2010	\$ 10 158 545	0.90	1.00	Bond et al. [4]

Unit	Scale Parameter	Base Value	Base Year	Base Price	Scaling Factor	Installation Factor	Literature Source
Hydroprocessing Reactor	Product flow (kg/h of Hydrocarbons)	6 875	2010	\$ 2 223 945	0.90	1.00	Bond et al. [4]
H <sub>2</sub> Compressor to Hydroprocessor	Work (kW)	4 064	2002	\$ 914 235	0.65	2.47	Spath et al. [135]

For the L-ETH-J process, the process section producing ethanol from lignocellulose (including the evaporation and cogeneration section) was costed using the study by Petersen [93]. The cost data of this section is given in Table 105.

Table 105: Installed capital cost of lignocellulose to ethanol process section, [93].

Scale Parameter	Base Value	Base Year	Base Price (TIC)	Scaling Factor <sup>1</sup>
HHV of lignocellulose feed (MW)	600	2010	\$ 193 776 751	0.6

<sup>1</sup> Based on [130].

The additional data which was used for determining the total capital cost of the L-ETH-J process is given in Table 106.

Table 106: L-ETH-J process - capital costs for equipment based on literature sources

Unit	Scale Parameter	Base Value	Base Year	Base Price	Scaling Factor	Installation Factor	Literature Source
Aerobic WWT Plant	Wastewater flow (kg/h)	360 000	2007	\$ 15 630 229	0.60	1.00	Humbird et al. [32]
Anaerobic WWT Plant	Wastewater flow (kg/h)	412 000	2007	\$ 13 268 925	0.60	1.00	Humbird et al. [32]
Cooling Tower	Cooling water flow (litre/s)	5 000	2007	\$ 2 923 425	0.90	2.47	Sinnott et al. [130]
Ethanol Reformer	Flow (Nm <sup>3</sup> /h of H <sub>2</sub> Produced)	52 510	2011	\$ 36 012 778	0.65	1.92	Jones et al. [98]
Molecular Sieve (ethylene drying)	Flow to column (kg/h)	152 107	2012	\$ 110 500	0.65	3.30	Cameron et al. [129]
Ethylene Compressor	Work (kW)	861	2012	\$ 1 403 400	0.65	3.30	Cameron et al. [129]
Ethylene Oligomerization Reactor	Flow to reactor (kg/h)	3 675	2006	\$ 6 320 000	0.60	1.00	Sinnott et al. [130]
C <sub>4+</sub> Oligomerization Reactor	Product flow (kg/h of Hydrocarbons)	6 875	2010	\$ 10 158 545	0.90	1.00	Bond et al. [4]
Hydroprocessing Reactor	Product flow (kg/h of Hydrocarbons)	6 875	2010	\$ 2 223 945	0.90	1.00	Bond et al. [4]
H <sub>2</sub> Compressor to Hydroprocessor	Work (kW)	4 064	2002	\$ 914 235	0.65	2.47	Spath et al. [135]

Table 107: FP-J process - capital costs for equipment based on literature sources

Unit	Scale Parameter	Base Value	Base Year	Base Price	Scaling Factor	Installation Factor	Literature Source
Biomass Feed Handling & Dryer	Biomass feed (dry MT/h)	41.67	2002	\$ 3 813 728	0.75	2.47	Phillips et al. [134]
Pyrolysis Reactor	Biomass feed (dry MT/h)	16.67	2009	\$ 38 000 000	0.70	1.00	Jones et al. [98]
Air Dryer	Area (m <sup>2</sup> )	606	2011	\$ 782 600	0.65	2.47	Klein-Marcusamer et al. [5]

Unit	Scale Parameter	Base Value	Base Year	Base Price	Scaling Factor	Installation Factor	Literature Source
Oil Filter	Biomass feed to pyrolysis reactor (dry MT/h)	83.5	2013	\$ 5 969 859	0.70	1.40	Jones et al. [98]
Cooling Tower	Cooling water flow (litre/s)	5 000	2007	\$ 2 923 425	0.90	2.47	Sinnott et al. [130]
Aerobic WWT Plant	Wastewater flow (kg/h)	32 724	2007	\$ 3 567 191	0.65	1.00	Jones et al. [55]
Hydrotreater	Reactor volume (m <sup>3</sup> )	342	2011	\$ 4 890 600	0.65	2.75	Jones et al. [98]
Post-hydrotreater HRSG	Area (m <sup>2</sup> )	333	2011	\$ 161 878	0.65	2.47	Klein-Marcuschamer et al. [5]
Post-hydrotreater High Pressure Flash	Flow to separator (kg/h)	83 220	2011	\$ 2 137 301	0.65	1.40	Jones et al. [98]
Hydrocracker	Feed flow (kg/h of Hydrocarbons)	4 355	2011	\$ 5 021 074	0.65	3.00	Jones et al. [98]
Product Recovery Section	Hydrocarbon flow to section (kg/h)	28 830	2011	\$ 3 602 661	0.65	1.00	Jones et al. [98]
Steam-Methane Reformer	Flow (Nm <sup>3</sup> /h of H <sub>2</sub> Produced)	52 510	2011	\$ 36 012 778	0.65	1.92	Jones et al. [98]
Pressure Swing Adsorption Unit	Flow (kg/h of H <sub>2</sub> Produced)	8 665	2002	\$ 4 855 471	0.60	2.47	Spath et al. [135]
Turbine Power Generator	Net work (MW)	25.6	2002	\$ 4 045 870	0.71	2.47	Spath et al. [135]

Table 108: GFT-J process - capital costs for equipment based on literature sources

Unit	Scale Parameter	Base Value	Base Year	Base Price	Scaling Factor	Installation Factor	Literature Source
Biomass Feed Handling & Dryer	Biomass feed (dry MT/h)	41.67	2002	\$ 3 813 728	0.75	2.47	Phillips et al. [134]
Gasifier	Biomass feed (dry MT/h)	20.83	2010	\$ 6 466 667	0.60	2.31	Dutta et al. [36]
Rectisol Unit	Feed flow (Nm <sup>3</sup> /h of Syngas)	200 000	2007	\$ 28 800 000	0.63	1.32	Kreutz et al. [104]
Fischer-Tropsch Reactor	Flow to reactor (kmol/h)	3 186	2003	\$ 10 500 000	0.72	1.00	Swanson et al. [69]
Pressure Swing Adsorption Unit	Flow (kg/h of H <sub>2</sub> Produced)	8 665	2002	\$ 4 855 471	0.60	2.47	Spath et al. [135]
Turbine Power Generator	Net work (MW)	25.6	2002	\$ 4 045 870	0.71	2.47	Spath et al. [135]
Auto-thermal reformer	Flow to reactor (Nm <sup>3</sup> /s of Gas)	100	2002	\$ 27 368 000	0.60	2.30	Leibbrandt [92]
Air Separation Unit	Flow of oxygen (MT/h of 99.5% oxygen)	24	2002	\$ 24 552 000	0.75	1.00	Leibbrandt [92]
Hydrocracker	Feed flow (kg/h of Hydrocarbons)	4 355	2011	\$ 5 021 074	0.65	3.00	Jones et al. [98]
Cooling Tower	Cooling water flow (litre/s)	5 000	2007	\$ 2 923 425	0.90	2.47	Sinnott et al. [130]
Chiller	Duty (kW)	1 000	2007	\$ 1 574 680	0.90	2.47	Sinnott et al. [130]
Aerobic WWT Plant	Wastewater flow (kg/h)	32 724	2007	\$ 3 567 191	0.65	1.00	Jones et al. [55]
HRSG	Area (m <sup>2</sup> )	65	2002	\$ 96 054	0.65	2.47	Phillips et al. [134]
FT Reactor Preheater	Area (m <sup>2</sup> )	606	2011	\$ 782 600	0.65	2.47	Klein-Marcuschamer et al. [5]
Incinerator & HRSG	Equivalent steam produced <sup>1</sup> (kg/h)	650 000	2011	\$ 11 272 996	0.86	1.02	Klein-Marcuschamer et al. [5]

<sup>1</sup> Based on 32 bar steam.

## Appendix D. Power and Water Calculations

In section 5 the net export of electricity and make-up water requirements for each of the investigated processes are given. This appendix shows the power and water calculations used to determine the net export of electricity and make-up water requirements.

### HEFA Process

Table 109: Power generation and usage of the HEFA process

Usage (MW)	
H <sub>2</sub> compressor	0.42
Hydrotreater feed pump	0.03
Hydrocracker feed pump	0.05
Steam generation pumps	0.05
Reforming section	0.15
WWT section	0.04
PSA compressor	1.13
H <sub>2</sub> recycle compressor	0.19
Cooling tower	0.31
Miscellaneous <sup>1</sup>	0.24
<b>Total usage</b>	<b>2.60</b>
Generation (MW)	
Expander	0.15
Steam turbine	2.45
<b>Total generated</b>	<b>2.60</b>
<b>Net export (MW)</b>	<b>0.00</b>

<sup>1</sup> Specified as 10% of electricity usage.

Table 110: Water inputs and outputs of the HEFA process

Water inputs (kg/h)	
Boiler feed (for power generation)	8 056
Steam reforming boiler feed	6 913
Cooling water to process	1 080 980
<b>Total water inputs</b>	<b>1 095 949</b>
Water outputs (kg/h)	
Steam condensate	8 056
Wastewater <sup>1</sup>	3 556
Cooling water from process	1 080 980
Boiler water <u>loss</u> <sup>2</sup>	161
Cooling water <u>loss</u> <sup>3</sup>	18 233
<b>Total water outputs</b>	<b>1 067 087</b>
<b>Make-up water required (kg/h)</b>	<b>28 862</b>

<sup>1</sup> Wastewater (from hydrotreater and hydrogen plant sections) is treated and then discarded; <sup>2</sup> 2% water purge in boiler water recycle; <sup>3</sup> Discussed in section 4.4.8.1.

## SYN-FER-J Process

Table 111: Power generation and usage of the SYN-FER-J process

Scenario	A.1	A.2	B
<b>Usage (MW)</b>			
Utilities <sup>1</sup>	5.63	5.50	5.49
Separation section	0.02	0.02	0.03
Oligomerization section	0.08	0.08	0.08
Hydroprocessing section	0.52	0.55	0.55
Hydrogen recovery plant	1.19	1.08	1.00
Gasification plant	4.71	5.00	10.60 <sup>2</sup>
Dehydration section	1.20	1.29	1.27
WWT plant <sup>3</sup>	8.72	8.47	7.78
Fermentation section <sup>4</sup>	4.09	1.80	0.38
Miscellaneous <sup>5</sup>	2.38	2.16	2.47
<b>Total usage</b>	<b>28.53</b>	<b>25.94</b>	<b>29.64</b>
<b>Generation (MW)</b>			
Expander	-	-	0.90
Steam turbine	28.65	26.23	29.80
<b>Total generated</b>	<b>28.65</b>	<b>26.23</b>	<b>30.7</b>
<b>Net export (MW) <sup>6</sup></b>	<b>0.00</b>	<b>0.00</b>	<b>0.00</b>

<sup>1</sup> Mainly for the cooling tower; <sup>2</sup> Scenario B has additional compressors to elevate the syngas pressure for the fermentation section; <sup>3</sup> Specified based on [32]; <sup>4</sup> Significantly larger for scenario A.1 due to higher recycle of syngas required; <sup>5</sup> Specified as 10% of electricity usage; <sup>6</sup> Although the electricity generated is slightly larger than the electricity required, no electricity is exported.

Table 112: Water inputs and outputs of the SYN-FER-J process

Scenario	A.1	A.2	B
<b>Water inputs (kg/h)</b>			
Gasification boiler feed	9 190	9 190	36 137
Water to fermentation	650 839	608 947	540 851
Scrubber feed	31 153	54 112	50 775
Cooling water to process	17 846 400	17 465 900	17 362 600
Boiler feed (for power generation)	250 945	240 261	238 770
<b>Total water inputs</b>	<b>18 788 526</b>	<b>18 378 410</b>	<b>18 229 133</b>
<b>Water outputs (kg/h)</b>			
Hydrogen recovery plant wastewater	117	101	70
Separation section wastewater	681 886	660 428	607 580
Dehydration section wastewater	6 380	6 832	6 756
Steam condensate	250 941	244 176	242 641
Cooling water from process	17 846 400	17 465 900	17 362 600
Cooling water <u>loss</u> <sup>1</sup>	301 009	294 592	292 849
Boiler water <u>loss</u> <sup>2</sup>	5 019	4 805	4 775
WWT water <u>loss</u> <sup>3</sup>	34 419	33 368	30 720
<b>Total water outputs</b>	<b>18 445 277</b>	<b>18 044 672</b>	<b>17 891 303</b>
<b>Make-up water required (kg/h)</b>	<b>343 249</b>	<b>333 737</b>	<b>337 831</b>

<sup>1</sup> Discussed in section 4.4.8.1.; <sup>2</sup> 2% water purge in boiler water recycle; <sup>3</sup> 5% water loss in WWT section based on [32].

## S-ETH-J Process

Table 113: Power generation and usage of the S-ETH-J process

Usage (MW)	
Sugarcane to ethanol plant <sup>1</sup>	4.90
Utilities <sup>2</sup>	4.20
Dehydration section	1.25
Oligomerization section	0.08
Hydroprocessing section	0.53
Hydrogen plant	0.49
WWT plant <sup>3</sup>	2.60
Miscellaneous <sup>4</sup>	1.41
<b>Total usage</b>	<b>15.46</b>
Generation (MW)	
Steam turbine	68.07
<b>Total generated</b>	<b>68.07</b>
<b>Net export (MW)</b>	<b>52.62</b>

<sup>1</sup> Specified as 22 kWh per wet ton of sugarcane in feed (based on [91]); <sup>2</sup> Mainly for the cooling tower;

<sup>3</sup> Specified based on [32]; <sup>4</sup> Specified as 10% of electricity usage.

Table 114: Water inputs and outputs of the S-ETH-J process

Water inputs (kg/h)	
Diffuser water	80 297
Juice treatment water	7 002
Scrubber feed	20 649
Make-up water to fermentation section	1 823
Boiler feed (for power generation)	273 943
Cooling water to process	13 492 800
Steam reforming boiler feed	629
<b>Total water inputs</b>	<b>13 877 142</b>
Water outputs (kg/h)	
Steam condensate	273 943
Multi-effect evaporator condensate	65 381
Water from dewatering bagasse	52 882
Vinasse <sup>1</sup>	108 468
Other process wastewater	19 425
Cooling water from process	13 492 800
Cooling water <u>loss</u> <sup>2</sup>	227 579
Boiler water <u>loss</u> <sup>3</sup>	5 479
WWT water <u>loss</u> <sup>4</sup>	21 809
<b>Total water outputs</b> <sup>5</sup>	<b>13 649 563</b>
<b>Make-up water required (kg/h)</b>	<b>227 579</b>

<sup>1</sup> The bottoms of the first ethanol distillation column; <sup>2</sup> Discussed in section 4.4.8.1; <sup>3</sup> 2% water purge in boiler water recycle; <sup>4</sup> 15.8% water loss in WWT section (chosen so that make-up water is only needed for meeting cooling water make-up); <sup>5</sup> Does not include vinasse as it is regarded as a neutral product.

## L-ETH-J Process

Table 115: Power generation and usage of the L-ETH-J process

Usage (MW)	
Pretreatment & conditioning section <sup>1</sup>	5.31
Hydrolysis & fermentation section <sup>1</sup>	1.51
Evaporation section	0.61
Steam & power plant section	0.17
Dehydration section	1.25
Oligomerization section	0.08
Hydroprocessing section	0.54
Hydrogen plant	0.49
WWT plant <sup>1</sup>	7.18
Utilities <sup>2</sup>	3.76
Other sections	0.73
Miscellaneous <sup>3</sup>	2.16
<b>Total usage</b>	<b>23.79</b>
Generation (MW)	
Steam turbine	42.84
<b>Total generated</b>	<b>42.84</b>
<b>Net export (MW)</b>	<b>19.05</b>

<sup>1</sup> Specified based on [32]; <sup>2</sup> Mainly for the cooling tower; <sup>3</sup> Specified as 10% of electricity usage.

Table 116: Water inputs and outputs of the L-ETH-J process

Water inputs (kg/h)	
Water plant feed	113 103
Diluting of pretreated solids	195 483
Scrubber feed	28 719
Cooling water to process	12 581 800
Steam reforming boiler feed	622
<b>Total water inputs</b>	<b>12 919 727</b>
Water outputs (kg/h)	
Water plant wastewater	368 648
Cooling water from process	12 581 800
Boiler & WWT water <u>loss</u> <sup>1</sup>	30 721
Cooling water <u>loss</u> <sup>2</sup>	212 213
<b>Total water outputs</b>	<b>12 707 514</b>
<b>Make-up water required (kg/h)</b>	<b>212 213</b>

<sup>1</sup> 8.2% water loss from boiler water & WWT section (chosen so that make-up water is only needed for meeting cooling water make-up); <sup>2</sup> Discussed in section 4.4.8.1.

## FP-J Process

Table 117: Power generation and usage of the FP-J process

Usage (MW)	
Feedstock grinding	4.96
Pyrolysis section	5.79
Quench section	0.19
Hydrotreating section	0.17
Hydrocracking & separation section	0.13
Hydrogen plant	10.70
Steam & power plant	1.65
Utilities	3.26
Miscellaneous <sup>1</sup>	2.69
<b>Total usage</b>	<b>29.55</b>
Generation (MW)	
Steam turbine	93.03
<b>Total generated</b>	<b>93.03</b>
<b>Net export (MW)</b>	<b>63.48</b>

<sup>1</sup> Specified as 10% of electricity usage.

Table 118: Water inputs and outputs of the FP-J process

Water inputs (kg/h)	
Boiler feed	344 731
Ash removal	1000
Chilled water to process	64 198
Cooling water to process	6 828 770
<b>Total water inputs</b>	<b>7 237 699</b>
Water outputs (kg/h)	
Steam condensate	303 195
Chilled water from process	64 198
Cooling water from process	6 828 770
Wastewater <sup>1</sup>	44 714
Boiler water <u>loss</u> <sup>2</sup>	0
Chilled water <u>loss</u> <sup>3</sup>	3 865
Cooling water <u>loss</u> <sup>4</sup>	207 321
<b>Total water outputs</b>	<b>6 985 978</b>
<b>Make-up water required (kg/h)</b>	<b>253 721</b>

<sup>1</sup> Wastewater (mainly from hydrotreater and hydrogen plant sections) is treated and then discarded; <sup>2</sup> No water purge in boiler water recycle (as steam is used in process, no build-up occurs); <sup>3</sup> 6% water purge from chilled water cycle (based on [32]); <sup>4</sup> Discussed in section 4.4.8.1.

## GFT-J Process

Table 119: Power generation and usage of the GFT-J process

Usage (MW)	
Gasification section <sup>1</sup>	3.77
Gas cleaning section <sup>2</sup>	2.55
Syngas compression	20.40
Upgrading and separation section	0.02
Hydrogen recovery plant	0.70
ATR section	1.97
ASU section <sup>3</sup>	3.60
Steam & power plant	1.00
Utilities <sup>4</sup>	3.66
WWT plant	0.60
Miscellaneous <sup>5</sup>	3.83
<b>Total usage</b>	<b>42.11</b>
Generation (MW)	
Steam turbine	54.65
<b>Total generated</b>	<b>54.65</b>
<b>Net export (MW)</b>	<b>12.53</b>

<sup>1</sup> Specified based on [134]; <sup>2</sup> Based on [108]; <sup>3</sup> Based on [104]; <sup>4</sup> Mainly for the cooling tower; <sup>5</sup> Specified as 10% of electricity usage.

Table 120: Water inputs and outputs of the GFT-J process

Water inputs (kg/h)	
Gasification boiler feed	44 159
Boiler feed (for power generation)	216 283
ATR boiler feed	2 592
Cooling water to process	15 297 200
<b>Total water inputs</b>	<b>15 560 234</b>
Water outputs (kg/h)	
Gasification knock-out water	25 894
Rectisol water removed	8 254
Fischer-Tropsch reactor aqueous product	15 547
Steam condensate	216 283
Cooling water from process	15 297 200
Cooling water <u>loss</u> <sup>1</sup>	258 013
Boiler water <u>loss</u> <sup>2</sup>	0
WWT water <u>loss</u> <sup>3</sup>	19 878
<b>Total water outputs</b>	<b>1 067 087</b>
<b>Make-up water required (kg/h)</b>	<b>274 946</b>

<sup>1</sup> Discussed in section 4.4.8.1; <sup>2</sup> No water purge in boiler water recycle (as steam is used in process, no build-up occurs); <sup>3</sup> 40% of treated wastewater is discarded.

## Appendix E. Additional Capital Costs

### SYN-FER-J Process

In section 6.2.1, the summary of capital costs for the SYN-FER-J process was only given for scenario A.1. The summary for scenarios A.2 and B are given in Table 121.

Table 121: Summary of the capital costs of the SYN-FER-J process, scenario A.2 and B

	<b>Scenario A.2</b>	<b>Scenario B</b>
<b>Process Area</b>	<b>Installed cost</b>	<b>Installed cost</b>
Feedstock handling	\$ 23 800 000	\$ 23 800 000
Gasification plant	\$ 43 500 000	\$ 47 500 000
Fermentation	\$ 18 100 000	\$ 10 500 000
Separation	\$ 7 300 000	\$ 8 600 000
Hydrogen recovery	\$ 7 600 000	\$ 7 400 000
Steam & power plant	\$ 16 800 000	\$ 18 000 000
Dehydration	\$ 18 600 000	\$ 18 500 000
Oligomerization	\$ 40 100 000	\$ 39 800 000
Hydroprocessing	\$ 4 700 000	\$ 4 600 000
Utilities	\$ 7 300 000	\$ 7 200 000
WWT	\$ 24 500 000	\$ 23 200 000
<b>Totals</b>	<b>\$ 212 300 000</b>	<b>\$ 209 100 000</b>
Additional Direct Costs	\$ 21 230 000	\$ 20 910 000
<b>Total Direct Costs (TDC)</b>	<b>\$ 233 500 000</b>	<b>\$ 230 000 000</b>
<b>Total Indirect Costs (TIC)</b>	<b>\$ 140 100 000</b>	<b>\$ 138 000 000</b>
<b>Fixed Capital Investment (FCI)</b>	<b>\$ 373 600 000</b>	<b>\$ 368 000 000</b>
Land	\$ 1 800 000	\$ 1 800 000
Working Capital	\$ 37 400 000	\$ 36 800 000
<b>Total Capital Investment (TCI)</b>	<b>\$ 412 800 000</b>	<b>\$ 406 700 000</b>
Lang Factor (FCI / total purchased cost)	4.06	3.92

## Appendix F. Capital Cost Comparison to Literature

As discussed in section 7.2.2, this appendix compares the capital costs of processes or process sections investigated in this study to studies in literature.

### HEFA Process

Detailed capital cost estimation for a vegetable oil upgrading to jet fuel process, similar to the HEFA process, was done by Klein-Marcuschamer et al. [5] (*Klein-Marcuschamer study*). A comparison between the capital cost of the HEFA process (*this project*) and the *Klein-Marcuschamer study* is done in Table 122. The capital costs by the *Klein-Marcuschamer study* were adjusted to *this project's* vegetable oil feed rate (14.9 MT/h) and to 2007 dollars.

Table 122: HEFA process capital cost comparison, (installed costs are in MM\$, in 2007)

Section or equipment	<i>This Project</i>	<i>Klein-Marcuschamer study</i> , [5]	Possible reasons for difference
Heat exchangers	2	17	Significant amounts of heat exchangers for <i>this project</i> are included in other sections.
Hydrotreater	4	11	The <i>Klein-Marcuschamer study</i> has three hydrotreaters (to extend catalyst life-time), whilst <i>this project</i> only has one. <sup>1</sup>
Hydrocracker	27	120	Capital costs from Jones et al. [55] were employed by <i>this project</i> and the <i>Klein-Marcuschamer study</i> . It seems as though the <i>Klein-Marcuschamer study</i> interprets the hydrocracker cost data differently to [55].
Compressors	7	23	The <i>Klein-Marcuschamer study</i> requires more compression due to additional hydrotreaters. Some compressors of <i>this project</i> are also included in the hydrogen production section.
Hydrogen production or recycling	37 <sup>2</sup>	45 <sup>3</sup>	-
Steam turbine	3	-	-
Separation	2	3	-
Other	11	3	-
<b>Totalled Installed Cost (MM\$)</b>	<b>92</b>	<b>220</b>	

<sup>1</sup> The catalyst replacement period for the hydrotreater of *this project* is therefore significantly smaller (1 year versus 10 year by the *Klein-Marcuschamer study*); <sup>2</sup> Consists of steam reforming for hydrogen generation and PSA; <sup>3</sup> Consists of an amine scrubber and new hydrogen feed.

### Ethanol to Jet Process Section

The only literature found which estimated the capital cost of the ethanol to jet fuel (ETH-J) process section was a study by Crawford [49] (for which the detail of the capital estimate is

uncertain). Comparing the FCI of the ETH-J sections at an ethanol feed rate of 10<sup>6</sup> MT per year and in 2007 dollars, the *Crawford study* had a FCI of \$41 million, whilst *this project's* ETH-J section had a FCI of \$101 million. The higher cost of *this project's* ETH-J process section might be due to the two-step oligomerization process employed by this study (instead of a single step). No further in-depth comparison can be performed as the *Crawford study* showed little detail on the specific equipment costs.

### Gasification and Syngas Fermentation Process Section

A capital cost evaluation for the gasification and syngas fermentation (SYN-FER) process was performed by Piccolo et al. [6] (*Piccolo study*). A comparison between the capital costs of *this project* and the *Piccolo study* is done in Table 123 (adjusting the capital costs of the *Piccolo study* to *this project's* lignocellulose feed rate (77.9 MT/h) and to 2007 dollars).

Table 123: SYN-FER process capital cost comparison, (installed costs are in MM\$, in 2007)

Section or equipment	<i>This Project</i> (Scenario A.1)	<i>Piccolo study</i> , [6]	Possible reasons for difference
Feedstock handling	24	36	-
Gasification plant	43	71	Different types of gasifiers were employed by the <i>Piccolo study</i> (oxygen-blown gasifier) and <i>this project</i> (DFB gasifier). <sup>1</sup>
Fermentation	22	12	Different types of fermentation were used by the <i>Piccolo study</i> (CSTR's) and <i>this project</i> (bubble column reactors).
Separation	7	3	-
Power generation	18	51	The difference is somewhat explained due to the difference in power generation. <sup>2</sup>
Heat exchangers	- <sup>3</sup>	9	-
ASU	-	26	<i>This project</i> does not have an ASU plant as it employs a DFB gasifier.
Balance of plant	47	63	-
<b>Totalled Installed Cost (MM\$)</b>	<b>162</b>	<b>271</b>	

<sup>1</sup> Oxygen-blown gasifiers are generally more capital intensive [134]; <sup>2</sup> The *Piccolo study* produces 39.4 MW electricity, whilst *this project* produces 28.6 MW; <sup>3</sup> Not calculated separately by *this project*.

### Sugarcane to Ethanol Process Section

As *this project's* cost estimation of the sugarcane to ethanol process section was obtained from the study by van der Westhuizen [91] (who after comparing capital costs of different literature, used the capital cost by Dias et al. [89]) no capital cost comparison will be done.

## Lignocellulose to Ethanol Process Section

*This project's* cost estimation of the lignocellulose to ethanol (L-ETH) process section was based on the study by Petersen [93]. Thorough capital cost estimation was performed by Humbird et al. [32] on the L-ETH process. Only the total installed costs of *this project* will be compared to the *Humbird study* [32]. The costs of the *Humbird study* were adjusted to *this project's* lignocellulose feed rate (77.9 MT/h) and to 2007 dollars. It is evident from the comparison in Table 124 that similar total installed costs were obtained by *this project* and the *Humbird study*.

Table 124: L-ETH process capital cost comparison

	<i>This Project</i>	<i>Humbird study</i> , [32]
<b>Total installed cost (2007 MM\$)</b>	196	207

## FP-J Process

Brown et al. [51] and Jones et al. [98] performed detailed capital cost estimations on the fast pyrolysis with upgrading to fuels (FP-F) process. A comparison between the capital costs of these two studies and the FP-J process of the current study (referred to as *this project*) is performed in Table 125. The capital costs by the *Brown study* and the *Jones study* are adjusted to *this project's* lignocellulose feed rate (83.5 MT/h) and to 2007 dollars.

Table 125: FP-F process capital cost comparison, (installed costs are in MM\$, in 2007)

Section or equipment	<i>This Project</i>	<i>Jones study</i> , [98]	<i>Brown study</i> , [51]	Possible reasons for difference
Feedstock handling	25	- <sup>1</sup>	16	-
Pyrolysis & combustion	145	145	68	The pyrolysis and combustion section by this project is based on the <i>Jones study</i> . There is considerable uncertainty surrounding the pyrolysis & combustion section capital cost.
Heat recovery & Filtration	36	12	-	Significantly higher cost for <i>this project</i> in comparison to the <i>Jones study</i> is due to heat recovery from pyrolysis vapours to drier air. <sup>2</sup> No oil filtration is performed by the <i>Brown study</i> .
Hydrotreating & Hydrocracking	80	117	44	The <i>Jones study</i> consists of extensive hydrotreating (stabilizer, and two stages of hydrotreating), whilst <i>this project</i> and the <i>Brown study</i> both only have one stage of hydrotreating. Hydrocracking of the total hydrotreated oil is employed by <i>this project</i> and the <i>Brown study</i> , whilst the <i>Jones study</i> only hydrocracks a heavy fraction from the separation section.

Section or equipment	<i>This Project</i>	<i>Jones study</i> , [98]	<i>Brown study</i> , [51]	Possible reasons for difference
Separation	2	4	13	The separation section by the <i>Brown study</i> is believed to include significant refinery units.
Power generation	38 <sup>3</sup>	-	67	No power generation is performed by the <i>Jones study</i> .
Hydrogen production	72	62	-	Hydrogen is not produced by the <i>Brown study</i> , but rather purchased.
Balance of plant	52	8	4	Balance of plant cost by <i>this project</i> includes significant amount of power generation section costs.
<b>Totalled Installed Cost (MM\$)</b>	<b>450</b>	<b>347</b>	<b>213</b>	

<sup>1</sup> The *Jones study* included the feedstock handling cost along with the biomass feedstock cost; <sup>2</sup> Excess cost mainly includes air compressors and heat exchangers; <sup>3</sup> See balance of plant section discussion.

### GFT-J Process

Ekblom et al. [48] and Swanson et al. [69] performed detailed capital cost estimations on the GFT process. A comparison between the capital costs of these two studies and the GFT-J process of the current study (referred to as *this project*) is performed in Table 126. The capital costs by the *Ekblom study* and the *Swanson study* are adjusted to *this project's* lignocellulose feed rate (77.9 MT/h) and to 2007 dollars.

Table 126: GFT process capital cost comparison, (installed costs are in MM\$, in 2007)

Section or equipment	<i>This Project</i>	<i>Ekblom study</i> , [48]	<i>Swanson study</i> , [69] <sup>1</sup>	Possible reasons for difference
Feedstock handling & gasification	67	130	42	<i>This project</i> consists of a DFB gasifier, whilst the other two studies employ pressurized oxygen-blown gasifiers. <sup>2</sup>
Gas cleaning & compression	52	63	31	The <i>Swanson study</i> utilizes amine scrubbing for acid gas removal, whereas the other two studies use a Rectisol unit.
FT plant, hydrocracking, separation & ATR	121	137	76	The <i>Swanson study</i> does not have a ATR section.
Power generation	24	34	35	-
Balance of plant (including ASU)	57	115	43	The oxygen requirements of the <i>Ekblom study</i> are much higher than <i>this project</i> resulting in a much more expensive ASU section. <sup>3</sup>
<b>Totalled Installed Cost (MM\$)</b>	<b>322</b>	<b>479</b>	<b>226</b>	

<sup>1</sup> The low-temperature gasification scenario; <sup>2</sup> Oxygen-blown gasifiers are generally more capital intensive [134]; <sup>3</sup> Both studies have ATR but the *Ekblom study* also employs an oxygen-blown gasifier.

## Appendix G. Operating Costs

This appendix provides the assumptions made for variable operating cost calculations as well as a complete summary of the investigated processes' variable operating costs.

### Variable Operating Cost Assumptions

Table 127: Assumptions for variable operating costs

Cost description	\$/MT (2007\$)	Literature Source
<b>Raw materials</b>		
Lignocellulose feedstock (dry) <sup>1</sup>	70.00	Based on in-house information, [32], [98] and [36]
Vegetable oil	700	[140]
Sugarcane (wet)	30.00	[141]
Trash (dry)	70.00	- <sup>2</sup>
Natural Gas	200.00	[140]
Nutrients (L-ETH-J process)	5% of feedstock cost	Humbird et al. [32]
Nutrients (SYN-FER-J process)	5% of feedstock cost	Assumption <sup>3</sup>
Olivine	223.76	Phillips et al. [134]
MgO	472.37	Phillips et al. [134]
Nitrogen	5.12	Cameron et al. [129]
H <sub>3</sub> PO <sub>4</sub>	815.48	van der Westhuizen [91]
Water (make-up)	0.18	Humbird et al. [32]
Distilled water	0.78	Assumption
Boiler feed water chemicals	4 996	Jones et al. [98]
Cooling tower water chemicals	3 569	Jones et al. [98]
Reformer catalyst	19 473	Jones et al. [55]
n-Heptane <sup>4</sup>	2 446.45	[150]
Catalyst for ethylene oligomerization	Equal to solvent cost	Assumption <sup>5</sup>
Auto-thermal reformer catalyst	19 474 <sup>6</sup>	Jones et al. [55]
Lime	81.55	[151]
Enzymes <sup>7</sup>	507	Kazi et al. [58]
Sulphur Dioxide	303.60	Humbird et al. [32]
Oxygen	24.46	[152]
Glucose	579.17	Humbird et al. [32]
<b>Waste disposal</b>		
Wastewater	0.73	Jones et al. [98]
Solids disposal cost	29.36	Jones et al. [98]
<b>By-products credits</b>		
Grid electricity	0.08 <sup>8</sup>	Assumption <sup>9</sup>
Naptha	1 176	[140]
Diesel	1 169	[140]
Gas oil	1 162	[140]

<sup>1</sup> For lignocellulose with 3.7 wt% ash; <sup>2</sup> Based on the lignocellulose cost; <sup>3</sup> Assumed to be similar to the L-ETH-J process [32]; <sup>4</sup> Ethylene oligomerization solvent; <sup>5</sup> Due to uncertainty surrounding the catalyst cost, it was assumed to be same cost as solvent (n-heptane) make-up; <sup>6</sup> Assume cost is the same as the reformer catalyst by [55]; <sup>7</sup> 10% broth as specified by [58]; <sup>8</sup> Cost is in \$/kWh; <sup>9</sup> Based on in-house information.

Table 128: Assumptions for periodic costs

Cost description	\$/MT (2007\$)	Replacement period (years)	Literature Source
Adsorbent	1 990	3	Cameron et al. [129]
Dehydration Catalyst	8 990	0.25	Cameron et al. [129]
C <sub>4+</sub> Oligomerization Catalyst	130 488	10	Bond et al. [4]
Hydrogenation Catalyst	293 527 <sup>1</sup>	10	Bond et al. [4]
ZnO & Shift Catalysts	19 474	5	Jones et al. [55]
Hydrotreater Catalyst	10 397 <sup>1</sup>	1	Klein-Marcuschamer et al. [5]
Hydrocracking Catalyst	10 397 <sup>1</sup>	1	Klein-Marcuschamer et al. [5]
FT Catalyst	33 069	3	Swanson et al. [69]
Baghouse bags	109 <sup>2</sup>	5	Humbird et al. [32]

<sup>1</sup> Cost is \$ per m<sup>3</sup>; <sup>2</sup> Cost of bag (\$ per bag).

## HEFA Process

Table 129: Variable operating costs of the HEFA process

Stream description	Usage (kg/h)	\$/MT (2007\$)	\$/hour (2007\$)	MM\$/year (2007\$)
<b>Raw materials</b>				
Vegetable oil	14 873	700.00	10 411.19	82.08
Water (make-up)	28 862	0.18	5.18	0.04
Boiler feed water chemicals	0.01	4 996.71	0.03	0.00
Cooling tower water chemicals	0.20	3 569.08	0.73	0.01
Reformer catalyst	1.62	19 473.86	31.58	0.25
<b>Subtotal</b>			<b>10 448.70</b>	<b>82.38</b>
<b>Waste disposal</b>				
Wastewater	8 009	0.73	5.86	0.05
Solids disposal	1.62	29.36	0.05	0.00
<b>Subtotal</b>			<b>5.91</b>	<b>0.05</b>
<b>By-product credits</b>				
Naphtha	1 705	1 176	2 005.26	15.81
Diesel	305	1 169	356.40	2.81
<b>Subtotal</b>			<b>2 361.66</b>	<b>18.62</b>
<b>Total variable operating costs</b>			<b>8 092.95</b>	<b>63.80</b>

Table 130: Periodic costs of the HEFA process

Cost description	Amount (MT)	MM\$ per period (2007\$)
ZnO & Shift Catalysts	31.78	0.619
Hydrotreater Catalyst	17.99 <sup>1</sup>	0.19
Hydrocracking Catalyst	10.91 <sup>1</sup>	0.11
Baghouse Bags	4320 <sup>2</sup>	0.47

<sup>1</sup> Amount is in m<sup>3</sup> catalyst; <sup>2</sup> Amount of baghouse bags.

**SYN-FER-J Process**

Table 131: Variable operating costs of SYN-FER-J (A.1) process

Stream description	Usage (kg/h)	\$/MT (2007\$)	\$/hour (2007\$)	MM\$/year (2007\$)
<b>Raw materials</b>				
Lignocellulose feedstock (wet)	155 763	35.00	5 451.71	42.98
Water (make-up)	343 249	0.26	88.71	0.70
Boiler feed water chemicals	0.17	4 996.71	0.84	0.01
Cooling tower water chemicals	3.37	3 569.08	12.04	0.09
Nutrients <sup>1</sup>	-	-	272.59	2.15
Olivine	210	223.76	47.05	0.37
MgO	2.72	472.37	1.29	0.01
Nitrogen	119	5.12	0.61	0.00
Solvent (n-heptane) make-up <sup>2</sup>	82.8	2 446.45	202.49	1.60
Catalyst for ethylene oligomerization <sup>3</sup>	-	-	202.49	1.60
<b>Subtotal</b>			<b>6 279.81</b>	<b>49.51</b>
<b>Waste disposal</b>				
Wastewater	110 229	0.73	80.63	0.64
Solids disposal	3 095	29.36	90.87	0.72
<b>Subtotal</b>			<b>171.50</b>	<b>1.35</b>
<b>By-product credits</b>				
Diesel	966	1169	1 129.95	8.91
<b>Subtotal</b>			<b>1 129.95</b>	<b>8.91</b>
<b>Total variable operating costs</b>			<b>5 321.35</b>	<b>41.95</b>

<sup>1</sup> Nutrient cost data based on [32]; <sup>2</sup> Solvent for ethylene oligomerization; <sup>3</sup> Uncertainty surrounding ethylene oligomerization catalyst cost, assumed to be same cost as solvent make-up.

Table 132: Variable operating costs of SYN-FER-J (A.2) process

Stream description	Usage (kg/h)	\$/MT (2007\$)	\$/hour (2007\$)	MM\$/year (2007\$)
<b>Raw materials</b>				
Lignocellulose feedstock (wet)	155 763	35.00	5 451.71	42.98
Water (make-up)	333 737	0.26	86.25	0.68
Boiler feed water chemicals	0.16	4 996.71	0.80	0.01
Cooling tower water chemicals	3.30	3 569.08	11.78	0.09
Nutrients <sup>1</sup>	-	-	272.59	2.15
Olivine	210	223.76	47.05	0.37
MgO	2.72	472.37	1.29	0.01
Nitrogen	127	5.12	0.65	0.01
Solvent (n-heptane) make-up <sup>2</sup>	88.6	2 446.45	216.84	1.71
Catalyst for ethylene oligomerization <sup>3</sup>	-	-	216.84	1.71
<b>Subtotal</b>			<b>6 305.79</b>	<b>49.71</b>

Stream description	Usage (kg/h)	\$/MT (2007\$)	\$/hour (2007\$)	MM\$/year (2007\$)
<b>Waste disposal</b>				
Wastewater	107 455	0.73	78.60	0.62
Solids disposal	3 095	29.36	90.87	0.72
<b>Subtotal</b>			<b>169.47</b>	<b>1.34</b>
<b>By-product credits</b>				
Diesel	1 035	1 169	1 210.01	9.54
<b>Subtotal</b>			<b>1 210.01</b>	<b>9.54</b>
<b>Total variable operating costs</b>			<b>5 265.25</b>	<b>41.51</b>

<sup>1</sup> Nutrient cost data based on [32]; <sup>2</sup> Solvent for ethylene oligomerization; <sup>3</sup> Uncertainty surrounding ethylene oligomerization catalyst cost, assumed to be same cost as solvent make-up.

Table 133: Variable operating costs of SYN-FER-J (B) process

Stream description	Usage (kg/h)	\$/MT (2007\$)	\$/hour (2007\$)	MM\$/year (2007\$)
<b>Raw materials</b>				
Lignocellulose feedstock (wet)	155 763	35.00	5 451.71	42.98
Water (make-up)	337 831	0.26	87.31	0.69
Boiler feed water chemicals	0.16	4 996.71	0.80	0.01
Cooling tower water chemicals	3.28	3 569.08	11.71	0.09
Nutrients <sup>1</sup>	-	-	272.59	2.15
Olivine	210	223.76	47.05	0.37
MgO	2.72	472.37	1.29	0.01
Nitrogen	126	5.12	0.64	0.01
Solvent (n-heptane) make-up <sup>2</sup>	87.6	2 446.45	214.38	1.69
Catalyst for ethylene oligomerization <sup>3</sup>	-	-	214.38	1.69
<b>Subtotal</b>			<b>6 301.85</b>	<b>49.68</b>
<b>Waste disposal</b>				
Wastewater	104 367	0.73	76.34	0.60
Solids disposal	3 095	29.36	90.87	0.72
<b>Subtotal</b>			<b>167.21</b>	<b>1.32</b>
<b>By-product credits</b>				
Diesel	1 023	1 169	1 196.28	9.43
<b>Subtotal</b>			<b>1 196.28</b>	<b>9.43</b>
<b>Total variable operating costs</b>			<b>5 272.78</b>	<b>41.57</b>

<sup>1</sup> Nutrient cost data based on [32]; <sup>2</sup> Solvent for ethylene oligomerization; <sup>3</sup> Uncertainty surrounding ethylene oligomerization catalyst cost, assumed to be same cost as solvent make-up.

Table 134: Periodic costs of the SYN-FER-J process scenarios

Cost description	Amount (MT)			MM\$ per period (2007\$)		
	A.1	A.2	B	A.1	A.2	B
Adsorbent	0.54	0.58	0.57	0.001	0.001	0.001
Dehydration Reactor Catalyst	98.54	105.52	104.32	0.89	0.95	0.94
C <sub>4+</sub> Oligomerization Catalyst	112.00	119.93	118.57	14.61	15.65	15.47
Hydrogenation Reactor Catalyst	6.08 <sup>1</sup>	6.51 <sup>1</sup>	6.44 <sup>1</sup>	1.78	1.91	1.89
Baghouse bags	4320 <sup>2</sup>	4320 <sup>2</sup>	4320 <sup>2</sup>	0.47	0.47	0.47

<sup>1</sup> Amount is in m<sup>3</sup> catalyst; <sup>2</sup> Amount of baghouse bags.

## S-ETH-J Process

Table 135: Variable operating costs of the S-ETH-J process

Stream description	Usage (kg/h)	\$/MT (2007\$)	\$/hour (2007\$)	MM\$/year (2007\$)
<b>Raw materials</b>				
Sugarcane (wet)	222 554	30.00	6 676.61	43.87
Trash	36 656	59.50 <sup>1</sup>	2 181.03	14.33
H <sub>3</sub> PO <sub>4</sub>	16.02	815.48	13.07	0.09
Lime	353	81.55	28.75	0.19
Water (make-up)	227 579	0.26	58.82	0.39
Cooling tower water chemicals	2.55	3 569.08	9.10	0.06
Reformer catalyst	0.103	19 473.86	2.00	0.01
Nitrogen	1811	5.12	9.27	0.06
Solvent (n-heptane) make-up <sup>2</sup>	57.4	2 446.45	140.33	0.92
Catalyst for ethylene oligomerization <sup>3</sup>	-	-	140.33	0.92
<b>Subtotal</b>			<b>9 259.28</b>	<b>60.83</b>
<b>Waste disposal</b>				
Wastewater	75 331	0.73	55.10	0.36
Ash disposal	6 708	29.36	196.96	1.29
<b>Subtotal</b>			<b>252.06</b>	<b>1.66</b>
<b>By-product credits</b>				
Grid electricity	52 617 <sup>4</sup>	0.08 <sup>5</sup>	4 209.33	27.66
Diesel	1 012	1 169	1 183.44	7.78
<b>Subtotal</b>			<b>5 392.77</b>	<b>35.43</b>
<b>Total variable operating costs</b>			<b>4 118.57</b>	<b>27.06</b>

<sup>1</sup> Based on the lignocellulose cost; <sup>2</sup> Solvent for ethylene oligomerization; <sup>3</sup> Uncertainty surrounding ethylene oligomerization catalyst cost, assumed to be same cost as solvent make-up; <sup>4</sup> Units is in kW; <sup>5</sup> Cost is in \$/kWh.

Table 136: Periodic costs of the S-ETH-J process

Cost description	Amount (MT)	MM\$ per period (2007\$)
Adsorbent	0.32	0.001
Dehydration Reactor Catalyst	103.20	0.93
C <sub>4+</sub> Oligomerization Catalyst	117.30	15.31
Hydrogenation Reactor Catalyst	6.37 <sup>1</sup>	1.87
ZnO & Shift Catalysts	2.01	0.04
Baghouse bags	4320 <sup>2</sup>	0.47

<sup>1</sup> Amount is in m<sup>3</sup> catalyst; <sup>2</sup> Amount of baghouse bags.

## L-ETH-J Process

Table 137: Variable operating costs of the L-ETH-J process

Stream description	Usage (kg/h)	\$/MT (2007\$)	\$/hour (2007\$)	MM\$/year (2007\$)
<b>Raw materials</b>				
Lignocellulose feedstock (wet)	155 763	35.00	5 451.71	42.98
Sulphur dioxide	1 455	303.60	441.65	3.48
Oxygen	2 726	24.46	66.69	0.53
Glucose	312	579.17	180.43	1.42
Nutrients <sup>1</sup>	-	-	254.86	2.01
Enzymes	8 139	507.00	4 126.28	32.53
Water (make-up)	212 213	0.26	54.84	0.43
Cooling tower water chemicals	2.4	3 569.08	8.49	0.07
Reformer catalyst	0.10	19 473.86	1.99	0.02
Nitrogen	125	5.12	0.64	0.01
Solvent (n-heptane) make-up <sup>2</sup>	87	2 446.45	212.15	1.67
Catalyst for ethylene oligomerization <sup>3</sup>	-	-	212.15	1.67
<b>Subtotal</b>			<b>11 011.9</b>	<b>86.82</b>
<b>Waste disposal</b>				
Wastewater	80 629	0.73	58.98	0.46
Ash disposal	3151	29.36	92.54	0.73
<b>Subtotal</b>			<b>151.51</b>	<b>1.19</b>
<b>By-product credits</b>				
Grid electricity	19 078 <sup>4</sup>	0.08 <sup>5</sup>	1 526.22	12.03
Diesel	1 012	1 169	1 182.94	9.33
<b>Subtotal</b>			<b>2 709.16</b>	<b>21.36</b>
<b>Total variable operating costs</b>			<b>8 454.23</b>	<b>66.65</b>

<sup>1</sup> Nutrient cost data based on [32]; <sup>2</sup> Solvent for ethylene oligomerization; <sup>3</sup> Uncertainty surrounding ethylene oligomerization catalyst cost, assumed to be same cost as solvent make-up; <sup>4</sup> Units is in kW; <sup>5</sup> Cost is in \$/kWh.

Table 138: Periodic costs of the L-ETH-J process

Cost description	Amount (MT)	MM\$ per period (2007\$)
Adsorbent	0.57	0.001
Dehydration Reactor Catalyst	103.89	0.93
C <sub>4+</sub> Oligomerization Catalyst	117.34	15.31
Hydrogenation Reactor Catalyst	6.36 <sup>1</sup>	1.87
ZnO & Shift Catalysts	2.00	0.04
Baghouse bags	4320 <sup>2</sup>	0.47

<sup>1</sup> Amount is in m<sup>3</sup> catalyst; <sup>2</sup> Amount of baghouse bags.

## FP-J Process

Table 139: Variable operating costs of the FP-J process

Stream description	Usage (kg/h)	\$/MT (2007\$)	\$/hour (2007\$)	MM\$/year (2007\$)
<b>Raw materials</b>				
Lignocellulose feedstock	166 922	35.98	6 006.69	47.36
Water (make-up)	253 721	0.26	65.57	0.52
Boiler feed water chemicals	1.54	4 996	7.73	0.06
Cooling tower water chemicals	2.32	3 569	8.29	0.07
Distilled water	1 357	0.78	1.05	0.01
Natural gas	2 642	200.00	2 362.40	18.63
Reformer catalyst	2 943	19 473	57.31	0.45
<b>Subtotal</b>			<b>8 509.04</b>	<b>67.09</b>
<b>Waste disposal</b>				
Wastewater	92 471	0.73	67.64	0.53
Solids disposal	912	29.36	152.66	1.20
<b>Subtotal</b>			<b>220.30</b>	<b>1.74</b>
<b>By-product credits</b>				
Grid electricity	63 480 <sup>1</sup>	0.08 <sup>2</sup>	5 078.37	40.04
Naptha	4 019	1 176	4 726.79	37.27
Diesel	1 878	1 169	2 195.71	17.31
Gas oil	1 711	1 035	1 987.57	15.67
<b>Subtotal</b>			<b>13 998.45</b>	<b>110.28</b>
<b>Total variable operating costs</b>			<b>-5 259.11</b>	<b>-41.46</b>

<sup>1</sup> Units is in kW; <sup>2</sup> Cost is in \$/kWh.

Table 140: Periodic costs of the FP-J process

Cost description	Amount (MT)	MM\$ per period (2007\$)
Hydrotreater Catalyst	212.96 <sup>1</sup>	2.21
Hydrocracking Catalyst	19.69 <sup>1</sup>	0.20
ZnO & Shift Catalyst	57.68	1.12
Baghouse bags	4320 <sup>2</sup>	0.47

<sup>1</sup> Amount is in m<sup>3</sup> catalyst; <sup>2</sup> Amount of baghouse bags.

**GFT-J Process**

Table 141: Variable operating costs of the GFT-J process

Stream description	Usage (kg/h)	\$/MT (2007\$)	\$/hour (2007\$)	MM\$/year (2007\$)
<b>Raw materials</b>				
Lignocellulose feedstock	155 763	35.00	5 451.71	42.98
Water (make-up)	274 946	0.258	71.06	0.56
Boiler feed water chemicals	0.56	4 997	2.82	0.02
Cooling tower water chemicals	2.89	3 569	10.32	0.08
Olivine	210	223.8	47.05	0.37
MgO	2.72	472.4	1.29	0.01
Auto-thermal reformer catalyst	3.55	19 474	69.13	0.55
<b>Subtotal</b>			<b>5 653.38</b>	<b>44.57</b>
<b>Waste disposal</b>				
Wastewater	80 557	0.73	58.92	0.46
Solids disposal	3 095	29.36	90.87	0.72
<b>Subtotal</b>			<b>149.79</b>	<b>1.18</b>
<b>By-product credits</b>				
Grid electricity	12 533 <sup>1</sup>	0.08 <sup>2</sup>	1 002.65	7.90
Naptha	2 388	1 176	2 808.84	22.14
<b>Subtotal</b>			<b>3 811.49</b>	<b>30.05</b>
<b>Total variable operating costs</b>			<b>1 991.69</b>	<b>15.70</b>

<sup>1</sup> Units is in kW; <sup>2</sup> Cost is in \$/kWh.

Table 142: Periodic costs of the GFT-J process

Cost description	Amount (MT)	MM\$ per period (2007\$)
FT Catalyst	471.88	15.60
Hydrocracking Catalyst	17.45 <sup>1</sup>	0.18
Baghouse bags	4320 <sup>2</sup>	0.47

<sup>1</sup> Amount is in m<sup>3</sup> catalyst; <sup>2</sup> Amount of baghouse bags.

## Appendix H. Discounted Cash Flow Sheets

### HEFA Process

Table 143: Discounted Cash Flow Sheet for Construction Period and Years 1-8 of the HEFA Process

Year	-2	-1	0	1	2	3	4	5	6	7	8
Fixed Capital Investment	\$ 4709746	\$ 35323096	\$ 18838985								
Land	\$ 1848000										
Working Capital			\$ 14717957								
Loan Payment				\$ 7887629	\$ 7887629	\$ 7887629	\$ 7887629	\$ 7887629	\$ 7887629	\$ 7887629	\$ 7887629
Loan Interest Payment	\$ 445071	\$ 3783104	\$ 5563388	\$ 5563388	\$ 5416960	\$ 5261308	\$ 5095850	\$ 4919968	\$ 4739006	\$ 4534264	\$ 4323002
Loan Principal	\$ 7084619	\$ 60049284	\$ 88307741	\$ 85983499	\$ 83512831	\$ 80886511	\$ 78094732	\$ 75127072	\$ 71972449	\$ 68619084	\$ 65054538
Jet Fuel Sales				\$ 70441823	\$ 93922431	\$ 93922431	\$ 93922431	\$ 93922431	\$ 93922431	\$ 93922431	\$ 93922431
By-Product Credit (Other Fuels)				\$ 13964469	\$ 18619291	\$ 18619291	\$ 18619291	\$ 18619291	\$ 18619291	\$ 18619291	\$ 18619291
Total Annual Sales				\$ 84406292	\$ 112541723	\$ 112541723	\$ 112541723	\$ 112541723	\$ 112541723	\$ 112541723	\$ 112541723
Annual Manufacturing Cost											
Feedstock				\$ 61561389	\$ 82081852	\$ 82081852	\$ 82081852	\$ 82081852	\$ 82081852	\$ 82081852	\$ 82081852
Catalyst cost				\$ 2220360	\$ 300537	\$ 300537	\$ 300537	\$ 300537	\$ 300537	\$ 300537	\$ 300537
Baghouse bags				\$ 472498							
Other Variable Costs				\$ 299501	\$ 342287	\$ 342287	\$ 342287	\$ 342287	\$ 342287	\$ 342287	\$ 342287
Fixed Operating Costs				\$ 9580999	\$ 9580999	\$ 9580999	\$ 9580999	\$ 9580999	\$ 9580999	\$ 9580999	\$ 9580999
Total Product Cost				\$ 74134746	\$ 92305674	\$ 92305674	\$ 92305674	\$ 92305674	\$ 92305674	\$ 92305674	\$ 92305674
Annual Depreciation											
General Plant Writedown				\$ 0	\$ 0	\$ 0	\$ 0	\$ 0	\$ 0	\$ 0	\$ 0
Depreciation Charge				\$ 21031960	\$ 36044276	\$ 25741706	\$ 18382728	\$ 13143135	\$ 13128417	\$ 13143135	\$ 6564209
Remaining Value				\$ 126147607	\$ 90103311	\$ 64361625	\$ 45978897	\$ 32835762	\$ 19707344	\$ 6564209	\$ 0
Net Revenue				\$ (16323802)	\$ (21225188)	\$ (10786966)	\$ (3242530)	\$ 2172945	\$ 1285258	\$ 2559649	\$ 9348838
Losses Forward				\$ (16323802)	\$ (37548990)	\$ (48315957)	\$ (51558486)	\$ (49385541)	\$ (48102283)	\$ (45542634)	\$ (36194797)
Taxable Income				\$ (16323802)	\$ (37548990)	\$ (48315957)	\$ (51558486)	\$ (49385541)	\$ (48102283)	\$ (45542634)	\$ (36194797)
Income Tax				\$ 0	\$ 0	\$ 0	\$ 0	\$ 0	\$ 0	\$ 0	\$ 0
Annual Cash Income				\$ 2389317	\$ 12348420	\$ 12348420	\$ 12348420	\$ 12348420	\$ 11257052	\$ 12348420	\$ 12348420
Discount Factor		1.19	1.09	1.00	0.91	0.84	0.77	0.70	0.64	0.59	0.54
Annual Present Value	\$ 87510485			\$ 2181077	\$ 10336442	\$ 9456946	\$ 8652283	\$ 7916087	\$ 6602428	\$ 6626287	\$ 6062477
Total Capital Investment + Interest	\$ 8365909	\$ 42743076	\$ 39120329	\$ 0	\$ 0	\$ 0	\$ 0	\$ 0	\$ 0	\$ 0	\$ 0
Net Present Worth			\$ 0								

Table 144: Discounted Cash Flow Sheet for Years 9-20 of the HEFA Process

Year	9	10	11	12	13	14	15	16	17	18	19	20
Fixed Capital Investment												\$ (1848000)
Land												\$ (14717957)
Working Capital												\$ 7887629
Loan Payment	\$ 7887629	\$ 7887629	\$ 7887629	\$ 7887629	\$ 7887629	\$ 7887629	\$ 7887629	\$ 7887629	\$ 7887629	\$ 7887629	\$ 7887629	\$ 7887629
Loan Interest Payment	\$ 4098431	\$ 3859711	\$ 3605953	\$ 3336207	\$ 3049467	\$ 2744663	\$ 2420656	\$ 2076237	\$ 1710120	\$ 1320936	\$ 907235	\$ 467400
Loan Principal	\$ 61265260	\$ 57237343	\$ 52955666	\$ 48404245	\$ 43566083	\$ 38423118	\$ 32956146	\$ 27144754	\$ 20967245	\$ 14400553	\$ 7420159	\$ 0
Jet Fuel Sales	\$ 93922431	\$ 93922431	\$ 93922431	\$ 93922431	\$ 93922431	\$ 93922431	\$ 93922431	\$ 93922431	\$ 93922431	\$ 93922431	\$ 93922431	\$ 93922431
By-Product Credit (Other Fuels)	\$ 18619291	\$ 18619291	\$ 18619291	\$ 18619291	\$ 18619291	\$ 18619291	\$ 18619291	\$ 18619291	\$ 18619291	\$ 18619291	\$ 18619291	\$ 18619291
Total Annual Sales	\$ 112541723	\$ 112541723	\$ 112541723	\$ 112541723	\$ 112541723	\$ 112541723	\$ 112541723	\$ 112541723	\$ 112541723	\$ 112541723	\$ 112541723	\$ 112541723
Annual Manufacturing Cost												
Feedstock	\$ 82081852	\$ 82081852	\$ 82081852	\$ 82081852	\$ 82081852	\$ 82081852	\$ 82081852	\$ 82081852	\$ 82081852	\$ 82081852	\$ 82081852	\$ 82081852
Catalyst cost	\$ 300537	\$ 300537	\$ 919406	\$ 300537	\$ 300537	\$ 300537	\$ 300537	\$ 919406	\$ 300537	\$ 300537	\$ 300537	\$ 300537
Baghouse bags				\$ 472498				\$ 472498				
Other Variable Costs	\$ 342287	\$ 342287	\$ 342287	\$ 342287	\$ 342287	\$ 342287	\$ 342287	\$ 342287	\$ 342287	\$ 342287	\$ 342287	\$ 342287
Fixed Operating Costs	\$ 9580999	\$ 9580999	\$ 9580999	\$ 9580999	\$ 9580999	\$ 9580999	\$ 9580999	\$ 9580999	\$ 9580999	\$ 9580999	\$ 9580999	\$ 9580999
Total Product Cost	\$ 92305674	\$ 92305674	\$ 93397042	\$ 92305674	\$ 92305674	\$ 92305674	\$ 92305674	\$ 93397042	\$ 92305674	\$ 92305674	\$ 92305674	\$ 92305674
Annual Depreciation												
General Plant Writedown												
Depreciation Charge												
Remaining Value												
Net Revenue	\$ 16137618	\$ 16376337	\$ 15538728	\$ 16899842	\$ 17186581	\$ 17491385	\$ 17815392	\$ 17068444	\$ 18525929	\$ 18915112	\$ 19328814	\$ 19768579
Losses Forward	\$ (36194797)	\$ (20057179)	\$ (3680842)	\$ 0	\$ 0	\$ 0	\$ 0	\$ 0	\$ 0	\$ 0	\$ 0	\$ 0
Taxable Income	\$ (20057179)	\$ (3680842)	\$ 11857886	\$ 16899842	\$ 17186581	\$ 17491385	\$ 17815392	\$ 17068444	\$ 18525929	\$ 18915112	\$ 19328814	\$ 19768579
Income Tax	\$ 0	\$ 0	\$ 3320208	\$ 4731956	\$ 4812243	\$ 4897588	\$ 4988310	\$ 4779164	\$ 5187260	\$ 5296231	\$ 5412068	\$ 5535202
Annual Cash Income	\$ 12348420	\$ 12348420	\$ 7936844	\$ 7616464	\$ 7536177	\$ 7450832	\$ 7360110	\$ 6477888	\$ 7161160	\$ 7052188	\$ 6936352	\$ 6813218
Discount Factor	0.45	0.41	0.38	0.34	0.31	0.29	0.26	0.24	0.22	0.20	0.18	0.17
Annual Present Value	\$ 5546639	\$ 5074693	\$ 2984197	\$ 2620061	\$ 2371860	\$ 2145470	\$ 1939019	\$ 1561388	\$ 1579213	\$ 1422856	\$ 1280407	\$ 1150665
Total Capital Investment + Interest	\$ 0	\$ 0	\$ 0	\$ 0	\$ 0	\$ 0	\$ 0	\$ 0	\$ 0	\$ 0	\$ 0	\$ (2718829)
Net Present Worth												

### SYN-FER-J Process

The discounted cash flow sheet will only be given for the SYN-FER-J process, scenario A.1. Similar sheets were developed for scenario A.2 and B.

Table 145: Discounted Cash Flow Sheet for Construction Period and Years 1-8 of the SYN-FER-J (A.1) Process

Year	-2	-1	0	1	2	3	4	5	6	7	8
Fixed Capital Investment			\$ 90 731 849	\$ 48 390 320							
Land	\$ 1848 000										
Working Capital			\$ 37 804 937								
Loan Payment				\$ 20 260 374	\$ 20 260 374	\$ 20 260 374	\$ 20 260 374	\$ 20 260 374	\$ 20 260 374	\$ 20 260 374	\$ 20 260 374
Loan Interest Payment	\$ 1 143 221	\$ 9 717 381	\$ 14 290 266	\$ 14 290 266	\$ 13 914 149	\$ 13 514 337	\$ 13 089 337	\$ 12 637 562	\$ 12 157 325	\$ 11 646 832	\$ 11 104 179
Loan Principal	\$ 18 146 370	\$ 154 244 144	\$ 226 629 623	\$ 229 859 115	\$ 214 933 291	\$ 207 787 264	\$ 200 598 217	\$ 192 973 405	\$ 184 870 356	\$ 176 258 914	\$ 167 006 619
Jet Fuel Sales				\$ 89 872 555	\$ 119 830 073	\$ 119 830 073	\$ 119 830 073	\$ 119 830 073	\$ 119 830 073	\$ 119 830 073	\$ 119 830 073
By-Product Credit (Other fuels)				\$ 6 681 420	\$ 8 908 560	\$ 8 908 560	\$ 8 908 560	\$ 8 908 560	\$ 8 908 560	\$ 8 908 560	\$ 8 908 560
Total Annual Sales				\$ 96 553 975	\$ 128 738 634	\$ 128 738 634	\$ 128 738 634	\$ 128 738 634	\$ 128 738 634	\$ 128 738 634	\$ 128 738 634
Annual Manufacturing Cost				\$ 32 235 981	\$ 42 981 308	\$ 42 981 308	\$ 42 981 308	\$ 42 981 308	\$ 42 981 308	\$ 42 981 308	\$ 42 981 308
Feedstock				\$ 19 941 572	\$ 5 183 043	\$ 5 183 043	\$ 5 184 122	\$ 5 183 043	\$ 5 183 043	\$ 5 184 122	\$ 5 183 043
Catalyst cost				\$ 472 498				\$ 472 498			
Baghouse bags				\$ 6 895 889	\$ 7 880 788	\$ 7 880 788	\$ 7 880 788	\$ 7 880 788	\$ 7 880 788	\$ 7 880 788	\$ 7 880 788
Other Variable Costs				\$ 20 289 668	\$ 20 289 668	\$ 20 289 668	\$ 20 289 668	\$ 20 289 668	\$ 20 289 668	\$ 20 289 668	\$ 20 289 668
Fixed Operating Costs				\$ 20 289 668	\$ 20 289 668	\$ 20 289 668	\$ 20 289 668	\$ 20 289 668	\$ 20 289 668	\$ 20 289 668	\$ 20 289 668
Total Product Cost				\$ 79 835 409	\$ 76 334 808	\$ 76 334 808	\$ 76 335 886	\$ 76 334 808	\$ 76 335 886	\$ 76 334 808	\$ 76 334 808
Annual Depreciation				\$ 0	\$ 0	\$ 0	\$ 0	\$ 0	\$ 0	\$ 0	\$ 0
General Plant Writedown				\$ 54 023 255	\$ 92 584 291	\$ 66 120 835	\$ 47 218 367	\$ 33 759 809	\$ 33 722 004	\$ 33 759 809	\$ 16 861 002
Depreciation Charge				\$ 324 026 117	\$ 231 441 826	\$ 165 320 990	\$ 119 102 624	\$ 84 342 815	\$ 50 620 811	\$ 16 861 002	\$ 0
Remaining Value				\$ (51 594 955)	\$ (54 094 615)	\$ (27 231 347)	\$ (7 904 958)	\$ 6 006 455	\$ 6 051 999	\$ 6 995 106	\$ 24 438 645
Net Revenue				\$ (51 594 955)	\$ (54 094 955)	\$ (105 689 570)	\$ (132 920 916)	\$ (140 825 872)	\$ (134 819 417)	\$ (128 767 418)	\$ (121 717 311)
Losses Forward				\$ (51 594 955)	\$ (105 689 570)	\$ (132 920 916)	\$ (140 825 872)	\$ (134 819 417)	\$ (128 767 418)	\$ (121 717 311)	\$ (97 332 667)
Taxable Income				\$ 0	\$ 0	\$ 0	\$ 0	\$ 0	\$ 0	\$ 0	\$ 0
Income Tax				\$ 0	\$ 0	\$ 0	\$ 0	\$ 0	\$ 0	\$ 0	\$ 0
Annual Cash Income				\$ (35 411 808)	\$ 32 143 452	\$ 32 143 452	\$ 32 142 374	\$ 32 143 452	\$ 31 670 954	\$ 32 142 374	\$ 32 143 452
Discount Factor		1.19	1.09	1.00	0.91	0.84	0.77	0.70	0.64	0.59	0.54
Annual Present Value	\$ 22 180 827			\$ (3 240 446)	\$ 26 906 189	\$ 24 616 824	\$ 22 521 499	\$ 20 605 906	\$ 18 575 485	\$ 17 247 923	\$ 15 780 880
Total Capital Investment + Interest	\$ 18 025 821	\$ 109 791 009	\$ 100 485 523	\$ 0	\$ 0	\$ 0	\$ 0	\$ 0	\$ 0	\$ 0	\$ 0
Net Present Worth				\$ 0	\$ 0	\$ 0	\$ 0	\$ 0	\$ 0	\$ 0	\$ 0

Table 146: Discounted Cash Flow Sheet for Years 9-20 of the SYN-FER-J (A.1) Process

Year	9	10	11	12	13	14	15	16	17	18	19	20
Fixed Capital Investment												\$ (1848 000)
Land												\$ (37 804 937)
Working Capital												\$ (37 804 937)
Loan Payment	\$ 20 260 374	\$ 20 260 374	\$ 20 260 374	\$ 20 260 374	\$ 20 260 374	\$ 20 260 374	\$ 20 260 374	\$ 20 260 374	\$ 20 260 374	\$ 20 260 374	\$ 20 260 374	\$ 20 260 374
Loan Interest Payment	\$ 10 527 339	\$ 9 914 158	\$ 9 262 346	\$ 8 569 470	\$ 7 832 944	\$ 7 050 015	\$ 6 217 763	\$ 5 333 078	\$ 4 392 559	\$ 3 392 993	\$ 2 330 348	\$ 1 200 756
Loan Principal	\$ 157 367 584	\$ 147 021 368	\$ 136 023 340	\$ 124 332 437	\$ 111 905 006	\$ 98 694 648	\$ 84 652 037	\$ 69 724 741	\$ 53 857 026	\$ 36 989 644	\$ 20 599 618	\$ (0)
Jet Fuel Sales	\$ 119 830 073	\$ 119 830 073	\$ 119 830 073	\$ 119 830 073	\$ 119 830 073	\$ 119 830 073	\$ 119 830 073	\$ 119 830 073	\$ 119 830 073	\$ 119 830 073	\$ 119 830 073	\$ 119 830 073
By-Product Credit (Other fuels)	\$ 8 908 560	\$ 8 908 560	\$ 8 908 560	\$ 8 908 560	\$ 8 908 560	\$ 8 908 560	\$ 8 908 560	\$ 8 908 560	\$ 8 908 560	\$ 8 908 560	\$ 8 908 560	\$ 8 908 560
Total Annual Sales	\$ 128 738 634	\$ 128 738 634	\$ 128 738 634	\$ 128 738 634	\$ 128 738 634	\$ 128 738 634	\$ 128 738 634	\$ 128 738 634	\$ 128 738 634	\$ 128 738 634	\$ 128 738 634	\$ 128 738 634
Annual Manufacturing Cost												
Feedstock	\$ 42 981 308	\$ 42 981 308	\$ 42 981 308	\$ 42 981 308	\$ 42 981 308	\$ 42 981 308	\$ 42 981 308	\$ 42 981 308	\$ 42 981 308	\$ 42 981 308	\$ 42 981 308	\$ 42 981 308
Catalyst cost	\$ 5 183 043	\$ 5 184 122	\$ 5 183 043	\$ 5 183 043	\$ 5 184 122	\$ 5 183 043	\$ 5 183 043	\$ 5 184 122	\$ 5 183 043	\$ 5 183 043	\$ 5 184 122	\$ 5 183 043
Baghouse bags	\$ 472 498											
Other Variable Costs	\$ 7 880 788	\$ 7 880 788	\$ 7 880 788	\$ 7 880 788	\$ 7 880 788	\$ 7 880 788	\$ 7 880 788	\$ 7 880 788	\$ 7 880 788	\$ 7 880 788	\$ 7 880 788	\$ 7 880 788
Fixed Operating Costs	\$ 20 289 668	\$ 20 289 668	\$ 20 289 668	\$ 20 289 668	\$ 20 289 668	\$ 20 289 668	\$ 20 289 668	\$ 20 289 668	\$ 20 289 668	\$ 20 289 668	\$ 20 289 668	\$ 20 289 668
Total Product Cost	\$ 76 334 808	\$ 76 335 886	\$ 76 807 306	\$ 76 334 808	\$ 76 335 886	\$ 76 334 808	\$ 76 334 808	\$ 76 808 384	\$ 76 334 808	\$ 76 334 808	\$ 76 335 886	\$ 76 334 808
Annual Depreciation												
General Plant Writedown												
Depreciation Charge												
Remaining Value												
Net Revenue	\$ 41 876 487	\$ 42 488 590	\$ 42 668 982	\$ 43 834 356	\$ 44 569 804	\$ 45 353 811	\$ 46 186 063	\$ 46 957 171	\$ 48 011 167	\$ 49 010 833	\$ 50 072 400	\$ 51 203 070
Losses Forward	\$ (97 332 667)	\$ (55 456 180)	\$ (12 967 590)	\$ 0	\$ 0	\$ 0	\$ 0	\$ 0	\$ 0	\$ 0	\$ 0	\$ 0
Taxable Income	\$ (55 456 180)	\$ (12 967 590)	\$ 29 701 392	\$ 43 834 356	\$ 44 569 804	\$ 45 353 811	\$ 46 186 063	\$ 46 957 171	\$ 48 011 167	\$ 49 010 833	\$ 50 072 400	\$ 51 203 070
Income Tax	\$ 0	\$ 0	\$ 8 316 390	\$ 12 273 620	\$ 12 479 545	\$ 12 699 067	\$ 12 932 098	\$ 13 047 208	\$ 13 443 127	\$ 13 723 033	\$ 14 020 272	\$ 14 338 860
Annual Cash Income	\$ 32 143 452	\$ 32 142 374	\$ 23 354 564	\$ 19 869 832	\$ 19 662 829	\$ 19 444 385	\$ 19 211 354	\$ 18 622 668	\$ 18 700 325	\$ 18 420 419	\$ 18 122 102	\$ 17 806 592
Discount Factor	0.45	0.41	0.38	0.34	0.31	0.28	0.26	0.24	0.22	0.20	0.18	0.17
Annual Present Value	\$ 14 438 194	\$ 13 209 194	\$ 8 781 121	\$ 6 835 216	\$ 6 189 170	\$ 5 599 019	\$ 5 061 224	\$ 4 488 687	\$ 4 123 894	\$ 3 776 521	\$ 3 445 226	\$ 3 007 306
Total Capital Investment + Interest	\$ 0	\$ 0	\$ 0	\$ 0	\$ 0	\$ 0	\$ 0	\$ 0	\$ 0	\$ 0	\$ 0	\$ (6 494 082)
Net Present Worth												

### S-ETH-J Process

Table 147: Discounted Cash Flow Sheet for Construction Period and Years 1-8 of the S-ETH-J Process

Year	-2	-1	0	1	2	3	4	5	6	7	8
Fixed Capital Investment			\$ 37 823 729								
Land	\$ 1848 000										
Working Capital			\$ 29 549 788								
Loan Payment				\$ 15 836 285	\$ 15 836 285	\$ 15 836 285	\$ 15 836 285	\$ 15 836 285	\$ 15 836 285	\$ 15 836 285	\$ 15 836 285
Loan Interest Payment	\$ 893 586	\$ 7 595 478	\$ 11 169 820	\$ 11 169 820	\$ 10 875 833	\$ 10 563 324	\$ 10 231 128	\$ 9 879 003	\$ 9 502 631	\$ 9 103 611	\$ 8 679 452
Loan Principal	\$ 14 183 898	\$ 120 563 137	\$ 177 298 731	\$ 172 632 266	\$ 167 671 813	\$ 162 398 852	\$ 156 793 695	\$ 150 835 412	\$ 144 501 758	\$ 137 769 084	\$ 130 612 251
Jet Fuel Sales				\$ 68 615 188	\$ 91 486 918	\$ 91 486 918	\$ 91 486 918	\$ 91 486 918	\$ 91 486 918	\$ 91 486 918	\$ 91 486 918
By-Product Credit (Other fuels + Electricity)				\$ 26 572 872	\$ 35 430 496	\$ 35 430 496	\$ 35 430 496	\$ 35 430 496	\$ 35 430 496	\$ 35 430 496	\$ 35 430 496
Total Annual Sales				\$ 95 188 060	\$ 126 917 414	\$ 126 917 414	\$ 126 917 414	\$ 126 917 414	\$ 126 917 414	\$ 126 917 414	\$ 126 917 414
Annual Manufacturing Cost				\$ 32 988 991	\$ 43 865 321	\$ 43 865 321	\$ 43 865 321	\$ 43 865 321	\$ 43 865 321	\$ 43 865 321	\$ 43 865 321
Feedstock				\$ 20 885 856	\$ 5 428 294	\$ 5 428 294	\$ 5 428 294	\$ 5 428 294	\$ 5 428 294	\$ 5 428 294	\$ 5 428 294
Catalyst cost				\$ 472 498				\$ 472 498			
Baghouse bags				\$ 16 296 178	\$ 18 624 204	\$ 18 624 204	\$ 18 624 204	\$ 18 624 204	\$ 18 624 204	\$ 18 624 204	\$ 18 624 204
Other Variable Costs				\$ 17 235 263	\$ 17 235 263	\$ 17 235 263	\$ 17 235 263	\$ 17 235 263	\$ 17 235 263	\$ 17 235 263	\$ 17 235 263
Fixed Operating Costs				\$ 17 235 263	\$ 17 235 263	\$ 17 235 263	\$ 17 235 263	\$ 17 235 263	\$ 17 235 263	\$ 17 235 263	\$ 17 235 263
Total Product Cost				\$ 87 788 786	\$ 85 153 082	\$ 85 153 082	\$ 85 153 719	\$ 85 153 082	\$ 85 625 580	\$ 85 153 719	\$ 85 153 082
Annual Depreciation				\$ 0	\$ 0	\$ 0	\$ 0	\$ 0	\$ 0	\$ 0	\$ 0
General Plant Writedown				\$ 42 226 648	\$ 72 367 432	\$ 51 682 580	\$ 36 907 686	\$ 26 387 961	\$ 26 358 411	\$ 26 387 961	\$ 13 179 206
Depreciation Charge				\$ 253 271 237	\$ 180						



## FP-J Process

Table 151: Discounted Cash Flow Sheet for Construction Period and Years 1-8 of the FP-J Process

Year	-2	-1	0	1	2	3	4	5	6	7	8
Fixed Capital Investment											
Land	\$ 23 015 098	\$ 172 613 236	\$ 92 060 393								
Working Capital			\$ 71 922 182								
Loan Payment				\$ 38 544 444	\$ 38 544 444	\$ 38 544 444	\$ 38 544 444	\$ 38 544 444	\$ 38 544 444	\$ 38 544 444	\$ 38 544 444
Loan Interest Payment	\$ 2 174 927	\$ 18 486 878	\$ 27 186 585	\$ 27 186 585	\$ 26 471 040	\$ 25 710 415	\$ 24 901 871	\$ 24 042 389	\$ 23 128 760	\$ 22 157 571	\$ 21 251 998
Loan Principal	\$ 34 522 647	\$ 293 442 502	\$ 431 533 091	\$ 420 175 232	\$ 408 101 827	\$ 395 267 797	\$ 381 625 224	\$ 367 123 169	\$ 351 707 484	\$ 335 320 611	\$ 317 901 365
Jet Fuel Sales				\$ 67 511 637	\$ 90 015 516	\$ 90 015 516	\$ 90 015 516	\$ 90 015 516	\$ 90 015 516	\$ 90 015 516	\$ 90 015 516
By-Product Credit (Other Fuels + Electricity)				\$ 22 537 322	\$ 30 049 763	\$ 30 049 763	\$ 30 049 763	\$ 30 049 763	\$ 30 049 763	\$ 30 049 763	\$ 30 049 763
Total Annual Sales				\$ 90 015 516	\$ 120 284 902	\$ 120 284 902	\$ 120 284 902	\$ 120 284 902	\$ 120 284 902	\$ 120 284 902	\$ 120 284 902
Annual Manufacturing Cost				\$ 109 525 708	\$ 146 034 278	\$ 146 034 278	\$ 146 034 278	\$ 146 034 278	\$ 146 034 278	\$ 146 034 278	\$ 146 034 278
Feedstock				\$ 35 571 531	\$ 47 356 708	\$ 47 356 708	\$ 47 356 708	\$ 47 356 708	\$ 47 356 708	\$ 47 356 708	\$ 47 356 708
Catalyst cost				\$ 4 234 861	\$ 2 418 959	\$ 2 418 959	\$ 2 418 959	\$ 2 418 959	\$ 2 418 959	\$ 2 418 959	\$ 2 418 959
Baghouse bags				\$ 472 498							
Other Variable Costs				\$ 18 782 227	\$ 21 465 402	\$ 21 465 402	\$ 21 465 402	\$ 21 465 402	\$ 21 465 402	\$ 21 465 402	\$ 21 465 402
Fixed Operating Costs				\$ 32 913 049	\$ 32 913 049	\$ 32 913 049	\$ 32 913 049	\$ 32 913 049	\$ 32 913 049	\$ 32 913 049	\$ 32 913 049
Total Product Cost				\$ 91 920 166	\$ 104 154 118	\$ 104 154 118	\$ 104 154 118	\$ 104 154 118	\$ 105 749 955	\$ 104 154 118	\$ 104 154 118
Annual Depreciation				\$ 0	\$ 0	\$ 0	\$ 0	\$ 0	\$ 0	\$ 0	\$ 0
General Plant Writedown				\$ 0	\$ 0	\$ 0	\$ 0	\$ 0	\$ 0	\$ 0	\$ 0
Depreciation Charge				\$ 102 776 798	\$ 176 137 423	\$ 125 791 896	\$ 89 830 805	\$ 64 226 508	\$ 64 154 586	\$ 64 226 508	\$ 32 077 293
Remaining Value				\$ 6 164 452	\$ 440 307 597	\$ 314 515 701	\$ 224 684 896	\$ 160 458 388	\$ 96 303 802	\$ 32 077 293	\$ 0
Net Revenue				\$ (7 165 826)	\$ (106 462 163)	\$ (55 356 011)	\$ (18 586 377)	\$ 7 877 402	\$ 7 267 117	\$ 9 762 220	\$ 42 943 808
Losses Forward				\$ 0	\$ 0	\$ 0	\$ 0	\$ 0	\$ 0	\$ 0	\$ 0
Taxable Income				\$ (7 165 826)	\$ (178 120 399)	\$ (233 476 410)	\$ (252 062 787)	\$ (244 185 384)	\$ (236 918 267)	\$ (227 156 047)	\$ (184 212 239)
Income Tax				\$ 0	\$ 0	\$ 0	\$ 0	\$ 0	\$ 0	\$ 0	\$ 0
Annual Cash Income				\$ 19 780 703	\$ 57 601 855	\$ 57 601 855	\$ 57 601 855	\$ 57 601 855	\$ 56 000 199	\$ 57 601 855	\$ 57 601 855
Discount Factor		1.19	1.09	1.00	0.91	0.84	0.77	0.70	0.64	0.59	0.54
Annual Present Value	\$ 420 269 497			\$ 18 079 325	\$ 48 216 552	\$ 44 113 954	\$ 40 360 434	\$ 36 926 289	\$ 32 848 363	\$ 30 099 739	\$ 28 279 725
Total Capital Investment + Interest	\$ 32 300 950	\$ 208 872 425	\$ 19 116 959	\$ 0	\$ 0	\$ 0	\$ 0	\$ 0	\$ 0	\$ 0	\$ 0
Net Present Worth				\$ 0	\$ 0	\$ 0	\$ 0	\$ 0	\$ 0	\$ 0	\$ 0

Table 152: Discounted Cash Flow Sheet for Years 9-20 of the FP-J Process

Year	9	10	11	12	13	14	15	16	17	18	19	20
Fixed Capital Investment												
Land												\$ (1848 000)
Working Capital												\$ (71 922 182)
Loan Payment	\$ 38 544 444	\$ 38 544 444	\$ 38 544 444	\$ 38 544 444	\$ 38 544 444	\$ 38 544 444	\$ 38 544 444	\$ 38 544 444	\$ 38 544 444	\$ 38 544 444	\$ 38 544 444	\$ 38 544 444
Loan Interest Payment	\$ 20 027 786	\$ 18 861 237	\$ 17 621 194	\$ 16 303 030	\$ 14 901 821	\$ 13 412 335	\$ 11 829 012	\$ 10 145 940	\$ 8 356 834	\$ 6 455 015	\$ 4 433 381	\$ 2 284 384
Loan Principal	\$ 299 384 706	\$ 279 701 498	\$ 258 778 248	\$ 236 536 834	\$ 212 894 210	\$ 187 762 100	\$ 161 046 668	\$ 132 648 164	\$ 102 460 554	\$ 70 371 124	\$ 46 260 061	\$ 0
Jet Fuel Sales	\$ 90 015 516	\$ 90 015 516	\$ 90 015 516	\$ 90 015 516	\$ 90 015 516	\$ 90 015 516	\$ 90 015 516	\$ 90 015 516	\$ 90 015 516	\$ 90 015 516	\$ 90 015 516	\$ 90 015 516
By-Product Credit (Other Fuels + Electricity)	\$ 110 284 902	\$ 110 284 902	\$ 110 284 902	\$ 110 284 902	\$ 110 284 902	\$ 110 284 902	\$ 110 284 902	\$ 110 284 902	\$ 110 284 902	\$ 110 284 902	\$ 110 284 902	\$ 110 284 902
Total Annual Sales	\$ 200 300 418	\$ 200 300 418	\$ 200 300 418	\$ 200 300 418	\$ 200 300 418	\$ 200 300 418	\$ 200 300 418	\$ 200 300 418	\$ 200 300 418	\$ 200 300 418	\$ 200 300 418	\$ 200 300 418
Annual Manufacturing Cost												
Feedstock	\$ 47 356 708	\$ 47 356 708	\$ 47 356 708	\$ 47 356 708	\$ 47 356 708	\$ 47 356 708	\$ 47 356 708	\$ 47 356 708	\$ 47 356 708	\$ 47 356 708	\$ 47 356 708	\$ 47 356 708
Catalyst cost	\$ 2 418 959	\$ 2 418 959	\$ 3 542 297	\$ 2 418 959	\$ 2 418 959	\$ 2 418 959	\$ 2 418 959	\$ 3 542 297	\$ 2 418 959	\$ 2 418 959	\$ 2 418 959	\$ 2 418 959
Baghouse bags				\$ 472 498								
Other Variable Costs	\$ 21 465 402	\$ 21 465 402	\$ 21 465 402	\$ 21 465 402	\$ 21 465 402	\$ 21 465 402	\$ 21 465 402	\$ 21 465 402	\$ 21 465 402	\$ 21 465 402	\$ 21 465 402	\$ 21 465 402
Fixed Operating Costs	\$ 32 913 049	\$ 32 913 049	\$ 32 913 049	\$ 32 913 049	\$ 32 913 049	\$ 32 913 049	\$ 32 913 049	\$ 32 913 049	\$ 32 913 049	\$ 32 913 049	\$ 32 913 049	\$ 32 913 049
Total Product Cost	\$ 104 154 118	\$ 104 154 118	\$ 105 749 955	\$ 104 154 118	\$ 104 154 118	\$ 104 154 118	\$ 104 154 118	\$ 105 749 955	\$ 104 154 118	\$ 104 154 118	\$ 104 154 118	\$ 104 154 118
Annual Depreciation												
General Plant Writedown												
Depreciation Charge												
Remaining Value												
Net Revenue	\$ 76 118 514	\$ 77 285 063	\$ 76 929 269	\$ 79 843 270	\$ 81 244 479	\$ 82 733 965	\$ 84 317 287	\$ 84 404 523	\$ 87 789 465	\$ 89 691 285	\$ 91 712 919	\$ 93 861 916
Losses Forward	\$ (184 212 239)	\$ (108 093 725)	\$ (30 808 662)	\$ 0	\$ 0	\$ 0	\$ 0	\$ 0	\$ 0	\$ 0	\$ 0	\$ 0
Taxable Income	\$ (108 093 725)	\$ (30 808 662)	\$ 46 120 607	\$ 79 843 270	\$ 81 244 479	\$ 82 733 965	\$ 84 317 287	\$ 84 404 523	\$ 87 789 465	\$ 89 691 285	\$ 91 712 919	\$ 93 861 916
Income Tax	\$ 0	\$ 0	\$ 12 913 770	\$ 22 356 116	\$ 22 748 454	\$ 23 165 510	\$ 23 608 840	\$ 23 633 266	\$ 24 581 050	\$ 25 113 560	\$ 25 679 817	\$ 26 281 136
Annual Cash Income	\$ 57 601 855	\$ 57 601 855	\$ 43 092 249	\$ 35 245 740	\$ 34 853 401	\$ 34 436 345	\$ 33 993 015	\$ 32 372 752	\$ 33 020 805	\$ 32 488 236	\$ 31 922 238	\$ 31 320 519
Discount Factor	0.45	0.41	0.38	0.34	0.31	0.29	0.26	0.24	0.22	0.20	0.18	0.17
Annual Present Value	\$ 25 873 490	\$ 23 671 995	\$ 16 202 326	\$ 12 124 524	\$ 10 969 405	\$ 9 915 960	\$ 8 955 447	\$ 7 802 918	\$ 7 281 903	\$ 6 554 869	\$ 5 892 645	\$ 5 289 635
Total Capital Investment + Interest	\$ 0	\$ 0	\$ 0	\$ 0	\$ 0	\$ 0	\$ 0	\$ 0	\$ 0	\$ 0	\$ 0	\$ (12 073 037)
Net Present Worth												

## GFT-J Process

Table 153: Discounted Cash Flow Sheet for Construction Period and Years 1-8 of the GFT-J Process

Year	-2	-1	0	1	2	3	4	5	6	7	8
Fixed Capital Investment											
Land	\$ 16 502 909	\$ 123 771 819	\$ 66 011 637								
Working Capital			\$ 5 157 1591								
Loan Payment				\$ 27 638 182	\$ 27 638 182	\$ 27 638 182	\$ 27 638 182	\$ 27 638 182	\$ 27 638 182	\$ 27 638 182	\$ 27 638 182
Loan Interest Payment	\$ 1 559 525	\$ 13 255 962	\$ 19 494 061	\$ 19 494 061	\$ 18 980 982	\$ 18 435 578	\$ 17 855 814	\$ 17 239 525	\$ 16 584 410	\$ 15 888 022	\$ 15 147 762
Loan Principal	\$ 24 755 364	\$ 210 412 092	\$ 309 429 547	\$ 301 285 427	\$ 292 628 227	\$ 283 425 624	\$ 273 643 256	\$ 263 244 600	\$ 252 190 828	\$ 240 440 668	\$ 227 950 249
Jet Fuel Sales				\$ 86 988 386	\$ 115 984 514	\$ 115 984 514	\$ 115 984 514	\$ 115 984 514	\$ 115 984 514	\$ 115 984 514	\$ 115 984 514
By-Product Credit (Other Fuels + Electricity)				\$ 22 537 322	\$ 30 049 763	\$ 30 049 763	\$ 30 049 763	\$ 30 049 763	\$ 30 049 763	\$ 30 049 763	\$ 30 049 763
Total Annual Sales				\$ 109 525 708	\$ 146 034 278	\$ 146 034 278	\$ 146 034 278	\$ 146 034 278	\$ 146 034 278	\$ 146 034 278	\$ 146 034 278
Annual Manufacturing Cost											
Feedstock				\$ 32 235 981	\$ 42 981 308	\$ 42 981 308	\$ 42 981 308	\$ 42 981 308	\$ 42 981 308	\$ 42 981 308	\$ 42 981 308
Catalyst cost				\$ 16 621 248	\$ 18 145	\$ 18 145	\$ 15 785 863	\$ 18 145	\$ 18 145	\$ 15 785 863	\$ 18 145
Baghouse bags				\$ 472 498							
Other Variable Costs				\$ 2 424 540	\$ 2 770 903	\$ 2 770 903	\$ 2 770 903	\$ 2 770 903	\$ 2 770 903	\$ 2 770 903	\$ 2 770 903
Fixed Operating Costs				\$ 25 383 330	\$ 25 383 330	\$ 25 383 330	\$ 25 383 330	\$ 25 383 330	\$ 25 383 330	\$ 25 383 330	\$ 25 383 330
Total Product Cost				\$ 77 137 598	\$ 71 316 993	\$ 71 316 993	\$ 66 921 404	\$ 71 316 993	\$ 71 789 491	\$ 66 921 404	\$ 71 316 993
Annual Depreciation											
General Plant Writedown											
Depreciation Charge				\$ 73 695 804	\$ 126 298 827	\$ 90 198 713	\$ 64 412 917	\$ 46 053 431	\$ 46 001 859	\$ 46 053 431	\$ 23 000 930
Remaining Value				\$ 442 020 108	\$ 315 712 882	\$ 225 522 568					

Table 154: Discounted Cash Flow Sheet for Years 9-20 of the GFT-J Process

Year	9	10	11	12	13	14	15	16	17	18	19	20
<b>Fixed Capital Investment</b>												
Land												\$ (1848 000)
Working Capital												\$ (51571591)
Loan Payment	\$ 27 638 182	\$ 27 638 182	\$ 27 638 182	\$ 27 638 182	\$ 27 638 182	\$ 27 638 182	\$ 27 638 182	\$ 27 638 182	\$ 27 638 182	\$ 27 638 182	\$ 27 638 182	\$ 27 638 182
Loan Interest Payment	\$ 14 360 866	\$ 13 524 395	\$ 12 635 226	\$ 11 690 040	\$ 10 685 307	\$ 9 617 276	\$ 8 481 959	\$ 7 275 117	\$ 5 992 244	\$ 4 628 550	\$ 3 178 943	\$ 1 638 011
Loan Principal	\$ 214 672 293	\$ 200 559 146	\$ 185 556 190	\$ 169 608 046	\$ 152 655 174	\$ 134 634 266	\$ 115 478 045	\$ 95 114 990	\$ 73 469 042	\$ 50 459 410	\$ 28 000 171	\$ 0
Jet Fuel Sales	\$ 115 984 514	\$ 115 984 514	\$ 115 984 514	\$ 115 984 514	\$ 115 984 514	\$ 115 984 514	\$ 115 984 514	\$ 115 984 514	\$ 115 984 514	\$ 115 984 514	\$ 115 984 514	\$ 115 984 514
By-Product Credit (Other fuels+ Electricity)	\$ 30 049 763	\$ 30 049 763	\$ 30 049 763	\$ 30 049 763	\$ 30 049 763	\$ 30 049 763	\$ 30 049 763	\$ 30 049 763	\$ 30 049 763	\$ 30 049 763	\$ 30 049 763	\$ 30 049 763
Total Annual Sales	\$ 146 034 278	\$ 146 034 278	\$ 146 034 278	\$ 146 034 278	\$ 146 034 278	\$ 146 034 278	\$ 146 034 278	\$ 146 034 278	\$ 146 034 278	\$ 146 034 278	\$ 146 034 278	\$ 146 034 278
<b>Annual Manufacturing Cost</b>												
Feedstock	\$ 42 981 308	\$ 42 981 308	\$ 42 981 308	\$ 42 981 308	\$ 42 981 308	\$ 42 981 308	\$ 42 981 308	\$ 42 981 308	\$ 42 981 308	\$ 42 981 308	\$ 42 981 308	\$ 42 981 308
Catalyst cost	\$ 18 145 1	\$ 15 785 863	\$ 18 145 1	\$ 18 145 1	\$ 15 785 863	\$ 18 145 1	\$ 18 145 1	\$ 15 785 863	\$ 18 145 1	\$ 15 785 863	\$ 18 145 1	\$ 18 145 1
Baghouse bags			\$ 472 498					\$ 472 498				
Other Variable Costs	\$ 2 770 903	\$ 2 770 903	\$ 2 770 903	\$ 2 770 903	\$ 2 770 903	\$ 2 770 903	\$ 2 770 903	\$ 2 770 903	\$ 2 770 903	\$ 2 770 903	\$ 2 770 903	\$ 2 770 903
Fixed Operating Costs	\$ 25 383 330	\$ 25 383 330	\$ 25 383 330	\$ 25 383 330	\$ 25 383 330	\$ 25 383 330	\$ 25 383 330	\$ 25 383 330	\$ 25 383 330	\$ 25 383 330	\$ 25 383 330	\$ 25 383 330
Total Product Cost	\$ 71 316 993	\$ 86 921 404	\$ 71 789 491	\$ 71 316 993	\$ 86 921 404	\$ 71 316 993	\$ 71 316 993	\$ 87 393 902	\$ 71 316 993	\$ 71 316 993	\$ 86 921 404	\$ 71 316 993
<b>Annual Depreciation</b>												
General Plant Writedown												
Depreciation Charge												
Remaining Value												
Net Revenue	\$ 60 356 419	\$ 45 598 478	\$ 61 609 560	\$ 63 027 245	\$ 48 427 566	\$ 65 100 009	\$ 66 235 326	\$ 51 365 258	\$ 68 725 041	\$ 70 088 735	\$ 55 933 930	\$ 73 079 274
Losses Forward	\$ (13 161 428)	\$ (7 125 786)	\$ (25 669 387)	\$ 0	\$ 0	\$ 0	\$ 0	\$ 0	\$ 0	\$ 0	\$ 0	\$ 0
Taxable Income	\$ (7 125 786)	\$ (25 669 387)	\$ 35 940 173	\$ 63 027 245	\$ 48 427 566	\$ 65 100 009	\$ 66 235 326	\$ 51 365 258	\$ 68 725 041	\$ 70 088 735	\$ 55 933 930	\$ 73 079 274
Income Tax	\$ 0	\$ 0	\$ 10 063 249	\$ 17 647 629	\$ 13 559 719	\$ 18 228 002	\$ 18 545 891	\$ 14 382 272	\$ 19 243 012	\$ 19 624 846	\$ 15 661 501	\$ 20 462 197
Annual Cash Income	\$ 47 079 103	\$ 31 474 691	\$ 36 543 356	\$ 29 431 475	\$ 17 914 973	\$ 28 851 101	\$ 28 533 212	\$ 16 619 921	\$ 27 836 092	\$ 27 454 257	\$ 15 813 191	\$ 26 616 906
Discount Factor	0.45	0.41	0.38	0.34	0.31	0.29	0.26	0.24	0.22	0.20	0.18	0.17
Annual Present Value	\$ 21 146 901	\$ 12 934 804	\$ 13 739 997	\$ 10 124 418	\$ 5 638 376	\$ 8 307 687	\$ 7 517 064	\$ 4 005 958	\$ 6 138 546	\$ 5 539 197	\$ 2 919 016	\$ 4 495 255
Total Capital Investment + Interest	\$ 0	\$ 0	\$ 0	\$ 0	\$ 0	\$ 0	\$ 0	\$ 0	\$ 0	\$ 0	\$ 0	\$ (8 745 247)
<b>Net Present Worth</b>												

## Appendix I. Indices

Table 155: Chemical Engineering Plant Cost Indices, [98].

Year	Index	Year	Index
1990	357.6	2002	395.6
1991	361.3	2003	402.0
1992	358.2	2004	444.2
1993	359.2	2005	468.2
1994	368.1	2006	499.6
1995	381.1	<b>2007</b>	<b>525.4</b>
1996	381.7	2008	575.4
1997	386.5	2009	521.9
1998	389.5	2010	550.8
1999	390.6	2011	585.7
2000	394.1	2012	584.6
2001	394.3	2013	567.6

Table 156: Inorganic Chemical Indices, [98].

Year	Index	Year	Index	Year	Index
1980	89.0	1991	125.6	2002	157.3
1981	98.4	1992	125.9	2003	164.6
1982	100.0	1993	128.2	2004	172.8
1983	100.3	1994	132.1	2005	187.3
1984	102.9	1995	139.5	2006	196.8
1985	103.7	1996	142.1	<b>2007</b>	<b>203.3</b>
1986	102.6	1997	147.1	2008	228.2
1987	106.4	1998	148.7	2009	224.8
1988	116.3	1999	149.7	2010	233.7
1989	123.0	2000	156.7	2011	249.3
1990	123.6	2001	158.4		

Table 157: Labour Indices, [98].

Year	Index	Year	Index
1990	12.85	2001	17.57
1991	13.30	2002	17.97
1992	13.70	2003	18.50
1993	13.97	2004	19.17
1994	14.33	2005	19.67
1995	14.86	2006	19.60
1996	15.37	<b>2007</b>	<b>19.55</b>
1997	15.78	2008	19.50
1998	16.23	2009	20.30
1999	16.40	2010	21.07
2000	17.09	2011	21.46

## **Appendix J. Aspen Plus Simulation Flow Sheets**

Appendix J contains the flow sheets of Aspen Plus<sup>®</sup> simulations for the sections which consisted of significant new work (where the writer performed 50%+ of the simulation). Stream tables accompany the Aspen Plus<sup>®</sup> flow sheets. The flow sheets and stream tables are named using a description with the associated Aspen simulation block included in brackets.

Although significant heat integration was performed on the processes, most of the heat and work streams were removed from the Aspen Plus<sup>®</sup> simulation flow sheets to ensure clarity of the figures (the duties of the work and heat streams are also not given).

**HEFA Process**

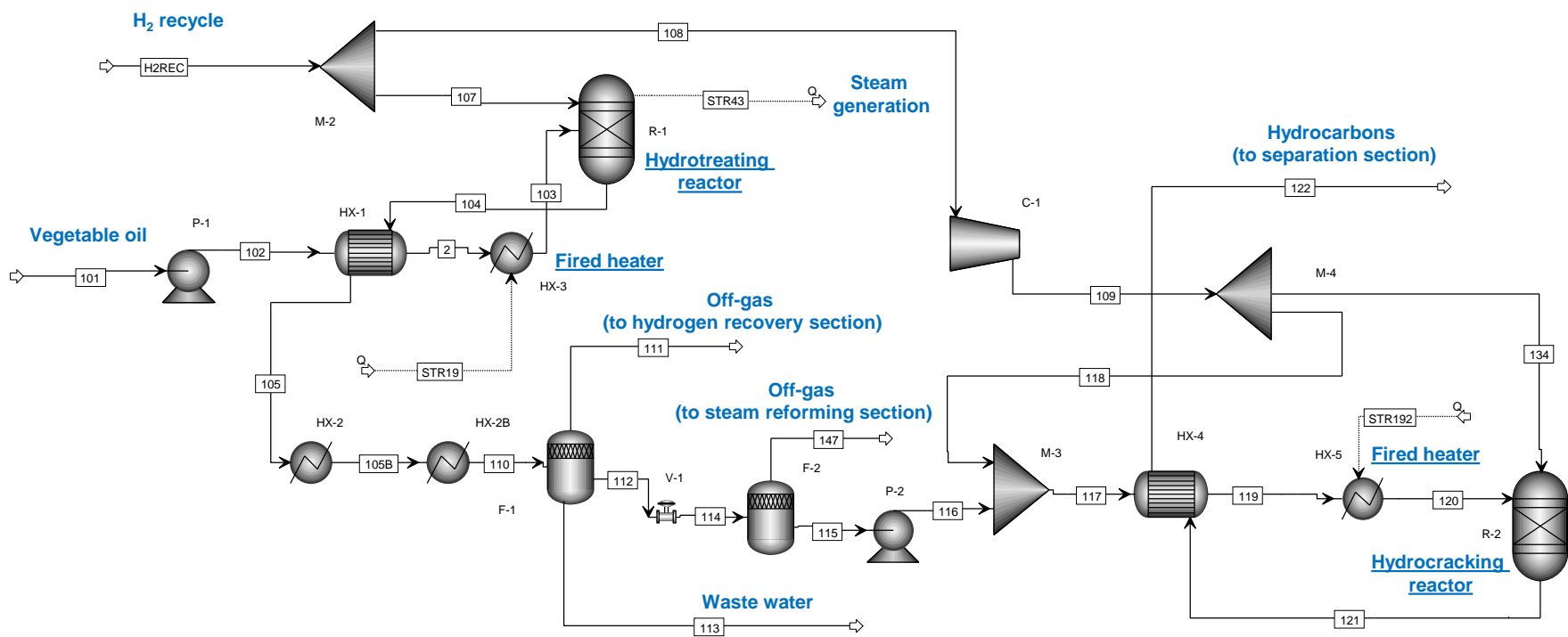


Figure 55: Hydrotreating and hydrocracking section (MAIN section)

Table 158: Stream table for hydrotreating and hydrocracking section (MAIN section)

Stream	101	104	105	107	109	110	111	113	114	115	117	121	122
Total Mass Flow (kg/hr)	14873.134	15642.74	15642.74	769.603	1185.803	15642.735	1430.895	1098.438	13113.408	12605.861	13700.879	13791.663	13791.663
Temperature (C)	25	350	152.6	59	146.2	35	42.5	42.5	35.1	30.8	75.9	278	130.9
Pressure (bar)	1.013	30	30	30	55.158	30	30	30	2	2	55.158	55.158	55.158
Vapour fraction	0	0.894	0.809	1	1	0.534	1	0	0.194	0	0.894	1	0.86
Enthalpy (Gcal/hr)	-7.672	-8.092	-10.548	0.093	0.505	-12.261	-1.561	-4.143	-6.557	-6.023	-5.514	-2.942	-5.307
Mass Flow (kg/hr)													
HYDROGEN	0	275.817	275.817	769.603	1185.803	275.817	262.496	0	13.321	0.062	1095.08	1082.156	1082.156
WATER	0	1108.417	1108.417	0	0	1108.417	9.389	1098.438	0.589	0.441	0.441	0.333	0.333
CAR-DIOX	0	732.041	732.041	0	0	732.041	535.525	0	196.517	24.074	24.074	23.64	23.64
CO	0	299.357	299.357	0	0	299.357	281.209	0	18.148	0.243	0.243	0.963	0.963
C2H4	0	79.087	79.087	0	0	79.087	53.887	0	25.201	2.919	2.919	0	0
C3H8	0	748.53	748.53	0	0	748.53	286.66	0	461.871	182.545	182.545	0	0
C4H10-01	0	1.276	1.276	0	0	1.276	0.233	0	1.044	0.72	0.72	301.62	301.62
C5H12-01	0	6.334	6.334	0	0	6.334	0.488	0	5.846	5.139	5.139	771.23	771.23
C6H14-01	0	13.866	13.866	0	0	13.866	0.427	0	13.439	12.879	12.879	1126.301	1126.301
C7H16-01	0	27.632	27.632	0	0	27.632	0.331	0	27.301	26.924	26.924	1491.554	1491.554
C8H18-01	0	30.063	30.063	0	0	30.063	0.138	0	29.925	29.793	29.793	1790.628	1790.628
C9H20-01	0	38.749	38.749	0	0	38.749	0.068	0	38.681	38.624	38.624	1827.535	1827.535
C10H2-01	0	34.94	34.94	0	0	34.94	0.023	0	34.917	34.9	34.9	1877.169	1877.169
C11H2-01	0	24.922	24.922	0	0	24.922	0.006	0	24.916	24.912	24.912	1417.74	1417.74
C12H2-01	0	17.425	17.425	0	0	17.425	0.002	0	17.424	17.423	17.423	1014.308	1014.308
C13H2-01	0	16.165	16.165	0	0	16.165	0.001	0	16.164	16.164	16.164	590.513	590.513
C14H3-01	0	16.151	16.151	0	0	16.151	0	0	16.151	16.151	16.151	272.349	272.349
C15H3-01	0	952.233	952.233	0	0	952.233	0.004	0	952.23	952.227	952.227	75.087	75.087
C16H3-01	0	921.848	921.848	0	0	921.848	0.002	0	921.847	921.846	921.846	38.18	38.18
C17H3-01	0	5022.045	5022.045	0	0	5022.045	0.005	0	5022.04	5022.039	5022.039	54.724	54.724
C18H3-01	0	4977.387	4977.387	0	0	4977.387	0.001	0	4977.386	4977.386	4977.386	24.18	24.18
C19H4-01	0	144.859	144.859	0	0	144.859	0	0	144.859	144.859	144.859	2.545	2.545
C20H4-01	0	90.059	90.059	0	0	90.059	0	0	90.059	90.059	90.059	2.545	2.545
C21H4-01	0	30.009	30.009	0	0	30.009	0	0	30.009	30.009	30.009	2.545	2.545
C22H4-01	0	17.646	17.646	0	0	17.646	0	0	17.646	17.646	17.646	2.545	2.545
C23H4-01	0	15.877	15.877	0	0	15.877	0	0	15.877	15.877	15.877	1.273	1.273
C57H1OLE	14873.134	0	0	0	0	0	0	0	0	0	0	0	0

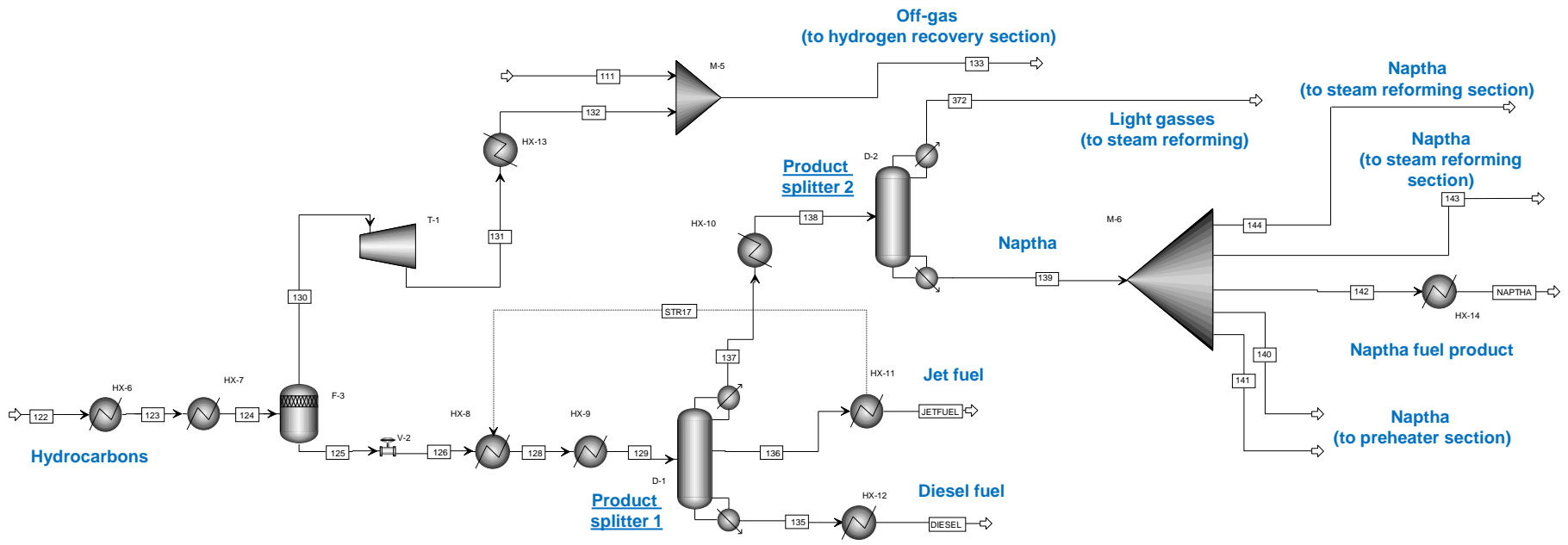


Figure 56: Separation section (MAIN section)

Table 159: Stream table for separation section (MAIN section)

Stream	111	122	129	130	133	137	138	139	143	144	372	DIESEL	JETFUEL	NAPTHA
Total Mass Flow (kg/hr)	1430.895	13791.663	12553.68	1237.985	2668.878	5109.767	5109.767	3867.013	1124.718	999.687	1242.752	304.812	7139.106	1704.918
Temperature (C)	42.5	130.9	150	23.6	36.2	95.1	70	86.6	86.6	86.6	47.2	35	40	35
Pressure (bar)	30	55.158	1.013	55	30	1.013	1.013	1.013	1.013	1.013	1.013	1.013	1.013	1.013
Vapour fraction	1	0.86	0.75	1	1	1	0.371	0	0	0	1	0	0	0
Enthalpy (Gcal/hr)	-1.561	-5.307	-4.996	-0.111	-1.632	-2.183	-2.531	-1.932	-0.562	-0.5	-0.592	-0.146	-3.535	-0.903
Mass Flow (kg/hr)														
HYDROGEN	262.496	1082.156	7.221	1074.935	1337.431	7.221	7.221	0	0	0	7.221	0	0	0
WATER	9.389	0.333	0.293	0.041	9.43	0.293	0.293	0	0	0	0.293	0	0	0
CAR-DIOX	535.525	23.64	3.905	19.736	555.26	3.905	3.905	0	0	0	3.905	0	0	0
CO	281.209	0.963	0.019	0.943	282.153	0.019	0.019	0	0	0	0.019	0	0	0
C2H4	53.887	0	0	0	53.887	0	0	0	0	0	0	0	0	0
C3H8	286.66	0	0	0	286.66	0	0	0	0	0	0	0	0	0
C4H10-01	0.233	301.62	243.641	57.978	58.211	243.641	243.641	4.876	1.418	1.261	238.765	0	0.001	2.15
C5H12-01	0.488	771.23	723.412	47.819	48.306	723.384	723.384	200.993	58.459	51.96	522.39	0	0.028	88.615
C6H14-01	0.427	1126.301	1104.125	22.177	22.603	1103.595	1103.595	717.357	208.643	185.449	386.237	0	0.53	316.274
C7H16-01	0.331	1491.554	1482.147	9.407	9.738	1473.344	1473.344	1391.081	404.595	359.617	82.263	0	8.802	613.31
C8H18-01	0.138	1790.628	1787.28	3.348	3.486	1554.223	1554.223	1552.564	451.562	401.363	1.659	0.001	233.057	684.506
C9H20-01	0.068	1827.535	1826.434	1.101	1.169	0.142	0.142	0.142	0.041	0.037	0	0.04	1826.251	0.063
C10H2-01	0.023	1877.169	1876.802	0.367	0.39	0	0	0	0	0	0	0.373	1876.429	0
C11H2-01	0.006	1417.74	1417.636	0.104	0.11	0	0	0	0	0	0	2.185	1415.451	0
C12H2-01	0.002	1014.308	1014.284	0.024	0.026	0	0	0	0	0	0	13.436	1000.848	0
C13H2-01	0.001	590.513	590.509	0.004	0.005	0	0	0	0	0	0	59.778	530.732	0
C14H3-01	0	272.349	272.348	0.001	0.001	0	0	0	0	0	0	102.944	169.405	0
C15H3-01	0.004	75.087	75.087	0	0.004	0	0	0	0	0	0	43.471	31.616	0
C16H3-01	0.002	38.18	38.18	0	0.002	0	0	0	0	0	0	24.071	14.11	0
C17H3-01	0.005	54.724	54.724	0	0.005	0	0	0	0	0	0	35.288	19.437	0
C18H3-01	0.001	24.18	24.18	0	0.001	0	0	0	0	0	0	15.72	8.461	0
C19H4-01	0	2.545	2.545	0	0	0	0	0	0	0	0	1.662	0.883	0
C20H4-01	0	2.545	2.545	0	0	0	0	0	0	0	0	1.667	0.878	0
C21H4-01	0	2.545	2.545	0	0	0	0	0	0	0	0	1.669	0.876	0
C22H4-01	0	2.545	2.545	0	0	0	0	0	0	0	0	1.671	0.874	0
C23H4-01	0	1.273	1.273	0	0	0	0	0	0	0	0	0.836	0.437	0

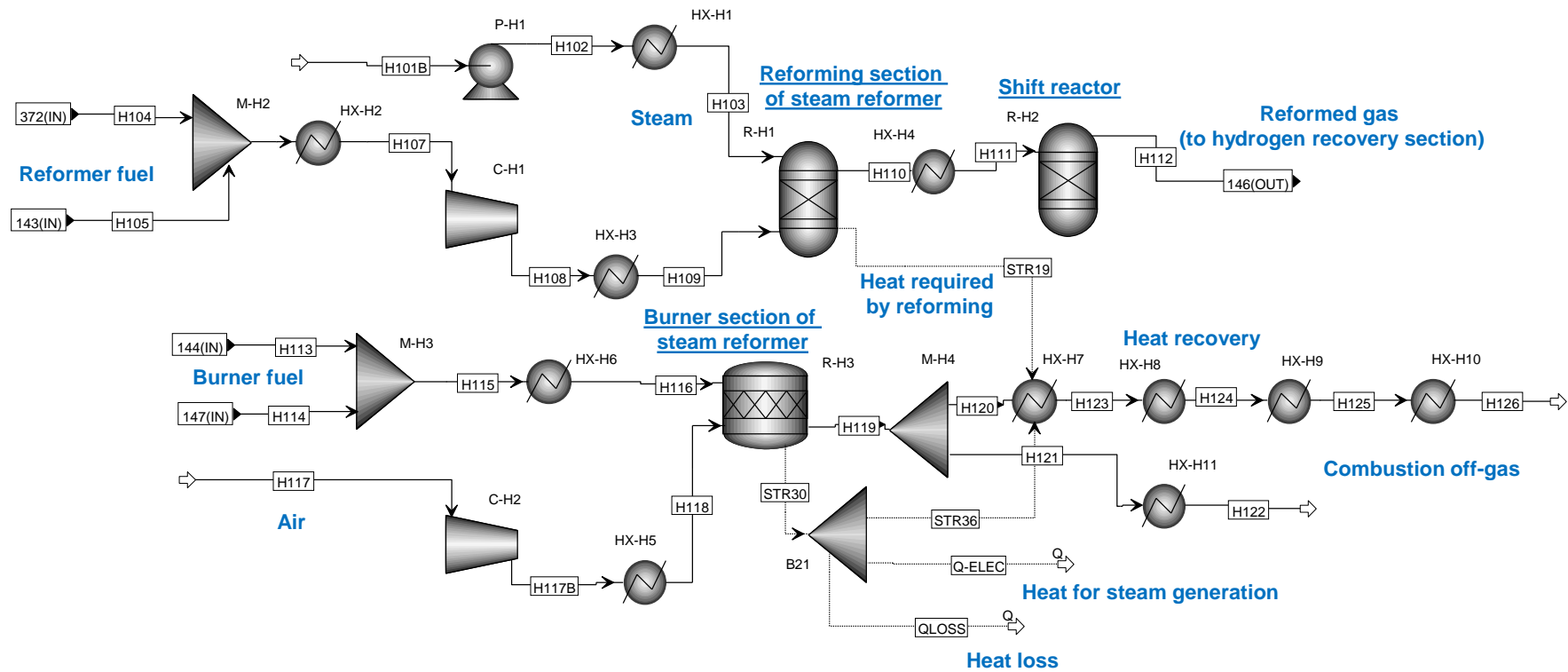


Figure 57: Hydrogen plant A; steam reforming (H2-PROD section)

Table 160: Stream table for hydrogen plant A; steam reforming (H2-PROD section)

Stream	H2-PROD.H101B	H2-PROD.H104	H2-PROD.H105	H2-PROD.H109	H2-PROD.H110	H2-PROD.H112	H2-PROD.H113	H2-PROD.H114	H2-PROD.H116	H2-PROD.H117	H2-PROD.H119	H2-PROD.H122	H2-PROD.H126
Total Mass Flow (kg/hr)	6912.883	1242.752	1124.718	2367.47	9280.353	9280.353	999.687	507.548	1507.234	24650.512	26157.746	3359.377	22798.368
Temperature (C)	25	47.2	86.6	565.6	850	353.1	86.6	30.8	250	25	900	160	159.6
Pressure (bar)	1	1.013	1.013	27.903	25.834	24.766	1.013	2	1.013	1.02	1.013	1.013	1.013
Vapour fraction	0	1	0	1	1	1	0	1	1	1	1	1	1
Enthalpy (Gcal/hr)	-26.194	-0.592	-0.562	-0.277	-14.482	-18.033	-0.5	-0.534	-0.813	-0.001	-9.013	-1.873	-12.714
Mass Flow (kg/hr)													
HYDROGEN	0	7.221	0	7.221	622.248	754.995	0	13.259	13.259	0	0	0	0
WATER	6912.883	0.293	0	0.293	3672.147	2485.828	0	0.148	0.148	0	2045.095	262.647	1782.448
CAR-DIOX	0	3.905	0	3.905	2173.155	5071.232	0	172.443	172.443	0	4186.821	537.703	3649.117
CO	0	0.019	0	0.019	2277.939	433.434	0	17.905	17.905	0	0	0	0
METHA-01	0	0	0	0	534.864	534.864	0	0	0	0	0	0	0
C2H4	0	0	0	0	0	0	0	22.282	22.282	0	0	0	0
C3H8	0	0	0	0	0	0	0	279.326	279.326	0	0	0	0
C4H10-01	0	238.765	1.418	240.183	0	0	1.261	0.324	1.584	0	0	0	0
C5H12-01	0	522.39	58.459	580.849	0	0	51.96	0.708	52.668	0	0	0	0
C6H14-01	0	386.237	208.643	594.88	0	0	185.449	0.56	186.009	0	0	0	0
C7H16-01	0	82.263	404.595	486.858	0	0	359.617	0.377	359.994	0	0	0	0
C8H18-01	0	1.659	451.562	453.221	0	0	401.363	0.132	401.495	0	0	0	0
C9H20-01	0	0	0.041	0.041	0	0	0.037	0.057	0.094	0	0	0	0
C10H2-01	0	0	0	0	0	0	0	0.017	0.017	0	0	0	0
C11H2-01	0	0	0	0	0	0	0	0.005	0.005	0	0	0	0
C12H2-01	0	0	0	0	0	0	0	0.001	0.001	0	0	0	0
C15H3-01	0	0	0	0	0	0	0	0.002	0.002	0	0	0	0
C16H3-01	0	0	0	0	0	0	0	0.001	0.001	0	0	0	0
C17H3-01	0	0	0	0	0	0	0	0.001	0.001	0	0	0	0
OXYGE-01	0	0	0	0	0	0	0	0	0	5669.618	944.936	121.356	823.58
NITRO-01	0	0	0	0	0	0	0	0	0	18980.894	18980.894	2437.671	16543.223



Table 162: Stream table for steam & power plant (ELEC section)

Stream	ELEC.E101	ELEC.E103	ELEC.E104	ELEC.E105	ELEC.E106	ELEC.E107	ELEC.E108	ELEC.E109	ELEC.E111	ELEC.E112
Total Mass Flow (kg/hr)	8056.301	8056.301	8056.301	8056.301	7906.229	7906.229	150.072	150.072	7906.229	7906.229
Temperature (C)	90	580	393.4	195.9	195.9	62.7	195.9	125	60.1	99.6
Pressure (bar)	1	86	24	4	4	0.2	4	4	1	1
Vapour fraction	0	1	1	1	1	0.927	1	0	0	0.017
Enthalpy (Gcal/hr)	-29.996	-23.828	-24.506	-25.222	-24.753	-25.554	-0.47	-0.553	-29.681	-29.286
Mass Flow (kg/hr)										
WATER	8056.301	8056.301	8056.301	8056.301	7906.229	7906.229	150.072	150.072	7906.229	7906.229

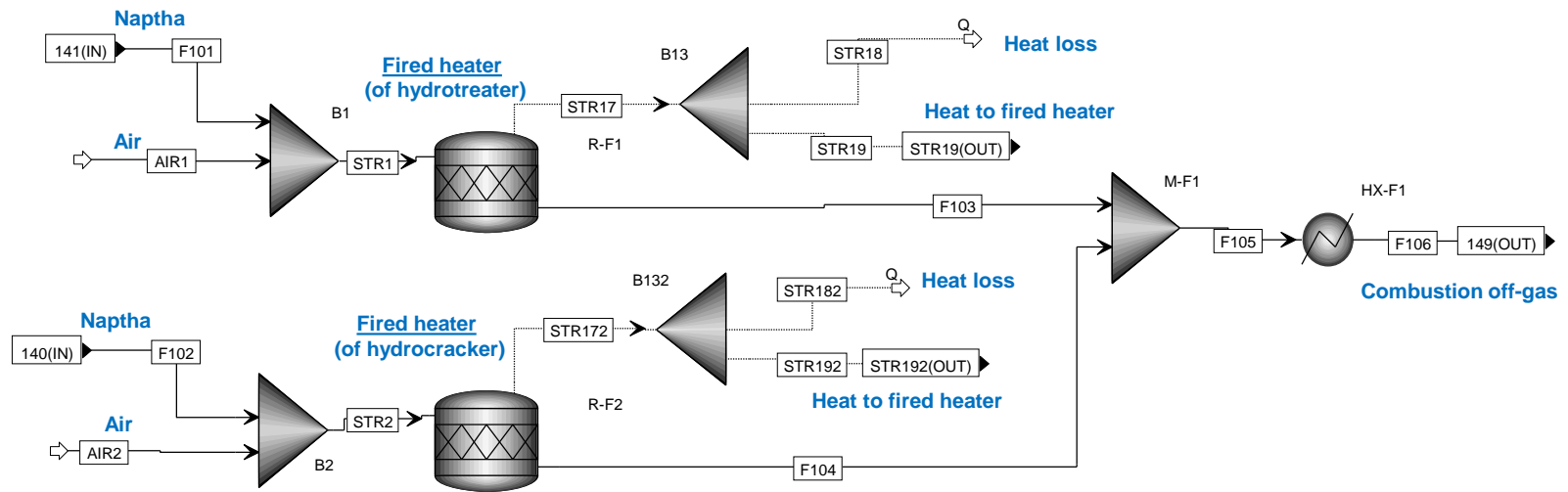


Figure 60: Utility section A; fired heater (PREHEAT section)

Table 163: Stream table for utility section A; fired heater (PREHEAT section)

Stream	PREHEAT.AIR1	PREHEAT.AIR2	PREHEAT.F101	PREHEAT.F102	PREHEAT.F103	PREHEAT.F104	PREHEAT.F105	PREHEAT.F106
Total Mass Flow (kg/hr)	248.927	470.671	13.038	24.652	261.966	495.325	757.291	757.291
Temperature (C)	25	25	86.6	86.6	705	711	708.9	110
Pressure (bar)	1	1	1.013	1.013	1	1	1	1
Vapour fraction	1	1	0	0	1	1	1	1
Enthalpy (Gcal/hr)	0	0	-0.007	-0.012	-0.097	-0.182	-0.279	-0.405
Mass Flow (kg/hr)								
WATER	0	0	0	0	18.757	35.466	54.223	54.223
CAR-DIOX	0	0	0	0	40.084	75.791	115.875	115.875
C4H10-01	0	0	0.016	0.031	0	0	0	0
C5H12-01	0	0	0.678	1.281	0	0	0	0
C6H14-01	0	0	2.419	4.573	0	0	0	0
C7H16-01	0	0	4.69	8.868	0	0	0	0
C8H18-01	0	0	5.235	9.898	0	0	0	0
C9H20-01	0	0	0	0.001	0	0	0	0
OXYGE-01	57.253	108.254	0	0	11.451	21.651	33.102	33.102
NITRO-01	191.674	362.417	0	0	191.674	362.417	554.091	554.091

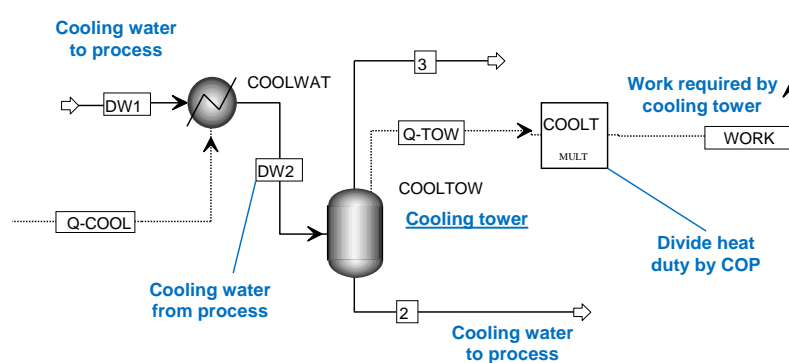


Figure 61: Utility section B; cooling tower (COOLT section)

Table 164: Stream table for utility section B; cooling tower (COOLT section)

Stream	COOLT.2	COOLT.3	COOLT.DW1	COOLT.DW2
Total Mass Flow (kg/hr)	1068110	12863.629	1080980	1080980
Temperature (C)	25	25	25	35
Pressure (bar)	0.032	0.032	1.013	1.013
Vapour fraction	0	1	0	0
Enthalpy (Gcal/hr)	-4047.255	-41.241	-4095.975	-4085.316
Mass Flow (kg/hr)				
WATER	1068110	12863.629	1080980	1080980

### SYN-FER-J Process

The Aspen Plus® simulation flow sheet will only be given for the SYN-FER-J process, scenario A.1. Similar simulations were developed for scenario A.2 and B.

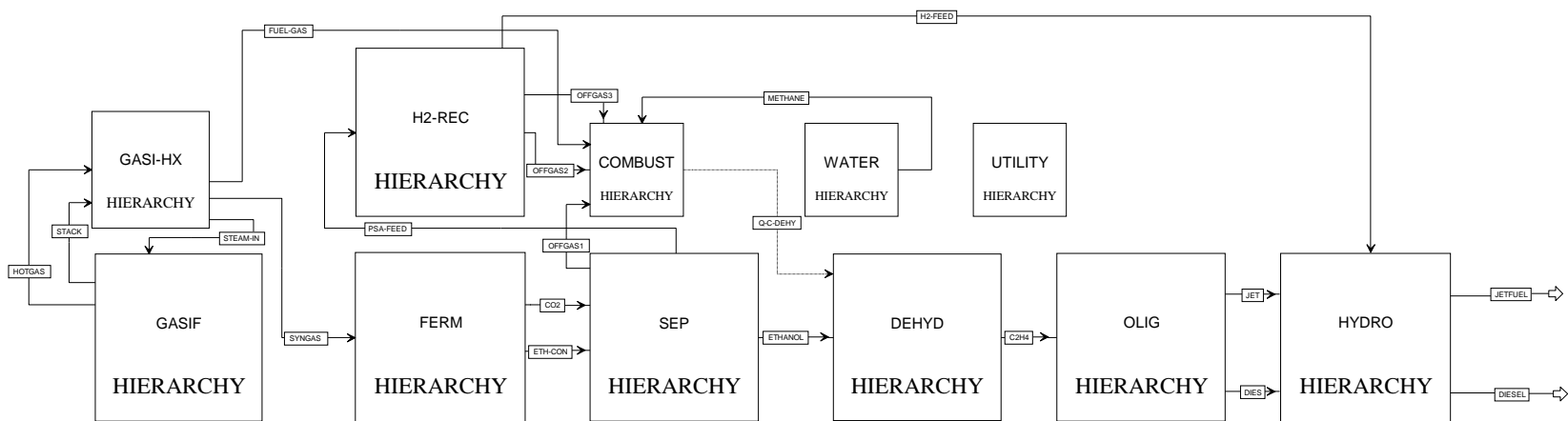


Figure 62: SYN-FER-J process overview

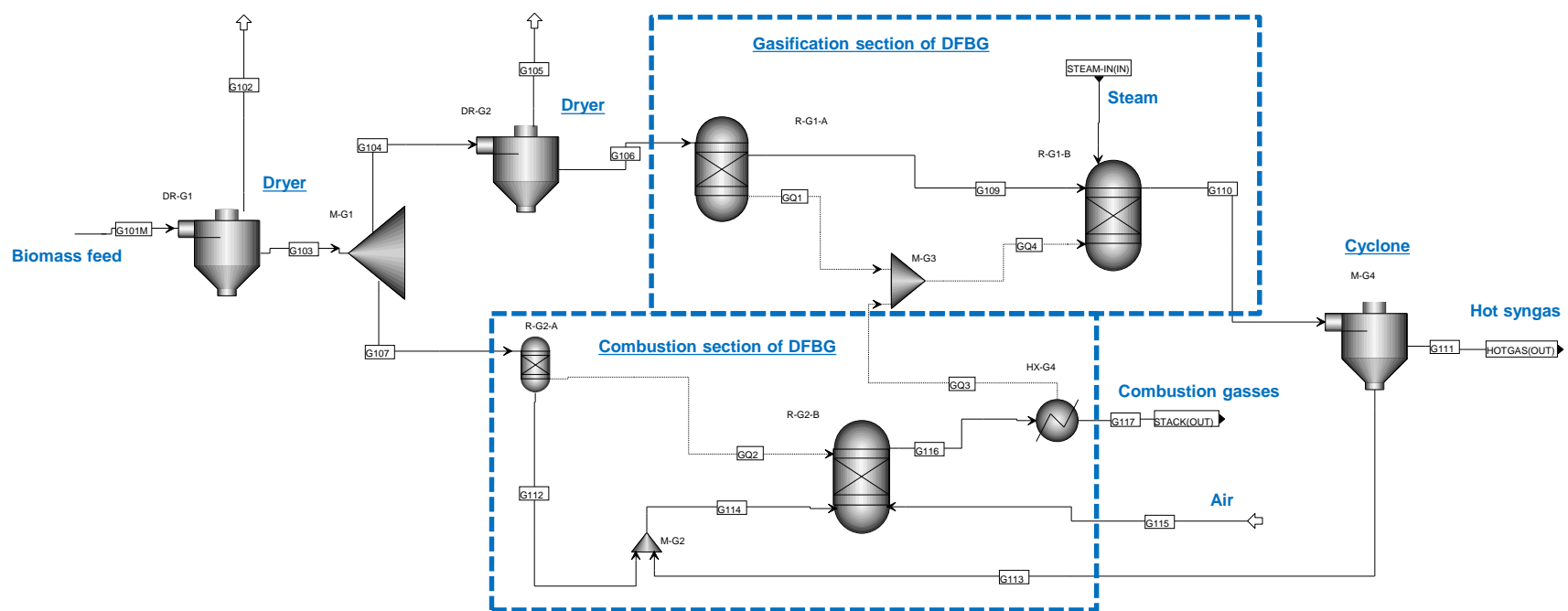


Figure 63: Gasification plant A; gasification (GASIF section)

Table 165: Stream table for gasification plant A; gasification (GASIF section)

Stream	GASIF.G101M	GASIF.G102	GASIF.G103	GASIF.G104	GASIF.G105	GASIF.G106	GASIF.G107	GASIF.G110	GASIF.G111	GASIF.G113	GASIF.G115	GASIF.G116	GASIF.G117
Total Mass Flow (kg/hr)	155763.24	69228.11	86535.13	51055.73	264.678	50791.05	35479.4	59981.083	58280.93	1700.156	259749.6	296929.113	296929.113
Temperature (C)	70.95	70.95	70.95	70.95	70.95	70.95	70.95	919.85	919.85	919.85	249.95	1648.45	959.25
Pressure (atm)	1	1	1	1	1	1	1	2	2	2	2	2	2
Vapour fraction	0	0	0	0	0	0	0	1	1	0	1	1	1
Enthalpy (Gcal/hr)	-393.586	-259.146	-134.44	-79.32	-0.991	-78.329	-55.121	-39.392	-35.13	-4.262	14.279	-45.104	-111.096
Mass Flow (kg/hr)													
H2O	77881.62	69228.11	8653.513	5105.573	264.678	4840.895	3547.94	2326.071	2326.071	0	0	19874.15	19874.15
O2	0	0	0	0	0	0	0	0	0	0	60524.24	18950.188	18950.188
N2	0	0	0	0	0	0	0	0	0	0	199225.3	198765.89	198765.89
NO2	0	0	0	0	0	0	0	0	0	0	0	2.088	2.088
NO	0	0	0	0	0	0	0	0	0	0	0	982.836	982.836
CO2	0	0	0	0	0	0	0	3765.906	3765.906	0	0	55403.545	55403.545
CO	0	0	0	0	0	0	0	48102.579	48102.58	0	0	67.794	67.794
H2	0	0	0	0	0	0	0	3891.023	3891.023	0	0	1.002	1.002
C	0	0	0	0	0	0	0	0	0	0	0	0	0
ASHO	0	0	0	0	0	0	0	1700.156	0	1700.156	0	2881.62	2881.62
CH4	0	0	0	0	0	0	0	195.336	195.336	0	0	0	0
C2H4	0	0	0	0	0	0	0	0.01	0.01	0	0	0	0
C2H6	0	0	0	0	0	0	0	0.002	0.002	0	0	0	0
BIOMASS	77881.62	0	77881.62	45950.16	0	45950.16	31931.46	0	0	0	0	0	0

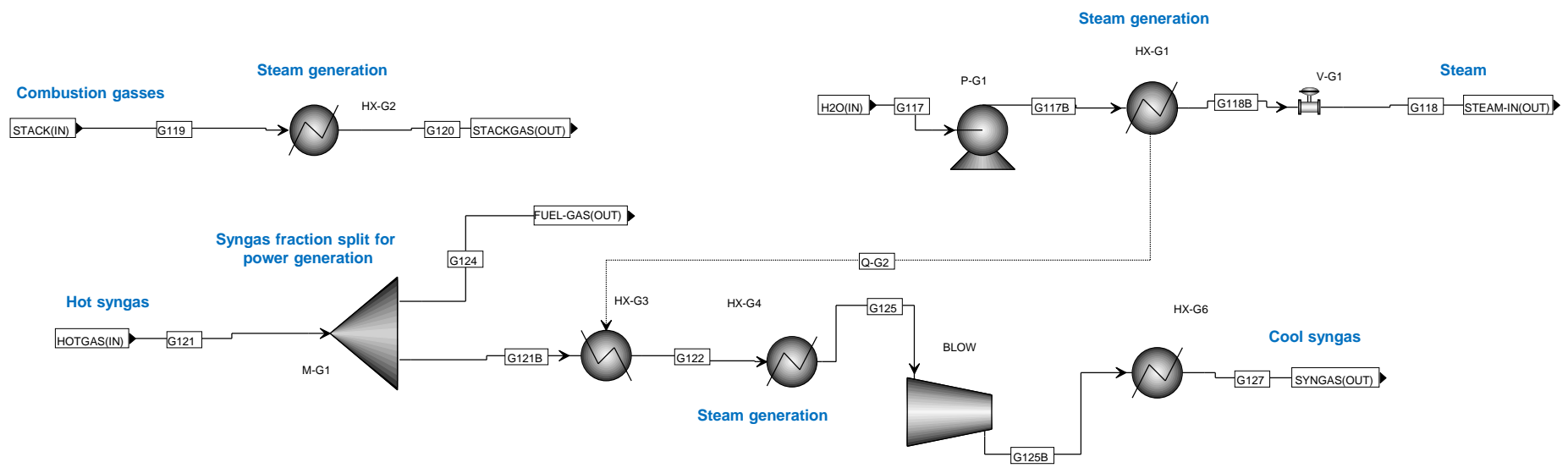


Figure 64: Gasification plant B; heat recovery (GASI-HX section)

Table 166: Stream table for gasification plant B; heat recovery (GASI-HX section)

Stream	GASI-HX.G117	GASI-HX.G117B	GASI-HX.G118	GASI-HX.G118B	GASI-HX.G119	GASI-HX.G120	GASI-HX.G121	GASI-HX.G121B	GASI-HX.G122	GASI-HX.G124	GASI-HX.G125	GASI-HX.G125B	GASI-HX.G127
Total Mass Flow (kg/hr)	9190.031	9190.031	9190.031	9190.031	296929.1	296929.1	58280.93	37882.6	37882.6	20398.33	37882.6	37882.6	37882.6
Temperature (C)	24.85	30.35	571.85	571.85	959.25	231.95	919.85	919.85	525.95	919.85	99.95	142.25	37.95
Pressure (atm)	1	87	2	87	2	1	2	2	2	2	1.5	2	2
Vapour fraction	0	0	1	1	1	1	1	1	1	1	1	1	0.999
Enthalpy (Gcal/hr)	-34.809	-34.762	-27.056	-27.056	-111.096	-173.396	-35.13	-22.834	-30.541	-12.295	-38.355	-37.599	-39.469
Mass Flow (kg/hr)													
H2O	9190.031	9190.031	9190.031	9190.031	19874.15	19874.15	2326.071	1511.946	1511.946	814.125	1511.946	1511.946	1511.946
O2	0	0	0	0	18950.19	18950.19	0	0	0	0	0	0	0
N2	0	0	0	0	198765.9	198765.9	0	0	0	0	0	0	0
NO2	0	0	0	0	2.088	2.088	0	0	0	0	0	0	0
NO	0	0	0	0	982.836	982.836	0	0	0	0	0	0	0
CO2	0	0	0	0	55403.55	55403.55	3765.906	2447.839	2447.839	1318.067	2447.839	2447.839	2447.839
CO	0	0	0	0	67.794	67.794	48102.58	31266.68	31266.68	16835.9	31266.68	31266.68	31266.68
H2	0	0	0	0	1.002	1.002	3891.023	2529.165	2529.165	1361.858	2529.165	2529.165	2529.165
ASHO	0	0	0	0	2881.62	2881.62	0	0	0	0	0	0	0
CH4	0	0	0	0	0	0	195.336	126.968	126.968	68.368	126.968	126.968	126.968
C2H4	0	0	0	0	0	0	0.01	0.006	0.006	0.003	0.006	0.006	0.006
C2H6	0	0	0	0	0	0	0.002	0.001	0.001	0.001	0.001	0.001	0.001

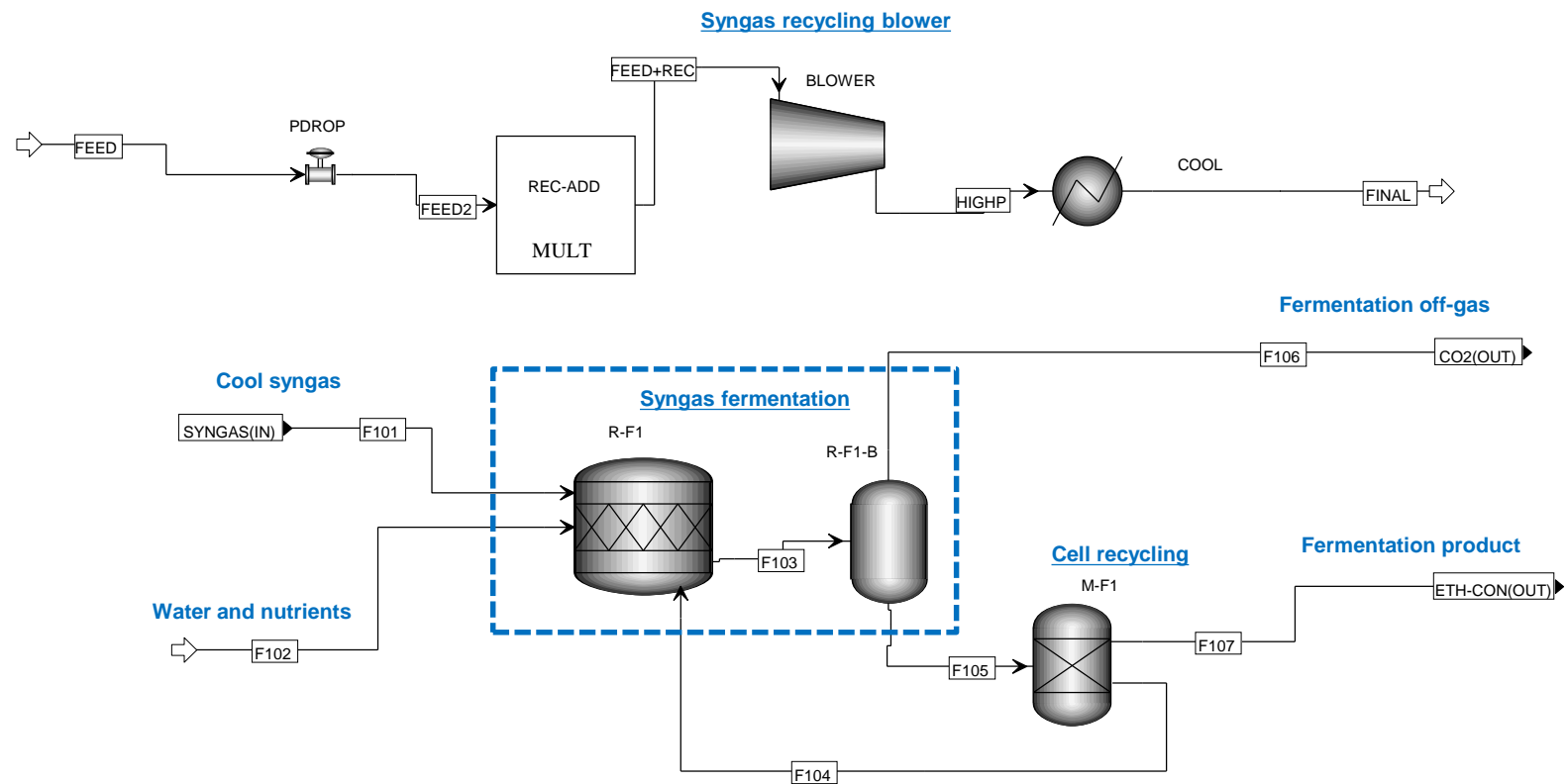


Figure 65: Fermentation section (FERM section)

Table 167: Stream table for fermentation section (FERM section)

Stream	FERM.F101	FERM.F102	FERM.F103	FERM.F104	FERM.F105	FERM.F106	FERM.F107	FERM.FEED+REC	FERM.FEED2	FERM.FINAL	FERM.HIGHP
Total Mass Flow (kg/hr)	37882.6	651016.4	690177.1	1278.428	670779.1	19397.96	669500.7	80500.53	37882.6	80500.53	80500.53
Temperature (C)	37.95	37.95	37.95	37.95	37.95	37.95	37.95	37.65	37.65	37.95	130.65
Pressure (atm)	2	1	1	1	1	1	1	1	1	2	2
Vapour fraction	0.999	0	0.019	0	0	1	0	1	1	1	1
Enthalpy (Gcal/hr)	-39.469	-2458.071	-2527.914	-1.612	-2488.419	-39.495	-2486.806	-83.858	-39.463	-83.858	-80.345
Mass Flow (kg/hr)											
H2O	1511.946	650838.5	652259.6	0	651417.2	842.353	651417.2	3212.886	1511.946	3212.886	3212.886
CO2	2447.839	0	16931.66	0	399.045	16532.61	399.045	5201.657	2447.839	5201.657	5201.657
CO	31266.68	0	1136.374	0	0.875	1135.499	0.875	66441.69	31266.68	66441.69	66441.69
H2	2529.165	0	475.264	0	0.337	474.927	0.337	5374.475	2529.165	5374.475	5374.475
CH4	126.968	0	126.968	0	0.145	126.823	0.145	269.808	126.968	269.808	269.808
C2H4	0.006	0	0.006	0	0.004	0.002	0.004	0.014	0.006	0.014	0.014
C2H6	0.001	0	0.001	0	0.001	0	0.001	0.002	0.001	0.002	0.002
ACETI-01	0	0	2956.323	0	2953.971	2.352	2953.971	0	0	0	0
ETHANOL	0	0	13733.04	0	13449.68	283.365	13449.68	0	0	0	0
CLOSTRID	0	0	2556.855	1278.428	2556.855	0	1278.428	0	0	0	0
AMMON-01	0	177.867	1	0	0.972	0.028	0.972	0	0	0	0

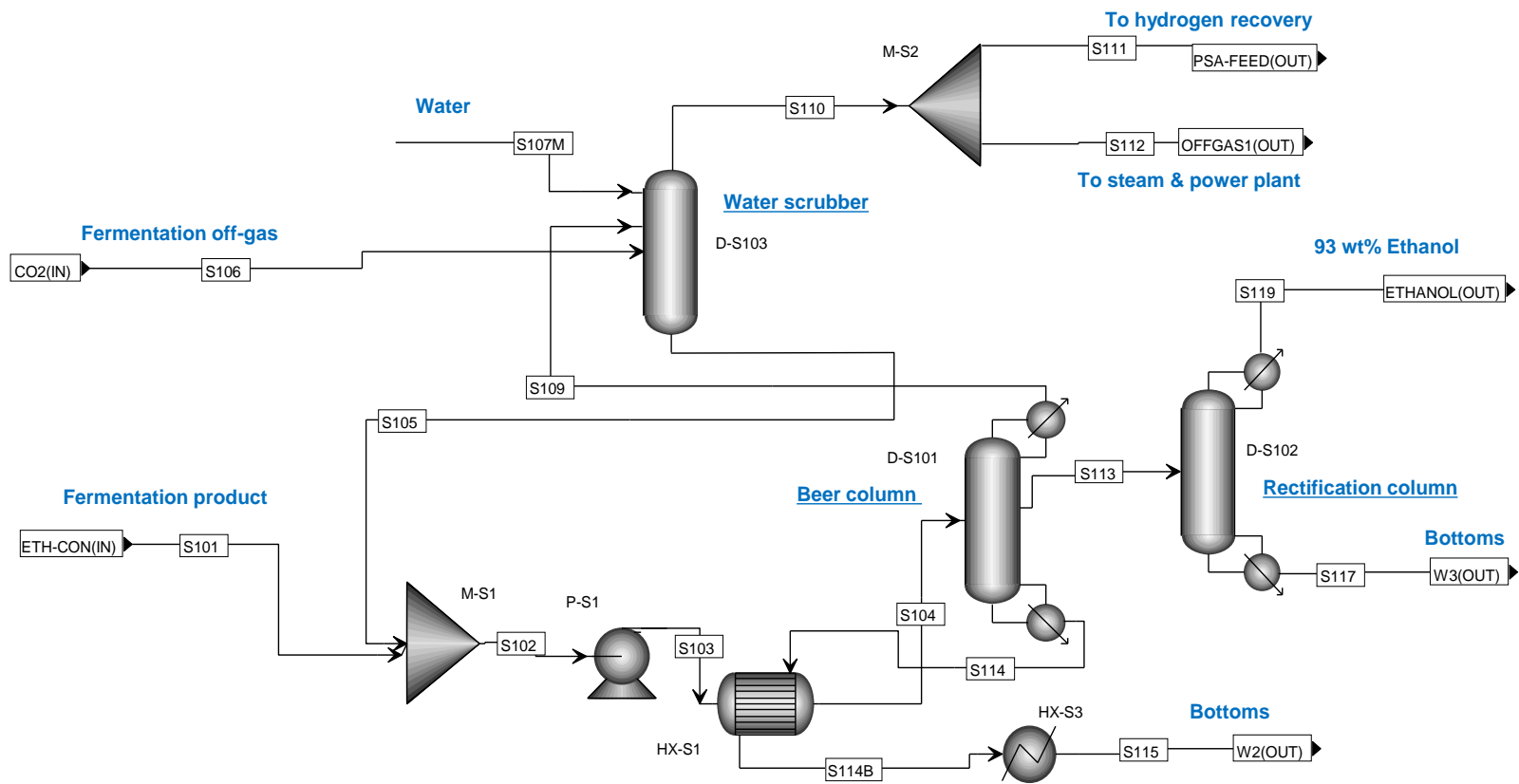


Figure 66: Separation section (SEP section)

Table 168: Stream table for separation section (SEP section)

Stream	SEP.S101	SEP.S103	SEP.S104	SEP.S106	SEP.S107M	SEP.S109	SEP.S110	SEP.S111	SEP.S113	SEP.S114	SEP.S115	SEP.S117	SEP.S119
Total Mass Flow (kg/hr)	669500.7	701698.8	701698.8	19397.96	31152.648	822.66	19175.14	6407.168	24929	675947.2	675947.2	10208	14721
Temperature (C)	37.95	38.05	76.95	37.95	24.95	88.65	28.75	28.75	102.55	115.05	34.95	114.15	86.25
Pressure (atm)	1	1.667	1.667	1	1	1.531	1	1	1.544	1.667	1	1.633	1.361
Vapour fraction	0	0	0	1	0	1	1	1	1	0	0	0	1
Enthalpy (Gcal/hr)	-2486.806	-2607.118	-2580.143	-39.495	-118.051	-1.735	-38.955	-13.017	-51.873	-2491.788	-2545.692	-37.682	-19.657
Mass Flow (kg/hr)													
H2O	651417.2	683099.3	683099.3	842.353	31152.648	183.943	496.853	166.018	11194.78	671720.6	671720.6	10165.43	1029.356
CO2	399.045	417.399	417.399	16532.61	0	417.291	16931.55	5657.497	0.113	0	0	0	0.113
CO	0.875	0.916	0.916	1135.499	0	0.916	1136.374	379.707	0	0	0	0	0
H2	0.337	0.353	0.353	474.927	0	0.353	475.264	158.804	0	0	0	0	0
CH4	0.145	0.152	0.152	126.823	0	0.152	126.968	42.425	0	0	0	0	0
C2H4	0.004	0.004	0.004	0.002	0	0.001	0.004	0.001	0.003	0	0	0	0.003
C2H6	0.001	0.001	0.001	0	0	0	0.001	0	0.001	0	0	0	0.001
ACETI-01	2953.971	2956.702	2956.702	2.352	0	0.379	0	0	22.154	2934.169	2934.169	22.154	0
ETHANOL	13449.68	13944.52	13944.52	283.365	0	219.605	8.125	2.715	13710.95	13.944	13.944	20.416	13690.53
CLOSTRID	1278.428	1278.428	1278.428	0	0	0	0	0	0	1278.428	1278.428	0	0
AMMON-01	0.972	1.018	1.018	0.028	0	0.02	0.002	0.001	0.997	0.001	0.001	0	0.997

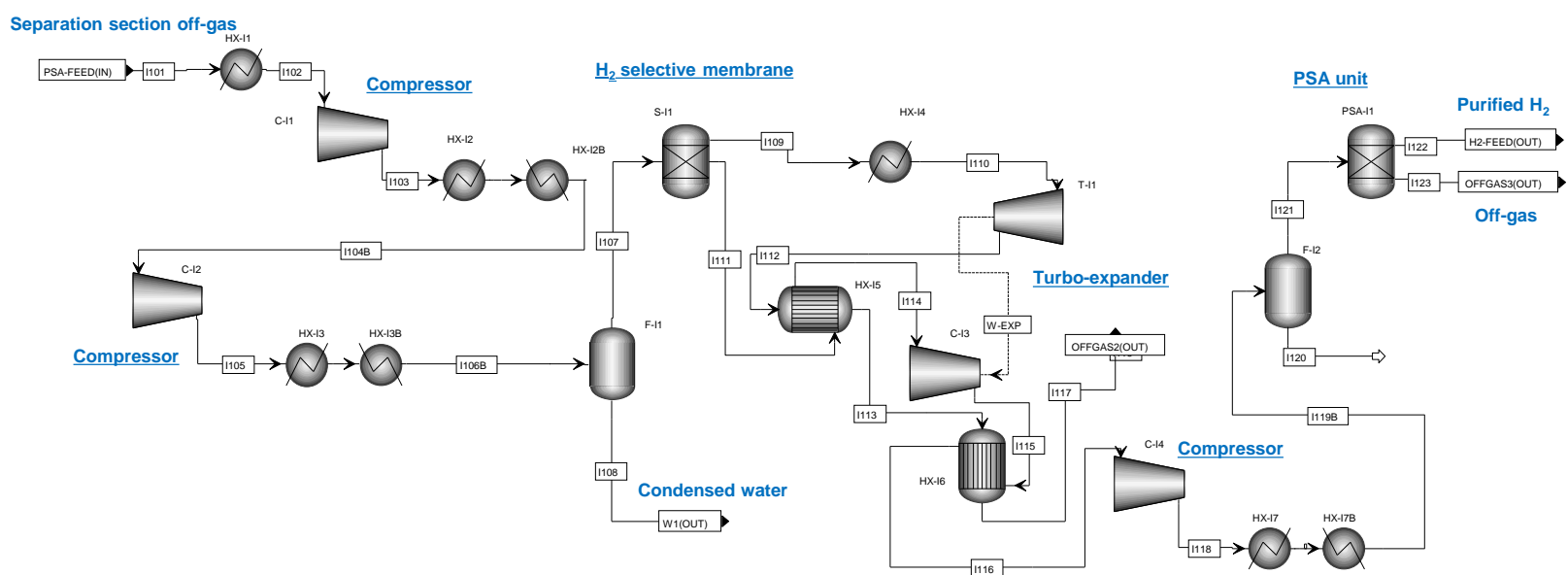


Figure 67: Hydrogen recovery plant (H2-REC section)

Table 169: Stream table for hydrogen recovery plant (H2-REC section)

Stream	H2-REC.1101	H2-REC.1103	H2-REC.1106B	H2-REC.1107	H2-REC.1109	H2-REC.1111	H2-REC.1114	H2-REC.1115	H2-REC.1116	H2-REC.1117	H2-REC.1118	H2-REC.1121	H2-REC.1122
Total Mass Flow (kg/hr)	6407.168	6407.168	6407.168	6254.187	5257.189	996.999	996.999	996.999	996.999	5257.189	996.999	996.999	101.627
Temperature (C)	28.75	257.65	79.95	79.95	79.95	79.95	45.15	240.45	101.65	81.65	243.75	34.85	34.85
Pressure (atm)	1	6.379	34.542	34.542	34.542	1.974	1.974	7.841	7.841	4.935	20	20	20
Vapour fraction	1	1	0.969	1	0.991	1	1	1	1	1	1	1	1
Enthalpy (Gcal/hr)	-13.017	-12.55	-12.982	-12.47	-10.75	-1.731	-1.752	-1.627	-1.717	-10.737	-1.625	-1.759	0.003
Mass Flow (kg/hr)													
H2O	166.018	166.018	166.018	48.842	48.842	0	0	0	0	48.842	0	0	0
CO2	5657.497	5657.497	5657.497	5623.482	4832.602	790.88	790.88	790.88	790.88	4832.602	790.88	790.88	0
CO	379.707	379.707	379.707	379.394	308.251	71.143	71.143	71.143	71.143	308.251	71.143	71.143	0
H2	158.804	158.804	158.804	158.792	31.758	127.034	127.034	127.034	127.034	31.758	127.034	127.034	101.627
CH4	42.425	42.425	42.425	42.351	34.41	7.942	7.942	7.942	7.942	34.41	7.942	7.942	0
C2H4	0.001	0.001	0.001	0.001	0.001	0	0	0	0	0.001	0	0	0
C2H6	0	0	0	0	0	0	0	0	0	0	0	0	0
ETHANOL	2.715	2.715	2.715	1.324	1.324	0	0	0	0	1.324	0	0	0
AMMON-01	0.001	0.001	0.001	0.001	0.001	0	0	0	0	0.001	0	0	0

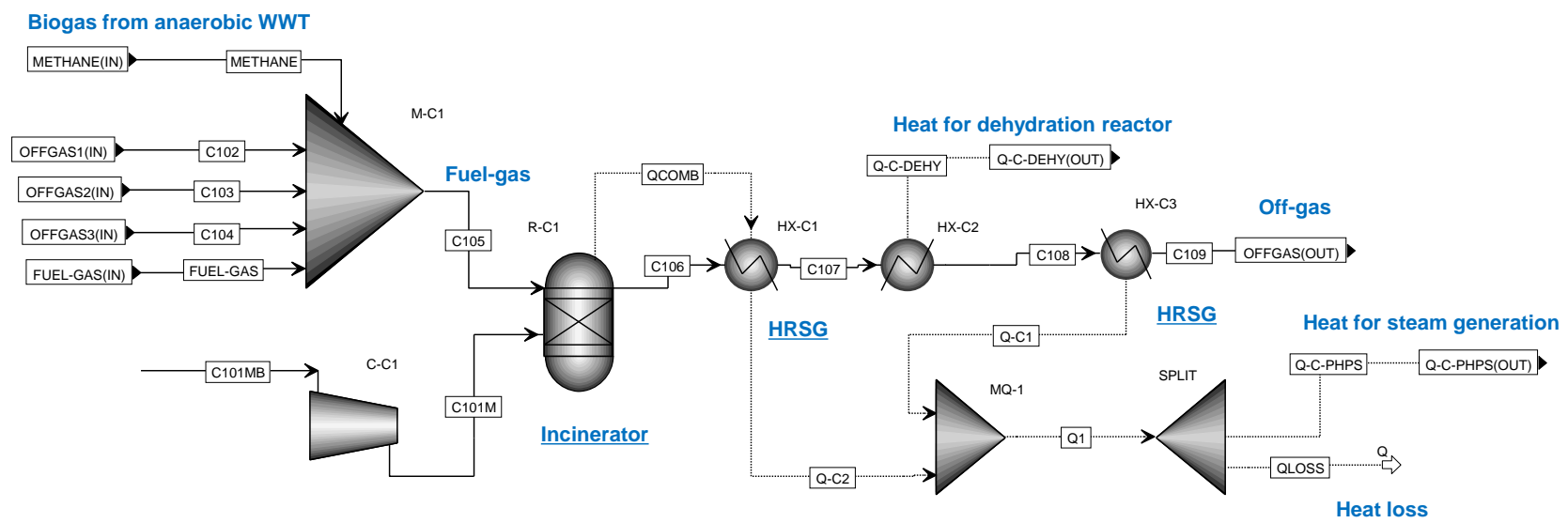


Figure 68: Steam & power plant A; incinerator and HRSG (COMBUST section)

Table 170: Stream table for steam & power plant A; incinerator and HRSG (COMBUST section)

Stream	COMBUST.C101M	COMBUST.C102	COMBUST.C103	COMBUST.C104	COMBUST.C106	COMBUST.C107	COMBUST.C108	COMBUST.C109	COMBUST.FUEL-GAS	COMBUST.METHANE
Total Mass Flow (kg/hr)	157138.757	12767.971	5257.189	895.372	198725.352	198725.352	198725.352	198725.352	20398.325	2267.739
Temperature (C)	26.15	28.75	81.65	34.85	850.05	419.95	358.45	159.95	919.85	35.15
Pressure (atm)	1.01	1	4.935	1.361	1	1	1	1	2	1
Vapour fraction	1	1	1	1	1	1	1	1	1	1
Enthalpy (Gcal/hr)	0.034	-25.939	-10.737	-1.762	-120.739	-146.439	-149.89	-160.628	-12.295	-4.24
Mass Flow (kg/hr)										
H2O	0	330.835	48.842	0	18731.392	18731.392	18731.392	18731.392	814.125	82.509
O2	32999.139	0	0	0	5499.798	5499.798	5499.798	5499.798	0	0
N2	124139.618	0	0	0	124136.108	124136.108	124136.108	124136.108	0	0
NO2	0	0	0	0	0.097	0.097	0.097	0.097	0	0
NO	0	0	0	0	7.459	7.459	7.459	7.459	0	0
CO2	0	11274.052	4832.602	790.88	50350.497	50350.497	50350.497	50350.497	1318.067	1517.681
CO	0	756.667	308.251	71.143	0.001	0.001	0.001	0.001	16835.903	0
H2	0	316.46	31.758	25.407	0	0	0	0	1361.858	0
CH4	0	84.543	34.41	7.942	0	0	0	0	68.368	667.486
C2H4	0	0.002	0.001	0	0	0	0	0	0.003	0
ACETI-01	0	0	0	0	0	0	0	0	0	0.032
ETHANOL	0	5.41	1.324	0	0	0	0	0	0	0.031
AMMON-01	0	0.002	0.001	0	0	0	0	0	0	0

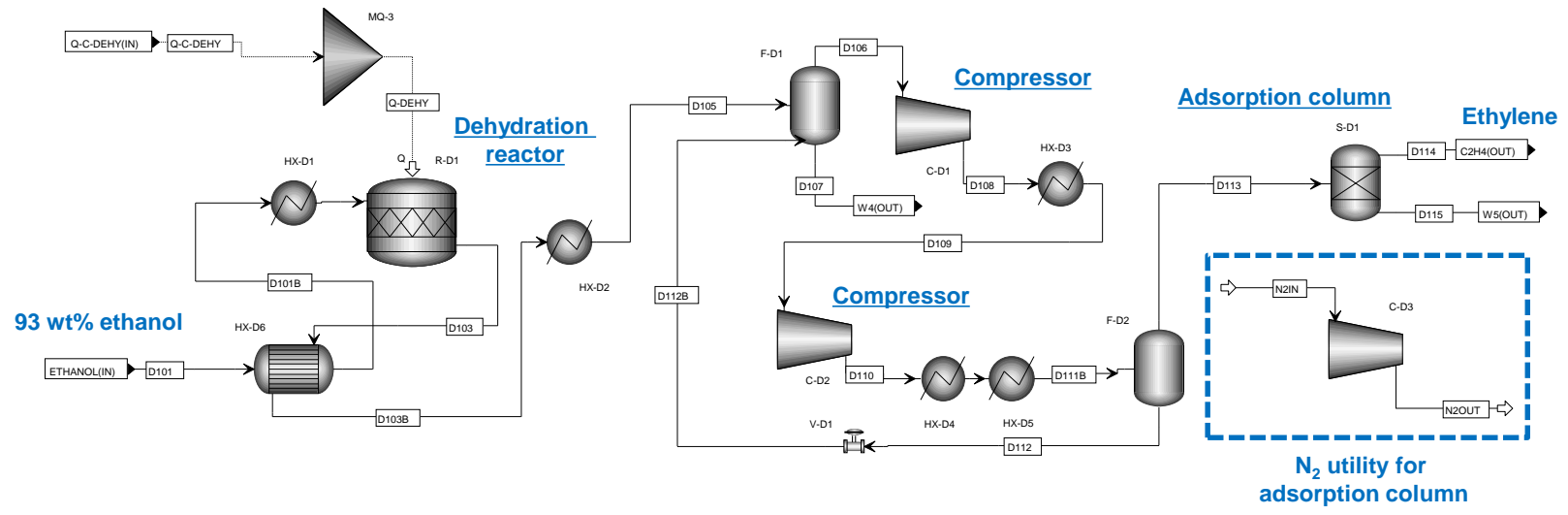


Figure 69: Dehydration section (DEHYD section)

Table 171: Stream table for dehydration section (DEHYD section)

Stream	DEHYD.D101	DEHYD.D101B	DEHYD.D103	DEHYD.D105	DEHYD.D106	DEHYD.D109	DEHYD.D111B	DEHYD.D112B	DEHYD.D113	DEHYD.D114	DEHYD.N2IN	DEHYD.N2OUT
Total Mass Flow (kg/hr)	14721.002	14721.002	14721.002	14721.002	8663.272	8663.272	8663.27	362.941	8300.329	8276.95	118.788	118.788
Temperature (C)	86.25	334.95	349.95	34.95	34.05	104.95	54.95	35.15	39.65	58.25	24.95	166.95
Pressure (atm)	1.361	1.361	1	1	1	5.251	22	1	22	22	1	2.79
Vapour fraction	1	1	1	0.466	1	1	0.908	0.131	1	1	1	1
Enthalpy (Gcal/hr)	-19.657	-17.885	-14.434	-20.2	2.796	3.034	2.652	-1.039	3.69	3.746	0	0.004
Mass Flow (kg/hr)												
H2O	1029.356	1029.356	6380.356	6380.356	298.383	298.383	298.383	283.188	15.195	0	0	0
N2	0	0	0	0	0	0	0	0	0	0	118.788	118.788
CO2	0.113	0.113	0.113	0.113	0.113	0.113	0.113	0.001	0.112	0	0	0
C2H4	0.003	0.003	8328.521	8328.521	8352.248	8352.248	8352.246	75.296	8276.95	8276.95	0	0
C2H6	0.001	0.001	0.001	0.001	0.001	0.001	0.001	0	0.001	0	0	0
ETHANOL	13690.532	13690.532	0	0	0	0	0	0	0	0	0	0
AMMON-01	0.997	0.997	0.997	0.997	1.005	1.005	1.005	0.072	0.933	0	0	0
C4H10O-5	0	0	11.014	11.014	11.522	11.522	11.522	4.384	7.138	0	0	0

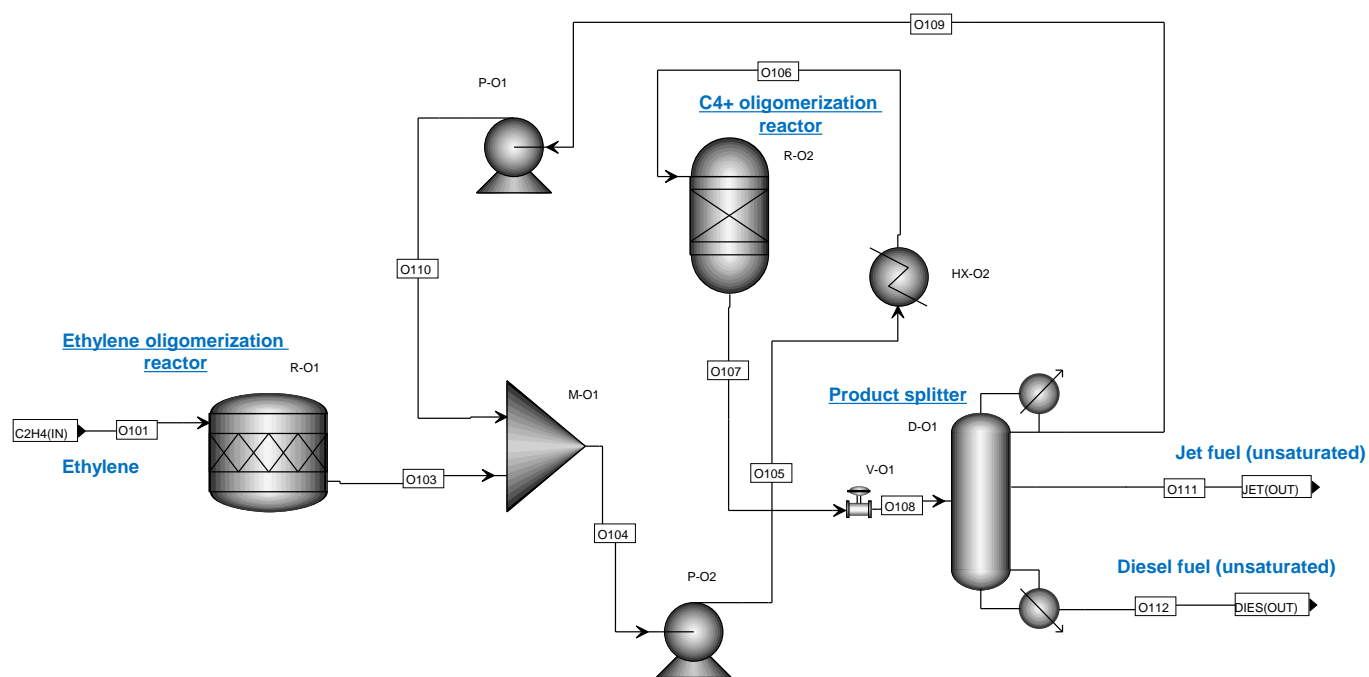


Figure 70: Oligomerization section (OLIG section)

Table 172: Stream table for oligomerization section (OLIG section)

Stream	OLIG.O101	OLIG.O103	OLIG.O104	OLIG.O105	OLIG.O106	OLIG.O107	OLIG.O108	OLIG.O109	OLIG.O110	OLIG.O111	OLIG.O112
Total Mass Flow (kg/hr)	8276.95	8276.95	16553.9	16553.9	16553.9	16553.899	16553.899	8276.951	8276.951	7319	957.947
Temperature (C)	58.25	54.95	44.55	50.05	234.95	234.95	172.75	33.45	31.65	184.25	286.15
Pressure (atm)	22	21.712	21.712	69.085	69.085	69.085	1	1	22	1	1
Vapour fraction	1	0	0	0	0	0	0.85	0	0	0	0
Enthalpy (Gcal/hr)	3.746	-0.634	-2.517	-2.461	0.015	-2.27	-2.27	-1.896	-1.882	-1.626	-0.182
Mass Flow (kg/hr)											
C2H4	8276.95	185.371	185.371	185.371	185.371	0	0	0	0	0	0
C4H8-1	0	6731.113	7967.836	7967.836	7967.836	1236.881	1236.881	1236.723	1236.723	0.159	0
C5H10-2	0	0	342.969	342.969	342.969	343.117	343.117	342.969	342.969	0.148	0
C6H12-3	0	1331.331	1563.429	1563.429	1563.429	232.434	232.434	232.099	232.099	0.335	0
C7H14-7	0	0	861.791	861.791	861.791	866.094	866.094	861.791	861.791	4.303	0
C8H16-16	0	29.135	3893.794	3893.794	3893.794	3941.93	3941.93	3864.659	3864.659	77.268	0
C9H18-3	0	0	1738.64	1738.64	1738.64	2700.595	2700.595	1738.64	1738.64	961.959	0
C10H20-5	0	0	0.07	0.07	0.07	1059.273	1059.273	0.07	0.07	1059.203	0.001
C11H22-2	0	0	0	0	0	1183.407	1183.407	0	0	1183.389	0.019
C12H24-2	0	0	0	0	0	1886.83	1886.83	0	0	1886.416	0.416
C13H26-2	0	0	0	0	0	959.966	959.966	0	0	956.977	2.99
C14H28-2	0	0	0	0	0	571.014	571.014	0	0	548.14	22.875
C15H30-2	0	0	0	0	0	637.219	637.219	0	0	440.349	196.868
C16H32-2	0	0	0	0	0	438.605	438.605	0	0	119.413	319.188
C17H3-01	0	0	0	0	0	206.889	206.889	0	0	36.19	170.698
C18H36-1	0	0	0	0	0	140.685	140.685	0	0	22.192	118.491
C19H4-01	0	0	0	0	0	91.031	91.031	0	0	13.885	77.146
1-EIC-01	0	0	0	0	0	57.929	57.929	0	0	8.674	49.255

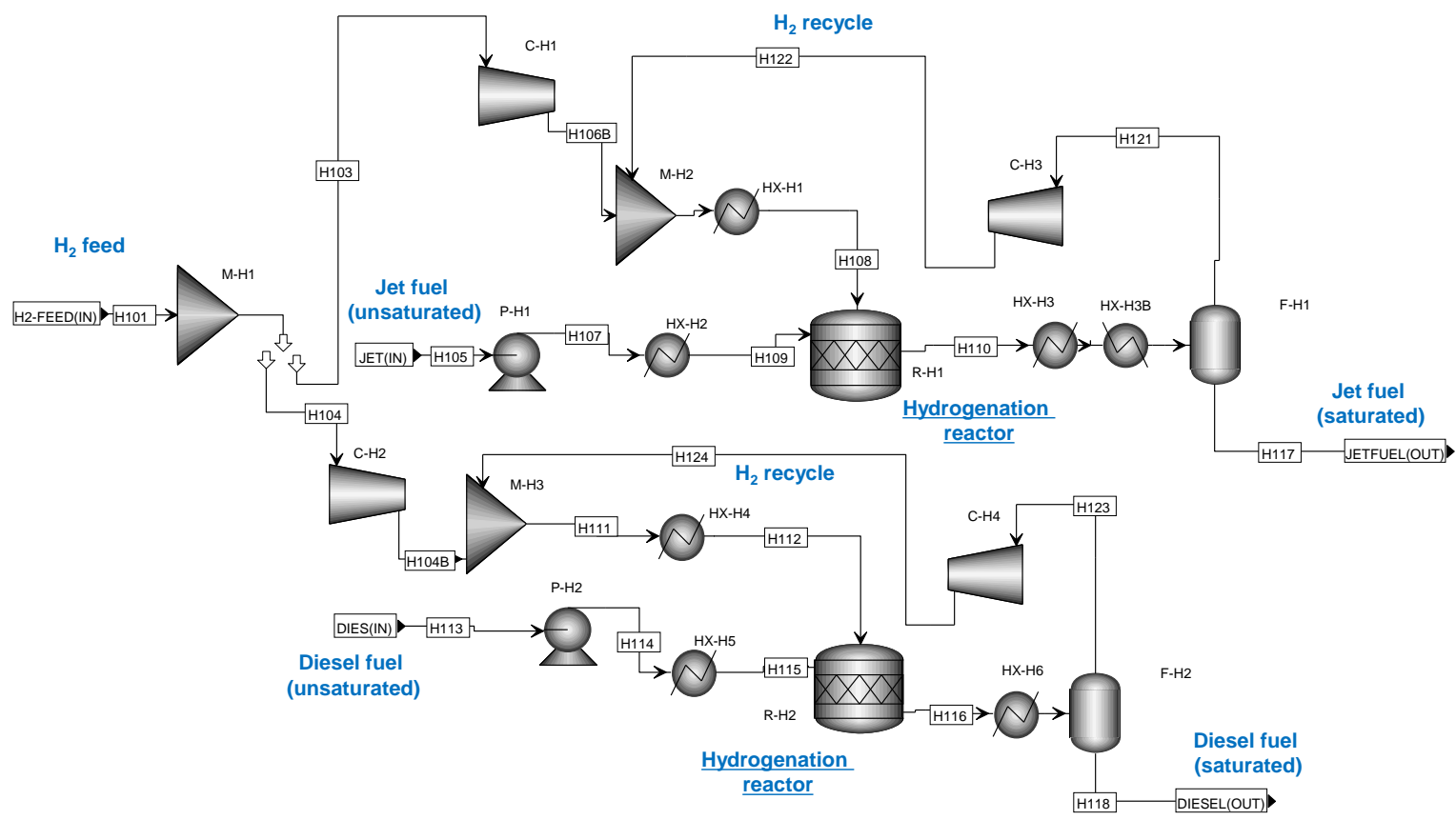


Figure 71: Hydroprocessing section (HYDRO section)

Table 173: Stream table for hydroprocessing section (HYDRO section)

Stream	HYDRO.H103	HYDRO.H104	HYDRO.H105	HYDRO.H108	HYDRO.H109	HYDRO.H110	HYDRO.H112	HYDRO.H113	HYDRO.H115	HYDRO.H116	HYDRO.H117	HYDRO.H118	HYDRO.H122	HYDRO.H124
Total Mass Flow (kg/hr)	93.184	8.443	7319	937.036	7319	8256.034	83.533	957.947	957.947	1041.482	7412.184	966.391	843.852	75.091
Temperature (C)	34.95	34.95	184.25	184.95	184.95	184.95	184.95	286.15	184.95	184.95	36.05	33.35	161.05	157.55
Pressure (atm)	20	20	1	34.049	34.049	34.049	34.049	1	34.049	34.049	14.049	14.049	34.049	34.049
Vapour fraction	1	1	0	1	0	1	1	0	0	1	0	0	1	1
Enthalpy (Gcal/hr)	0.003	0	-1.626	0.51	-1.612	-2.039	0.047	-0.182	-0.248	-0.267	-3.624	-0.455	0.388	0.035
Mass Flow (kg/hr)														
H2	93.184	8.443	0	922.794	0	830.514	83.529	0	0	75.176	0.905	0.09	829.61	75.087
C4H8-1	0	0	0.159	0	0.159	0	0	0	0	0	0	0	0	0
C5H10-2	0	0	0.148	0	0.148	0	0	0	0	0	0	0	0	0
C6H12-3	0	0	0.335	0	0.335	0	0	0	0	0	0	0	0	0
C7H14-7	0	0	4.303	0	4.303	0	0	0	0	0	0	0	0	0
C8H16-16	0	0	77.268	0	77.268	0	0	0	0	0	0	0	0	0
C9H18-3	0	0	961.959	0	961.959	0	0	0	0	0	0	0	0	0
C10H20-5	0	0	1059.203	0	1059.203	0	0	0.001	0.001	0	0	0	0	0
C11H22-2	0	0	1183.389	0	1183.389	0	0	0.019	0.019	0	0	0	0	0
C12H24-2	0	0	1886.416	0	1886.416	0	0	0.416	0.416	0	0	0	0	0
C13H26-2	0	0	956.977	0	956.977	0	0	2.99	2.99	0	0	0	0	0
C14H28-2	0	0	548.14	0	548.14	0	0	22.875	22.875	0	0	0	0	0
C15H30-2	0	0	440.349	0	440.349	0	0	196.868	196.868	0	0	0	0	0
C16H32-2	0	0	119.413	0	119.413	0	0	319.188	319.188	0	0	0	0	0
C17H3-01	0	0	36.19	0	36.19	0	0	170.698	170.698	0	0	0	0	0
C18H36-1	0	0	22.192	0	22.192	0	0	118.491	118.491	0	0	0	0	0
C19H4-01	0	0	13.885	0	13.885	0	0	77.146	77.146	0	0	0	0	0
1-EIC-01	0	0	8.674	0	8.674	0	0	49.255	49.255	0	0	0	0	0
C4H10-1	0	0	0	0.336	0	0.5	0	0	0	0	0.164	0	0.336	0
C5H12-1	0	0	0	0.095	0	0.247	0	0	0	0	0.152	0	0.095	0
C6H14-1	0	0	0	0.07	0	0.413	0	0	0	0	0.343	0	0.07	0
C7H16-1	0	0	0	0.293	0	4.684	0	0	0	0	4.391	0	0.293	0
C8H18-1	0	0	0	1.691	0	80.347	0	0	0	0	78.656	0	1.691	0
C9H20-1	0	0	0	7.146	0	984.466	0	0	0	0	977.32	0	7.146	0
C10H22-1	0	0	0	2.68	0	1077.105	0	0	0	0.001	1074.426	0.001	2.68	0
C11H24	0	0	0	1.17	0	1200.02	0	0	0	0.019	1198.85	0.019	1.17	0
C12H26	0	0	0	0.634	0	1909.643	0	0	0	0.421	1909.009	0.421	0.634	0
C13H28	0	0	0	0.099	0	967.655	0	0	0	3.024	967.556	3.023	0.099	0
C14H30	0	0	0	0.021	0	553.788	0.001	0	0	23.11	553.767	23.11	0.021	0.001
C15H32	0	0	0	0.006	0	444.574	0.002	0	0	198.757	444.568	198.755	0.006	0.002
C16H34	0	0	0	0.001	0	120.487	0.001	0	0	322.057	120.486	322.055	0.001	0.001
C17H36	0	0	0	0	0	36.496	0	0	0	172.141	36.496	172.141	0	0
C18H38	0	0	0	0	0	22.369	0	0	0	119.438	22.369	119.438	0	0
C19H40	0	0	0	0	0	13.99	0	0	0	77.729	13.99	77.729	0	0
C20H42	0	0	0	0	0	8.736	0	0	0	49.609	8.736	49.609	0	0

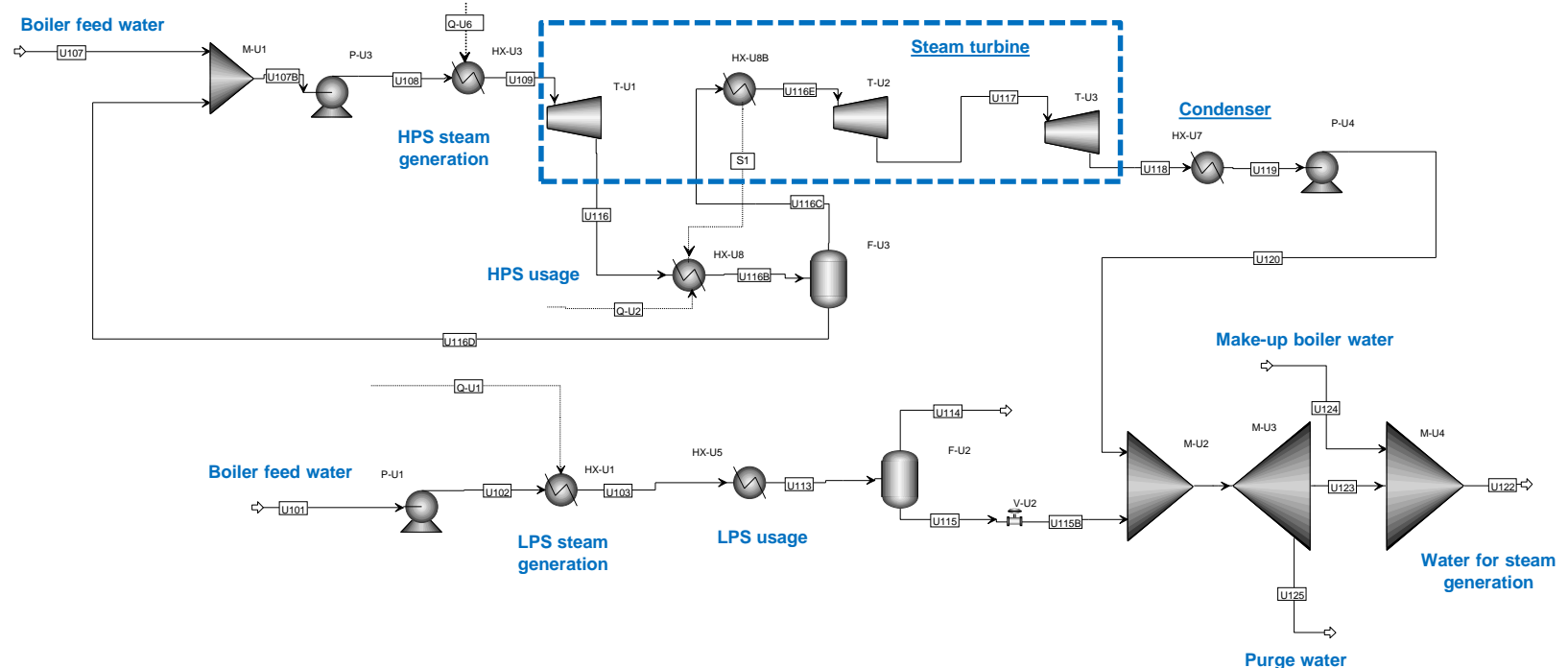


Figure 72: Steam & power plant B, steam turbine (UTILITY section)

Table 174: Stream table for steam & power plant B; steam turbine (UTILITY section)

Stream	UTILITY.U101	UTILITY.U103	UTILITY.U107	UTILITY.U109	UTILITY.U113	UTILITY.U115	UTILITY.U116	UTILITY.U116D
Total Mass Flow (kg/hr)	159917.26	159917.26	91027.472	92822.669	159917.26	159917.26	92822.669	1795.197
Temperature (C)	89.95	151.85	89.95	546.85	140.95	140.95	395.55	221.85
Pressure (atm)	1	4	1	86	4	4	23.686	23.686
Vapour fraction	0	1	0	1	0	0	1	0
Enthalpy (Gcal/hr)	-595.618	-503.962	-339.035	-274.476	-587.366	-587.366	-282.425	-6.44
Mass Flow (kg/hr)								
H2O	159917.26	159917.26	91027.472	92822.669	159917.26	159917.26	92822.669	1795.197

Stream	UTILITY.U116E	UTILITY.U117	UTILITY.U118	UTILITY.U120	UTILITY.U122	UTILITY.U124	UTILITY.U125
Total Mass Flow (kg/hr)	91023.609	91023.609	91023.609	91023.609	250940.87	5018.947	5018.947
Temperature (C)	395.95	210.05	62.75	60.05	99.95	24.95	99.95
Pressure (atm)	23.686	3.948	0.197	1	1	1	1
Vapour fraction	1	1	0.935	0	0.014	0	0.022
Enthalpy (Gcal/hr)	-276.082	-284.411	-293.782	-341.748	-930.204	-47.546	-46.456
Mass Flow (kg/hr)							
H2O	91023.609	91023.609	91023.609	91023.609	250940.87	12547.044	12547.044

Table 175: Stream table for cooling tower (UTILITY section); based on Figure 61 of the HEFA process

Stream	UTILITY.2	UTILITY.3	UTILITY.DW1	UTILITY.DW2
Total Mass Flow (kg/hr)	17634100	212372.63	17846400	17846400
Temperature (C)	25	25	25	35
Pressure (atm)	0.031	0.031	1	1
Vapour fraction	0	1	0	0
Enthalpy (Gcal/hr)	-66823.391	-680.866	-67627.779	-67449.914
Mass Flow (kg/hr)				
H2O	17634100	212372.63	17846400	17846400

**S-ETH-J Process**

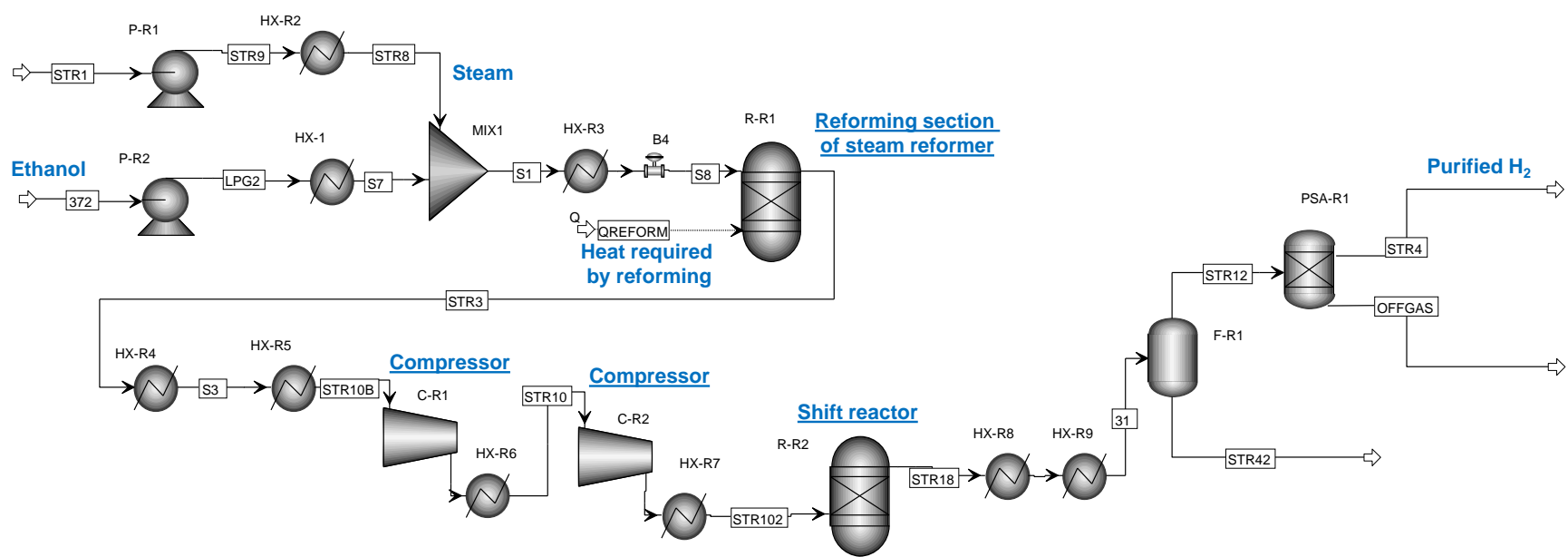


Figure 73: Hydrogen plant; steam reforming & hydrogen recovery (REFORM section)

Table 176: Stream table for hydrogen plant; steam reforming & hydrogen recovery (REFORM section)

Stream	REFORM.31	REFORM.372	REFORM.S1	REFORM.STR1	REFORM.STR3	REFORM.STR4	REFORM.STR10B	REFORM.STR18	REFORM.STR102
Total Mass Flow (kg/hr)	1242.891	614.311	1242.891	628.58	1242.891	106.422	1242.891	1242.891	1242.891
Temperature (C)	35	86.2	565.6	25	800	35	100	353.1	244.2
Pressure (atm)	24.442	1.361	84.875	0.987	1	24.442	1	24.442	25.1
Vapour fraction	0.906	0	1	0	1	1	1	1	1
Enthalpy (Gcal/hr)	-2.427	-0.956	-2.533	-2.383	-1.657	0.004	-2.198	-2.094	-2.094
Mass Flow (kg/hr)									
ETHANOL	0	571.309	571.309	0	0	0	0	0	0
H2O	166.872	42.997	671.577	628.58	328.207	0	328.207	166.872	328.207
CO2	755.631	0.005	0.005	0	361.503	0	361.503	755.631	361.503
CH4	24.951	0	0	0	24.951	0	24.951	24.951	24.951
CO	170.234	0	0	0	421.08	0	421.08	170.234	421.08
H2	125.203	0	0	0	107.15	106.422	107.15	125.203	107.15

**L-ETH-J Process**

Table 177: Stream table for hydrogen plant; steam reforming & hydrogen recovery (REFORM section); based on Figure 73 of the S-ETH-J process

Stream	REFORM.31	REFORM.372	REFORM.S1	REFORM.STR1	REFORM.STR3	REFORM.STR4	REFORM.STR10B	REFORM.STR18	REFORM.STR102
Total Mass Flow (kg/hr)	1235.075	613.406	1235.076	621.67	1235.075	105.732	1235.075	1235.075	1235.075
Temperature (C)	35	86.3	565.6	25	800	35	100	353.1	244.1
Pressure (atm)	24.442	1.361	86	1	1	24.442	1	24.442	25.1
Vapour fraction	0.905	0	1	0	1	1	1	1	1
Enthalpy (Gcal/hr)	-2.414	-0.963	-2.519	-2.357	-1.648	0.004	-2.186	-2.083	-2.083
Mass Flow (kg/hr)									
ETHANOL	0	566.897	566.897	0	0	0	0	0	0
H2O	166.535	46.506	668.176	621.67	326.929	0	326.929	166.535	326.929
CO2	751.163	0.003	0.003	0	359.334	0	359.334	751.163	359.334
CH4	24.515	0	0	0	24.515	0	24.515	24.515	24.515
CO	168.472	0	0	0	417.855	0	417.855	168.472	417.855
H2	124.39	0	0	0	106.442	105.732	106.442	124.39	106.442



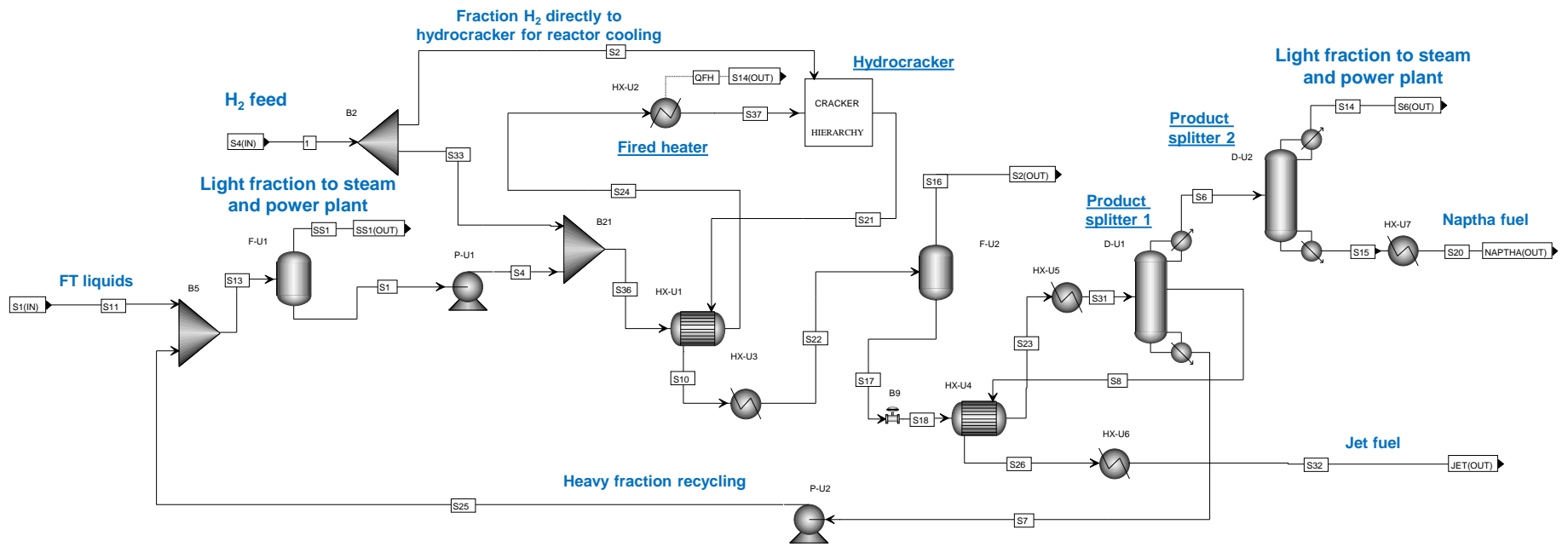


Figure 75: Upgrading and separation section (UPGRADE section)

Table 179: Stream table for upgrading and separation section (UPGRADE section)

Stream	UPGRADE.S1	UPGRADE.S2	UPGRADE.S4	UPGRADE.S6	UPGRADE.S7	UPGRADE.S8	UPGRADE.S11	UPGRADE.S14	UPGRADE.S15	UPGRADE.S16	UPGRADE.S21	UPGRADE.S22	UPGRADE.S31	UPGRADE.S37
Total Mass Flow (kg/hr)	2563.06	169.45	20162.47	2660.12	8791.06	7926.19	11764.4	271.97	2388.15	3179.50	22556.35	22556.35	19376.85	22556.16
Temperature (C)	40.75	40.75	177.65	99.05	332.85	186.65	39.55	-3.35	77.45	34.95	349.95	34.95	219.95	349.95
Pressure (atm)	34.542	34.542	34.542	1	1	1	19.738	1	1	34.542	34.542	34.542	1	34.542
Vapour fraction	1	1	0	1	0	0	0	1	0	1	0.99	0.916	0.576	0.98
Enthalpy (Gcal/hr)	0.138	0.009	-7.981	-1.139	-2.355	-3.16	-5.952	-0.153	-1.215	-0.557	-2.414	-9.89	-6.689	-2.234
Mass Flow (kg/hr)														
H2O	0	0	3.34	1.873	0	0.016	3.983	1.615	0.259	1.451	3.34	3.34	1.889	3.34
N2	0	0	0.226	0.001	0	0	0.786	0.001	0	0.224	0.226	0.226	0.001	0.226
CO2	0	0	40.469	2.266	0	0.004	76.093	2.266	0	38.198	40.468	40.468	2.27	40.469
CO	0	0	26.994	0.174	0	0	96.27	0.174	0	26.818	26.992	26.992	0.174	26.994
H2	2563.064	169.445	0	5.355	0	0.002	0	5.355	0	2318.248	2323.605	2323.605	5.357	2393.691
CH4	0	0	48.421	3.31	0	0.003	119.556	3.31	0	196.118	199.432	199.432	3.313	48.421
C2H6	0	0	21.831	7.92	0	0.018	36.638	7.92	0	91.88	99.818	99.818	7.938	21.831
C3H8	0	0	76.184	41.367	0	0.173	105.25	41.357	0.01	145.347	186.886	186.886	41.539	76.184
C4H10	0	0	197.14	143.722	0	1.096	239.485	141.061	2.662	155.235	300.049	300.049	144.814	197.14
C5H12-1	0	0	335.645	321.889	0	4.431	377.394	67.891	253.997	107.613	433.921	433.921	326.308	335.645
C6H14-1	0	0	431.883	511.882	0	12.768	463.433	0.995	510.887	56.513	581.144	581.144	524.631	431.883
C7H16-1	0	0	485.562	673.762	0	31.642	506.743	0.025	673.736	25.464	730.843	730.843	705.379	485.562
C8H18-1	0	0	510.643	765.007	0	98.779	523.936	0.001	765.006	10.014	873.771	873.771	863.757	510.643
C9H20-1	0	0	519.002	179.892	0	814.26	527.183	0	179.892	3.945	998.081	998.081	994.135	519.002
C10H22-1	0	0	517.006	1.678	0	1094.76	521.934	0	1.678	1.49	1097.916	1097.916	1096.426	517.006
C11H24	0	0	507.87	0.018	0	1164.27	510.941	0	0.018	0.619	1164.89	1164.89	1164.271	507.87
C12H26	0	0	493.986	0	0	1200.10	495.803	0	0	0.218	1200.306	1200.306	1200.088	493.986
C13H28	0	0	476.655	0	0.006	1200.95	477.697	0	0	0.067	1201.009	1201.009	1200.942	476.655
C14H30	0	0	457.728	0	0.798	1174.5	457.554	0	0	0.025	1175.308	1175.308	1175.283	457.728
C15H32	0	0	535.644	0	99.988	1020.48	436.107	0	0	0.008	1120.463	1120.463	1120.455	535.644
C16H34	0	0	1339.353	0	926.137	101.412	413.926	0	0	0.003	1027.517	1027.517	1027.514	1339.353
C17H36	0	0	1305.058	0	914.025	5.72	391.451	0	0	0.001	919.711	919.711	919.71	1305.058
C18H38	0	0	1191.898	0	823.119	0.702	369.022	0	0	0	823.791	823.791	823.791	1191.898
C19H40	0	0	1072.593	0	725.841	0.088	346.89	0	0	0	725.903	725.903	725.903	1072.593
C20H42	0	0	968.815	0	643.648	0.01	325.242	0	0	0	643.634	643.634	643.634	968.815
C30H62	0	0	8598.521	0	4657.50	0	3941.03	0	0	0	4657.323	4657.323	4657.323	8598.521

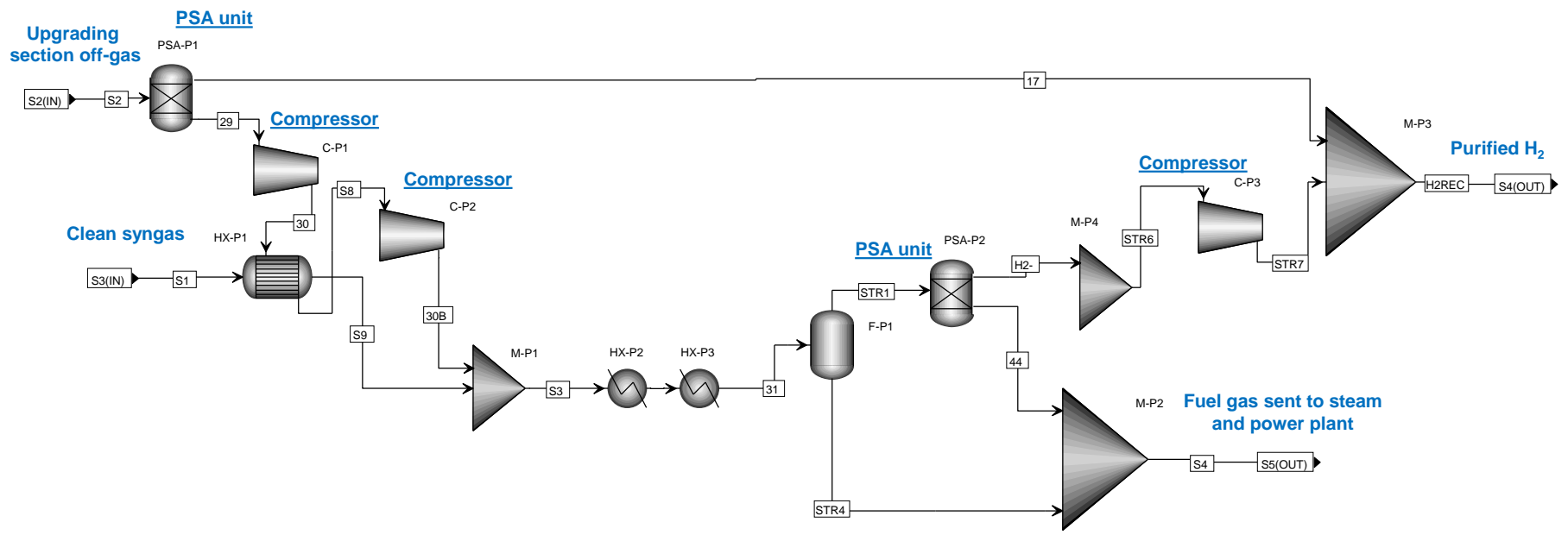


Figure 76: Hydrogen recovery plant (PSA section)

Table 180: Stream table for hydrogen recovery plant (PSA section)

Stream	PSA.17	PSA.30	PSA.30B	PSA.31	PSA.H2-	PSA.H2REC	PSA.S1	PSA.S2	PSA.S3	PSA.S4	PSA.STR4	PSA.STR7
Total Mass Flow (kg/hr)	1970.511	1208.988	1208.988	4704.927	592.553	2563.064	3495.938	3179.499	4704.927	4112.373	0.216	592.553
Temperature (C)	36.15	223.65	214.75	44.95	44.95	40.75	-38.85	34.95	147.75	44.95	44.95	56.15
Pressure (atm)	34.542	8.685	31.582	31.582	31.582	34.542	31.582	34.542	31.582	1.974	31.582	34.542
Vapour fraction	1	1	1	1	1	1	1	1	1	1	0	1
Enthalpy (Gcal/hr)	0.075	-0.324	-0.339	-3.587	0.04	0.138	-3.147	-0.557	-3.199	-3.628	0	0.063
Mass Flow (kg/hr)												
H2O	0	1.451	1.451	1.451	0	0	0	1.451	1.451	1.451	0.002	0
N2	0	0.224	0.224	18.068	0	0	17.844	0.224	18.068	18.068	0	0
CO2	0	38.198	38.198	111.615	0	0	73.417	38.198	111.615	111.615	0	0
CO	0	26.818	26.818	2943.041	0	0	2916.223	26.818	2943.041	2943.041	0	0
H2	1970.511	347.737	347.737	740.692	592.553	2563.064	392.954	2318.248	740.692	148.138	0	592.553
CH4	0	196.118	196.118	291.618	0	0	95.5	196.118	291.618	291.618	0	0
C2H6	0	91.88	91.88	91.88	0	0	0	91.88	91.88	91.88	0	0
C3H8	0	145.347	145.347	145.347	0	0	0	145.347	145.347	145.347	0.001	0
C4H10	0	155.235	155.235	155.235	0	0	0	155.235	155.235	155.235	0.004	0
C5H12-1	0	107.613	107.613	107.613	0	0	0	107.613	107.613	107.613	0.009	0
C6H14-1	0	56.513	56.513	56.513	0	0	0	56.513	56.513	56.513	0.014	0
C7H16-1	0	25.464	25.464	25.464	0	0	0	25.464	25.464	25.464	0.019	0
C8H18-1	0	10.014	10.014	10.014	0	0	0	10.014	10.014	10.014	0.021	0
C9H20-1	0	3.945	3.945	3.945	0	0	0	3.945	3.945	3.945	0.024	0
C10H22-1	0	1.49	1.49	1.49	0	0	0	1.49	1.49	1.49	0.026	0
C11H24	0	0.619	0.619	0.619	0	0	0	0.619	0.619	0.619	0.029	0
C12H26	0	0.218	0.218	0.218	0	0	0	0.218	0.218	0.218	0.026	0
C13H28	0	0.067	0.067	0.067	0	0	0	0.067	0.067	0.067	0.018	0
C14H30	0	0.025	0.025	0.025	0	0	0	0.025	0.025	0.025	0.013	0
C15H32	0	0.008	0.008	0.008	0	0	0	0.008	0.008	0.008	0.006	0
C16H34	0	0.003	0.003	0.003	0	0	0	0.003	0.003	0.003	0.003	0
C17H36	0	0.001	0.001	0.001	0	0	0	0.001	0.001	0.001	0.001	0